International Atomic Energy Agency

INDC(CCP)-409
Distr.: L

INDC INTERNATIONAL NUCLEAR DATA COMMITTEE

SELECTED ARTICLES TRANSLATED FROM JADERNYE KONSTANTY (NUCLEAR CONSTANTS) VOLUME 1, 1996

Translated by Dr. Alex Lorenz

August 1997

Reproduced by the IAEA in Austria
August 1997

INDC(CCP)-409
Distr.: L

SELECTED ARTICLES TRANSLATED FROM JADERNYE KONSTANTY (NUCLEAR CONSTANTS) VOLUME 1, 1996

Translated by Dr. Alex Lorenz

August 1997

Contents

DEVELOPMENT OF A NATIONAL NEUTRON DATABASE FOR NUCLEAR TECHNOLOGY

A.V. Ignatyuk, V.N. Kononov, B.D. Kuzminov, V.N. Manokhin
M.N. Nikolaev, B.I. Furzov

State Research Centre of the Russian Federation
Institute of Physics and Power Engineering, Obninsk

Abstract

This paper describes the stages of a many years activities at the IPPE consisting of the measurement, theoretical description and evaluation of neutron data, and of the establishment of a national data bank of neutron data for nuclear technology. A list of libraries which are stored at the Nuclear Data Centre is given.

Introduction

Currently, nuclear technology has found wide applications in a number of fields in science and technology consisting of:

- nuclear energy (nuclear fission reactors, nuclear fission reactors, radioisotopic sources)
- nuclear transmutation (production of radioisotopes for medical and other applications, burn-up of long-lived radio nuclides, radiation alloying of semiconducting materials, etc...)
- nuclear instrumentation in industry (activation analysis, nuclear micro-analysis, control of fissile materials, etc...)
- scientific investigations (nuclear physics, nuclear astrophysics, medicine, radiobiology, agro-radiology, ecology, etc...).

In the sphere of nuclear technology, a number of processes use more than 500 stable and radioactive nuclides in a broad energy range. To ascertain the proper functioning of nuclear installations which have various functions and applications in industrial projects and scientific investigations, there is a need for nuclear data that characterize the properties of nuclear reactions. The reliability of radiation and nuclear safety, the ecological acceptance, and the economical planning of nuclear installations, all depend on the completeness, quality and accuracy of nuclear data. To satisfy that need, a concerted effort spanning many years of research in the field of neutron data at the FEI and other research institutes have led to the

creation of the National Library of Recommended Evaluated Data, BROND.

This systematically planned research effort consisted of the following activities:

- the determination of the main requirements and optimal accuracies of the nuclear data;
- the measurement of cross sections and other parameters which characterize the interaction of neutrons with fissile, structural and technological materials, the minor actinides and fission products;
- experimental and theoretical research to determine the mechanisms of nuclear reactions needed for the development of models used to ensure the required accuracy of calculational results;
- the development of evaluation methods and the evaluation of neutron data including all results obtained from experimental measurements and theoretical calculations;
- the creation of a domestic system of files of recommended evaluated neutron data, and their storage in computer data banks, and the satisfaction of users' requests.

The data survey includes data published since 1972 until now in accordance with State projects (established in accordance with the Council of Ministers decree No. 474-163, dated 15.06.1976. Listing of federal goal-oriented programs, P.11 - Scientific and technological programs) and specialized programs (in accordance with decrees No. 0156 dated 30.06.71; No. 086 dated 22.04.82, No. 0187 dated 23.07.76 and No. 770 dated 10.10.88, of the long-term Russian research program in the field of nuclear data for the years 1995-2005).

Goal-oriented research which would have the objective to guarantee the availability of neutron data to problems related to the following fields of activities:

- fast and intermediate neutron power reactors;
- nuclear safety and internal reactor safety;
- external fuel cycle;
- ecologically safe handling of long-lived radioactive waste (burial and transmutation);
- radiation resistant materials;
- disassembly of used up reactors:
- usage of weapons and reactor plutonium;
- development of the international fusion reactor project;
- manufacturing of radioisotopes for medical application, diagnostics and therapeutics;
- radiation protection of defense oriented problems;
- geophysical, astrophysical and a number of other applied problems in the national economy.

The research was executed primarily by the staff of the Institute of Physics and Power Engineering (FEI). Some of the work was performed by scientists of other Russian institutes, namely:

- the Russian Federal Nuclear Centre - VNIIEF
- the Radium Institute - RI
- the Russian Science Centre - Kurchatov Institute
- the State Science Centre - NIIAR
- the Institutes of the Russian Academy of Sciences

- NIYaFS (S.Petersburg)
- Iyal (Moscow) and others;

- the Institute of Nuclear Research of the Ukrainian Academy of Sciences - Iyal UAN
- the Institute of Nuclear Energy of the Byeloruss Academy of Sciences - IAE BAN, and currently,
- the Institute of Radiation Physical Chemistry - IRKhFP.

The coordination of the research was executed by the Russian Commission on Nuclear Data and the FEI institute.

The considerable demand for a high quality of needed neutron data, the enormous number of stable and radioactive nuclides which are involved in nuclear technology, and the wide energy range of the interactive particles (which at the present time extends from fractions of electron volts (eV) to a few GeV) has inevitably led to international cooperation so as to be able to cope with the solution of nuclear data problems.

I. Structure of the Nuclear Data Activities

The generation of nuclear data, which is a complex scientific activity, requires the participation of highly qualified staff and the availability of highly precise instrumentation. Neutron data exists in a variety of forms:

- differential experimental neutron data which characterize nuclear interaction at a fundamental level;
- reference or standard neutron data, which require extreme exactness and precision in their production;
- theoretical data, resulting from calculational models;
- integral neutron data which characterize the properties of a combination of nuclear interactions in various media or differential characteristics averaged over a broad energy range;
- evaluated neutron data generated from a combination of experimental data and theoretical models of nuclear reactions;
- task-dependent data.

The principal objective of the generation of neutron data is the creation of a universal library of evaluated neutron data which could serve as the underlying source of information for the solution of specific nuclear technology tasks. Figure.1 shows the interdependence of nuclear data activities. Nuclear data users specify the accuracy requirements in the calculation of parameters or formalisms which characterize the properties of the projected nuclear installation. Based on these objective-oriented requirements, specialists formulate a list of needed neutron data and their required accuracy. At the initial stages of the project, when the viability of the project is being investigated, the accuracy of the nuclear data is not of great importance. At subsequent stages, however, when the conceptual aspects of the project are being investigated, and the safety and economical aspects come into play, much more accurate data are needed. Should the accuracy of the existing experimental and evaluated neutron data

not satisfy the stated requirements, a special program, designed to generate new data or improve the accuracy of the existing data, is then implemented. The measurement of differential neutron data are performed either to validate nuclear models, to merge the calculated results with the existing experimental data in order to improve their accuracy, or to create data for special applications. The results of differential neutron data measurements serve as the principle source of information in the generation of evaluated data.

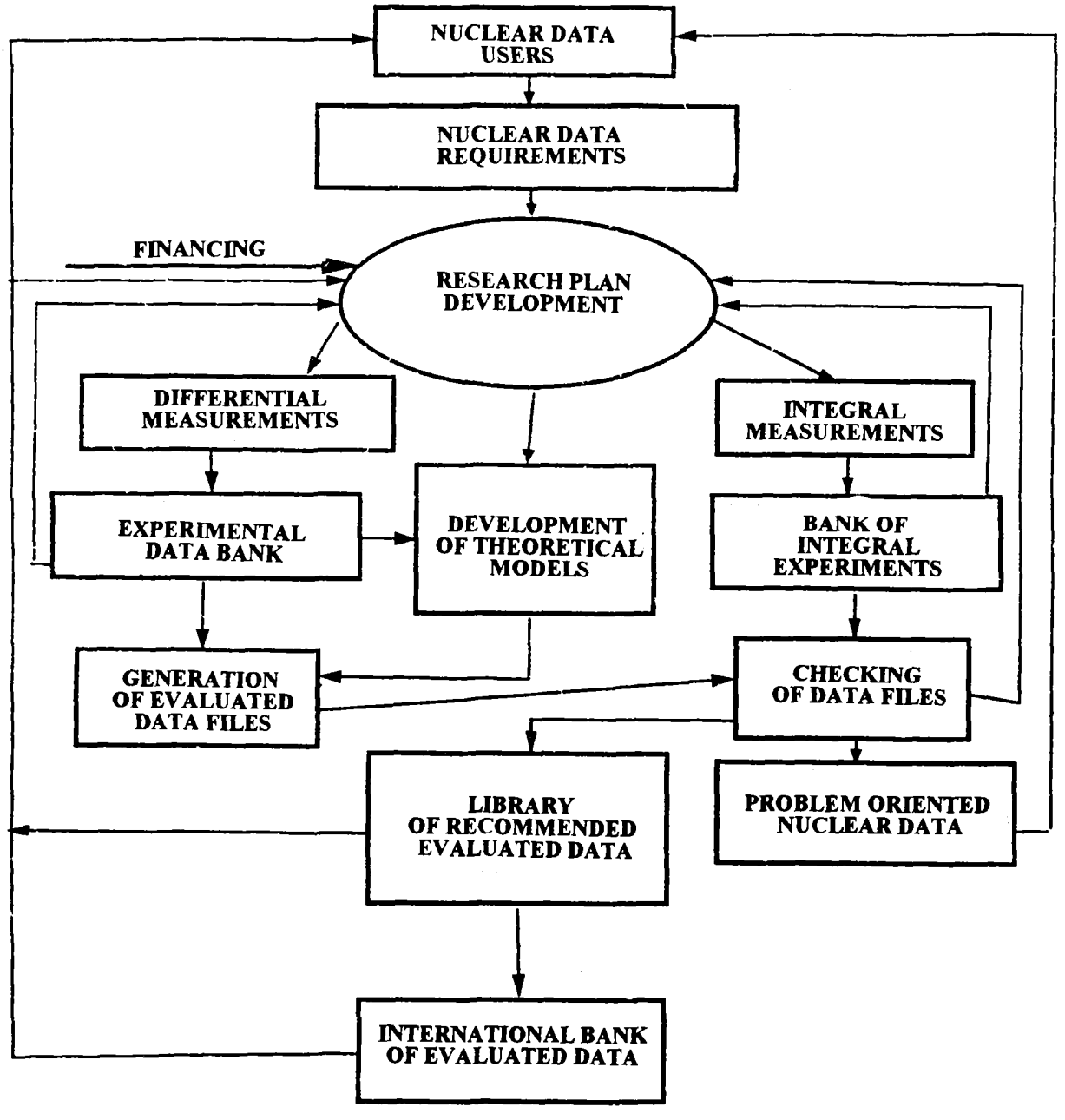

Figure 1. Structure of nuclear data activities

Currently, theoretical modeling of neutron interactions plays an important role in satisfying existing requirements of neutron data inasmuch as trying to satisfy the neutron data demand by means of their measurement alone is not practical because they cost too much and take too long to implement. Calculations using theoretical models give a realistic representation of the shape of the dependence; however, the values of calculated reaction cross sections are not accurate enough. In order to increase the accuracy of the calculational results, it is necessary to normalize the calculated curves to experimental data.

Thus, theoretical and experimental results complement each other: theory generates the shape of continuous curves, and the measurements provide accurate values of the data. At the same time data measurements yield a number of parameters (such as fission barrier characteristics, level densities, optical model parameters, and others), which enter into the theoretical model calculations.

An enormous amount of experimental and theoretical data has accumulated over the years. However, before they can be used in nuclear technology projects these data must go through an evaluation stage During that stage, scientist collect all of the available information for a given element or isotope, and perform a critical analysis of the experimental and theoretical data; they then select the best values and enter them into files of evaluated data in a standard international computer format. After the processed evaluated file had been subjected to a format and physical check, it is added to the domestic library of evaluated nuclear data.

Results of integral measurements are used in the testing of evaluated data and the substantiation of the calculational methods. As a rule, integral data are measured for a specific nuclear apparatus/installation, and are used in the formulation of problem oriented data. Differential data serve as the basic information in the formulation of such data. They are used in the extrapolation of calculation of apparatus/installation of various types, for the prediction of the operation of these installations as a function of time, for other energy generating applications and others.

In engineering calculations, the data information used is not in the form of evaluated data, but in the form of group constants derived from the evaluated data files. Group constants, which are used to described the interaction of neutrons with the environment, consist of cross sections averaged over rather broad energy intervals. Inasmuch as cross sections within such energy intervals may vary by a number of orders of magnitude, the effect of such averaging must take a number of factors into account (e.g., nuclide concentration in the medium, temperature). In order to take such dependencies into consideration, special selfshielding factors are introduced in the group constants. Supplementary group constants describe the neutron spectrum and the angular distribution of scattered neutrons.

In the process of group constants formulation, special features of the calculational system are taken into consideration to the fullest extent, in particular, the heterogeneous nature of the reactor core, the degree of burn-up, etc...

The BNAB-78 multi group set is an example of such a system of group constants actually being used ; it takes into account the totality of all experimental and theoretical information available at that time. A comparison of this data file with integral experiments, and an

international testing of the BNAB-78 constants has shown a high degree of reliability of this system. It was chosen as the standard for the calculation of fast neutron reactors.

A new version of the system of group constants, BNAB-90, was constructed from the domestic BROND-2 library of evaluated neutron data. This system allows for up to 300 energy groups and is universal in that it can be used to calculate all types of reactors, as well as their safety and radiation environment. The BNAB-90 group constants have been tested using international verification checks and have been compared with reactor experiments.

The Nuclear Data Centre (TsYaD) plays a large role in the provision of neutron data to users. It collects and compiles numerical and bibliographic data, carries out the computer servicing of data banks, participates in the development of evaluated data files, coordinates the overall nuclear data evaluation effort, supplies information to data users in accordance with their requirements, etc...

Because of Russian participation in international cooperation, the domestic files of experimental data include practically all published results of experimental data measurements worldwide (approximately 8000 in all). The library of evaluated data also includes practically all existing evaluated neutron data in the world .

International cooperation was implemented through the IAEA as well as by bilateral agreements. The international exchange of experimental and evaluated nuclear data, the participation in international nuclear data projects and the participation in joint experimental and theoretical studies - all of these facilitated considerably the accesses to nuclear data information in each of the participating countries. This situation created conditions for an unbiased evaluation of the quality of nuclear data, and allowed the utilization of data which were not available in our domestic files due to the state of experimental technology in our laboratories.

Our participation in this international cooperation was made possible only because the quality of the domestic neutron data was commensurate with the world standard, and because the quantity of data was comparable to that of the USA or Western Europe. This level was achieved in Russia because of the development of original measurement techniques, parallel measurement, in-depth analysis of experimental results and high level theoretical approaches in the representation of the mechanisms of neutron interaction with nuclei.

The extensive complex of works which has been included in this effort is a salient example of goal-oriented fundamental research performed to satisfy current and future needs in the national economy.

As a result of this experimental and theoretical research effort, the national economy now has a collection of neutron data which in its quality and quantity is commensurate to the body of nuclear data existing in the leading western countries.

II. Current Requirements of Nuclear Data

The development of nuclear technology is achieved by implementing traditional methods as well as by the implementation of techniques adopted from a large number of other spheres of activity. This development inevitably generates new nuclear data requirements. As a result, the nuclear data which have been generated in previous years, are continuously changing due to the enhancement in their quantity and quality. At the same time, because of the continuously changing situation in the field of nuclear data, their earlier requirements do not correspond to the need of the users. Furthermore, the achieved experimental and theoretical level in nuclear physics and the material investment in nuclear data research further enhanced this situation.

The greatest demand with respect to quantity of nuclear data and the associated degree of their accuracy are due to the growing requirements in the field of nuclear energy. In this field alone, nuclear data are needed for a number of applications:

- for the understanding of physical processes, which are at the basis of the operation of nuclear power reactors;
- for the calculation and optimization of reactor parameters;
- for the calculation of reactor safety and for the analysis of possible reactivity problems;
- for the prediction of fuel cycle problems , and problems in the transmutation of radioactive waste;
- for the development of alternative modes of nuclear energetics;
- for the evaluation of safe methods in the utilization of reactor grade and military grade plutonium.

Specific nuclear data requirements are also generated in connection with the development of thermonuclear installations, nuclear medicine and others.

Nuclear data must also be universal so that their applications not be limited, neither by their specific application nor by other characteristics of the nuclear installation or device being studied. This is especially important in the analysis of reactivity related accidents, when neutron spectra can change significantly from thermal to fast.

Nuclear data must have the quality of complexity so as to be able to be used in the calculation of neutron fields, gamma ray fields induced radioactivity and its evolution as a function of time, reactor kinetics, etc... The investigation of electro-nuclear installations requires taking into account reactions in energy ranges of up to a few GeV.

Nuclear data must be specified with a required accuracy because their uncertainties lead to ambiguities and inaccuracies in the prediction of reactor parameters. Large ambiguities, in their turn, lead to large increases in the cost of the project.

The necessary accuracy of nuclear data results from target accuracies determined by the consideration required for the prediction accuracy of one or the other nuclear reactor parameter determined by technological or economical considerations. For instance, the

requirements for the accuracy of the effective multiplication coefficient κ_{eff} or in the calculation of the critical mass, the possibilities to compensate the corresponding uncertainty without having to change the construction of the reactor or the composition of heat exchange elements is substantiated . The contribution to the overall uncertainty due to the inaccuracies of the nuclear data must not exceed the contribution from the uncertainty in the manufacturing of the heat exchange elements or any other technological uncertainties. In the formulation of nuclear data requirements for fast reactors, a significant role is played as well by specific contributing accuracies from: - the breeding of the nuclear fuel, -the change of the reactivity due to the burn up of the fuel and the accumulation of actinides and fission products, - the effect of the heterogeneous fuel distribution,- the irradiation of the nuclear materials,- the Doppler and sodium effects on reactivity,- the induced activity of the irradiated fuel, heat exchange medium and construction materials, and others.

Scientists at the FEI institute solved the problem in the determination of the nuclear data accuracy requirements on the basis of individual target accuracies. A mathematical formalism was developed to represent the formulation of requirements, which would guarantee the calculational accuracy of a number of reactor parameters taking into account microscopic and integral experiments, using specific assumptions regarding the correlational properties of experimental uncertainties,. The value of this exercise was that it identified those data whose measurement needed to be emphasized under conditions of limited resources.

It can be expected that the requirement for greater accuracies of nuclear data will increase with the development of nuclear technology. In particular, the improvement in the increase of the degree of burn up of the reactor fuel elements has inevitably raised the accuracy requirement for the capture cross sections of fission products and the quantitative prediction of the influence of inelastic scattering of neutrons by fission products in the reactor. In addition, there is an increase in the production of minor actinides which consequentially raises the accuracy requirement for their nuclear data. An increase in the role played by nuclear data used for the analysis of the reactor core can also be expected.

As nuclear data and their uncertainties may vary considerably, depending on the nature of their application, their requirements listed below are given separately for various fields of application.

1. The economical and safe energy production by operating nuclear power reactors

The contemporary concept of nuclear energy production is based on ecological acceptance and economical expediency. The full adherence to these premises significantly raises the competitive and profitable nature of such power stations. As a matter of fact, the construction parameters of many power stations have built-in safety factors which were determined on the basis of the accuracy of the underlying integral experiments and of the data errors achieved at the time of the design phase of the reactor. By using contemporary improved nuclear data for the reactor calculations, it was possible to improve the effectiveness and reliability of the power plant operation which is required for the required safety level.

In addition, the following considerations must be taken into account.

The recalculation of the required fuel enrichment and of the amount of burned up of absorbers permitting the optimization of the energy removal cycle, of fuel loading and reloading, thus avoiding an unnecessary overcautious fuel loading.

The determination of a maximum local energy production with a minimum degree of uncertainty opens the possibility to increase the overall energy yield of the reactor.

The improvement in the determination of the neutron fluence, in the number of displaced atoms and in the intensity of the release of gaseous products in the reactor vessel makes it possible to justifiably extend the life of a reactor.

The recalculation of the prediction of the burned up additives to guarantee the possibility to shut the reactor at any point in time taking the fuel burn up into account, the accumulation of the fission products and minor actinides can permit the extension of the lifetime of the reactor core and increase the overall energy production of the reactor.

The reevaluation of the kinetic parameters (the yield of delayed neutrons, the temperature and power coefficients, the lifetime of the reactor) will permit judging the safety level of the reactor with a higher degree of reliability.

The decrease in the uncertainty of the calculated determination of the radiation burden subjected by the reactor structure and the reactor personnel is an important consideration in the evaluation of the correspondence of these parameters as standards and for the reduction in the safety margins of the shielding.

The organization of the safe storage of the irradiated fuel requires an exact knowledge of the residual heat generation resulting from fission product and actinide decay, so as to be able to calculate its criticality in various geometric configurations to a high degree of reliability.

In order to improve the characteristics of nuclear reactors mentioned above, it is necessary to have a thorough knowledge of neutron and gamma ray cross sections, decay schemes and decay constants for a wide range of materials and radioactive nuclides. Fuel elements consist of isotopes of uranium, plutonium, of some of the heavier actinides as well as fission product nuclides. Structural materials, heat exchange materials, burn up absorbers and control element are made up of isotopes of zirconium, iron, hydrogen, oxygen, nitrogen, sodium, hafnium, boron, gadolinium, erbium, silver, indium.

At the present time, many neutron reaction cross sections and decay data are known to a satisfactory degree of accuracy; even so, in a number of cases, the quality of nuclear data are not adequate.

The evaluation of residual heat, caused by the decay of uranium-235 and/or plutonium-239 fission products, performed by different specialists differ in some time intervals by as much as 10%. These uncertainties have to be compensated by expensive margin increases in the emergency cooling systems, prolonging the holding and storage time of the spent fuel. These

uncertainties increase dramatically when dealing with fuel having a complex composition (such as recycling of burned up plutonium, and transmutation of actinides).

There is a need for new measurements of fission product yields and decay data which contribute significantly in given time intervals where differences can be observed. Also, there is a need to investigate the effect of a changing neutron spectrum on fission product yields and other contributions: delayed neutron fission, decay of minor actinides, transmutation of fission products, activation of structural materials. For an operating fuel lifetime of 60 Gw/t, approximately 50 isotopes are in need of being investigated.

The existing uncertainties in the fission and capture cross sections of the actinides lead to the situation that even considering the use of unrecycled uranium or plutonium fuel only, and for a high degree of burn up, it is necessary to make allowances of 10% to 15% for the transport of allowable quantities of fuel in a single container. Dealing with recycled fuel, or with fuel containing transmutated actinides, allowances are significantly higher. It is absolutely necessary to improve the quality of the neutron fission and capture cross sections, and reduce the fission product capture cross section uncertainties to 10%.

Average cross section data for the basic structural materials above 1 MeV are still not satisfied (the uncertainty of the scattering cross section for iron is as high as 20%). Average cross sections in the 1-5 MeV energy range are important in the evaluation of radiation damage of structural materials and to estimate the effect on reactivity. There is a need for new measurements having a total uncertainty of 5% for iron and 10% for chrome and nickel.

There are persistent discrepancies between calculation and measurement values of the moderator temperature coefficient. New measurements of the uranium-238 capture cross section and of the quantity η for uranium-235 have confirmed the incorrectness of earlier nuclear data. There is also a need for future measurements of the resonance shape of uranium-238 in the form of UO_2 at different temperatures.

In order to satisfy the existing discrepancies of nuclear data, there is a need for new measurements of the uranium-238 cross section and neutron inelastic scattering spectra, and of yields and delayed neutron spectra of uranium-238.

2. Advanced nuclear reactors

a) Reactors with an intrinsic internal safety factor

One of the primary objectives in the design of new reactors or in the modernization of existing operating reactors is to make these reactors intrinsically safe. Instead of implementing engineering methods to guarantee the safe operation of reactors, the method used relies on the inherent characteristics of nuclides and materials. This circumstance puts an especially high demand on a large number nuclear data.

One of the most important factors which determines the intrinsic internal safety of reactors is the Doppler temperature reactivty coefficient, which has a large enough negative value for

uranium-238 reactors. In reactors using thorium as the absorber of "extra" neutrons, this effect has the same sign and a value that is not any smaller; however the uncertainty of the calculated evaluation increases from 10% to 20-25%. In the case of transmutation reactors (as well as for blankets of electro-nuclear installations used for transmutation) where the excess neutrons in the chain reaction are absorbed by burned out actinides, the Doppler effect can be determined to a much smaller accuracy. The resulting error could in some cases be as high as 100% (that is, the Doppler coefficient could even have a positive value). This increase of the inaccuracy of the calculated prediction of the Doppler effect is evident.

b) Increase of the fuel burn up

Increased fuel burn up is another characteristic of new generation reactors. In order to avoid building in excess reactivity in the design of reactors, there is a need for more accurate nuclear data for the minor actinides and fission products. In particular, the need for the neutron inelastic scattering cross sections and for more accurate neutron radiation capture cross sections for these nuclides become more acute. Table 1 summarizes the required accuracies of nuclear data taking into account the development of reactor technology.

Table 1. Required accuracies of nuclear data (in %)

Nuclear Characteristics	Fuel materials	Minor actinides	Raw materials	Structural materials	Fission products
Fission c.s.	1	1	5	-	-
Number of secondary neutrons	0.5	1	3	-	-
Neutron capture c.s.	3	2	5	5	5
Neutron inelastic scattering c.s.	5-10	5	10	5	5
(n,2n) c.s.	5	5	10	10	10
Total c.s.	2	3	5	5	5
H, T, He output c.s.	15	15	20	15	15

c) Utilization of reactor grade and weapons grade plutonium

The accumulation of weapons grade plutonium and plutonium produced in power reactors and movable nuclear reactors presents a problem as far as its utilization is concerned. To deal with this problem, a number of projects have been initiated which are designed to utilize plutonium in tight lattice thermal reactors. This requires a meticulous study of the resonances in the cross sections of plutonium-239 and of some of its heavier isotopes noting also that there are noticeable discrepancies in the evaluated capture and fission cross sections in the resonance energy range. In thermal as well as in fast reactors, a small fraction of all fissions occur in that energy range and the above-noted discrepancy has a weak effect on the results. However, in the case of intermediate spectra which occur in tight lattice thermal reactors designed for

the burning of plutonium; these discrepancies become substantial and must be resolved.

In order to diminish the accumulation of new plutonium, it is necessary to minimize the quantity of uranium-238 present in the reactors. The replacement of the depleted uranium in fast reactors with structural materials (such as steel) will entail a sharp increase in the accuracy requirement of the data of iron, chrome and nickel which are the major components of steel.

Another method to burn plutonium-239 is already being considered in the design of fast neutron reactors where the uranium-238 is replaced with thorium-232. In such a scheme, the burning of plutonium-239 is accompanied by the production of uranium-233 which happens to be an effective fuel for thermal and fast reactors. Until recently, there has been no expressed need for nuclear data for isotopes of the thorium cycle, as a result there exist only part of the needed nuclear data which would be needed to solve this problem. There is therefore a need to create a nuclear data file for the thorium cycle. The accuracy requirements for these data would not have to be as severe as those given in Table 1 because this stage would consist of preliminary calculations for a feasibility study.

The following nuclides are being investigated: thorium-232, protoactinium-231,-232,-233 and uranium-232,-233-,234 in the thermal and resonance neutron energy range up to 20 MeV. The accuracies required are: 3-5 % for the fission cross section, 3-5 % for the radiative capture cross section and 20% for the inelastic scattering cross section.

d) Other technological innovations

There is a need to investigate the nuclear data uncertainties for nuclides which enter into fuels of novel composition (such as mixed fuel, fuels that contain actinides, fuels that are based on the uranium-thorium fuel cycle, and others), and into new heat exchange materials (such as lead, liquid salts and others). In particular, the error in the total cross section of lead in the energy range of a few hundreds of keV contributes considerably to the calculational uncertainty of critical characteristics of the lead breeder and to a significant degree to the criticality safety parameters of the target of the transmutation accelerator that is cooled by a lead coolant.

3. Transmutation of radioactive wastes

The assurance that the method chosen for the transmutation of long-lived radioactive wastes is reliable and accurate depends to a large extent on the quantity and quality of the nuclear data used in the calculational transmutation models.

Two basic transmutation models are investigated: waste burning reactors (~ 1.5 GeV) and proton accelerators coupled with a subcritical reactor which serves as a target or as a blanket.

a) Waste burning reactors.

The criticality safety of an installation used for the transmutation of actinides depends substantially on the effective fraction of delayed neutrons. The problem consists not only on the fact that the fraction and energy spectra of delayed neutrons for the minor actinides are

not known to a high enough accuracy, but also to the fact that the weight of delayed neutrons in systems using fuels that have a fission threshold, depends to a high degree on the inelastic scattering cross section of the actinides being transmuted for which there are only evaluations based on calculations. In this regard, it is absolutely necessary to improve the quality of the nuclear data for the minor actinides in the reactor energy range, considering that their abundance in the fuel can be as high as tens of percents. To satisfy these requirements, the following nuclear data are needed: delayed neutron yields, fission product yields for neptunium-237, americium-242,243 and for plutonium-238, cross sections and spectra of neutron inelastic scattering for neptunium-237, plutonium-238 and for the isotopes of americium, neutron fission and radiative capture cross sections for the curium isotopes.

Table 2 shows a one-group evaluation of cross section uncertainties of the fissile nuclides and their required accuracy in the fast neutron energy range. There is also a need for neutron fission and radiative capture cross sections for short-lived nuclides of uranium-237,239, neptunium-238,239, plutonium-243, americium-242,244 in the thermal neutron energy range.

Table 2. Cross section errors of the most important transuranium isotopes

Nuclide	$\Delta\sigma_{n,\gamma}$ %		$\Delta\sigma_{n,\gamma}$ %		$\Delta\sigma_{n,\gamma}$ %	
	achieved	required	achieved	required	achieved	required
Np-237	15	5	7	5	30	10
U-238	5	3	3	3	10	10
Pu-238	25	10	1-	5	40	20
Pu-239	6	4	3	3	20	15
Pu-240	10	5	5	3	20	15
Pu-241	15	5	5	3	20	25
Am-242m	30	10	15	5	40	20
Am-243	30	10	10	5	30	20
Cm-242	50	10	15	5	30	30
Cm-243	50	10	15	5	30	30
Cm-244	50	10	10	5	30	30

There are noticeable discrepancies among the evaluated neutron spectrum shape. It has been shown in the calculation of power reactors, that the actual lack of neutrons that can split uranium-238 may be compensated by increasing the uranium-238 cross section. However, in reactors that contain actinides which have a high fission threshold (such as plutonium-240 and neptunium-237), the effect of such compensation will not occur. As a result, there is a need to improve the accuracy of the fission spectra.

The uncertainties in the neutron radiative capture data of the actinides present a considerable problem, inasmuch as it is extremely difficult to measure the cross sections of these nuclides. Since the heavy actinides are generated by neutron capture, the error in the existing correlation in the capture cross section data leads to a corresponding increase in the uncertainties in the results obtained in the modeling of heavy actinide accumulation. One of the most important problem to be solved in this connection is the development of greatly improved theoretical models to calculate the radiative capture cross sections.

b) accelerators coupled with a subcritical reactor which serves as a target or as a blanket

Since the transmutation in this process takes place in a subcritical reactor which has a neutron flux similar to the spectrum of a waste burning reactor, or in a thermal neutron flux, all of the nuclear data noted above are required for this process as well. In addition there is a need for a tremendous amount of nuclear data in the energy range of 20 MeV to 1.5 GeV. A list of such required nuclear data would include neutron production differential cross section in the target materials, neutron and gamma ray emission cross sections, activation cross sections, and cross sections for heat production, radiation damage and gas generation in structural and shielding materials, and others.
The following materials could conceivably be included in such a system:

1. Actinides: ^{238}U, ^{237}Np, ^{238}Pu, ^{239}Pu, ^{240}Pu, ^{241}Pu, ^{242}Pu, ^{241}Am, ^{242m}Am, ^{243}Cm, ^{224}Cm, ^{244}Cm, ^{245}Cm, ^{246}Cm.
2. Target materials: Ta, W, Pb, Bi.
3. Structural, shielding, and heat transfer materials: H, C, N, O, Na, Mg, Al, Ar, K, Ca, Cr, Mn, Fe, Co, Ni, Cu, Zn, Zr.

The existing experimental data in the 20 MeV to 1.5 GeV energy range are not systematized, fragmented and require a thorough analysis and translated into the computer EXFOR format. The existing theoretical models and systematics to describe nuclear processes in the specified range cannot guarantee the required accuracy of the resulting calculations.

It is advisable to support and join the effort aimed at the generation of the more important nuclear data for the accelerator transmutation method on-going in other countries. This effort consists of:

1. establishing a nuclear data library of neutron and proton nuclear data for the mor important nuclides in the 20 - 200 MeV energy range;
2. establishing a library consisting of files of standard reference data up to 1.5 GeV; these data could be used in measurements as reference data or in testing and comparison of data generated from theoretical models and computer programs;
3. establishing a library of activation cross sections with energies up to 100 MeV for neutrons and protons.

4. Thermonuclear installations.

For the construction of thermonuclear installations, such as proposed the ITER project, there is a need for a comprehensive nuclear database for the calculation of reaction rates of

thermonuclear reactions in plasma; predict the neutron and gamma ray distribution in the component materials of a fusion reactor; to calculate the rate at which tritium is generated in the reactor blankets; to calculate the nuclear heating generated by the induced radioactivity and the release of decay heat; the prediction of the gas generation rate, and of the number of atomic displacements used as a predictor of radiation damage in the component materials.

The most likely materials to be used in the construction of the ITER reactor are:

- Structural materials: Fe, Cr, Mn, Ni, Ti, Al, V.
- Blanket materials for the generation of tritium and its cooling: ^{6}Li, ^{7}Li, Pb, H, O, Ga, Na, K.
- Neutron multiplier materials: Be, Pb.
- Magnetic materials and associated shielding materials: Fe, Cr, Ni, Cu, Nb, Sn, Ti, Al, V, W, ^{10}B, ^{11}B, C, H, O, Na, K, Li, Ga.
- First wall (adjacent to the plasma): Mo, Nb, W, Cu, Fe, Cr, Fe, Cr, Ni, Ti, Al, V.
- Biological shielding: B, C, O, Si, Ca, Ba.

Cross section data for all neutron reactions in the energy range from a few eV to 20 MeV are needed for all of these elements (approximately 30) and their stable isotopes.
Many of the data, in the 0 to 10 MeV energy range that have been produced for the development of fission reactors may be used for the calculational analysis of fission reactors.

Table 3 summarizes the acceptable nuclear data errors (in %) for various neutron interactions and fission reactor components.

Table 3. Cross section errors for thermonuclear reactors (given in %)

Neutron cross sections	Blanket ^{3}H production	Neutron multiplication	Magnets	First wall	Shielding
σ_{tot} 10 MeV	3	3	3	3	-
σ_{tot} > 10 MeV	3	3	3	3	3
Neutron emission (θ, E')	10	10	20	-	5
Neutron multip. (n,2n), (n,3n), etc	-	3	-	-	-
(n,n') (θ)	10	10	20	-	3

However, the energy range from 7-20 MeV is of specific importance to thermonuclear reactors, and here the data requirements are much more stringent and exacting than those that were generated to satisfy the demands of the fission reactor technology. Furthermore, data requirements for thermonuclear reactors include such reactions as(n,n'),(n,2n), (n,3n), (n,p), (n,np), (n,α), (n,nα) and the energy and angular distribution of the secondary particles

generated by these reactions. In order to evaluate the sensitivity of the calculated characteristics of thermonuclear reactors to the neutron cross section uncertainties it is absolutely necessary to have the covariance matrices for the basic elements of the more important materials.

The situation of the nuclear data at energies close to 14 MeV is generally satisfactory, however, in the energy interval of 7-14 MeV there is a need to improve the quality of the double differential neutron emission cross sections and of gamma ray emission.

The required accuracy of 3% has not been achieved for the 6Li(n,n'α)T reaction cross section. Data for the (n,xp), (n,xα) reactions are not complete and are not reliable. There is a need to initiate a measurement and theoretical project to investigate these reaction.

The achieved accuracies of dosimetry reactions is not the same for various reactions and varies from 2% to 30%. The uncertainties in the vicinity of the reaction threshold and in the energy range above 17 MeV increases the errors significantly between these boundaries. The problem with regard to the covariance matrices has not been resolved.

The condition of the activation reaction cross section data is not satisfactory. There are big gaps and discrepancies in all types of experimental activation cross sections, and the quality of most of the available data for these cross sections, obtained from calculational models which cannot guarantee acceptable qualities. Some of the half-life data are also not reliable.

Existing thermonuclear charged particle induced reaction data files, namely DATLIB (Austria), ECPL (USA) and ECPNDL (Russia), encompass all nuclear fusion reactions, pertinent to the (d,t) cycle.

The cross section errors range from 3% for the D(d,n) and D(d,p) reactions, 8% for the T(t,n) and 3He(d,p) reactions and 2% for the T(d,n) reaction, which satisfy the requirements for thermonuclear reactor applications.

5. Nuclear Medicine

The use of nuclear science and technology in medicine has reached significant proportions and is continuously growing in its application for the diagnosis and healing of a number of diseases, namely cancer, cardiovascular disorder, malfunctioning of the brain, and others, as well as in biochemical and physiological research.

The main nuclear medical tools are radio nuclides and irradiation therapy. The production of medical radioisotopes in operational accelerators and nuclear reactors is guaranteed by an adequate availability of nuclear data. However, in order to optimize a specific application of radioisotopes and at the same time minimizing deleterious side effects, it is necessary to have a more exact knowledge of nuclear interaction processes, especially in the cases of thick target applications. A large amount of deleterious radioactivity lowers the acceptable amount of the beneficial radionuclide that can be administered to the patient.

There is a need for more exact data for the decay schemes of the ^{90}Y, ^{186,187}Re and ^{153}Sm

isotopes which are used in internal radiotherapy, in order to be able to calculate the radiation dose received by the patient within an acceptable uncertainty.

The application of accelerators producing particles of a few MeV in the production of medical radioisotopes in spallation reactions or in other reactions require a knowledge of the cross section for the production of these isotopes.

Fast neutron reactors can be used for the production of some isotopes for internal therapy. Cross section data in the epithermal and fast neutrons for many of the interesting nuclides are either absent altogether or have high uncertainties. There is also a need for cross sections for the evaluation of the formation of reaction products in the same energy range.

Photon and positron tomography is used effectively in medical diagnostics, for the study of biochemical, physiological and pharmacological processes at the molecular level. Physiological preparations and medications used in these methods are labeled with short-lived radio nuclides which emit photons or positrons. Radio nuclides that have a dominant gamma ray line with an energy of 70-250 keV, such as ^{99m}Tc, ^{123}I and ^{201}Tl are used in photon diagnostics; nuclides such as ^{11}C, ^{13}N, ^{15}O and ^{18}F are used extensively in positron diagnostics. Cyclotrons that produce particles in the 10-30 MeV energy range are used in the production of the above-mentioned short-lived positron emitters. Cross section data for the production of these isotopes are available but many of them do not agree with each other.

There are some 100 prospective positron emitters for which there is a need of production cross section and decay schemes. Part of them are produced as impurities in the production of the above-mentioned positron emitters and present a problem in the dosimetry of positron tomography.

The possibility to produce short-lived isotopes for positron tomography with 2-4 MeV proton, deuteron or He3 beams, using tabletop cyclotrons, is currently investigated. Such accelerators are nowadays accessible for most clinics. In this energy range, the cross section data are either unavailable or in most cases discrepant.

In radiotherapy, geometrically focussed external beams of charged particles or neutrons are used. In order to optimize the design of the beam collimator and associated shielding, there is a need for the measurement and evaluation of the most important component elements, namely H, Be, C, N, O, Ca, Fe, Ni, Cu, Zr, W and Pb, in the 20-70 MeV energy range.

There is a need for a better description of nuclear interactions at higher energies, in particular for the effect of spallation in biological tissues and their influence on the dose absorbed by the patient. Data on the fragmentation process for the heavier ions are entirely absent.

One of the more promising approaches in selective radiotherapy is the use of beams of radioactive nuclides having a fixed E/m value. The main advantage in the use of such beams is that the region of the Breggov (?) peak is a sensitive function of the E/m value which makes it possible to create a beam with a high localization of the therapeutic effect. The cross section for the formation of such nuclides as a result of the bombardment of a target by the primary beam is absent as well. It is necessary to implement research in this area.

In order to predict the effect of neutron beams, it is necessary to perfect the existing data on the interaction of neutron with biological tissue at energies below 20 MeV. Such data do not exist in the 20 to 70 MeV range. Kerma factor data for C, O and other nuclides in the same energy range are also needed.

With regard to neutron capture therapy, which consists of a preliminary infusion of nuclides which have a high charged particle production cross section into the biological tissue, it is necessary to have detailed knowledge of the energy release mechanism at the end of the particle track.

It would be of great practical usefulness to publish a bulletin devoted to medical radioisotopes which would list yields of every type, pathlengths and differential energy loss in biological tissues.

6. Decommissioning of nuclear reactors

In a few years, a significant number of operating reactors will have completed their operating life, and will have to be removed from service and eventually disassembled.

The main question in this problem revolves around the knowledge on the activation of structural materials (the reactor vessel and the internal machinery) and of the concrete shield. These would be needed for the determination of the radiation dose load during the disassembly process, the cooling time prior to disassembly and the determination of the materials subject to isolation or burial. If the activation level of these materials will require their burial, and since we are concerned here with tens of thousands cubic meters of concrete and thousands of tons of metal, the problem assumes a very significant importance from a technological as well as economical point of view.

This problem must be taken into account during the design phase of new nuclear installations by using materials which have a low activation cross section or a short decay lifetime of the radioactive nuclides produced during irradiation. It must be recognised that the induced radioactivity results to some extent from alloy additives and impurities, whose contents are not always known to a high degree of accuracy. The main contributors to the long-lived activation levels of steel used in the VVER reactor vessel and to the serpentine based concrete used in the construction of the main reactor shield are:

-for steel : ^{55}Fe(2.6 yrs), ^{54}Mn(312 days), ^{60}Co(5.27 yrs), ^{59}Ni(7.5·105 yrs), ^{63}Ni(100 yrs) , ^{108m}Ag(418 yrs), ^{110m}Ag(249 days) ;

-for concrete: ^{41}Ca(1.03·105 yrs, ^{45}Ca(154 days), ^{55}Fe(2.68 yrs), ^{54}Mn(312days), ^{60}Co(5.27 yrs), ^{108m}Ag(418 yrs), ^{134}Cs(2.06 yrs), ^{151}Sm(90 yrs), ^{152}Eu(13.2yrs), ^{154}Eu(8.8 yrs).

These radionuclides are formed principally by neutron capture processes whose cross sections in the thermal and epithermal neutron energy ranges are well known. However, in the case of radionuclides formed in isomeric states (e.g., Eu and Ag), their isomeric ratios are not well determined even at energies of 14.8 MeV, and experimental measurements of the energy

depends of the cross section for the formation of isomers is absent. There is therefore a need for measurements of excitation functions for the above listed isomers in absorption reactions, as well as for an improvement in the accuracy of the neutron capture cross section of Ca and the rare earth elements such as Eu, Re, Hf, Ir, which enter into the composition of structural materials of fast neutron reactors to the same extent as for alloy admixtures and impurities.

7. Reference cross sections and standards.

Practically all countries have adopted the set of nuclear data standards recommended by the IAEA, published in report INDC(SEC)-101. This system of reference data is under continuous review and development.

In the 0-20 MeV energy range, the standards require an accuracy of 1%, however, the achieved accuracy is 2-3 %. The standards used above 20 MeV consist of the hydrogen scattering cross section and of the uranium-235 fission cross section. There is a need to develop theoretical models for these reactions and to initiate a search for other reactions that could be used as standards at high neutron and proton energies.

The following reactions could be considered as possible candidates to serve as additional standards at energies above 20 MeV:

- standard for scattering reaction
  C(n,n) and ^{4}He(n,n);
- standard for the capture and inelastic scattering reactions
  ^{12}C(n,n'γ), ^{56}Fe(n,n'γ), ^{208}Pb(n,n'γ), ^{7}Li(n,n'γ), ^{27}Al(n,γ), ^{54}Fe(n,2nγ);
- standard for the charged particle production reaction
  ^{12}C(n,p), ^{3}He(n,p), ^{3}He(n,d), ^{46}Ti(n,p), ^{51}V(n,xα);
- standard for the fission and fragmentation reactions
  ^{232}Th(n,f), ^{235}U(n,f), ^{209}Bi(n,f), ^{208}Pb(n,f).

8. Nuclear data for the microanalysis of materials.

For the nuclear, atomic and molecular microanalysis of gas production, structural and technological materials, it is necessary to measure nuclear cross sections for the interaction of thermal and fast neutrons as well as proton, deuterons and alpha particles with these materials in the enrgy range of 0.5 to 2.5 MeV. In addition, there is a need to measure and evaluate the production cross sections and yields of characteristic X-rays for intermediate and heavy nuclei, as well as to measure the yields of secondary ions as a result of the bombardment by atoms of hydrogen, helium, argon and others.

These data are needed for the specific physico-nuclear microanalysis of structural materials used in nuclear energy applications, and to resolve other problems:

- to develop the production technology and the machining of structural materials;
- to study the corrosion of steel in contact with liquid metal coolants;
- to study separate problems, such as resistance oPf materials to radiation;
- to investigate the effect of impurities on monocrystaline materials;

- to investigate single and multiple layer depositions in microelectronic applications (distribution in depth, presence of impurities, interactive diffusion, etc...).

9. Safeguarding of fissile materials.

The technology used in the non-destructive testing/control of the quantity and type or nuclear materials stored in any given intallation, is based on recording of spontaneous or induced radiation. In order to extract the pertinent information from the measured data, there is a need for a variety of highly accurate nuclear data.

Most often, the first indication of the presence of fissile material is the detection of fission neutron. In this regard, there is a need for data on the distribution of prompt neutrons generated by induced fission of ^{239,240,241}Pu, ^{235,238}U as a function of the excitation energy of the fissile nuclei, and spontaneous fission of ^{238,240,242}Pu, ^{238}U. There are also unsatisfied requests for halflives and delayed neutron yields for ^{234,236}U and ^{237}Np. There is a need for the improvement of information on the (α,n) reaction cross section and the spectra of neutrons generated as a result of the intrinsic α-radioactivity of fissile isotopes. In many cases, data and theoretical models for the calculation of various characteristics of the fission process already exist, and can be applied to the detection of fissile materials.

It is evident that there is a need for further research on the fission process; the more details are known about the fission process in individual nuclides, the better the possibilities for the identification of these nuclides.

10. Space applications

Space exploration programs foresee lengthy space misssions, such as the planned mission to Mars, which will expose electronic equipment and man to cosmic radiation. In addition, the most likely energy source on a space vehicle will be a nuclear reactor providing its own source of radiation.

The reduction of the radiation dose burden subjected by the cosmonauts at the expense of adequate shielding leads to large expenditures, and are deemed to be too expensive. In order to minimize shield weight, nuclear data used in calculations must be as accurate as possible. Furthemore, it is necessary to evaluate the effect of radiation on the electronics and on all on-board computers. The uncertainty of the calculated results, determined by nuclear data, must not exceed 15%.

In addition to the applications identifyed above, neutron data are of importance in other fields of activity, such as geophysics, geology, ecology, archeology, astrophysics and others. A large number of neutron reactions are used in applied geophysics in the determination and composition of rocks. Astrophysics uses nuclear data for the study of stellar, galactic and universe evolution. Neutron activation analysis is used extensively in industry. The use of this method is predicated on the exact knowledge of the neutron activation cross section, decay data, and the intensity and energies of the secondary radiation.

Depending on the type of reactions and nuclides entailed in various nuclear technological processes, acceptable neutron uncertainties are determined on the basis of developed formalisms and physical considerations in a broad neutron energy range.

III. Measurement of Nuclear Data Characterizing the Interaction of Neutrons with Nuclei

The measurement of nuclear data is the most expensive and time consuming activity of all nuclear data production. The severe demand that is put on the generation of reliable and highly accurate nuclear data used in the calculation of a multitude of various problems in nuclear technology has stimulated the creation of complex experimental installations for the precise measurements of the interaction of neutrons with nuclei.

The contemporary experimental facilities which provide powerful sources of neutrons consists of reactors and accelerators of various types. Linear electrostatic acelerators are widely used in the measurement of neutron data. Their high energy resolution (10^{-4} to 10^{-5}), their ability to vary the energy of the accelerated particles in a wide dynamic range, the favorable conditions for the organization of various pulse regimes and the simplicity of their use - all of these attributes have facilitated their effective utilization in the field of nuclear data measurements. Practically all types of neutron interactions important to nuclear technology have been measured on five FEI accelerators covering an energy range from a few tens of keV up to 20 MeV.

Pulsed neutron sources, having the ability to produce white spectra of fast neutrons, have substantially improved the arsenal of measurement methodology and has allowed to perform measurements simultaneously over wide energy intervals. Such a facility, based on an electron linear accelerator, has operated, among others, at the VNIIEhF laboratory. This includes also single pulsed neutron sources based on nuclear explosions. The use of a moderating target on pulsed neutron sources made it possible to obtain short enough pulses of slowed down neutrons so as to be able to measure resolved resonances (IAEh, PIYaF, RAN, LNF, OIYaI). Resonances at low energies were studied with the aid of mechanical selectors (choppers) installed on thermal neutron reactor beams. In particular, a series of measurements of the structure of low lying levels of heavy radiactive nuclei were performed on the SM-2 (NIIAR) reactor using an energy selector.

In fast reactors, the basic process takes place in the energy range where the most advanced of the contemporary spectrometers will not be able to resolve separate resonances. However, for practical purposes, there is no real need for a detailed resonance structure in this energy range; as a rule it is only necessary to know average characteristics of that structure which is needed to calculate the resonance selfshielding effect. The averaged information on the resonance structure can be obtained from experiments on the transmission of neutrons using a wide enough thickness range.

A list of the FEI facilities, used in the measurement of neutron data is given in Table 4.

Table 4. List of facilities used for the measurement of neutron interaction data

Facility	Neutron energy	Mode regime
Cascade accelerator KG-03	14 MeV	pulsed
Cascade accelerator KG-2.5	0.03-1.2; 3.5-6 MeV	continuous
Electrostatic accelerator EhG-2.5	0.03-1.2; 3.5-6 MeV	continuous
Electrostatic accelerator EhG-1	0.03-7.5 MeV	pulsed continuous
Charge exchange accelerator EhGP-10M	1.5 - 20 MeV	pulsed continuous
Cyclotron	9 MeV	pulsed
Reactor BR-10	fission spectrum thermal neutrons	continuous

A number of neutron transmission measurements were performed on the FEI electrostatic generators. The results of these experiments made it possible to take into account the resonance structure of the uranium-238 cross section, as well as those of structural materials, to a high degree of accuracy in the calculation of fast reactors. Experiments to study the neutron transmission function for nuclear fuel materials performed on the IBR reactor at the FEI laboratory were analyzed together with measurements performed at the LNF and OIYaI laboratory as part of a joint effort. The self-indication method which was used in these measurements made it possible to obtain explicit information on the resonance selfshielding of the capture and fission reactions. The temperature dependence of resonance selfshielding, which is needed for the calculation of the Doppler temperature coefficient of reactivity in reactors, was also studied.

The level of experimental techniques achieved at the present time is reflected in the cumulative error of the measured results, composed to a significant extent by various corrections. The neutron beam collimation, the average value of the initial neutron energy, the geometry of the experiment, the geometrical and physical characteristics of the sample being investigated, the effectiveness of the radiation detection, the intermittent and amplitudinal effects and the stability of the detection electronics, the reliability of the used standards, the degree to which the whole process is understood - all of these and many other factors, inevitably have an effect on the formulation of the total error of the final result of the measurement. The magnitude of the corrections is determined from measurements as well as from calculations. The problem involved in the determination of corrections occupies a significant place in the overall effort spent in obtaining experimental results. Thus, in the course of measuring the value of ν, there

arose the necessity to perform special studies to investigate the effect of counting fission events on the actual measurement of the value of ν. This correction could be as high as 5%, while the required accuracy of the measurement was 1%.

In the process of measuring the Np-237(n,2n) reaction cross section in order to determine the energy characteristics of neutrons generated in the gas target of the EhGP-10M accelerator, the nuclear magnetic resonance method as well as the time of flight method were used to determine the initial energy of the deuterons incident on the target. The energy and shape of the neutron energy distribution was controlled by allowing the transmission of neutrons through carbon in the vicinity of the 6.293±0.005 MeV resonance. A computer model to understand the process involved in the interaction of charged particles with the detailed characteristics of the target structure and the target gas was developed.

The following reactions cross sections that had different energy dependencies were used as reference: Al-27(n,α), U-238n,f), U-238(n,2n).

Because of the inevitability to have uncertainties associated with the measurement, due to effects of selfshielding, multiple scattering, energy loss in the sample, and others, it is highly desirable to use a large enough number of samples so as to obtain a high statistical measurement accuracy. In particular, the correction for multiple scattering in U-238 samples used for the measurement of the inelastic scattering cross section on the EhGP-10M accelerator, and for the measurement of the capture cross section using the time-of-flight method on the EhG-1 accelerator, have introduced an error of approximately 2 to 3 % to the final result. One major problem consists in the calibration of the energy dependence of the effectiveness of the neutron detectors because the resulting error is added directly to the error of the measured neutron spectrum shape. In most cases , errors caused by various corrections are combined as independent random values. One way to diminish the role of these errors is to use different methods of measurement to determine the same nuclear data quantity, inasmuch as different methods have different correction structures, or would have at least a different weight in the determination of compound error.

The development of measurement methods was accompanied by an increase in the accuracy and information content of the measured results, as well as by an increase in the number of non-correlated measurement of one and the same quantity in order to avoid the risk of having hidden errors stemming from separate methods.

The measurement of nuclear data has been separated into two categories: absolute and relative. The first category consists of precision data measurements of a relatively small group of reactions and nuclei that are used as standards. The nuclear data standards that have been recommended by the IAEA have been adopted in our country as well. These international standards were determined with the participation of Russian specialists. Thus, precise results for the $^{27}Al(n,\alpha)$ reaction cross section, the ^{197}Au neutron capture cross section, the ^{252}Cf spontaneous fission spectrum, and others were measured at the FEI laboratory. The measurements made at the FEI laboratory showed that the choice of the 27Al(n,α) reaction cross section to serve as a standard is not very successful because the energy dependence of this cross section is non-monotonic. When this reaction is used for the monitoring of the neutron flux there is a sharp increase in the requirement in the determination of the energy of

the incident neutrons and its dispersion. It was shown that the $^{58}Ni(n,p)$ reaction cross section which is used for dosimetry inside of reactors, undergoes fluctuations at neutron energies of 8 MeV.

The category of relative measurements consists of a much larger body of nuclides and reactions. Investigations include such diverse processes as nuclear fission, elastic and inelastic scattering of neutrons, radiative capture of neutrons, processes involving the multiple emission of neutrons and charged particles, and others, in the energy range from thermal to 20 MeV.

High accuracy demand are put on the nuclear data of the fuel and fertile isotopes which make up the reactor. The most important nuclear data quantities which make it possible to have a chain reactor are the fission cross section $\sigma_f(E_n)$ and the average number of neutron per fission ν-bar (E_n). A great deal of attention has been given to these quantities and to their dependence on neutron energy, not only because of their basic importance but also because of their use in special applications.

If it is possible to limit the study of ν-bar (E_n) to relatively small number of nuclides which determine the neutron balance in the reactor, namely the constituents of nuclear fuel (Pu-239, U-235, and U233) and the fertile isotopes (U-238 and Th-232), and those that are produced in significantly large quantities during reactor operations, namely (U-236, Np-237, Pu-240, Pu-241, Pu-242, Am-241 and Am-243), the demand for the fission cross section is substantially larger. The fission cross section is not only functional in determining the generation of neutrons but also in the burnup of nuclides in the reactor; among them are those that create the detrimental radiation environment as a result of the reprocessing of the fuel (U-232, Cm-242, -243,-244,-245,-246 and -247), and those that inadvertainly participate in their creation (Np-237, Pu-236, Am-241 and Am-243). In the process of studying a variety of applied problems related to the multiple capture or emission of neutrons (e.g., astrophysical processes, the kinetics of nuclear explosions, the synthesis of superheavy elements, etc...), there is a need for fission probability data for an even greater number of nuclides which have such a short lifetime that their direct measurement is not possible using contemporary technology.

Most of the relative measurements of ν-bar (E_n) were performed in the energy range that is of most practical interest, namely, $E_n = 0 - 7$ MeV. The neutron detectors used were He-3 counters embedded in a block of polyethylene, and the fissioning of nuclides was initiated by monoenergetic neutrons. Fission fragments were registered using pulsed ionization chambers, depending on the specific alpha activity of the target. A variety of data registration schemes were used, and special investigations were conducted to study the influence of various effects on the ν-bar (E_n) quantity being measured. On a number of occasions, stilbene detectors were used in the measurement of ν-bar(E_n).

Table 5. Lists the nuclides for which the energy dependence of ν-bar(E_n) has been measured. An example of the measured energy dependence of ν-bar is shown in Fig. 2. The results of measurements performed by Russian scientists contributed significantly to the international collection of the ν-bar(E_n) values. Basically, the requested accuracies of ν-bar(E_n) for the most important nuclides have been satisfied.

Table 5. Measurements of the energy dependence of ν-bar(E_n)

Nuclide	Measurement method	Average measurement accuracy in %	Energy range in MeV
Th-232	(see annotation 1 below)	1.0 - 2.0	1.48 - 3.27
Th-232	(see annotation 1 below)	0.8 - 1.2	1.35 - 6.35
U-233	A	0.5 - 0.8	Thermal - 4.9
U-235	(see annotation 2 below)	0.8 - 1.5	Thermal - 3.2
U-236	B	0.5 - 1.3	0.8 - 5.9
U-238	B	0.4 - 1.0	1.3 - 5.9
U-238	A	0.5 - 1.2	1.2 - 4.9
Np-237	B	0.5 - 0.7	1.0 - 5.9
Pu-239	A	0.5 - 0.8	Thermal - 4.9

Annotations: 1. Neutron detector: helium counter with polyethylene moderator; continuous registration of neutrons; Cf-252 used as standard.
2. Stilbene scintillation neutron detector

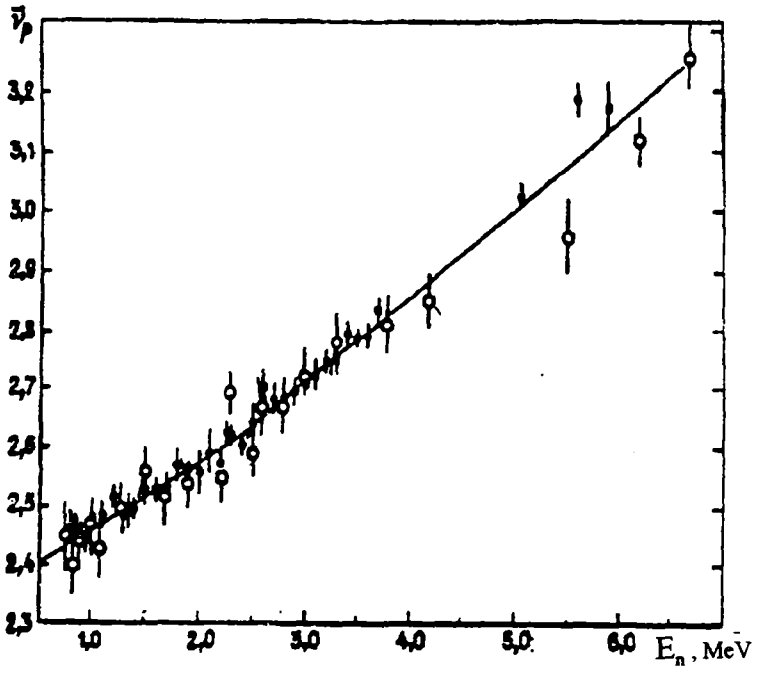

Figure 2. Energy dependence of ν-bar(E_n) for ^{236}U.
Closed circles - FEI results
Open circles - Sweden results
Curve - FEI evaluation

The comprehensive collection of relative fission cross section measurements, including some 15 nuclides, ranging from thorium-232 to californium-249, and ranging in neutron energies up to 10 MeV, have been measured at the FEI laboratory on electrostatic generators. The standards used in these measurements were uranium-235 (for most nuclides) and plutonium-239. The measurements were planned and executed in such a way so as to be able to plot the relative shape of the curve in its entirety and use it in the evaluation of the data.

Considerable attention was given to the accuracy of the normalization of the energy dependence of the cross section, and to the various methods used in comparing the number of nuclei in the measured target with that of the standard (e.g., method of weighing in a beam of thermal neutrons, the method of isotope additives, alpha spectrometry), as well as taking various corrections and backgrounds into consideration.

Up to 7 MeV of these measurements, solid tritium and deuterium targets were used in an uninterrupted beam of protons and deuterons. In order to eliminate various sources of spurious neutrons, which increases with energy, a pulsed synchronization methodology was developed; this consisted of an accelerator (operating in a pulsed mode in a nanosecond time frame) that generated a neutron beam whose energy was selected using the time-of-flight method and a gaseous deuterium target. This technique made it possible to widen the energy range up to 10 MeV, as well as to double and sharpen the measurements in the 5.5 - 7 MeV neutron energy range. As a result, the precision of the measured cross section ratios, typical for the contemporary world standard, was achieved in the entire neutron energy range: namely 1.0 - 1.5 % for the basic isotopes, and up to 3 - 4 % for the other nuclides for which the requirements are considerably lower.

Figure 3 shows an example of the measured fission cross section results for a number of nuclides which reflects the state of the data. Figure 4 shows the results for uranium-232, which illustrates the quality of the achieved accuracy for an experimentally complicated measurement. The evaluations of the fission cross sections of the plutonium-239 and -242 isotopes performed in our country rely mainly on the FEI measurement results of $\sigma_f(E_n)$. These evaluations are included in the IAEA library of nuclear data, and were used in the US evaluations.

The acquisition of similar experimental information for the isotopes of curium and for heavier isotopes, in particular for even-even nuclei, is severely impeded because of their high alpha decay and spontaneous fission activities. The method of pulsed synchronization on electrostatic accelerators was used to suppress the existing background in the measurements of the energy dependence of the fission cross sections of curium-244,-246,-248. Table 6 lists the nuclides whose fission cross sections were measured at the FEI laboratory.

Contemporary spectroscopy of secondary neutrons (in fission reactions and neutron inelastic scattering) is based on a complex detection apparatus operating in a nanosecond time frame and pulsed sources of monoenergetic neutrons with bursts of short duration. The amount of experimental nuclear data that describe angular and energy distributions of secondary neutrons resulting from neutron spectroscopy research, can be counted in the thousands.

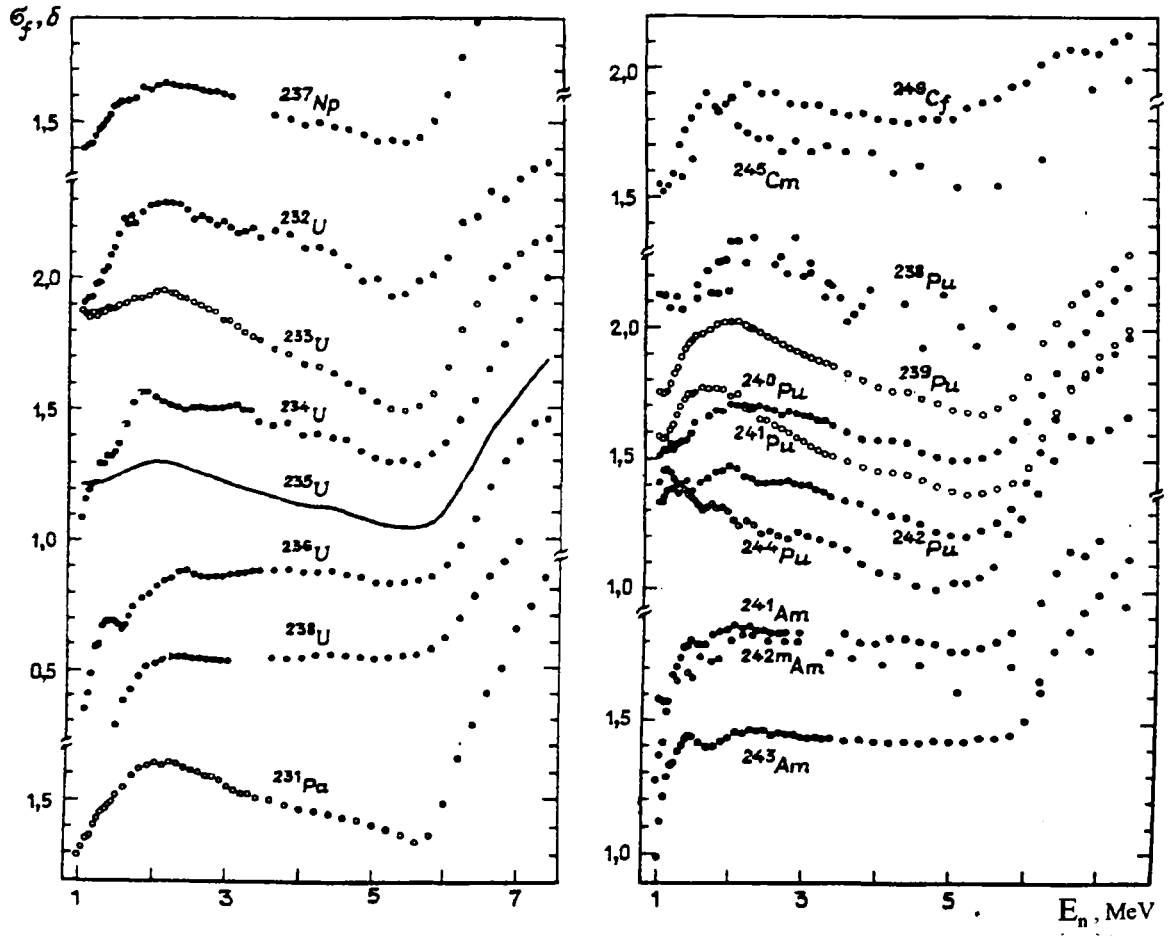

Figure 3. Fission cross-sections of transuranium nuclides measured at the FEI laboratory, of ^{244}Pu measured in the USA; evaluation of ^{235}U from ENDF/B-5.

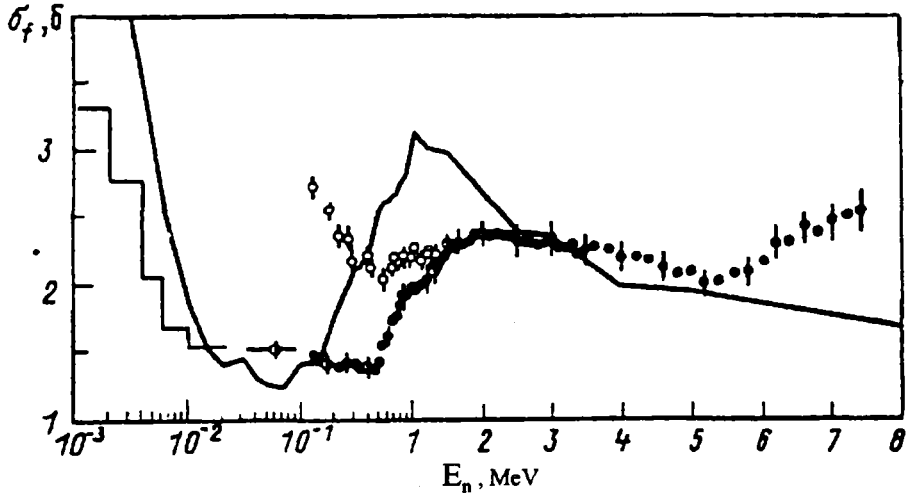

Figure 4. ^{232}U fission cross-section . Black dots - FEI, white dots - RNTs KI, histogram - USA, solid curve - ENDF/B-5 evaluation.

Table 6. Fast neutron fission cross section measurements

	Measurement methods	
Nuclides	A (see below)	B (see below)
Th-232	+	+
Pa-231	+	
U-232, -233	+	
U-234,-236,-238	+	+
Np-237	+	+
Pu-238,-239,-240,-241,-242	+	
Am-241,-242m	+	
Am-243	+	+
Cm-245,-247	+	
Cf-249	+	

A. Accelerators EhG-1 and KG-2.5, double ionization chamber, track detectors, measurement accuracy: 1 - 2 %, energy range: 1 - 7 MeV.
B. Accelerator EhGP-10M, pulsed synchronization, fast ionization chamber; measurement accuracy 2 - 3 %, energy range: 4 - 10 MeV.

Table 7. Parameters of the FEI spectrometers

Parameters	KG-0.3	Cyclotron	EhG-1	EhGP-10M
Pulse current, mA	2	1	1.5	0.6
Repeat frequency, MHZ	2	2.9	1.2	5
Pulse duration, ns	2.5	2.5	2.0	1.0
Flight length, m	2 and 7	2.84	2	2
Neutron energy, MeV	2.5 and 14	9.1	0.1 - 6	1.5 - 20

Four neutron spectrometers based on the time-of-flight method for neutrons generated by the KG-0.3 neutron generator, the cyclotron, the EhG-1 accelerator and the tandem generator EhGP-10M, were built at the FEI laboratory for the study of the (n,n'), (n,2n), (n,xn) reactions and of the neutron fission spectrum in a wide energy range. This array of instrumentation made it possible to measure double differential cross sections for the above named reactions in the neutron energy range of 1.5 to 20 MeV with high enough accuracies to satisfy practical requirements. This resulting body of information also served to improve the

knowledge of nuclear structure and the mechanism of nuclear reactions. The parameters of the spectrometers are listed in Table 7.

By increasing the flight path of the KG-0.3 spectrometer to 7 meters and by taking the neutron detectors beyond the confines of the target room, allowed for a significant reduction of the background, improve the total resolution to 0.6 ns/m, and made it possible to measure the hard part of the neutron spectrum from the (n.n') reaction with a distinct separation from the elastic scattering neutron peak.

The use of the time-of-flight neutron spectrometer on the 1.5 m FEI cyclotron made it possible to perform spectrometrical measurements for an initial neutron energy of 10 MeV. This arrangement made it possible to eliminate substantial difficulties stemming from the high repeat frequency of ion clusters (11.6 MHZ), a low modulating frequency of the beam and a substantial reduction of the background resulting from the (p.n.) reactions occurring in structural materials. During normal operation of the spectrometer systems to stabilize the resonance frequency, to eliminate the asymmetrical potential of the cyclotron dee, to automatically control the frequency and to lower the ion cluster repeat frequency are used. .

The use of the neutron time-of-flight spectrometer with the EhGP-10M accelerator made it possible to increase the energy range from 1.5 MeV to 20 MeV: from 1.5 to 9 MeV in the case of using a tritium gas target and the T(p.n.) reaction; up to 12 MeV when using a deuterium gas target and the (d-d) reaction; up to 20 MeV when using a tritium gas target and the T(d,n) reaction. The use of the neutron spectrometer with the EhG-1 accelerator it was possible to lower the energy of the primary neutrons to 0.01 MeV.

Double differential neutron inelastic cross sections and neutron emission in those cases when the initial neutron energy allowed other neutron emission reactions, namely (n,2n), (n,np) and (n,f) to take place, were measured using the FEI spectrometers. Double differential cross sections were measured as a rule at five scattering angles (30° - 150°). The lower energy detection limit for secondary neutron was set at 0.2 MeV.

These measurements embraced a large number of nuclides (e.g., from Li-6 to Np-237). The choice of nuclides to be measured was based not only on practical requirements defined by the designers of nuclear power installations (e.g., fast neutron reactors, fusion reactors), but also on the requirements in the field of nuclear defense. This concerted measurement program resulted in a large body of information consisting of some hundred thousands of individual data points which contained practical information as well as data needed for the development of theoretical models of nuclides and nuclear reactions. Many of the cross section measurement were preliminary, others were significantly accurate. In order to improve the accuracy of the measured data, a considerable effort was devoted to the study of the energy dependence of the neutron detector effectiveness. This dependence was determined using different experimental means: by using known double differential cross sections of the T(p.n.) reaction, the standard Cf-252 neutron fission spectrum, the hydrogen (n,p) cross section and the cross sections of reactions used as standards. The experimentally determined effectiveness of neutron detectors was useful not only in the study of nuclear processes, but also in the study of the influence of electronic instrumentation and the geometry (factors that are normally not taken into account in the determination of the effectiveness).

A number of characteristics of the studied spectra which were identified in this process required the development of new approaches for their understanding. Among such observed characteristics was a significant spectrum hardening and an asymmetry (with respect to Θ=90°) in the distribution of emitted neutrons. Table 8 lists the nuclides which were used in the spectrometric neutron emission studies.

In some cases a number of measurements had to be performed to solve one specific problem. An example of such a case was to study the accumulation of uranium-232 and plutonium-238 in fast reactors from the initial uranium-238 fuel. This study was performed with the cooperation of three laboratory (FEI, RI, and the Debrecen University). The study included some of the most important problems concerning the chain of reactions in reactor neutron energy range, taking into account the loss or absorption of a neutron by a nuclide or the disappearance of a nuclide as a result of its fissioning. The measurements for neptunium were the first to perform systematic investigations of this reaction in the lower energy range which made it possible to predict the cross section in the full energy range.

The method devised for the measurement of the (n,2n) reaction cross section for plutonium-237 was also applied to thorium-232, for which data did not exist. For the case of non-fissionable nuclides, particularly those for which the activation method is not practical, a method to determine the (n,2n) was developed on the basis of the analysis of the spectrometric information, information derived from the spectrum determination and the second evaporation cascade. When it was possible, the data obtained by this method were compared with results obtained using the activation method and the method of neutron detection using a large scintillation tank. The agreement of the results from the three methods was satisfactory. This method was used to measure the (n,2n) reaction cross sections for titanium, vanadium, chrome, iron, cobalt, nickel, copper, zinc, ittrium and niobium.

The need to measure the neutron fission spectra is substantiated by the fact that the theoretically calculated spectra are deficient. In order to be able to predict accurately the variation in the neutron emission spectra of fissile nuclei as a function of the energy of the primary neutrons, it is necessary to know the corresponding energy dependence of the components that make up the spectrum.

The initial efforts at the FEI laboratory were concentrated on precise measurements of the neutron induced fission spectrum of uranium-238 as a function of neutron energy (E_o = 2.47, 6.01, 7.02, 8.01, 8.94 and 14.3 MeV. Subsequently, the following nuclides were also measured: Th-232, U-235, Np-237, Pu-239 (see Table 9). Figure 5 shows the variation of the effective Maxwellian temperature T as a function of the initial neutron energy. One of the effects that must be noted, is the change in the hardness of the spectrum in the region of the reaction threshold (n,n'f) caused by the appearance of low energy neutrons that are emitted prior to the fission event. Another effect is the lowering of the excitation energy of the fissioning uranium-238 following the preliminary emission of the neutron. This effect was first observed experimentally.

A number of threshold reactions, including those that lead to the generation of hydrogen, tritium, and helium have been studied extensively at 14 MeV. 14 MeV generators are widely available in scientific laboratories and research institutes. The results of experimental

Table 8. Nuclides used in the spectrometric analysis of neutron interactions

Nuclide	Initial E_n
Li-6,-7	8.9
Be	14.3
C	9.2, 21
Mg-24	1 - 7
Al-27	9.2
Ti	1-7, 14.36
Cr-50,-52,-54	1-7, 9.1, 14.36
Fe-54,-56	1-7, 9.1, 14.36
Co	4.9 - 9.1, 14.36
Ni-58,-60,-62,-64	1-7, 9.1, -14.36
Cu	9.1, 14.36
Zn-64,-66,-68	1-7, 14.36
Se-76,-78,-80,-82	1-7
Y-89	4.86 - 9.1, 14.36

Nuclide	Initial E_n
Zr	14.36
Nb-93	5.23 - 9.1, 14.36
Mo-92,-94	1-7, 5.23-8.5, 14.3
Cd	14.36
In-113,-115	5.34-8.53, 14.36
Sn	9.1, 14.36
Ta	5-8.5, 14.36
W	14.36
Pb	14.36
Bi	5-9.1
Th	1.5, 4.9, 6
U-235	4.9, 6
U-238	2.47, 6.9, 14.3
Np-237	14.3

Annotation: if a number of mass numbers are given for the name of the element, the measurements were made with the isotopes having a corresponding mass number.

measurements performed on these generators are used as reference points in theoretical descriptions of the energy dependence of the corresponding cross sections. The EhGP-10M accelerator at the FEI laboratory, can serve as a source of neutrons ranging in energy from 2 to 20 MeV, and has been used extensively to study these threshold reactions over a wide energy range. The EhG-1 accelerator with the KG-2.5 grid ionization chamber were used to study the Ni-58 (n,α) reaction in the 3.5 to 7 MeV range, Ar-36 in the 3.5 to 5.5 MeV range and O-17 in the 0.3 to 1.1 energy range. The techniques used to measure the neutron radiative capture reactions require a complex and precise technology. A large number of neutron radiative capture cross sections for fissile and fission product nuclides have been measured at the FEI laboratory using the time-of-flight method on the electrostatic accelerator (see Table 10). Neutron capture events were recorded by registering the prompt gamma rays with a total absorption detector. The neutron flux was measured relative to the $^{6}Li(n,\alpha)$ and $^{10}B(n,\alpha\gamma)$ reactions. The normalization of the radiative capture cross sections was performed using the saturated resonance and amplitude weighting methods.

This method was also used to measure the total cross sections. The capture to fission ratio quantity, alpha, which plays a very important role in the evaluation of the fuel breeding coefficient in fast reactors, was measured in the 10 to 1100 keV energy range for the most important fuel isotopes, namely uranium-235 and plutonium-239.

Table 9. Measured neutron fission spectra

Nuclide	E_n initial (MeV)	Energy range
Th-232	1.5	2.6 - 8.0
Th-232 *	7.3	2.0 -10.0
Th-232	14.6	0.35 - 12.0
Th-232	17.7	0.35 - 14.0
U-235	0.5	0,3 - 12.0
U-235	1.5	2.0 - 10.0
U-235	5.0	0.3 - 13.0
Np-237	4.9	0.3 - 12.0
Np-237 *	7.8	1.5 - 12.0
Pu-239	1.5	2.0 - 10.0
Pu-239 *	7.5	0.6 - 6.3

Nuclide	E_n initial (MeV)	Energy range
Pu-239 *	10.0	0.6 - 6.3
U-238	2.47	0.3 - 10.0
U-238	6.01	0.3 - 10.0
U-238	7.02	0.3 - 10.0
U-238	8.01	0.3 - 10.0
U-238	8.94	0.3 - 10.0
U-238	13.2	0.3 - 11.0
U-238	14.3	0.3 - 10.0
U-238	16.0	0.3 - 11.0
U-238	17.7	0.3 - 13.0
-	-	-

Annotation: * these measurements were performed in cooperation with the Dresden Technical University

Investigations using the spectrometers of the IBR-30 were executed in the resonance energy range by scientists from the LNF OIYaI institute. The measurement of the average lead cross section was performed on the neutron slowing down spectrometer by scientists from the IYaI RAN and FEI institutes. The activation method was also widely used in the measurement of the radiative capture cross section for a number of fissile, structural and fission product nuclides (see Table 11). The registration of the gamma ray count was measured using germanium-lithium detectors in conjunction with (β-γ) coincidences. The neutron flux was measured using the hydrogen scattering cross section and other standards cross sections. Figure 6 shows the experimental results of the U-236 neutron radiative capture cross section measurements performed at the FEI and other laboratories. It can be seen that the evaluation of the capture cross section used in the USA, which is based on earlier US measurements, falls higher than the contemporary values by about 40%.

Neutron radiative capture cross section measurement results of much higher precision (1% to 2%) have been obtained in the last few years in joint efforts of the GNTs RF, FEI and FZKA Karlsruhe, Germany) laboratories. These measurements were made using the time-of-flight spectrometer method on the basis of an electrostatic accelerator in the neutron energy range of 3 to 225 keV and a (4π-BaF_2) detector for the lead-114,-118,-120, gadolinium-152,-154,-158 and neodinium-142,-146, and -148 isotopes.

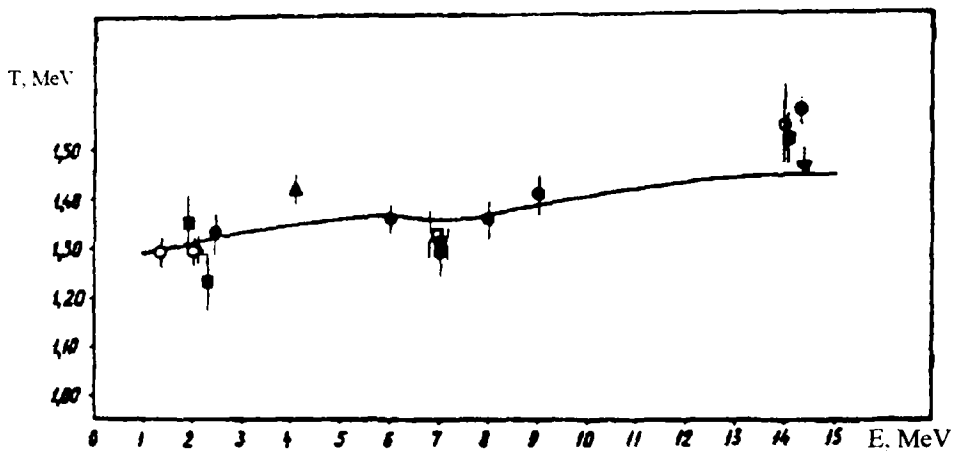

Figure 5. Depndence of the ^{238}U prompt neutron fission Maxwellian distribution T parameter as a function of initial neutron energy. Black dots - experimental FEI results, white dots - swedish results, solid curve - FEI calculation.

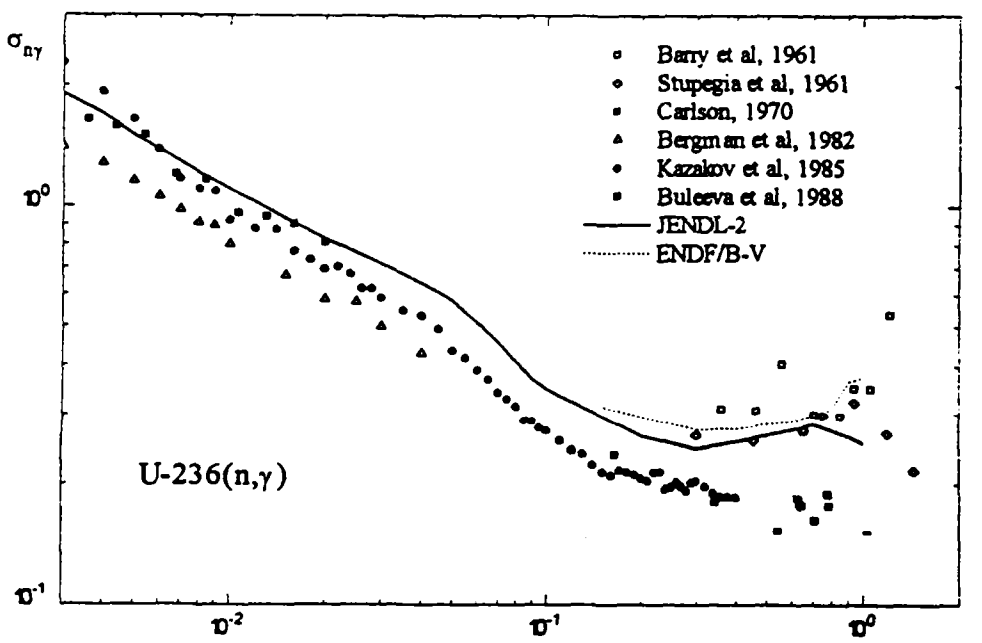

Figure 6. ^{236}U neutron radiative cross-section. Black dots - FEI measurements by time-of-flight method.

Table 10. Radiative capture cross sections measured by the time-of-flight method

Nuclides	E_n (keV)
Ru-103	5 - 400
Ag-107, -109	4 - 400
Sn-112,-114,-120,-122,-124	20 - 460
Cs-133	5 - 400
Nd-143,-145	4 - 400
Nd-142,-144,-146, -148,-150	7 - 350
Sm-147,-152	5 - 400
Eu-151,-153	5 - 400
Gd-154,-157	5 - 70
Gd-158,-160	5 - 400
Tb-159	5 - 400
-	-

Nuclides	E_n (keV)
Dy-160,-164	5 - 400
Ho-165	5 - 400
Eu-166,-168,-170	5 - 70
Yb-170,-172	5 - 400
Yb-173,-174,-176	16 - 450
Lu-175	5 - 400
Hf-176,-179	16 - 450
Ta-181	5 - 400
W-180,-182,-184,-186	5 - 400
Os-187	5 - 400
Au-197	4 - 460
U-236,-238	4 - 460

Thus, a whole array of research tools and techniques, developed for neutrons, gamma rays and charged particle spectrometry, were created in order to be able to measure nuclear data which characterize the interaction of neutrons with stable and radioactive nuclides. In pursuing this task, practically all important types of interactions of neutrons with nuclei had to be taken into account. Mathematical models of neutron physics were developed in order to understand the ongoing processes in targets and samples, and to identify side effects which distorted the measurement results.

Experimental results obtained in our country (whose total volume is measured in hundreds of thousands of individual values, and represents approximately 15% of the totality of the nuclear data existing in the world) are characterized by a high degree of reliability which substantiates their importance in their contribution to the international nuclear data exchange system.

IV. Experimental and Theoretical Investigations of the Mechanisms of Neutron Interactions with Nuclides

In order to use the potential of the nuclear processes in industry most effectively , it is necessary to have the means to be able to perform a comparative analysis of the characteristics

of the most varied nuclear reactions and spontaneous decay data for all of the nuclides existing in nature as well as for the enormous number of artificially produced nuclides. To obtain such a large body of nuclear data information from experiments in the foreseeable future is impossible. Aside from that, there is a large number of important short-lived nuclides whose properties are not possible to measure given the contemporary experimental technology. The only way to acquire such information is by means of theoretical representation. Therefore, one of the most important task facing physicists today is the development of theoretical models that simulate the processes of neutron interaction with nuclide, providing the required reliability to calculational results. Without a thorough understanding of nuclear physical processes it is not even possible to perform precision measurements of nuclear data. This is stipulated by the necessity to correctly taking into consideration various specific properties of the investigated phenomena which are reflected in the results of the measurement.

To understand the nuclear reaction mechanism is the first step in the analysis of neutron cross sections. Only after having acquired a sufficiently complete understanding of the mechanism, is it possible to effectively devise a theoretical model for the simulation of a large number of nuclear data.

Table 11. Radiative capture cross section measured using the activation method

Isotope	E_n (MeV)	Isotope	E_n (MeV)
Al-27	0.01 - 3.5	Sb-121,-123	0.01 - 3.5
Cl-37	0.01 - 3.5	Te-128,-130	0.01 - 3.5
Mn-55	0.01 - 3.5	Cs-133	0.01 - 3.5
Cu-65	0.01 - 3.5	Ba-138	0.01 - 3.5
Zn-68	0.01 - 3.5	W-186	0.01 - 3.5
Ga-69,-71	0.01 - 3.5	Os-192	0.01 - 3.5
Ge-74,-76	0.01 - 3.5	Ir-192	0.01 - 3.5
Se-80	0.01 - 3.5	Au-197	0.166 - 1.0
Rb-87	0.01 - 3.5	Tl-205	0.01 - 3.5
Nb-93	0.01 - 3.5	Th-232	th., 0.166 - 1.0
Y-89	0.01 - 3.5	U-236	th., 0.166 - 1.0
Mo-98,-100	0.01 - 3.5	U-238	0.024-7.0; 15 - 20
Sn-116,-122,-124	0.01 - 3.5	Np-237	0.03 - 2.5

A concerted effort to investigate the contribution of direct and compound (statistical) mechanisms to the scattering of neutrons on low-lying levels of light and intermediate nuclides was mounted by FEI in cooperation with the Ukrainian Academy of Sciences Institute of Nuclear Research and the Dresden Technical University. The analysis of observed total neutron cross sections and of elastic and inelastic differential cross sections resulted in the determination of individual and universal sets of neutron optical potential parameters. It was shown that by taking the direct transitions into account, the value of the integral cross section of neutron scattering by the compound nucleus is lowered, and at the same time alters the value of the neutron adhesion coefficient correspondingly. Consequently, it makes it possible to obtain a consistent description of these changes in the framework of the generalized optical model. A typical example of a theoretical description of existing experimental data for ^{80}Se is shown in Figure 7. The calculated parameters of the generalized optical potential give a good representation of the basic characteristics of the energy dependence and isotopical variations of the neutron cross sections, and they can be used successfully in most practical applications of the optical model.

The time-of-flight spectrometers installed on the four different accelerators at the FEI laboratory made it possible to implement a complex program of experimental investigations of equilibrium and non-equilibrium processes including the (n,n'), (p.n.), (α,n) and (n,2n) reactions for a large number of nuclides and over a wide range of excitation energies. As a result of this research project input parameters to the non-equilibrium processes and their dependence on energy and type of incident particles were derived. A salient example of how the variety of input parameters to describe non-equilibrium processes in inelastic scattering and charge exchange reactions can yield neutron spectra from the In-133(n,n') and Cd-113(p.n.) reactions, in which the same compound nucleus is formed for the same excitation energy, is shown in Figure 8. A substantial difference in the hard part of the spectrum can be seen clearly from the experimental data, namely, a significant contributions from the direct processes in the case of the (n.n') reaction, and a practical match of the spectra at lower neutron energies (i.e., large excitation energies), where the contribution of direct processes is negligibly small. As one would expect, these difference can also be seen in the angular distribution of the emitted neutrons. On the basis of a combined analysis of the double differential (n,n') and (p.n.) reaction cross sections, a change was noted in the contributions of the equilibrium and non-equilibrium reaction mechanisms for different energies of the incident particles for a large number of intermediate and heavy nuclides.

The negligibly small contribution of direct processes in the (p.n.) reactions for proton energies up to approximately 12 MeV makes it possible to use these reactions for the analysis of the equilibrium component of neutron spectra, and in part to obtain information on the level density of excited nuclei. If one would normalize the statistical description of the neutron spectra over the region of excitation of known discrete levels, then it would be possible to determine, concurrently with the level density energy changes, their absolute values as well. An analysis of the (p.n.) reaction spectra for incident proton energies of 5 MeV to 11 MeV for 27 nuclides was performed at the FEI laboratory. The resulting level density data were discussed extensively in the framework of the IAEA Coordinated Research Program and at the international meeting on level densities held in Bologna in 1989, were highly praised on both occasions.

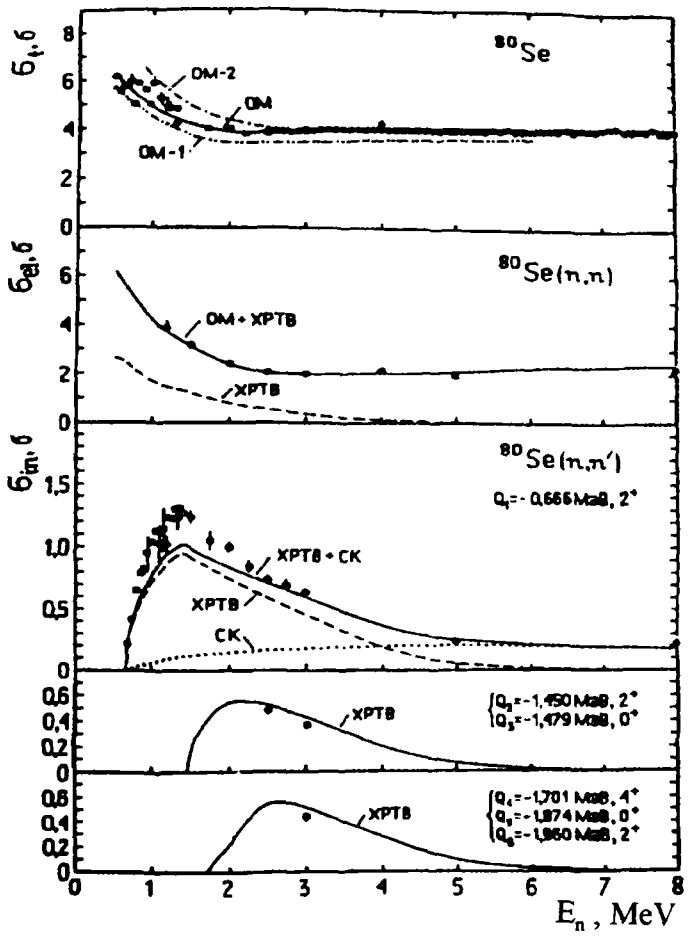

Figure 7. Energy dependenceof the total and integralelastic and inelastic scattering cross-sections for 0.5 to 8.0MeV neutrons. The solid curves represents cross-sections calculated using the coupled channels method. D0tted curve includes the compound nucleus contribution. The dashed curves includes the direct transition contribution. For σ_{tot}, results of different optical model calculations are shown. (I.A. Korzh, et al., "Neutron Physics", Moscow. Atomin-form , 1984, Vol.3, p. 173).

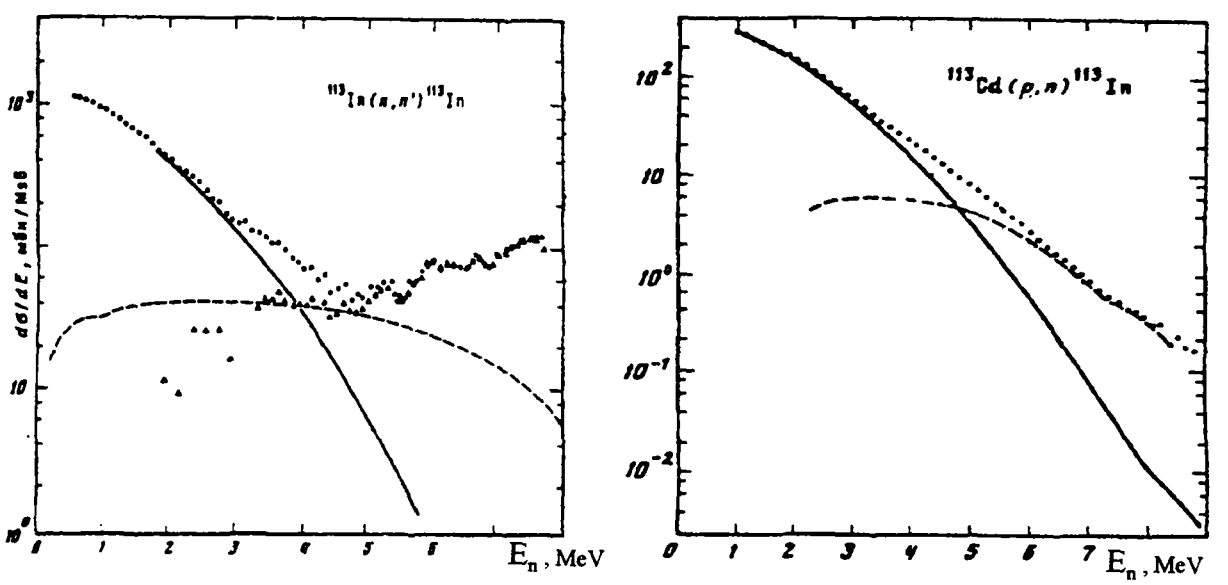

Figure 8. Integral spectra of neutrons from (n,n') and (p,n) reactions leading to the same compound nucleus. Solid curves represent the contribution from the equilibrium mechanism for neutron evaporation. Dashed curves shows the pre-equilibrium component. Triangular points represent the total non-equilibrium component of the inelastic neutron scattering spectrum.
(Lovtchikova, et al., Yadernaya Fizika 1982, Vol.36, p.6)

The analysis of the entire set of fast neutron double differential inelastic scattering data provided the possibility to study the contribution of direct processes for incident neutron energies ranging from 5 to 25 MeV for a large number of nuclides. Effective theoretical methods to describe single- and double-step direct transitions were developed. At higher neutron energies the number of linked channels which must be included in the generalized optical model in order to correctly interpret the multi step direct processes, is so large that it can't even be calculated using contemporary computers.

One possible method to avoid this difficulty is to use the generalized exciton model. In this approach, only the most intensive single step collective excitations are described by using the rigorous model of direct transitions, and the multi-step transitions are analyzed using the exciton model of the pre-equilibrium decay of nuclides. An important part in the use of such a generalized exciton model is the representation of the leading particle which reflects the initial conditions of the angular distribution of the multi-step transitions as well as a consistent choice of level densities of multi-step compound transitions. The given approach was successively applied to the analysis of neutron spectra for incident neutron energies higher than 14 MeV. Figure 9 shows a typical example describing the various components of the inelastic neutron scattering spectrum for the ^{209}Bi nuclide for incident neutron energies of 5.0, 14.1 and 25 MeV.

The fundamental concept of the statistical theory of nuclear reactions was also successively verified in its application to the analysis of radiative capture of fast neutrons with energies up to 1 - 2 MeV. An example of a good agreement between measurement results of various experiments and theory can be seen in Figure 10. Theoretical analysis of the radiative capture cross section can be used to derive radiation strength functions as well as neutron strength functions of p- and d-neutrons. For many nuclides, this information significantly supplements and improves the quality of the data which result from the analysis of average neutron resonance parameters.

The fission process has always occupied an important place in the research program at the FEI. At the end of the 1950s, O.Bohr proposed the concept of fission channels consisting of discrete transition states lying above the fission barrier; and in the case of even-even nuclei, in the form of low lying exiting states. By the mid-1960s, the accumulated experimental measurements and their theoretical analysis confirmed a number of qualitative predictions of Bohr's channel model. At the same time this information revealed significant contradictions between the observed variations in the anisotropy of the fission process in the near-threshold region and the classical representation of a single hump barrier model. These discrepancies could only be eliminated by adopting the double hump barrier model proposed by Strutinski. FEI physicists made considerable contributions to the adoption and development of that concept: formulae to represent the penetration of the double hump barrier in the quasi-classical approximation were derived, statistical rules governing the fluctuation of fission widths were determined, and observed even-odd differences in the fission thresholds and serious characteristic variations in the angular anisotropy at sub-barrier and near-barrier energies were explained.

Systematic measurements of fission product angular distributions for neutron energies up to 7 MeV were performed for a large number of actinides. The effective moments of inertia of

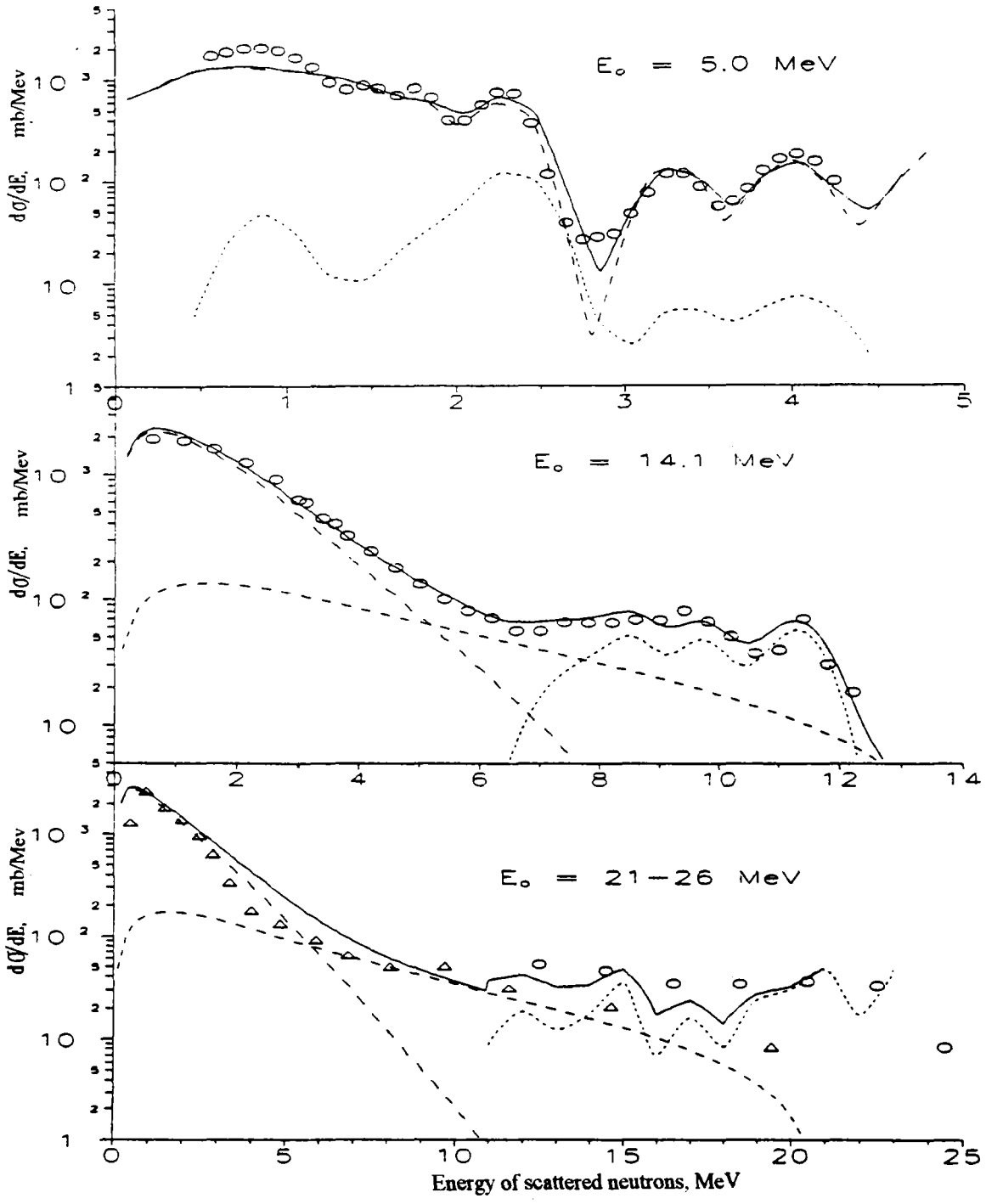

Figure 9. Spectra of inelastically scattered neutron on ^{209}Bi at energies of 5.0, 14.1 and 21-26 MeV. Experimental results at 5 MeV (Lovchikova et al.); at 14.1 MeV (Lychagin et al.), at 25.6 MeV (Martsinkovskiy et al.) are given by open circles. At 20.6 MeV (Prokopets et al.) are given by triangles. Calculated curves: direct process contributions by short dashes; equilibrium process contributions by long dashes; pre-equilibrium process contributions by dashes; total contributions by solid curves.

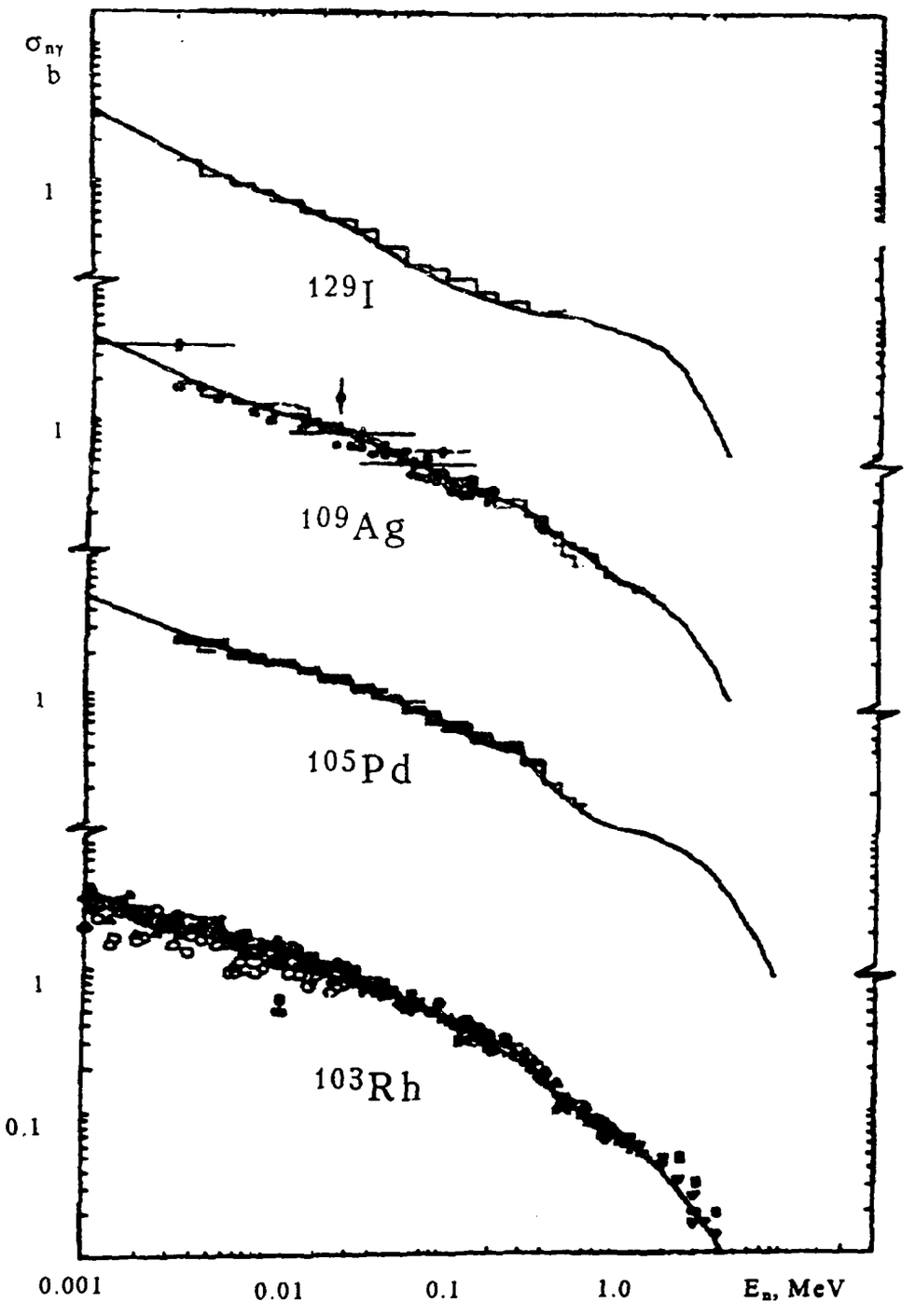

Figure 10. Fast neutron radiative capture cross-sections. Experimental data shown by points and histograms. Recommended evaluated data by solid curves.

transition states of fissioning nuclei, their dependence on the mass number and on the fissionability parameter which were derived from these fission product data, helped support the hypothesis that the angular distributions were formed in the inner hump.

Due to the simple kinematics of the angular momentum in photo-fission FEI physicists were among the first to realize the importance of that reaction in the study of the channel structure model. Research on photo-fission was conducted for twenty years in cooperation with the IFP AN SSSR institute, the laboratory that created the microtron which has served as a source of gamma rays of required energies and intensities. Quadrupole photo-fission which dominates at sub-barrier gamma ray energies was discovered and studied extensively.

It was shown that the relative position of the anisotropy maxima and of the photo-fission thresholds, as well as the resonance structure and isomeric shelves which are noticeable at deep sub-barrier energies, all serve as strong arguments to support the model of a double-hump barrier in photo-fission. The body of data obtained as a result of photofission research makes it possible to determine the basic parameters of a double-hump barrier for the most important even-even isotopes of thorium, uranium and plutonium.

The "physical" systematics based on double-hump barrier parameters and on the fissionability of actinides, constructed on the basis of the comprehensive information on fission barriers of heavy nuclei, which was obtained from neutron and gamma ray research, and supplemented by results from studying the fissionability of nuclei in reactions with charged particles, proved to be considerably more reliable than the earlier empirical models. The fission cross sections in the region of the first plateau shown in Figure 11, which were predicted by the systematics, together with the existing experimental data and the results based on earlier systematics. (Translator's note: incomplete sentence in the original). The new systematics can be used to evaluate the fission cross sections of all transuranium nuclides, including those that are neutron deficient or neutron rich, to an accuracy of approximately 15%. The experimental measurement of these nuclides is made extremely difficult by the high radioactivity of the target.

In reactor applications, data of considerable high accuracy is required regarding the neutron yield quantity $<\nu>$, which has demanded a great deal of attention to its measurement and analysis. A series of systematic measurements of the energy dependence of $<\nu>$ in the neutron energy range up to 7 MeV for ^{232}Th, $^{233,235,236,238}U$, ^{237}Np and ^{239}Pu were performed at FEI using two independent methods. Special attention was given to the non-monotone variations of $<\nu>$ at near-threshold energies. Simultaneously with the $<\nu>$ analysis, the average kinetic energy of fission fragments, the output from symmetrical fission and the dispersion of angular distributions, have shown a strong correlation of the observed variations in the indicated quantities with the spectrum of the transition states on the fission barrier. The analysis of the energy balance in various fission products, the concurrent collection of experimental data on ν, and the average kinetic energies of fragments, has given us a basis for the development of a systematic regarding the energy dependence of $<\nu>$ which has a wide application in the evaluation of neutron emission for all transuranium isotopes.

In the process of the development of new neutron spectrometric methods, emphasis was put on rather detailed measurements of prompt neutron fission spectra. Measurements of prompt

neutron spectra resulting from fission by monoenergetic neutrons of ^{232}Th, $^{233,235,238}U$, ^{237}Np, and ^{239}Pu were performed using the time-of-flight method. In cooperation with the TsIFI (Budapest), the shape of the soft part of the neutron spectrum , resulting from the thermal fission of $^{233,235}U$ and ^{239}Pu and from the spontaneous fission of ^{252}Cf, was analyzed using the lithium glass method. The resulting data proved to be of great importance in the evaluation of the neutron spectra as well as in testing the theoretical methods used to describe the emission of neutrons from fission products.

To study the mechanism of the emission of neutrons from the spontaneous fission of ^{252}Cf, measurements were made of the number and spectra of prompt neutrons emitted by the fission fragments at angles of 0° and 90° with respect to the direction of the two fission fragments, as well as of the angular distribution of neutrons (10 angles) independent of the fragment parameters.

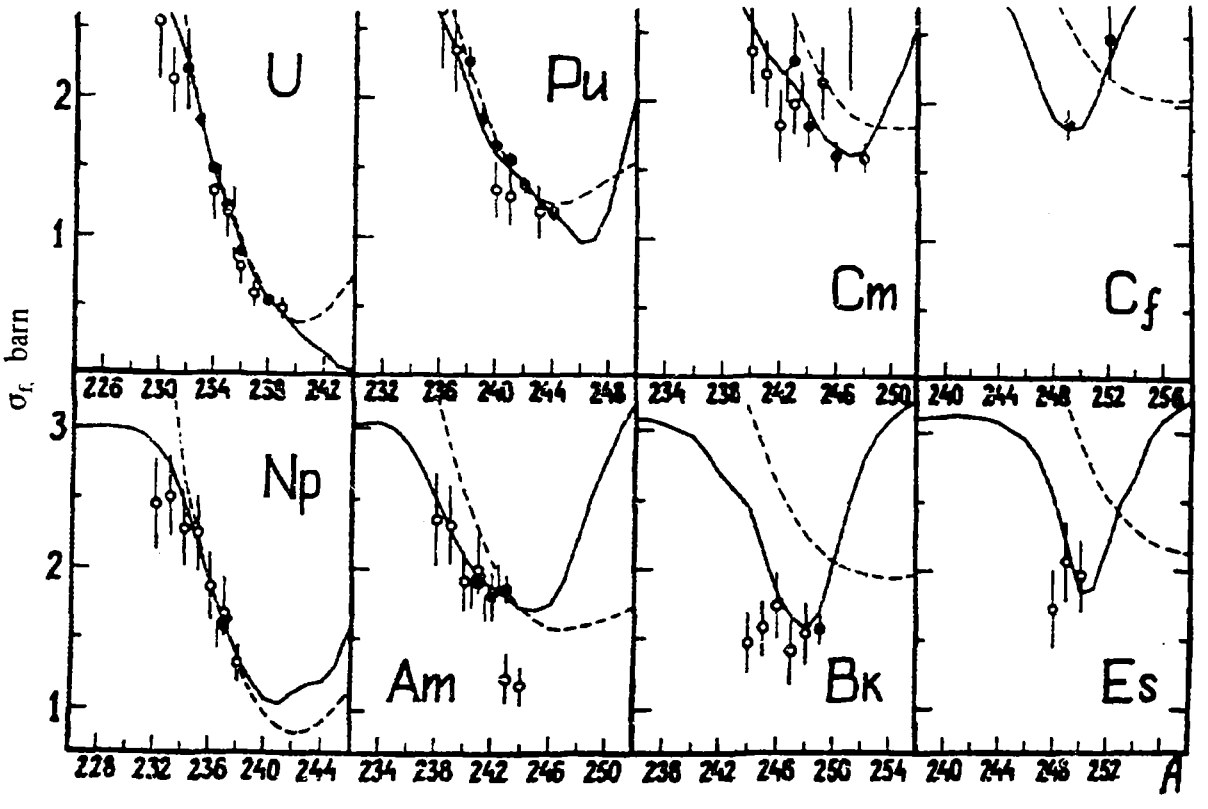

Figure 11. Fast neutron fission cross-sections in the "plateau" region as a function of the mass number of the target nuclide A. Experimental data: dark circles - neutron data, light circles - direct reaction data. Systematics: solid curves - FEI , dashed curves - Livermore Laboratory (USA).

The results of these measurements confirmed that the dominant process consists of the evaporation of neutrons from the entirety of the accelerated fragments. The observed temperature spectra of the fragments served to derive level density parameters, which confirmed the existence of a deep shell depression in the vicinity of mass number 132.

At high enough excitation energies, the level densities of excited nuclei begin to play a decisive role in the statistical theory. A large number of direct experimental data on level densities for many nuclei are found in the narrow energy interval near the neutron binding energy. However, this resolved resonance region gives only a single point in the energy dependence of the level density, and then only for one or two spin values.

The combined analysis of the shell, superfluidity and collective effects is most important in the analysis of level densities. Follow up microscopic methods to describe such effects as well as phenomenological systematics to describe changes in the level density energies, were developed at the FEI laboratory. Taking the superfluidity and collective effects into consideration noticeably lowers the level density parameter "a", derived from the analysis of the neutron resonance density, and eliminates most of the contradictions in the results of the analysis of various sources of information on nuclear level densities (see Figure 12). On the same level of importance as the level densities in the statistical theory of nuclear reactions, is the cross-section for the absorption of the particle by the excited nucleus (reverse action cross-section. Scientists at FEI developed microscopic methods for the analysis of collective excitation of heated nuclei which made it possible to analyze changes in the characteristics of collective modes as a result of increases in the temperature or in the energy of the excited nucleus.

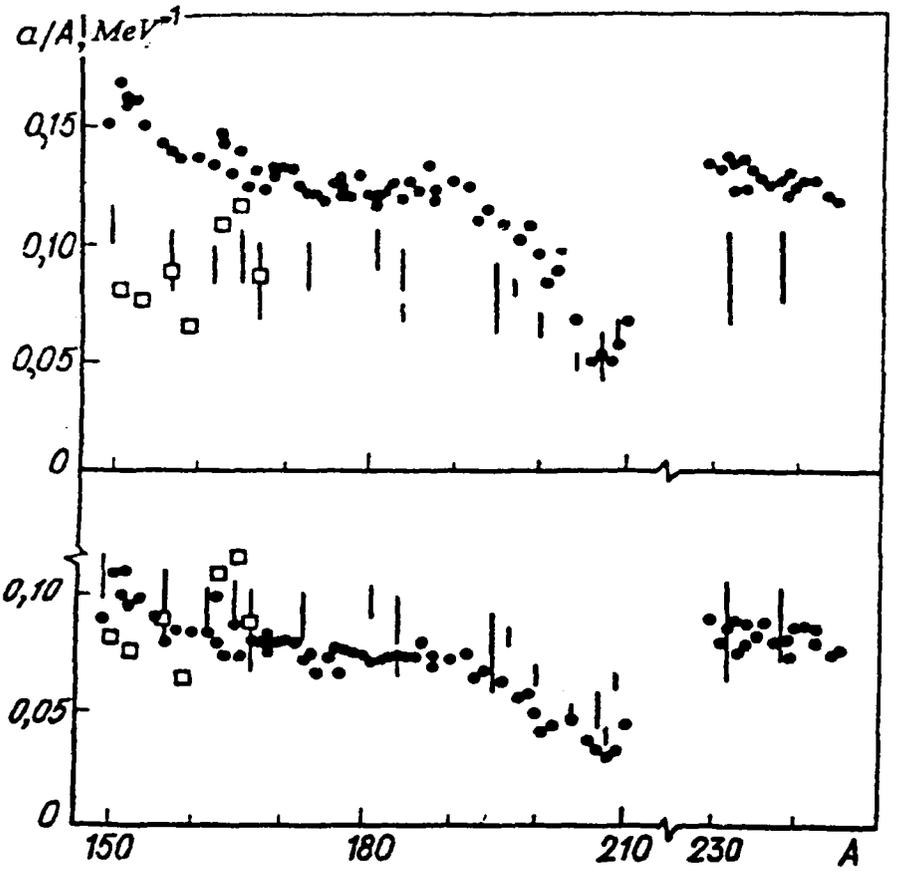

Figure 12. Comparison of level density parameters for heavy nuclides derived from inelastic neutron scattering (|) and fission product neutron spectra (□) with results of neutron resonance density analysis (•) using the Fermi-gas model (top) and using the coordinated collectve effect (bottom).

Taking the effect of temperature changes in the reverse reaction cross-sections into account can play an important role in the description of radiation strength functions and radiation widths, as well as in the analysis of the soft evaporation part of the spectra of neutrons emitted by the excited nucleus. Only a limited amount of experimental information on the effect of temperature changes on the collective properties of nuclei exist at the present time. There is no doubt that future research on reverse reaction cross-sections will have a signicant effect on the development of theory as well as for practical applications.

The results of experiments and of theoretical research on the physics of the interaction of neutrons with nuclides have not only enriched and widened our understanding of the properties of nuclei and mechanisms of nuclear reactions, but have also served as the basis for the development of systematics and the evaluation of nuclear data.

V. The Evaluation of Nuclear Data

The existence of the large body of experimentally measured data which characterize the interaction of neutrons with nuclei does not in itself offer the solution of providing nuclear data in a form required to perform project computations. This is due to the fact that each measurement is associated with a statistical and systematic error. Because of the difficulties associated with their identification, the differences in the results of a given experiment by different authors very often exceeds the magnitude of the assigned experimental error. In order to obtain a more objectively determined numerical value, and to determine its reliability, requires a special analysis of the data. Furthermore, to be useful, the data must be represented in the form of a curve or a histogram which is given for a specified interval. The experimental data are characterized over different energy or angular ranges, whose widths are dictated by the specifications and resolution of the measuring apparatus, nor do they encompass all nuclides, nuclear reactions and required energy ranges.

The objective of the nuclear data evaluation process is to construct a continuous curve, describing one or the other characteristic of a neutron interaction with a given nuclide in a reactor energy range, associated with a derived uncertainty, on the basis of existing experimental data and theoretical model representations. A file of evaluated data is made up of an internally consistent set of characteristics of neutron interactions with a given nuclide. For instance, a file for fissile nuclides includes the total neutron interaction cross-section, the neutron radiative capture cross-section, the fission cross-section, the elastic and inelastic scattering cross-sections, the (n,2n) cross-section, the average number of prompt and delayed fission neutrons, the spectra and energy distributions of secondary neutrons, etc..., for energies ranging from 0 to 20 MeV.

Scientists at FEI have developed a full set of consistent neutron data evaluation methods covering the total energy range of practical interest. With the aid of programs that incorporate these methods, a full array of neutron data for all basic reactor and shielding materials has been compiled. Using a collection of specially designed programs, a comprehensive verification of the library of neutron data files was performed which guaranteed its practical utilization.

As a rule, all evaluated neutron data files are represented in the international ENDF-B format. A short description of the basic features of the consistent evaluation methods and of the library of evaluated neutron data files is given below. In the resolved resonance region, the energy dependence of the cross-sections is represented by the parameters of individual resonances, these are normally evaluated by the experimenters

The features of the adopted evaluation methods in this domain consist of the following:

1. Differences in the methods used by experimenters, evaluators and those used in the development of the evaluated data files to calculate resonance cross-sections are analyzed; depending on the method used, parameters are corrected and the corrections are evaluated.

2. The results of cross-section measurements in the thermal region are described with the use of selected parameters of observed bound states of nuclei, together with resolved resonance parameters.

3. Use is made of perfected resonance formulae, which preserve the principle of unitarity, and which allow a non-contradictory description of the energy dependence of the cross section without resorting to artificial procedures (i.e., representation of fluctuating background cross sections, and others). In the case of fuel materials (e.g., Pu-239) use of well measured total and fission cross sections can be made to improve the quality of a badly measured absorption cross section.

4. The file is comprised of resonance parameters not only in the fully resolved resonance region, but also where only s-resonances are resolved. In the earlier versions of ENDF-B, this possibility was not foreseen. Its inclusion was possible without modification of the format (and eventually, it was also included in most processing programs) by using the implicit options of this format.

In the unresolved resonance region, the existence of the resonance structure is evident, but cannot be resolved with existing neutron spectrometers. In the case of the fuel nuclides, that region extends over an energy range between a few hundreds or thousands of eV to 100-200 keV. In fast multiplying systems, most processes which determine the neutron balance, take place in this region, which makes this region so important. Here the evaluation task consists not only in the determination of reliable average neutron reaction cross sections, but also of the structure of these cross sections which must take the resonance selfshielding into account. Pioneering research was conducted in this region by the FEI, and work in this region is still regarded to be of high priority.

The features of the adopted cross section evaluation procedures in the unresolved resonance region consist of the following:

1. On the basis of the statistical theory of nuclear reactions it is possible to describe all characteristics of the interaction of neutrons with nuclei, which can also be measured in the unresolved resonance region: the total cross section, the capture cross secction, the transmission functions, the anisotropy of scattering , and others.

2. Values of the strength functions and of the scattering radius - parameters used in the theoretical description - are evaluated as a function of spin and parity, using the statistical analysis of the data from the resolved resonance region. An array of evaluation methods have been developed to implement this. Methods developed outside of Russia are also used. The use of different methods increases the reliability of results. In the search for the optimum values of average resonance parameters it is stipulated that they do not deviate from their initial value by not more than their evaluated error.

3. In the process of searching for the optimal parameters, it is also required that they can also be used to describe cross sections in the region that is slightly higher than the unresolved resonance region, so as to ensure their agreement with the evaluation of the cross section in the non-resonance region. As the non-statistical effects, which manifest themselves at higher energies do not show any prominence in the unresolved resonance region, they are treated as corrections.

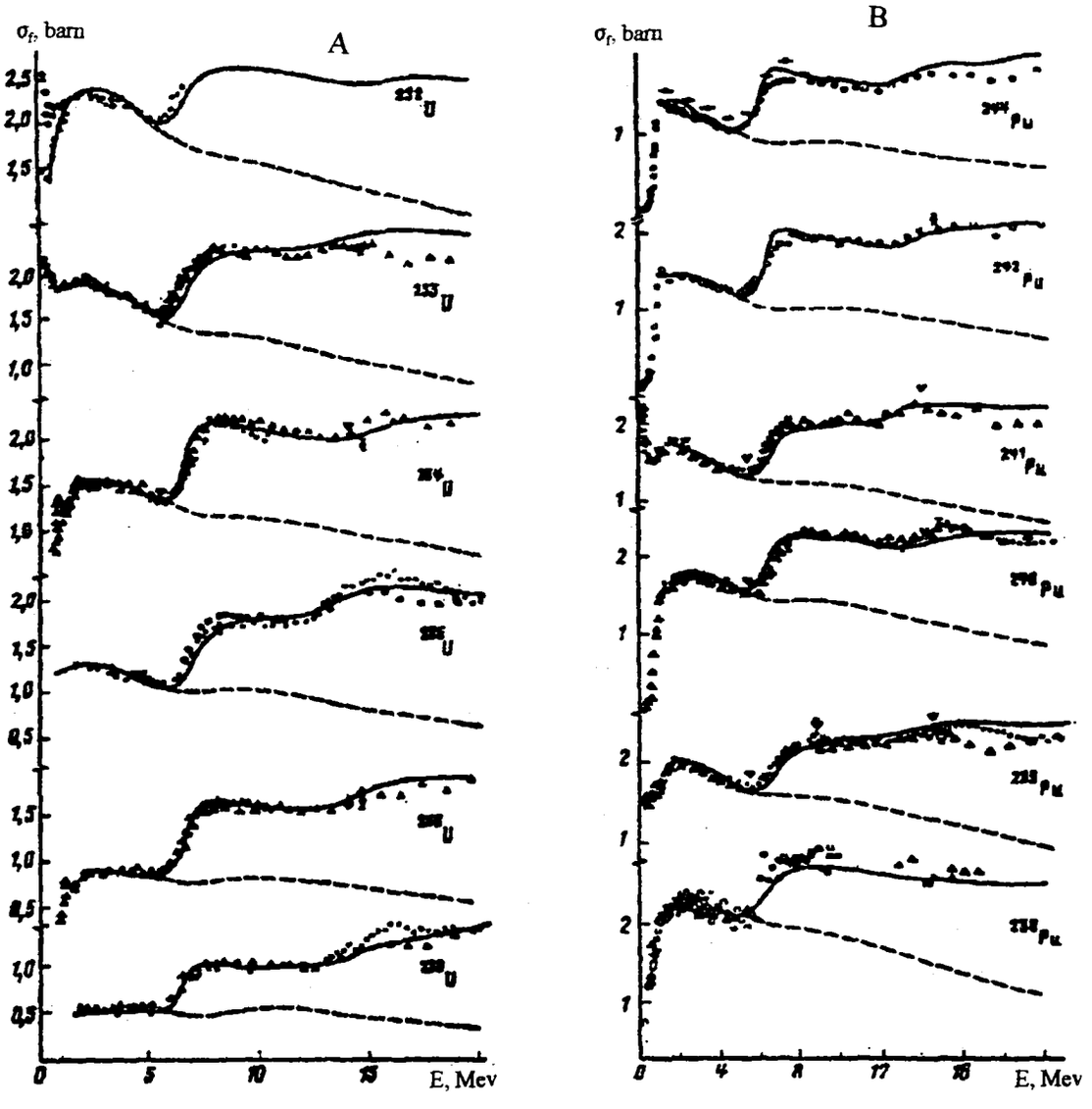

Figure 13. Contribution of the (n,f), (n,n'f) and (n,2nf) processes to the fission cross section of the uranium (A) and plutonium (B) isotopes.

The methodology for the evaluation of cross sections in the unresolved resonance region , described above, has been implemented in our country only for the fertile isotopes U-238 and Th-232 for which the inclusion of the unresolved structure cross section is very important. Because of that the uncertainty in the evaluated data turned out to be considerably smaller than the uncertainties in the experimental data. Now, this methodology has been recommended to be widely used at the IAEA meeting on nuclear data evaluation methods.

In the nonresonance energy region, the main evaluation task consists of the specification of the existing experimental data on the basis of their theoretical description in the framework of the optical-statistical model. The basic features of this approach to neutron cross section evaluation are as follows:

1. Optical potential parameters are determined for each material to be evaluated; this makes it possible to describe existing experimental data in terms of these parameters, namely, the total cross section, the elastic scattering cross section and angular distributions of scattered neutrons, the cross sections of inelastic processes, as well as data on strength functions in the unresolved resonance region. For those nuclides for which experimental data are not available or incomplete, the optical potential parameters are derived from systematics.

2. Fission barrier parameters are determined for fissile nuclides on the basis of existing experimental data. Collective and shell effects in level densities of neutron and fission channels and superfluidity effects are taken into account collectively. The character of the deformation of the nucleus in the saddle point is evaluated on the basis of characteristics of the fission process. Fission barrier parameters derived from the analysis of neutron data are correlated with information on the fissionability of nuclei initiated by charged particles. Principles derived from this information made it possible to perform a phenomenological evaluation of the fission cross sections for nuclides for which experimental data was not available or incomplete (e.g., U-237, Pu-243, and others). Nuclides for which the fission cross section was measured well, their theoretical analysis makes it possible to separate the individual contributions into the (n,f), (n,n'f) and (n,2nf) processes which must be known so as to be able to evaluate the (n,2n) and (n,3n) reaction cross sections and their spectra of secondary neutrons (see Figure 13).

3. The inelastic scattering cross section with excitation of discrete levels, calculated using the coupled channels model, are compared with experimental data (which are often very sparse and contradictory). Linkage of highly excited channels are taken into consideration in the framework of the exciton model. Knowing the cross section of the excitation of low-lying levels makes it possible to evaluate and calculate the contribution of inelastic scattering from the measurement results of the scattering anisotropy, and obtain clean data for the elastic scattering process. The latter are used as reference data in the determination of optical potential parameters.

4. The inelastic scattering cross section, as well as the (n,2n) and (n,3n) reaction cross sections for intermediate and heavy nuclei are determined on the basis of the statistical model which conserves spin and parity on all cascades of the decaying nucleus. In

addition, an improved method to describe level densities, developed at FEI, is used in the evaluation of the fissionability of nuclei including the possibility to have a preliminary emission of a first neutron. This approach guarantees an internally consistent evaluation of the (n,n'), (n,2n), (n,3n), and (n,nf), (n,n'f), (n,2nf) reactions as well as of the (n,p), (n,α), (n,n'p) etc....reactions on non-fissioning nuclei. The spectra of neutrons emitted in these reactions are evaluated correctly as well. Figure 14 shows some examples of the discrepancy between the Russian and foreign evaluations of the (n,2n) reaction in the region of their maximum value (namely, at 10-12 MeV). After reviewing new versions of evaluations performed outside of Russia, cross sections for the (n,2n) and (n,3n) reactions from these evaluations, which were in fact close to the data recommended by Russian physicists, were adopted.

The national library of evaluated neutron data consists of evaluation performed by the FEI and IyaEh BAN institutes. The standard data used in these evaluations consists of data recommended by the IAEA with the participation of Russian specialists. For a number of nuclides of secondary importance, for which there were no new experimental data, it was agreed by the expert to use the best evaluation results from non-Russian evaluation files. A brief description of the evaluated data included in the national file is as follows:

Fuel materials.

The evaluation of the basic fuel material that comprise the national file were taken from the following sources:

- IyaEh BAN : U-235, Pu-239,-240,-241,-242;
- FEI : Th-232, U-238;
- IAEA: Np-237
- Substantially modified European evaluations of Am-241 and Am-243.

The national evaluations have been given priority for two reasons: first, they include the latest experimental data in their evaluations; and second, because of a more extensive theoretical analysis these evaluations reflect a more contemporary understanding of the neutron-nuclide interactions, and are therefore deemed to be more reliable.

Thus, for instance there is a substantial difference between our evaluation of the U-235 neutron inelastic scattering cross section and spectrum and that of the one given in ENDF/B-5. The reason for this is that our evaluation makes a better accounting of the direct processes contribution, the weight given to fission, and a number of other factors.

In the case of the unresolved resonance region of U-238, our evaluation is performed with a simultaneous theoretical description of all types of data, in the non-Russian evaluation on the other hand, such a correlation is not taken into account.

The Russian evaluated data have been noted for their high quality and reliability at the international nuclear data meetings held at Mito, Japan in 1988, and Julich, Germany in 1991.

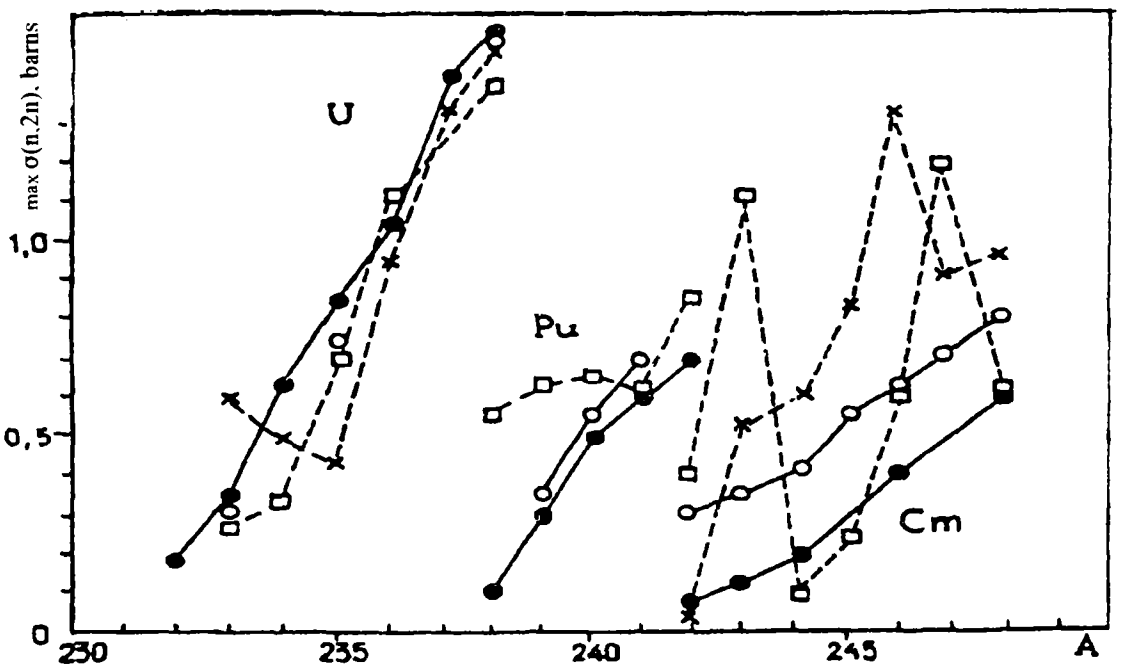

Figure 14. Maximum values of the (n,2n) reaction cross section as a function of mass numbers for the isotopes of uranium,plutonium and curium. - x - ENDF/B-V evaluation; - □ - ENDL-2 evaluation; - •- Nuclear Data Centre TsYaD evaluation.

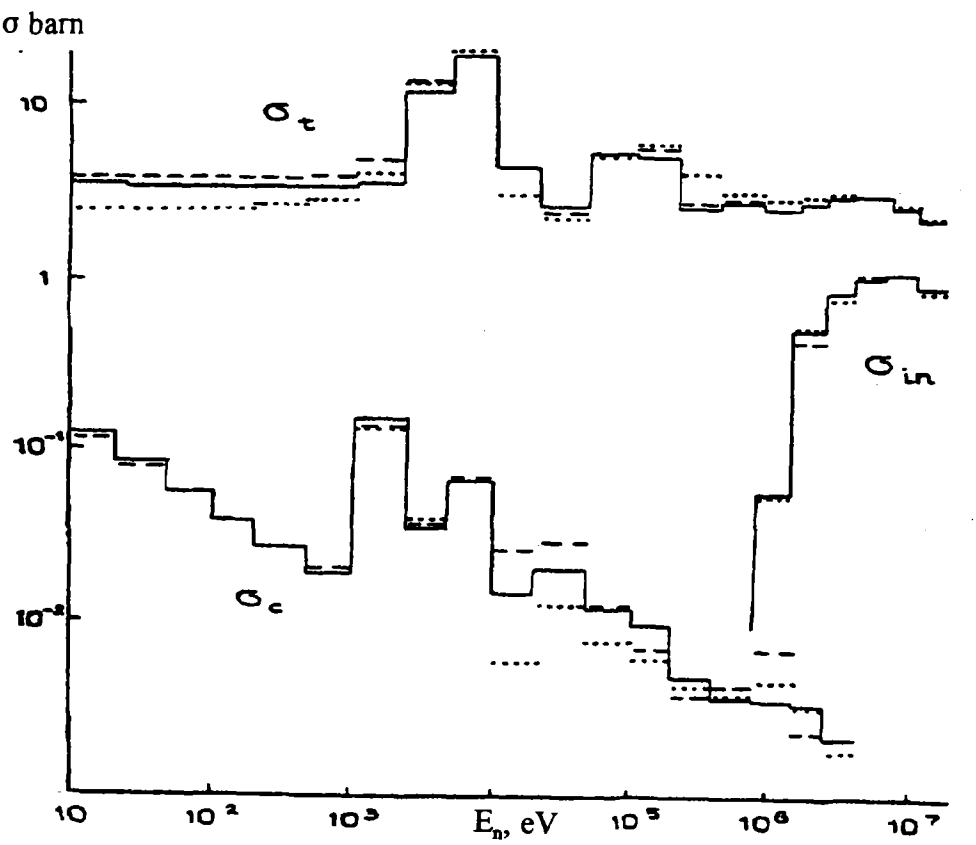

Figure 15. Comparison of various evaluated neutron cross sections for natural iron. - solid curve - BROND-2 evaluation; - short dashes - JENDL-2 evaluation; - long dashes - ENDF/B-V evaluation.

Structural and technological materials.

Most chemical elements that enter in the composition of structural materials consist of a few isotopes. Evaluations were first performed for each stable isotope separately; they were then combined in accordance to the weight of their composition., and finally analyzed and corrected so as to correspond with the results of separate measurements of each individual element. Until now, such correlation was only implemented in the Japanese library JENDL. In comparison with this and other non-Russian evaluations, our evaluations have significant advantages. Let us demonstrate using iron as an example.

Figure 15 shows results of various evaluations of the total neutron cross section, the radiative capture and the neutron inelastic scattering cross sections for natural iron. For convenience, the results are represented in the form of 74 energy groups. The boundary of the resolved resonance region is 60 keV in the case of ENDF/B-V, 250 keV in the case of JENDL-2 and 850 keV in our evaluation. The differences in the full consideration of the resolved resonance data affects and causes differences in the evaluation results below 1 MeV. For the analysis of the cross sections of the inelastic processes in the energy range above 3 MeV, where the experimental data are sparse and discrepant, it is of utmost importance to have a simultaneous analysis of all open neutron reaction channels and of the corresponding secondary neutron spectra; this approach was implemented in the Russian evaluation methodology.

The same approach, characterized by the internal consistency and completeness of the data, was applied to the other files of structural and technological data evaluations. It must be noted that in the case of the deuterium evaluation the correlation between the neutron spectrum from the (n,2n) reaction and the neutron emission angle was considered first. At the same time the contribution of the direct processes were taken into consideration as well. In the case of the sodium evaluation, the transmission function experiments were taken into consideration, which considerably increased the reliability of the evaluation of the neutron transparency in large amounts of sodium.

Fission products

Fission product data are needed for the calculation of the degree of their accumulation in nuclear reactors, as well as for the evaluation of radiation characteristics of the burned up fuel.

Fission product data on neutron radiative capture are of most interest. In non-Russian evaluations, it is often difficult to separate one set of capture data from another. Furthermore, since the time of these evaluations, a considerable number of new experimental capture data have been measured. For that reason, FEI has undertaken a complete analysis of the entire body of experimental information on the capture cross section and on resonance parameters using the evaluation methodology described above. The reasons for the differences between the earlier non-Russian evaluations can be attributed to the following factors:

- the inclusion of new experimental data on resonance parameters and capture cross sections in the energy range up to 100 KeV;

- the introduction of a new region of unresolved resonances, for those fission products which have a large yield, which makes it possible to improve the quality of the resonance selfshielding effect;
- the expansion of the evaluation range to the region above 8 MeV, using the empirical systematics of experimental data and the direct collective neutron capture model.

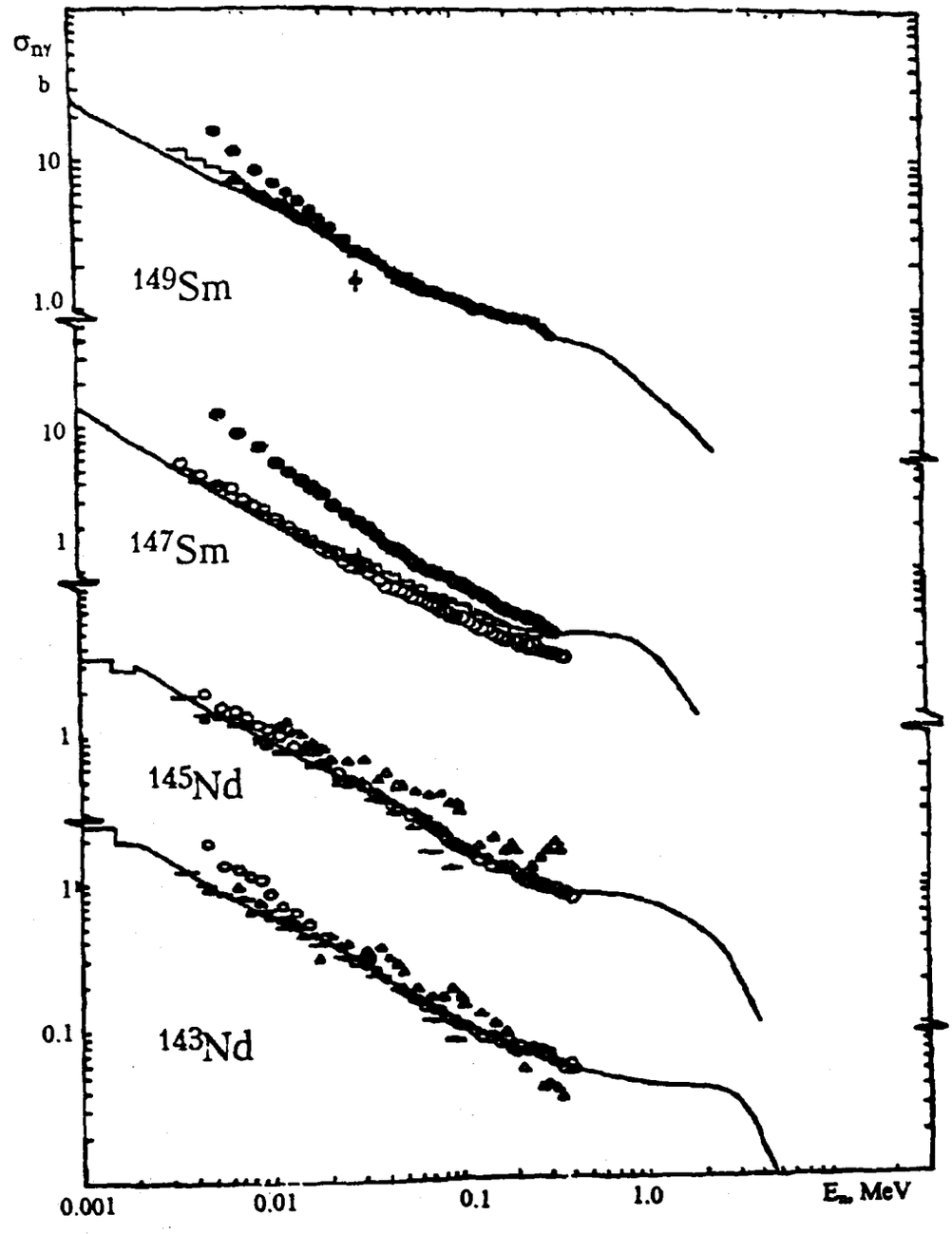

Figure 16. Comparison of recommended evaluations with experimental data for odd isotopes of neodynium and samarium

Table 12. Characteristics of fission product evaluations included on BROND-2.

No	Isotope	% contribution to absorption	Res. Num	E_{res} keV	$E_{non\text{-}res}$ keV	Evaluation used		% error in capture
						capture	scattering	
1	^{105}Pd	9,9	199	2,0	283	ФЭИ	ФЭИ	10
2	^{99}Tc	8,6	107	1,4	141	-"-	-"-	10
3	^{101}Ru	7,7	40	1,0	120	-"-	-"-	10
4	^{107}Pd	6.2	60	0,7	300	-"-	-"-	15
5	^{103}Rh	5,5	164	2,0	92	-"-	JENDL-3	15
6	^{133}Cs	4,9	160	3,5	-	JENDL-2	-"-	10
7	^{147}Pm	3,5	43	0,30	100	ФЭИ	-"-	25
8	^{149}Sm	3,4	70	0,12	520	-"-	-"-	20
9	^{145}Nd	3,4	114	2,0	30	-"-	-"-	20
10	^{102}Ru	3,3	8	1,3	100	-"-	-"-	10
11	^{135}Cs	3,0	-	0,03	-	-"-	-"-	30
12	^{97}Mo	2,5	64	1,8	100	JENDL-3	-"-	15
13	^{109}Ag	2,7	64	1,0	132	ФЭИ	ФЭИ	10
14	^{106}Ru	2,3	-	0,5	-	-"-	-"-	30
15	^{143}Nd	2.3	65	2,5	30	-"-	-"-	20
16	^{131}Xe	1,9	39	1,0	164	-"-	-"-	25
17	^{151}Sm	1,9	76	0,10	10	-"-	-"-	30
18	^{95}Mo	1,5	55	2,0	100	JENDL-3	JENDL-3	15
19	^{104}Ru	1,3	8	1,2	100	ФЭИ	-"-	10
20	^{153}Eu	1,3	72	0,01	10	ENDF/B-V	ENDF/B-V	15
21	^{98}Mo	1,2	161	32	100	JENDL-3	JENDL-3	20
22	^{144}Ce	1,1	-	0,5	-	ФЭИ	ФЭИ	30
23	^{129}I	1,0	5	2,0	500	-"-	-"-	30
24	^{100}Mo	0,9	158	26	100	JENDL-3	JENDL-3	20
25	^{141}Pr	0,9	15	0,99	-	ENDF/B-V	ENDF/B-V	10
26	^{147}Sm	0,3	120	0,75	120	ФЭИ	ФЭИ	20
27	^{151}Eu	-	92	0,01	10	ENDF/B-V	ENDF/B-V	15

To obtain data in the 1-8 MeV energy region, in which there is an absence of experimental data and which is relatively unimportant from a practical point of view, use is made of earlier theoretical evaluations. For the most important fission products, the recommended evaluated neutron radiative capture data, given together with the existing experimental data, are shown in Figure 16.

A complete file of neutron data for fission product nuclides has been assembled on the basis of evaluated resonance cross sections and capture cross sections in the non-resonance region. In addition, scattering cross sections and threshold reaction cross sections in the non-resonance region were taken from the latest non-Russian evaluations; there have been no new data for these reactions in the last few years, furthermore, from the point of view of reactor physics, their role is not significant. The most important fission products are tabulated in Table 12 in

the order of their diminishing contribution to the composite capture due to all fission products. The table also gives the number of considered resonances included in the evaluation of the capture and scattering cross sections, and the accuracy of the evaluated capture cross section in the energy region of importance to fast reactors. The error in the composite fission product capture cross section does not exceed 10%, which is entirely acceptable from a practical point of view.

Table 13. List of files included in the BROND-2 library

Isotopes	Eval./rev.	Authors
H-2,3	1988	Nikolaev M.N.
He-3,4	1988	Nikolaev M.N.
He-4	1976	Nikolaev M.N. et al.
Li-6	1989	Nikolaev M.N.
Li-7	1984	Bondarenko I.M.
N-14,15	1988/1993	Blokhin A.I. et al.
O-16	1977	Nikolaev M.N. et al.
F-19	1990	Blokhin A.I. et al.
Na-23	1978	Nikolaev M.N. et al.
Si-000	1985/1993	Hermsdorf D., Blokhin A.
P-31	1989	Koscheev V.N.
Cl-000	1990	Nikolaev M.N. et al.
Cr-000	1984/1988	Pronyaev V.G. et al.
Cr-50,52, 53, 54	1987	Blokhin A.I. et al.
Fe-000	1985/1994	Pronyaev V.G. et al.
Fe-54, 56, 57,58	1985	Pronyaev V.G. et al.
Ni-000	1984	Blokhin A.I. et al.
Ni-58, 60, 61, 62,64	1985	Blokhin A.I. et al.
Cu-000	1981	Nikolaev M.N. et al.
Zn-000	1989	Nikolaev M.N. et al.
Sr-90	1990	Grudzevich O.T.et al.
Zr-000	1988	Grudzevich O.T.et al..
Zr-90,91, 92, 94,96	1988/1993	Grudzevich O.T. et al./ Blokhin A.I.
Zr-93,95	1989	Grudzevich O.T.et al..
Nb-93	1988/1993	V.G.Pronyaev et al.
Nb-95	1990	Grudzevich O.T. et al. .
Tc-99	1984	Ignatyuk A., Kravchenko I.
Ru-101,102, 104, 106	1984	Ignatyuk A., Kravchenko I.
Rh-103	1985	Ignatyuk A et al...
Pd-105, 107	1985	Ignatyuk A., Kravchenko I.
Pd-106, 108	1987	Belanova T.., Ignatyuk A.
Ag-109	1985	Ignatyuk A.,Kravchenko I.
Sn-000	1990/1993	Pronyaev V.G.et al.
I-129,	1985	Ignatyuk A.,Kravchenko I.
Xe-131	1985	Ignatyuk A.,Kravchenko I.

Isotopes	Eval./rev.	Authors
Cs-135	1985	Ignatyuk A., Kravchenko I..
Ce-140, 142, 144	1990	Ignatyuk A., Ulaeva M.
Nd-143, 145	1985	Ignatyuk A., Kravchenko I.
Pm-147	1985	Ignatyuk A., Kravchenko I.
Sm-000, 144,154	1989	Belanova T.S. et al.
Sm-147, 149,151	1985	Ignatyuk A., Kravchenko I.
Sm-148, 150,152	1987	Zakharova S, Ignatyuk A.
Eu-153	1985	Ignatyuk A., Kravchenko I.
Gd-000, 152, 154, 155,156, 157,158, 160	1989	Blokhin A.I.
Er-162, 164, 166, 167,168, 170	1976	Zakharova S.M. et al
Ta-181	1988	Manturov G., Korchagina G.
W-182, 183, 184, 186	1983	Abagyan L., Manturov G.
Re-000	1988	Nikolaev M.N. et al.
Os-000	1990	Nikolaev M.N.
Ir-000	1990	Nikolaev M., Zabrodskaja S.
Pb-000	1984/1994	Hermsdorf D./ Blokhin A.I.
Pb-204, 206,207, 208	1990/1993	Blokhin A.I. et al.
Bi-209	1990/1993	Blokhin A.I. et al
Th-232	1983	Nikolaev M.N. et al.
Pa-231, 233	1994	Blokhin A.I. et al.
U-233	1990	Sukhovitsky E., Klepatsky A
U-235,236	1986	Konshin V.A. et al.
U-238	1980	Nikolaev M.N. et al.
Pu-238	1987	Sukhovitsky E., Klepatsky A
Pu-239, 240, 241, 242	1980	Konshin V.A. et al.
Am-241, 242, 242m, 243	1990/1994	Blokhin A.I., Maslov V.M.
Cm-242, 244	1987	Sukhovitsky E. et al.

The errors in the evaluated data

The uncertainty in the evaluated data is represented in the form of errors assigned to individual groups of a multi group data sets, in a form that can be used (and which are actually used) in computational programs designed to calculate the accuracy characteristics of reactors and shielding.

Table 14. Additional files included in the FOND library.

El.	Eval/Rev	Origin	Comments
*H	1989/1993	ENDF/B-6	Capture data were modifyed.
Be	1983/1993	-"-	Thermal sig cap was corrected.
B	1989	-"-	B-10 and B-11 files were used.
*N	1983-1990	-"-	N-14 and N-15 files were used.
*O	1990	-"-	
*F	1990	-"-	
Mg	1987	JENDL-3	
AL	1988	JENDL-3	
*Si	1989	JENDL-3	
*S	1979/1993	ENDF/B-6	INT low for MT=103 was corrected.
*Cl	1979/1993	ENDF/B-6	INT low for MT=103-107 was corrected.
Ar	1979	JEF-1	
K	1987	JENDL-3	
Ca	1987/1993	JENDL-3	$\Gamma_{comp}(E)$ was added.
Sc	1988	JENDL-3	
Ti	1988/1993	JENDL-3	Ethresh for 1-st inelastic level was corrected.
V	1982	ENDL-83	
Mn	1988	ENDF/B-6	
Co	1989	ENDF/B-6	
*Ni	1989/1993	ENDF/B-6	Ni-59,60,61,62,64 files were used and missed P-resonances were added.
*Cu	1987	JENDL-3	
Ga	1982	ENDL-83	
Ge	1974	ENDF/B-6	Ge-70,73,74,76 files were used, and RP for Ge-70 were modifyed.
As	1982	ENDL-83	
Se	1974/1993	ENDF/B-6	Data in resonance and fast regions was revised.
Br	1974/1992	ENDF/B-6	Br-79,81 files were used and (n,2n) reaction was added.
Kr	1974-1984	ENDF/B-6	Kr-78,80,82,83,84,86 files were used.
Rb	1984	JEF-1	Rb-85,87 files were used.
Sr	1984/1992	ENDF/B-6	Sr-84,86,87,88 files were used and (n,2n) reaction was added.
Y	1977	JENDL-3	
Mo	1989	JENDL-3	Mo-nat,95,97,98,100 files were used.
Ru	1990	ENDF/B-6	Ru-96,98,99,100 files were used,other from BROND-2.
Pd	1980-1991	ENDF/B-6	Pd-102,104 files were used, other - from BROND-2.
Ag	1977	JENDL-3	Ag-107 was used, Ag-109 - from BROND-2.
Cd	1975/1991	ENDF/B-6	Cd-nat and Cd-113 files were used. Energy spectrum (n,2n) reaction was corrected.

El.	Eval/Rev	Origin	Comments
In	1974-1979	ENDF/B-6	In-113,115 files were used.
Sb	1974-1979	ENDF/B-6	Sb-121,123,125 files were used.
Te	1974-1980	ENDF/B-6	Te-120,122,123,124, 125, 126,128,130 files were used.
I	1980	ENDF/B-6	
Xe	1978	ENDF/B-6	Xe-124,126,128,129, 130,132, 134,136 files were used.
Cs	1974-1978	ENDF/B-6	Cs-134,137 files were used.
	1984/1991	FOND-1	Cs-131 file was used.
Ba	1978	ENDF/B-6	Ba-134,135,136,137,138 files were used. Ba-130,132 were considered as Ba-134.
La	1977	JENDL-3	
Pr	1984/1991	FOND-1	
Nd	1974/1980	ENDF/B-6	Nd-142,144,146,148, 150 files were used. Nd-143,145 - from BROND-2.
Eu	1986	ENDF/B-6	Eu-151 was.used, Eu-153 - from BROND-2.
Tb	1980	ENDF/B-6	
Dy	1974-1980	ENDF/B-6	Dy-160,161,162,163,164 files were used with res. param. modified. Dy-156,158 were considered as Dy-160.
Ho	1974/1980	ENDF/B-6	
Lu	1967/1980	ENDF/B-6	Lu-175 and Lu-176 files were used.
Hf	1989	JENDL-3	Hf-nat,174,176,177, 178,179, 180 files were used.
*Ta	1989	JENDL-3	
Pt	1982/1991	ENDL-83	Some errors were found and removed.
*Pb	1989	JENDL-3	Based on integral experimental considerations.
Th	1981	JENDL-3	Th-228,229 files were used.
	1982/1993	ENDF/B-6	Th-230 was used. Thermal cross sections was corrected
Pa	1977-1978	ENDF/B-6	Pa-231,233 were files used.
*U	1978-1989	ENDF/B-6	U-232,234,235 files were used.
Np	1978/1990	ENDF/B-5	Np-237 aws used and (n,2n) cross section was modified.
	1989	JENDL-3	Np-239 file was used.
*Pu	1987/1993	JENDL-3	Pu-239 was used; LIPAR-5 lib. was used below 100 ev.
	1976-1978	ENDF/B-6	Pu-243,244 files were used.
Cm	1976-1978	ENDF/B-6	Cm-243,245,246,247, 248 files were used.
	1987	JENDL-3	Cm-249 and Cm-250 files were used.
Bk	1986	ENDF/B-6	Bk-249 file was used.
Cf	1975-1986	ENDF/B-6	Cf-249,250,251,252, 253 files were used.
Es	1975	ENDF/B-6	Es-253 file was used.

The status of the evaluated neutron data library

The content of the evaluated neutron data library is listed in Tables 13 and 14. The library includes data for basic nuclear fuels, reactor construction and technological materials, for the most important fission products, and component elements of the air and of the ground.

The neutron data evaluation for the basic reactor and shielding materials, performed by the FEI and IyaEh BAN institutes were subjected to a review by specialists from other institutes. The observations and comments were discussed at meetings organized by the TsYaD nuclear data centre. The accepted recommendations were incorporated in the revised files by the authors and subjected to a comprehensive algorithmic analysis. Documentation of the files was included in the library and the library was stored on magnetic tapes. Copies of the evaluated data library stored on magnetic tapes were then distributed to interested organization on request.

The evaluated data were then converted at the FEI institute to multi group data sets used in reactor and shielding calculations, and its introduction into practical engineering computations was thus guaranteed.

VI. The Nuclear Data Centre TsYaD

The nuclear data centre at the FEI institute was set up in 1963. From the very beginning of its operation, it was a member of the international network of nuclear data centres organized under the aegis of the IAEA, and participated in the scientific/technological effort in the creation and development of a neutron data base, its international exchange and at the same time making it available to scientists in our country.

The centre has the following tasks:

- to compile bibliographical data on the measurement, calculations and evaluations of neutron data performed in Russia, and to enter them in the international catalog of microscopic neutron data CINDA;
- to compile numerical experimental neutron data measured in Russia and to enter them into the international library EXFOR;
- to determine the nuclear data requirements in all applications;
- to evaluate nuclear data for their inclusion in national and international data libraries;
- to establish and develop an applied mathematical base in order to be able to carry out the formulation, verification, correction, search and retrieval, processing and graphical presentation of numerical data;
- to provide nuclear data to Russian institutes and organizations;
- to publish the topical " Nuclear Constants"journal;
- to promote the exchange of data with other national centres and the IAEA.

The TsYaD centre is equipped with contemporary programming facility for the calculation of nuclear reaction data using theoretical models, the processing of data into multi-group sets of data, the verification and testing of data, the performance of activation analysis calculations and the evaluation of radiation damage to the materials of nuclear installation components.

The TsYaD centre is equipped with state-of-the-art computers. Having these computational and programming resources makes it possible to have on-line access to the data stored at the centre as well as those available from other centres.

The TsYaD data centre database is continuously supplemented by new Russian and non-Russian
data, new calculational programs; at the same time data stored at the centre are continuously processed, searched, sorted, checked, improved and widened; the data are transformed and reformatted for the benefit of the users, and exchanged with other centres. There are large numbers of service programs to treat data in ENDF-6 format and a complex of NJOY programs for the preparation of multi-group data and the performance of reactor calculations.

Each year the centre receives approximately 100 requests for neutron data from Russian users, 40 of which originate from fields other than nuclear.

At the present time, the following individual data libraries compose the total body of nuclear data available at the centre:

1. The international catalog of bibliographical neutron data CINDA which comprises the entire bibliographical information on neutron data including references to both experimental and theoretical works. CINDA also serves as the catalog to the experimental data library EXFOR. In addition the centre also has a number of programs for the formatting of data, as well as programs for searching and retrieving information according to any desired parameter.

2. The international library of experimental neutron data EXFOR which contains experimental data from 8000 individual neutron physics measurements (comprising more than 45000 sets of data composed of 3.5 million data records). In addition, the EXFOR library has associated with it a number of computer programs for checking the integrity of the library, for searching and retrieving data from the library, for reformatting the information and to represent them in a graphical form.

3. The international library of nuclear structure and decay data ENSDF which contains all available data on nuclear decay schemes, half-lives and the spectroscopic properties of nuclear transitions.

4. The Russian library of evaluated neutron data BROND-2.2 which contains 121 complete files for fissile, construction and technological materials, for fission products, stored in the ENDF/B-VI format. This library is serviced by a series of programs, written for the ENDF-6 format.

5. The U.S. library of evaluated neutron data ENDF/B-VI which contains 250 files for the stable and actinides isotopes, and 70 fission product files. This is supplemented by specialized libraries, namely: - thermal scattering law neutron data, - radioactive decay data, - fission product decay data, - photon interaction data, - data on the interaction of neutrons and protons with the isotopes ^{12}C, ^{56}Fe, ^{208}Pb and ^{209}Bi at high energies.

6. The Japanese library of evaluated nuclear data JENDL-3 which contains data for 324 nuclides (including 172 fission product files) in ENDF-6 format.

7. The Chinese library of evaluated nuclear data CENDL-2 which contains 53 full files of neutron data.

8. The west European library of evaluated nuclear data JEF-2 which contains evaluated data for 303 elements and isotopes and 4 specialized libraries: - thermal scattering law data, - nuclear decay data, - fission product yield data, - photon interaction data.

9. The Russian activation data library ADL-3 which contains more than 30000 neutron reaction excitation functions for stable and radioactive nuclides, including isomeric states.

10. The European library of activation data EAF-2 which contains neutron induced cross section for 11000 reactions with 667 nuclides.

11. The Russian library of evaluated nuclear data for intermediate energies MENDL which contains 60000 excitation functions for 500 nuclides for incident neutron energies up to 100 MeV.

12. The international (IAEA) dosimetry file IRDF-90 which contains data for 44 reactions used in reactor dosimetry and as standards in neutron data measurements.

13. The Russian dosimetry file RDF-94 which contains 40 reactions used in reactor dosimetry and as standards in neutron data measurements.

14. The Russian library of photoneutron data BOFOD which contains cross sections for the interaction of photons with nuclides of 27 materials ranging from Be-9 to Am-243.

15. The Russian library of fission product yield data ACIYaD which contains fission product yield data for 21 fissile nuclei, ranging from uranium to curium.

Conclusion

This article describes the achievement of the research that has led to the establishment of a national data bank of nuclear data for the benefit of the national economy. The following has been achieved:

- Requirements for the need of nuclear data in the most important fields of nuclear technology have been identified, and methods to optimize the required uncertainties in evaluated nuclear data have been formulated.

- A program for the experimental and theoretical research aimed at investigating nuclear structure and the mechanisms of the interaction of neutrons with nuclides has been implemented. This program has the objective to devise theoretical models to guarantee the reliability of calculated results.

- Improved and newly derived physical representations of the optical properties of the nucleus, the nuclear level densities, equilibrium or non-equilibrium processes, the structure of the fission barrier, fission channels, the dynamics of fission and others, are reflected in new theoretical models and were implemented in the generation of evaluated neutron data files.

- Using the result of a critical analysis of the international body of experimentally determined data, and using contemporary theoretical models of the interaction of neutrons with nuclei has made it possible to generate evaluated neutron data and to create a national library of recommended evaluated neutron data.

- The activity of the TsYaD centre in the collection of neutron data and the exchange of these data with the IAEA has made it possible to make available the entire body of experimental and evaluated neutron data to the Russian users.

Based on this technical and theoretical foundation, this system has the ability to solve new problems in the measurement of neutron data as well as in the generation of improved files of evaluated neutron data.

BNAB-93 GROUP DATA LIBRARY
PART 1: NUCLEAR DATA FOR THE CALCULATION OF NEUTRON AND PHOTON RADIATION FIELDS

G. N. Manturov, M.N. Nikolaev, A.M. Tsibulya

State Research Centre of the Russian Federation
Institute of Physics and Power Engineering, Obninsk

Abstract

This paper is the first in a series of publications dedicated to the description of the new Russian multigroup data set BNAB-93. The first part of this series is devoted to the description of the neutron and photon data and their formats, and to their use in calculations.

Foreword

This paper is the first in a series of publications dedicated to the complete description of the new BNAB-93 Russian multigroup data system. This system is specifically intended for the computation of the design of nuclear reactors of various spectral classes, radiation shielding, the evaluation of the overall radiation environment as well as other practical problems. The BNAB-93 multigroup data set incorporates a system of algorithms designed for the processing and preparation of the data; these are then used in the calculation of the CONSYST2 data which serve as the State standard reference data (SSRD). These data are then certified and added to the category of recommended State reference data (RSRD), certified by the VNITsSMV licence No. 444, dated 01.08.95.

This license was issued on the basis of information compiled in a special verification report [1] and on the recommendation of a committee of experts confirming the suitability of the BNAB-93 multigroup data set to be used in engineering computations in various fields of nuclear technology. The proposed series of publications is designed to complement the verification documentation whose content is presented in a rather condensed form. On the other hand, it is also intended to include in this series of publications a variety of information obtained after the release of the above mentioned documentation.

The first part of this report describes the general structure of the BNAB-93 data set and the neutron and photon data formats. Subsequent parts of this documentation will consist of the description of supplementary data required for the calculation of a radiation environment

resulting from spent nuclear fuel and recovered reactor components. The sources of information used in the derivation of the BNAB-93 data and the methodology used in actual multigroup calculations will also be described. Test results using the BNAB-93 data and their comparison with evaluated macroscopic and integral experiments, as well as the comparison of results using BNAB-93 data with corresponding international reactor and shielding test calculations will be presented. It is also foreseen to present the evaluation methodology used in the determination of the uncertainties in the calculational predictions when using the BNAB-93 multigroup data.

Introduction

In the field of nuclear technology, a number of different nuclear data are needed to perform a variety of calculations:

- neutron cross sections and spectra of scattered neutrons are needed in reactor and shielding calculations, in the calculations of nuclear safety at fuel processing plants,
- data on the formation of gamma rays in neutron reactions and their interactions with matter are needed in shielding calculations and calculate the heating generated in reactor components,
- cross sections of reactions leading to the formation of radionuclides; the decay characteristics of these nuclides are needed in the calculation of the isotopic composition and radiation emission characteristics of the reactor fuel and reactor components.

The calculations that require various nuclear data are not only performed in the field of nuclear technology, but also in the fields of radiation medicine, mineral exploration, activation analysis, and in a number of other fields.

What is the source of these data?

At the present time there exist a few large computerized libraries of so-called evaluated nuclear data. In our country, the name of such a library is called BROND [2] - the Library of Recommended Evaluated Neutron Data. The quality and completeness of the data in this library is not any worse than the equivalent libraries in other countries, such as ENDF/B in the USA, JENDL in Japan and JEF in Western Europe. Non-neutron nuclear data (e.g., decay characteristics, nuclear structure data, etc...) are stored in another large computerizes library, called ENSDF, which is also accessible to Russian specialists. There are also computerized libraries of data on the interaction of gamma rays with matter.

However, even though the data are available, it does not necessarily mean that the accuracy of the existing data meets the required accuracy specifications. The problem is that the volume of the data stored in these data libraries is very large, and that the structure of the data themselves is at the same extremely complex. Therefore, a straight forewarn treatment of the evaluated data in engineering calculations is unthinkable (at least from a practical point of view). The nuclear data that are used in engineering computational programs are called "nuclear constants".

These nuclear constants are the same nuclear data that have been transformed into a more

compact and convenient format that is adaptable to practical computations. It stands to reason that the transformation of nuclear data into a compact format is inadvertently coupled with a loss of information and accuracy that were contained in the original evaluated nuclear data libraries. However, it turns out that there are means to obtain nuclear constants for which the loss of information becomes insignificant from a practical point of view, and which at the same time reduces the volume of the transformed information by factors of ten. This simplifies and standardizes the structure of the data considerably.

Thus, what is needed for practical calculations, is not the actual nuclear data but the nuclear constants which have been derived from them.

As mentioned above, various nuclear constants are needed for various computational tasks. In addition to the fact that the most complex requirements for nuclear constants are for neutron physics calculations, the structure of neutron data is extremely complex. The smooth energy dependence of some neutron cross sections is interrupted by an immense number of resonances of the most different shapes; also, the spectra of scattered neutrons can be quite complicated, especially if they are correlated with their angular distributions which are themselves by no means simple.

The multigroup method, its description and theory [3] has been developed in order to have a practical means to treat the interactions of neutrons with matter. The group constants which are used in the application of multigroup calculations, describe the interaction of neutrons with matter, by means of cross sections which have been averaged over wide energy intervals. Inasmuch as the actual cross sections can vary by orders of magnitude in these intervals, the averaging results depends on a number of factors (e.g., the concentration of nuclides in the material, the temperature, etc...). In order to take these dependencies into consideration, so-called selfshielding factors are entered into the group constants as a correction. Additional group constants describe neutron spectra and angular distributions.

The number of groups needed to describe the dependence of the cross section without substantially loosing the accuracy of the cross section value, varies from a few tens to a few hundreds (based on the current knowledge of neutron cross sections).

The interaction of photons with matter is similarly described by multigroup approximations. As the photon interaction cross sections, which are important primarily at energies that are not too low, their dependence on energy is much more straightforward than the neutron cross section dependence; it is therefore acceptable to use a smaller number of groups (i.e., varying from one to a few tens). The generation of photons in neutron reactions are described by matrices of the form of $\gamma^{l}_{g\,j}$, where photons from group number j, are formed by the interaction of a neutron from group g with nuclide l.

In the course of the last few years (since the beginning of the 1960's), a group of multigroup specialists at the FEI institute, has been working on the creation of multigroup constants for the calculation of fast breeder reactors that have been developed at the institute. In 1962, this group, under the leadership of I.I. Bondarenko, concluded the development of the 26-group set of constants which was later given the designation BNAB-64 (the designation was

composed by using the first letters of each of the four authors of the working group (namely, I.I. Bondarenko, M.N. Nikolaev, L.P. Abagyan and N.O.Bazazyants) and the year of its release [6]. In 1970, this multigroup set of data was updated in order to take into account results of new experimental measurements of the fuel nuclide cross sections and data on $\alpha=\sigma_c / \sigma_f$ for ^{235}U and ^{239}Pu . That multigroup set was given the designation BNAB-70, which was successfully implemented in fast reactor calculations. One of the main features of the BNAB-64 set was the incorporation of cross section selfshielding factors (so-called Bondarenko factors) and the Doppler effect in order to take resonances into account. Another improvement in the representation of resonance selfshielding, proposed by M.N.Nikolaev, was the introduction of subgroups [7]. The conversion of the BNAB-70 set to the new version was accomplished using the ARAMAKO program [8]. The new BNAB-ARAMAKO set of group constants was implemented not only for the calculation of fast reactors, but for radiation shielding design as well. For that purpose, it was necessary to introduce additional information on the anisotropy of elastic scattering using P_5 approximations (in the BNAB-64 multigroup set, the scattering anisotropy was taken into account using P_1 approximations), and on a photon generation matrix in order to describe the interaction of photons with matter. As a result of these improvements, the new BNAB-70 multigroup data set became in fact the first complete version of the BNAB multigroup system

The second complete version of the BNAB data system was developed in the year 1978. Although it was only published in 1981 [9], it was designated as BNAB-78. This multigroup set included data for a large number of nuclides, and incorporated data for a zeroeth and a minus first energy groups which allowed extending the investigated energy range from 10.5 MeV to 15 MeV, thus including the range of interest to fusion. But the most important attribute of this set, was that it was certified and corrected on the basis of results obtained from the analyses of many fast critical assemblies and integral experiments; this increased the reliability and usefulness of this set of constants considerably and of their use in the calculations of fast reactors. This multigroup set also included covariance matrices for the group constants' uncertainties which made it possible to perform quantitative evaluations of the accuracies of computed predictions. The BNAB-78 multigroup set together with the improved version of the ARAMAKO-C1 [10] program has been accepted as the standard computational system for the calculation of fast reactors. It was also widely used for the calculation of radiation shielding. In the 1980's, the BNAB multigroup constants were expanded to be able to perform thermal reactor calculations, and to describe the interaction of neutrons with matter in the unresolved and non-resonance regions of energy [11]. The BNAB-78 set of data together with the ARAMAKO-C1 program became the second complete version of the BNAB multigroup system.

The BNAB-93 multigroup set, described in this paper, is the third complete version of this system. The principal task assigned to this set of data was to create a universal multigroup system, that is, the applicability of the system to the calculation of neutron reactors of any spectral class, to the design of any required radiation shielding, to the analysis of thermonuclear blankets and electro-nuclear installation, as well as to the evaluation of the radiation environment at nuclear power plants. The existence of such a system is a prerequisite so as to be able to compare results obtained at different installations, as well as to guarantee the correct analysis of an investigated emergency situation which may be coupled with a sharp oscillation of the neutron spectrum in the reactor core (e.g., the loss of the

coolant/moderator in a thermal reactor, the penetration of water or oil into the core of a fast reactor).

Another important aspect of the viability of such a system is the preservation of the world-wide collection of nuclear data in a format adaptable for their immediate use in calculations. The situation that stimulated the development of the new set of constants was the change-over from the EhVM-EC computer, for which the ARAMAKO-C1 program was written, to IBM PC personal computers. In addition there was a need to be able to assimilate a number of computer programs written in the West for reactor, shielding and radiation environment calculations.

In order to achieve the assigned task , it was first of all necessary to develop this system using the latest evaluated nuclear data. It was also necessary to enlarge the list of the types of constants, to maximize the number of nuclides, and to be able to perform calculations using a substantially larger number of groups than the maximum 28 possible in the BNAB-78 multigroup system. On the basis of a series of calculations, it was found that by increasing the number of groups by a factor of ten, it was possible to lower the systematic component of the calculated error to a level lower than the error introduced by the inexact knowledge of the neutron cross sections. The new, more detailed energy grouping was arrived at by subdividing each earlier energy group into a few narrower ones. By subdividing the thermal energy region into a number of finer groups, it was possible to accurately describe the thermalization of neutrons. The maximum possible number of groups in the new system is 299. However, this limitation does not prevent the user from using a smaller number of groups, and in routine engineering calculations, it is recommended to perform 28 or 26 group calculations. Normally, the 299 group approximation is used primarily in the determination of the group constants.

The BNAB designation of this multigroup system unfortunately does not reflect the composition of the original group of specialists that worked on this task (as half of the authors of the BNAB-64 system have already died). However, by keeping this same designation does not only reflect an attempt to maintain the continuity of this effort, but also by the fact that the same principles that were developed by the original group (primarily by I.I.Bondarenko) in the formulation of the BNAB-64 were used in the development of the BNAB-93 system. Namely, deriving the evaluated data from the results of differential nuclear physics experiments, the checking of the data against the results from integral and macroscopic experiments, and the insistent identification and elimination of the underlying reasons for discrepancies. The methodologies recommended for the practical use of the BNAB-93 system of constants are the same as those developed during the utilization of earlier versions of the BNAB systems.

2. Structure of the BNAB-93 Library of Nuclear Constants

2.1 The standard BNAB format

The BNAB library contains the following types of nuclear constants:

- various neutron constants, including constants required to calculate the generation of photons in nuclear reactions,
- constants required for the description of the interaction of photons with matter, and
- constants describing the radiation characteristics of radionuclides which are generated in neutron induced neutron reactions .

All these constants are stored in the BNAB library in the form of so-called "standard format tables" which differ depending on whether a) the data are presented in a clear manner, which is important if the data are to be checked visually, or b) the data can be read using a universal standard procedure independent of the concrete content of the tabulated data. Thus, it can be said that the data tabulated in the BNAB library are stored simultaneously in a "people-readable" and a "computer-readable" format.

It can be said that the BNAB standard format tables have a formalized structure.
The information content of the BNAB library can be separated into two parts: a) the headers, which contain the description of the data, and b) the data themselves.

The BNAB constants are grouped according to nuclides, and each individual nuclide group is subdivided into files. A special algorithm was written to retrieve BNAB tabulated data and allows the consolidation of data into one file.

Each data file is composed of a few standard BNAB tables, each of which containing data of a given type. The description of the format and the rules to use each type of data shall be described in a separate chapter.

The header part of the BNAB library data has the same general appearance as the data tabulation for a given nuclide: that is, it consists of a few standard tables. The file bears the standard designation "HEAD".

The standard BNAB table format is rather general and is independent of the specific group subdivision, for instance that which was adopted in the BNAB-93 system. Nevertheless, in order to be able to understand the specific description of tables of constants of a given type, one has to take into account the cross section group structure incorporated in the BNAB constants. This structure is as follows: the neutron energy range under investigation is subdivided into a number of energy intervals (28 intervals in the case of the current version), and neutrons having an energy which fall within the same interval are consolidated into one group.

Each energy group is subdivided into a specific number of energy subgroups, whereby they must not necessarily be of the same width. If the boundaries of groups are arbitrary, generally speaking, then all subgroups of each group must necessarily be equal in the lethargy scale. The only exception is in the case of the lowest "thermal" energy group, where the widths of the subgroups on the lethargy scale must not be equal.

In the BNAB-93 system of constants, the number of groups is equal to 28 (traditionally, they are numbered from -1 to 26), and the number of subgroups within groups varies from 5 to 12, but in the thermal group there are 25 subgroups.

In the case of photons, the dependence of their cross sections on energy is limited to group subdivision only. The number of photon groups in the BNAB-93 system is 15.

The standard BNAB table consists of text information consisting of rows (so-called in ASCI representation). Each row consists of no more than 72 Hollerith characters. The * character in the first location of a line is a flag indicating that this line contains only commentary information; in the case of algorithmic notation, these lines are ignored.

The standard BNAB table consists of two "header rows" and the actual tabulated data. The structure of the data in the standard BNAB table can best be described by an example:

Decay characteristics of isotopes

```
 NAM=FE       LIB=NUCL  MF=  90 MT=   0 AWR= 55.3650     DAT= .010393
 LV = 12      L  =  13  LC=  12 LS=  12  LF= (I4,2A2,E6.0,5E7.0,3E8.0)
```

* A	T1/2	BETA+	BETA-	IT	ALFA	SF	E-GAM	E-LOC	E-TOT
520 - h	8.275	100.					0.740	0.193	0.933
521 - s	45.9	100.					3.63	2.00	5.63
530 - m	8.51	100.					1.152	1.042	2.194
531 - m	2.5			100.			3.011		3.011
540 A				5.8					
550 - y	2.7	100.					0.00169	0.0042	0.006
560 A				91.7					
570 A				2.2					
580 A				0.3					
590 - d	44.53		100.				1.19	0.117	1.307
600 - y	1.0+5		100.					0.0491	0.049
610 - m	6.0		100.				1.391	1.055	2.446
620 - s	68.		100				0.506	0.844	1.350

The meaning of the used abbreviations is as follows:

NAM - field for the designation of the Hollerith name of the nuclide for which the data is given in the data table in (A12) format;

LIB - field to indicate the source of the data used to determine the group constants (A4) format;

AWR - field for numerical data parameter of a general nature (here, it gives the ratio of the nuclide mass to the mass of the neutron) in (E8.0) format;

DAT - field for a second numerical parameter in (E8.0) format (note that in a table of this type the entry of a numerical parameter is not foreseen, and in this example, the parameters are entered to illustrate the possibilities available to use this field);

MF - identification number of the type of table, identifying its content;

MT - additional number identifying the type of table, giving more content information;

LT - the number of data lines comprised in the table;

LC - the number of columns in the table;

LS - parameter used if the table is divided into parts (if the table is composed of one part only, then LS=LC), and the number of columns in all parts of the table is the same, with the exception of the last part. For example, if LC is so large that the LC number of columns takes up more than 72 row positions, it is subdivided into a few parts. The number of such parts is determined by LC=(LC-1)/(LS+1). So that the first part consists of the first LS columns, occupying not more than 72 row positions, in the second part, the first header column is repeated and is followed by the LS-1 columns which did not fit in the first part of the table (the total number of columns is equal to LS). The header column is always the first in all the parts of the table. In the last part of the table, the header column is followed by the remaining LC-1- LS(P-1) columns.

All parts of a table have the same reading format.

LF - data reading format. The main part of the FORMAT operator determines the data reading format of the quantities entered on one part of the table. If the main part of the FORMAT operator is too large to be accommodated on the remaining part of the row, then that part of the row is filled up with blanks, and the main part of the FORMAT operator is entered on the next row;

LV - identifier that specifies the order of the quantities of various types. The quantities may be of INTEGER type, or of CHARACTER type, or of REAL type. There are two possible variants in which quantities of various types may be ordered. In the first variant, the LI quantities of INTEGER type are first, followed by LH quantities of CHARACTER type, followed by LR=LS-LI-LH quantities of type REAL. In the second variant, LH quantities of type CHARACTER come first, followed by LI quantities of INTEGER type, and the quantities of type REAL are as before last. There are limitations in both variants: LH≤ 8 always and LI≤ 8 for LR≠0. LI=9 is permissible , but that means that LI=LS-LH. The values of LI and LV and the quantities of various types that follow are determined by the identifier LV:

a) if LV > 0 the first quantity order variant is used: LI=LV/10 (LI≤ 9)
LH=LV-LI (LH≤ 8)

b) if LV < 0 the second quantity order variant is used: LH=-LV/10 (LH≤8)
LI=-LV-LH (LI≤9)

(The values LI=0 and/or LH=0 is permissible as well)

c) if the LV field is omitted, the standard quantity order variant is used: for subgroup data and blocking factors, the first two INTEGER fields and the remaining LS-2 REAL type fields, and for the other data types, the first INTEGER field and the remaining LS-1 REAL type fields.

The main body of the standard BNAB table is not described in this part of the report. However, it is clear that the tabulated data correspond structurally to the description given in the FORMAT operator.

The coding formats of two standard header row are as follows:

FORMAT(4X,A8,5X,A4,1X,2(4X,I4),2(5X,E12.0)),
FORMAT(4X,I3,10X,I4,1X,2(4X,I4),5X,A29).

It is mandatory that the values assigned to the identifiers, NAM, MF, MT, LT, LC, LS as well as to the quantity LV which determines LI and LH, are consistent and are in agreement with the values entered in the body of the FORMAT operator. The assignment of quantities to the identifiers BIB, AWR, and DAT are not required for all tables. If the content of the table does not require the assignment of specific values to these parameters, then these parameters and their identifiers in the header may be omitted. The identifiers of the latter, optional parameters can be designated by any three letter word (even by a four letter designator if the space used by the identifier is available).

As a rule, numerical data of the REAL type are represented as fixed point variables. This simplifies considerably the visual data analysis, and the detection of errors introduced either in the course of the processing of the original evaluated data or during the reprocessing of the data. It is essential for the benefit of those responsible for the visual analysis of the tabulated BNAB data, that these data be presented in a most convenient form.

2.2 Numerical content of the BNAB-93 library

As indicated above, all BNAB tables are characterized by two parameters, MF and MT. One describes the physics content of the table, and the other contains additional specifications. In addition to the MF and MT specifications there is the possibility to use additional abbreviated semantic specifications in the form of [MF,MT]; for instance [1,0] for a BNAB table where MF=1 and MT=0.

The following lists all BNAB type constants that can be used in the BNAB library.

MF	MT	Content
0	0	- BNAB-93 library catalog (a list of all nuclides for which there is information, list of data table types for each of these nuclides, etc...)
0	1	- Group structure of the neutron data.
0	2	- List of dilution cross sections, for which values of resonance selfshielding factors are entered.
0	3	- List of temperatures for which resonance selfshielding factors are entered. Currently this list consists of three temperatures: T=300K, T=900K and T=2100K.
0	4	- Energies at which cross section values in the thermal energy range are entered.
0	5	- Group structure for photon data.

(Other values for MT for MF=0 tables containing general information for the whole library are not specified at this time.)

MF	MT	Content (continued)
1	0	- Basic neutron constants required for neutron transport calculations.
2	0	- Cross section matrix for the inter-group transitions in inelastic scattering $p_{in}^{g\to k}$.
2	1	- First angular momentum matrix for inter-group transitions in inelastic $\omega_{in}^{g\to k}$ scattering. The moments were determined such that the differential slowing down cross section from group g to group k in the P_1 approximation is equal to

$$\sigma_{in}^{g\to k}\left(\overline{\Omega}\right)=\frac{\sigma_{in}}{4\pi}\times\left(p_{in}^{g\to k}+3\times\omega_{in,1}^{g\to k}\times\overline{\Omega}\right). \qquad (2.1)$$

3	0	- Angular momentum probability matrix for inter-group transitions in inelastic scattering, leaving the neutron in the group.
3	1	- Angular momentum probability matrix for inter-group transitions in inelastic scattering with the accompanying slowing down to the neighboring group.
3	k	- Angular momentum probability matrix for inter-group transitions in inelastic scattering with the accompanying slowing down from group g to group (g+k)

$$\sigma_{e}^{g\to k}\left(\overline{\Omega}\right)=\frac{\sigma_{e}}{4\pi}\times\sum_{n=0}^{N}(2n+1)\times\omega_{e}^{g\to k}\times P_n(\mu). \qquad (2.2)$$

4	k	- Resonance selfshielding factors for cross sections at the minimum temperature of 300K:

For k=1	factors for the total cross section
For k=2	factors for the inelastic scattering
For k=18	factors for the fission cross section
For k=102	factors for the capture cross sections.

5	k	- Resonance selfshielding Doppler shift factor:

For k=1	for the total cross sections
For k=2	for the inelastic scattering cross sections
For k=18	for the fission cross sections
For k=102	for the capture cross sections.

For the total cross section, the Doppler shift factors are determined by averaging over the spectrum:

$$\Delta f_{t,1}^{(1)}=f_{t,1}(T_2=900K)-f_{t,1}(T_1=300K) \qquad (2.3a)$$

$$\Delta f_{t,1}^{(2)}=f_{t,1}(T_3=2100K)-f_{t,1}(T_2=900K) \qquad (2.3б)$$

MF MT Content (continued)

For the inelastic scattering, capture and fission cross sections, the Doppler shift factor is determined in the same manner using:

$$\Delta f_e^{(1)} = f_e\left(T_2 = 900K\right) - f_e\left(T_1 = 300K\right) \quad (2.4a)$$

$$\Delta f_e^{(2)} = f_e\left(T_3 = 2100K\right) - f_e\left(T_2 = 900K\right) \quad (2.4б)$$

6 0 - Subgroup parameters for the resonance cross section structure. For LC=5, parameters are determined for the minimum 300K temperature. For LC=11, the subgroup cross sections are given for all of the listed temperatures. Subgroup contributions do not depend on temperature.

7 0 - Westcott G-factors for the averaging of the thermal group cross sections.

8 0 - Energy emission characteristics in neutron reactions.

9 0 - Neutron reaction cross sections and characteristics of material damage.

10 0 / 1 -Multiplicity of photons generated in specific energy groups $\gamma_{g,r}^{j}$ as a result of neutron interactions; where g is the number of the neutron group, j the number of the photon group, r the reaction type (when r=c or r=in or r=f).

11 0 - Cross sections for the interactions of photons with matter.

15 0 - Characteristics of delayed fission neutrons.

The above listed quantities are available in the form of 28-group constants. Subgroup data are given under the designation MF=MF+300.

70 0 - Parameters α_l^g (l=0,1,2,3,4,5) which determine the lth angular momentum of the cross section for the transition from one energy group to another for slowing down in hydrogen.

70 1 - Parameters β_l^g (l=0,1,2,3,4,5) which determine the lth angular momentum of the cross section for the transition for slowing down in hydrogen.

The following MF numbers, from 71 to 79, are assigned to data that characterizes fission product characteristics:

71 0 - Description of isobaric fission product decay chains.

72 0 - Cumulative yields of poisonous fission products.

72 ½/3 - Independent fission product yields for three energy ranges: MT=1 - thermal neutrons, MT=2 - fast neutrons, and MT=3 - fusion neutrons.

73 10 - Data for the calculation of delayed heat generation as a result of radioactive decay of fission products.

The following MF numbers, from 90 to 99 are assigned to radionuclide decay data.

90 0 - Decay characteristics of radioactive isotopes (half lives, branching ratios, total energy emission by photons and charged particles), and isotopic abundances for stable nuclides.

91 4 - Multiplicity of photons generated during the radioactive decay of nuclides. Group spectra and yields for the four strongest gamma ray row. The value for MT=4 gives the number of the gamma ray.

The following data tables for MF>300 are assigned to subgroup constants.

301 0 - Basic neutron subgroup constants.

302 g - First angular momentum probability matrix for inter-group transitions in inelastic scattering of group g neutrons.

303 k - Angular momentum probability matrix for inter-group transitions in inelastic scattering with slowing down from subgroup (g,m) to the subgroup having a value k larger.

304 k - Resonance shielding factors for cross sections:
- For k=1 for the total cross sections
- For k=2 for the inelastic cross sections
- For k=18 for the fission cross sections
- For k= 102 for the capture cross sections.

305 k - Resonance selfshielding Doppler shift factor:
- For k=1 for the total cross sections
- For k=2 for the inelastic cross sections
- For k=18 for the fission cross sections
- For k=102 for the capture cross sections.

306 0 - Subgroup parameters for multigroups

307 TEM - Thermalization scattering matrix, where TEM is the temperature of the neutron gas.

370 0/1 - The $\alpha_l^{g,m}$ и $\beta_l^{g,m}$ (l=0,1,2,3,4,5) parameters for the calculation of angular momentum transition matrix for scattering in hydrogen.

3. General Characteristics of the BNAB-93 Constants

3.1 Naming of materials

For ease of searching, materials (nuclides) in the BNAB system are represented by an eight-digit word, even though many existing programs use four-digit words for that purpose. However, in order to simplify the introduction of the new version of the BNAB systems, at the present time the designators used in the new system will consist of the first four symbols of the material designator. The following rules are used in the designation of materials.

The first two symbols are used to enter the chemical symbol of the nuclide. If the chemical symbol consists of only one digit (e.g., H, B, U and others), the following three possibilities exist: 1) if the nuclide in question consists of the natural mixture of isotopes, the second location is a blank; 2) if the atomic number of the nuclide is smaller than 100, the second symbol is a dash; 3) if the atomic number is greater than 100, the second symbol is the one hundred number of the atomic number. Thus, for hydrogen the designator is "H ", for boron it is "B-", and for iodine and uranium they are "I1" and "U2".

The second two symbols in the nuclide designator are used normally to indicate the isotope; in the case of a natural mixture of isotopes, these two locations are filled with blanks. An exception to this rule is the case of hydrogen H (and the natural mixture of the hydrogen isotopes); in this case, D is used for deuterium and T is used for tritium.

In the naming of the isotope, the last two locations are normally used to indicate the tens and ones numbers of the atomic number of the nuclide in question. For instance: ^{63}Cu is designated by "CU63", ^{98}Mo is designated by "MO98", and ^{100}Mo by "MO00" (natural molybdenum is designated bu "MO"), ^{127}I by "I127", ^{235}U by "U235".

In addition, there are the following exceptions to the general rules:

- helium and lithium isotopes are identified by a dash "-": HE-3, HE-4, LI-6 and LI-7.
- isomeric states are identified by the symbol "M" or "N" in the last position ("M" for the first isomeric state and "N" for the second). The third symbol is the number of digits in the atomic number of the nuclide; for instance: ^{242}Am^{m} by AM2M, and ^{192}Ir^{m1} by IR2N which is the second (long-lived) isomer of iridium-192.

- In addition, there are a number of artificial materials in the BNAB system for which neutron data can be given; these designators are as follows:

  "CAPT" - pure absorbers (capture cross sections in all groups are given the value of 1 barn, and are equal to the total cross section);
  "SCAT" - pure scatterers (inelastic cross sections in all groups are given the value of 1 barn and are equal to the total cross section; scattering is isotropic and slowing down is absent);
  "D-SC" - pure delta scatterers (scattering cross sections are equal to 1 barn, neither the direction nor the energy of the scattered neutrons are changed upon scattering);
  "HYDR" - hydrogen with an effective inter-group transition matrix (the slowing down occurs only to the neighboring group):
  "FP35" - uranium-235 fission product yields excluding the contribution of six poison fission products: ^{113}Cd, ^{135}Xe, ^{149}Sm, ^{151}Sm, ^{155}Gd and ^{157}Gd.
  "FP39" - plutonium-239 fission products excluding the contribution of six poison fission products;
  "SLAG" - uranium-235 fission products excluding the contribution of fifteen poison fission products (in addition to the above-mentioned: ^{99}Tc, ^{103}Rh, ^{109}Ag, ^{131}Xe, ^{133}Cs, ^{143}Nd, ^{147}Pm and ^{152}Sm;

In the BNAB-93 system of constants, there are large numbers of neutron data for materials subjected to the above-listed rules. However, there are additional materials for which special data types are called for, for instance to have inter-group scattering matrices to account for the thermal movement of atoms and their effects on molecules and crystals. The current version of the BNAB-93 data library does not have any general rules to include such materials. Materials can be described using any eight symbol designator, such as "H(H2O)', "H(ZRH)", "BE(BEO)", "C(GRAPH)", etc... The list of designators of all materials which require a thermalization matrix will be given in the next chapter.

The designator "HEAD" is used to describe the material and associated information contained in the BNAB tables. The identification of the nuclides as such is entered as part of the data table information. For instance, the designation of the nuclide which results from a neutron reaction is required in the table of neutron reaction cross sections. In such cases, the nuclides are not described to be accessed by using a text search method, rather, they are coded in the form of a six symbol word in the form of (Zx10000)+(Ax10)+M ; where Z is the atomic number of the isotope, A is the mass number and M is the isomeric state designator (and zero for the ground state).

3.2 The content of the BNAB-93 library

The content of the BNAB-93 library of nuclear constants is described in the MF=0 and MT=0 table of the "HEAD" file (see Table 1). The body of the table [0,0] contains, on one row after the other, each file included in the library, except for the heading. If a file for a given nuclide, whose designator is included in the given row, does not include a table having the designator MF, then, the field in that column is filled with blanks; if on the other hand there is at least one table, then the number of such tables is entered. In some special cases, the value of MT for the one table is entered instead of the number of tables given by the given value of MF. Note that the [0,0] table does not contain information on the presence of fission product data and thermalization matrix data in the library. Such data are stored in separate libraries.

Table 1. Content of the BNAB-93 library of nuclear constants

```
NAM=HEAD      BIB=BN93  MF=  0  MT=  0                    DAT= .010393
LV = -19      LT =150   LC= 20  LS= 20  LF = (A4,11I3,6I4,2I3)

*NAM  1  2  3  4  5  6  7  9 10 11 15 301 302 303 304 305 306 90 91
H     1     15                1  1  1      1                      1  1
D     1  2  5
T     1  2  5
HE    1     4                 1     1                           1  1
HE-3  1  2  5
LI                            1     1                           1  1
LI-6  1  2  3                    1
LI-7  1  2  3                    1
BE    1  2  3                 1  1  1                           1  1
B                             1     1                           1  1
B-10  1  2  3                                1
B-11  1  2  3
C     1  2  3  2     1        1  1  1      1        7            1  1
N     1  2  2  3     1        1  1  1                           1  1
N-15  1  2  2  2     1
O     1  2  2  3     1        1  1  1      1        5  3         1  1
F     1  1  2  3     1        1  1  1                           1  1
NE                            1                                 1  1
NA    1  2  2  3     1        1  1  1      1  1     4  3         1  1
MG    1  1  2  3     1        1  1  1                           1  1
AL    1  1  2  3     1        1  1  1                           1  1
```

Table 1. (Continued)

*NAM	1	2	3	4	5	6	7	9	10	11	15	301	302	303	304	305	306	90	91
SI	1	1	2	3		1		1	1	1								1	1
P	1	1	2	3		1		1	1	1								1	1
S	1	1	2	3		1		1	1	1								1	1
CL	1	1	2	3		1		1	1	1								1	1
AR	1	1	2					1	1									1	1
K	1	1	2	3		1		1	1	1								1	1
CA	1	1	2	3		1		1	1	1								1	1
SC	1	1	2					1	1	1								1	1
TI	1	1	2	3		1		1	1	1								1	1
V	1	1	2	3		1		1	1	1								1	1
CR	1	1	2	3		1		1	1	1								1	1
MN	1	1	2	3		1		1	1	1								1	1
FE	1	1	2	3	1	1		1	1	1		1	1	3	4		1	1	1
CO	1	1	2	3		1		1	1	1								1	1
NI	1	1	2	3		1		1	1	1								1	1
CU	1	1	2	3		1		1	1	1								1	1
ZN	1	1	2	3		1		1	1	1								1	1
GA	1	1	2	3		1		1	1	1								1	1
GE	1	1	2	3				1	1	1								1	1
AS	1	1	2	3	3	1		1	1	1								1	1
SE	1	1	2					1	1	1								1	1
BR	1	1	2	3		1		1	1	1								1	1
KR								1											1
RB								1											1
SR	1	1	2	1				1											1
SR89	1	1	2																
SR90	1	1	7																
Y	1	1	2	3	3	1		1	1	1								1	1
ZR	1	1	2	3	3	1		1	1	1								1	1
NB	1	1	2	3	3	1		1	1	1								1	1
MO	1	1	2	3	3	1		1	1	1								1	1
MO95	1	1	2	3	3														
MO97	1	1	2	3	3														
TC	1	1	2	3	3	1		1	1	1								1	1
RU	1	1	2					1	1	1								1	1
RU01	1	1	2	3	3														
RH	1	1	2	3	3	1		1	1	1								1	1
PD	1	1	2					1	1	1								1	1
PD05	1	1	2	3	3														
PD07	1	1	2	3	3														
AG	1	1	2	3	3	1		1	1	1								1	1
AG09	1	1	2	3	3														
CD	1	1	2	3	3	1	1	1	1	1								1	1
CD13	1	1	2																
IN	1	1	2					1	1	1								1	1
SN	1	1	2					1	1	1								1	1
SB	1	1	2	3	3	1		1	1	1								1	1
TE	1	1	2					1	1	1								1	1
I	1	1	2	3	3	1		1	1	1								1	1
I129	1	1	2	3	3														
XE								1		1								1	1
XE31	1	1	2	3	1														

Table 1. (Continued)

*NAM	1	2	3	4	5	6	7	9	10	11	15	301	302	303	304	305	306	90	91
XE35	1	1	2																
CS	1	1	2	3	3	1		1	1	1								1	1
CS35	1	1	2																
CS37	1	1																	
BA	1	1	2					1	1	1								1	1
LA	1	1	2	3	3	1		1	1	1								1	1
CE	1	1	2					1	1	1								1	1
PR	1	1	2	3	3	1		1	1	1								1	1
ND	1	1	2					1	1	1								1	1
ND43	1	1	2	1	1														
ND45	1	1	2	1	1														
PM								1		1								1	1
PM47	1	1	2	3	1	1													
SM	1	1	2					1	1	1								1	1
SM49	1	1	2	3	1														
SM51	1	1	2	3	1														
SM52	1	1	2	3	1														
EU	1	1	2	3	3	1		1	1	1								1	1
EU55	1	1	2				1												
GD	1	1	2	3	3	1		1	1	1		1						1	1
GD55	1	1	2	1			1												
GD57	1	1	2	1			1												
TB	1	1	2	3	3	1		1										1	1
DY	1	1	2			1		1	1	1								1	1
HO	1	1	2					1	1	1								1	1
ER	1	1	2					1	1	1								1	1
TM	1	1	2	3				1										1	1
YB								1										1	1
LU	1	1	2	3				1		1								1	1
HF	1	1	2	3	3	1	1	1	1	1								1	1
TA	1	1	2	3	3	1	1	1	1	1								1	1
W	1	1	2	3	3	1		1	1	1								1	1
RE	1	1	2	3	3	1		1	1	1								1	1
OS	1	1	2					1	1	1								1	1
IR	1	1	2					1	1	1								1	1
PT	1	1	2	3		1		1	1	1								1	1
AU	1	1	2	3	3	1		1	1	1								1	1
HG								1										1	1
TL								1										1	1
PB	1	1	2	3	1	1		1	1	1								1	1
BI	1	1	2	3		1		1	1	1								1	1
TH								1										1	1
TH30	1	1	2	3	3														
TH32	1	1	2	3	3	1			1	1	1								
PA								1		1								1	1
PA31	1	1	2	4	4	1	1		1		1								
PA33	1	1	2	3	3	1	1		1										
U								1		1								1	1
U232	1	1	2	4	4		1				1								
U233	1	1	2	4	4		1				1								
U234	1	1	2	3	3						1								
U235	1	1	2	4	4	1	1		1		1	1			4		1		
U236	1	1	2	3	3		1				1								

Table 1. (Continued)

*NAM	1	2	3	4	5	6	7	9	10	11	15	301	302	303	304	305	306	90	91
U238	1	1	2	3	3	1	1		1		1	1	1		3	3	1		
NP								1		1								1	1
NP37	1	1	2	3	3	1	1		1		1								
NP39	1	1	2																
PU								1		1								1	1
PU36	1	1	2	3	3														
PU38	1	1	2	3	3	1					1								
PU39	1	1	2	4	4	1	1				1	1			4	4	1		
PU40	1	1	2	4	4	1	1				1	1			4				
PU41	1	1	2	4	4		1				1	1			4				
PU42	1	1	2	3	3						1	1			3				
AM								1										1	1
AM41	1	1	2	3	3		1				1								
AM2M	1	1	2	3			1				1								
AM43	1	1	2	3	3		1				1								
CM								1										1	1
CM42	1	1									1								
CM43	1	1	2	4	4						1								
CM44	1	1									1								
CM45	1	1									1								
CM46	1	1	2																
CM48	1	1	2																
FP35	1	1																	
FP39	1	1																	

3.3 Entering group data into the BNAB-93 library

The 28 basic groups and 299 subgroup of nuclear data entered into the BNAB-93 data library are described in table [0,1] is shown in Table 2 below. The following designations are used in Table 2:

NG - number of the neutron group;
MS - number of subgroups;
EH - upper energy boundary of a group, in eV;
EL - lower energy boundary of a group, in eV;
DU- group width in lethargy units, DU=ln(EH/EL);
DUS - subgroup width in lethargy units;
R - flag indicating which spectrum was used in the averaging of constants within a group:

- for $R \le 2$ $\Phi(E) = E^R$
- for $2<R<10$ Watt spectrum: $\Phi(E) = \exp(-E/a) \times sh\sqrt{b \times E}$, where $a = 0{,}966(0{,}8+0{,}083R)$. $b = 2{,}243/(0{,}8+0{,}083R)^2$,
- for $R=10$ $\Phi(E) = \delta(E-0{,}0253эВ)$;
- for $R=20$ $\Phi(E) = 1$, if the energy falls within the boundaries of the lowest energy subgroup, and $\Phi(E) = 0$, if the energy falls outside of the boundaries;

- for R>20 $\Phi(E)$ is the Maxwellian spectrum with a temperature T=R degrees Kelvin:

$$1/<1/V>=13{,}831\times\left[\frac{\int_{EL}^{EU}\Phi(E)E^{-1/2}dE}{\int_{EL}^{EU}\Phi(E)dE}\right]^{-1}$$ Km/s — average velocity of neutrons of a given group (for the lifetime calculation);

$$EAV=\frac{\int_{EL}^{EU}\Phi(E)E\,dE}{\int_{EL}^{EU}\Phi(E)dE}$$ eV — average energy of neutrons of a given group;

where, BD is the dose factor which is defined as the ratio of the biological dose (given in units of millirem per second) and neutron flux density (in units of neutrons per cm^2 per second). The characteristics of the BNAB neutron energy groups are entered in the first 28 row of the table. The characteristics of the subgroups are entered in the following 25 row; the 26th being the thermal group. The analogous characteristics of the subgroups of the higher energy groups are easily calculated from the tabulated data, inasmuch as all subgroups of any of these groups have the same width in lethargy units. The number of the 26th group in the last 25 row is not entered. The BNAB-93 group subdivision for the description of the energy dependence of the cross section for the interaction of photons with matter is illustrated in table [0,5] (see Table 2). The same designations as those used in table [0,1] are used in this table. The standard spectrum used in all of the groups is F(E)=constant (i.e., R=0). The table also includes dose factors in the form of *K* coefficients, which represent the ratio of the dose (in microrems per second) to the neutron flux density (in MeV per cm^2 per second).

Table 2. Group structure for photons

NAM=HEAD BIB=BN93 MF= 0 MT= 5
LV = 10 LT = 15 LC= 4 LS= 4 LF =
(I4,2(2E10.0,E5.0))

* NG	EL	EU	R	EAV	K
1	9.00+ 6	11.00+ 7	0.	10.000+ 7	2.97- 4
2	7.00+ 6	9.00+ 6	0.	8.000+ 6	3.10- 4
3	5.50+ 6	7.00+ 6	0.	6.250+ 6	3.31- 4
4	4.50+ 6	5.50+ 6	0.	5.000+ 6	3.49- 4
5	3.50+ 6	4.50+ 6	0.	4.000+ 6	3.72- 4
6	2.50+ 6	3.50+ 6	0.	3.000+ 6	4.05- 4
7	1.75+ 6	2.50+ 6	0.	2.125+ 6	4.46- 4
8	1.25+ 6	1.75+ 6	0.	1.500+ 6	4.91- 4
9	0.75+ 6	1.25+ 6	0.	1.000+ 6	5.35- 4
10	0.35+ 6	0.75+ 6	0.	0.550+ 6	5.62- 4
11	0.15+ 6	0.35+ 6	0.	0.250+ 6	5.32- 4
12	0.08+ 6	0.15+ 6	0.	0.115+ 6	4.51- 4
13	0.04+ 6	0.08+ 6	0.	0.060+ 6	2.66- 4
14	0.02+ 6	0.04+ 6	0.	0.030+ 6	1.33- 4
15	0.00	0.02+ 6	0.	0.010+ 6	0.44- 4

Table 3. BNAB-93 group structure for neutrons

NAM=HEAD BIB=BN93 MF= 0 MT= 1 DAT= .010393
LV = 20 LT = 43 LC= 11 LS= 11 LF = (2I3,4E10.0,E5.0,2E8.0.E5.0)

*NG	MS	EL	EU	DU	DUS	R	1/<1/V>	EAV	BD
-1	5	13.9818+6	20.0+6	0.07160	0.071595	20.	52580.	14.45+6	40.
0	4	10.5 +6	13.9818+6	0.28638	0.071595	2.4	46770.	11.51+6	40.
1	6	6.5 +6	10.5 +6	0.47957	0.079929	2.4	37920.	7.607+6	41.
2	6	4.0 +6	6.5 +6	0.47000	0.078334	2.4	30390.	4.903+6	38.
3	6	2.5 +6	4.0 +6	0.48551	0.080918	2.4	24310.	3.138+6	35.
4	8	1.4 +6	2.5 +6	0.57982	0.072477	-1.	18830.	1.896+6	36.
5	8	0.8 +6	1.4 +6	0.55962	0.069953	-1.	14164.	1.071+6	37.
6	9	0.4 +6	0.8 +6	0.69315	0.077017	-1.	10341.	0.577+6	28.
7	9	0.2 +6	0.4 +6	0.69315	0.077017	-1.	7312.	0.288+6	16.
8	9	100.0 +3	200.0 +3	0.69315	0.077017	-1.	5170.	0.144+6	11.
9	12	46.4159+3	100.0 +3	0.76753	0.063961	-1.	3585.	69810.	6.2
10	12	21.5443+3	46.4159+3	0.76753	0.063961	-1.	2442.	32400.	3.5
11	12	10.0 +3	21.5443+3	0.76753	0.063961	-1.	1664.	15040.	2.0
12	12	4.64159+3	10.0 +3	0.76753	0.063961	-1.	1133.6	6981.	1.6
13	12	2.15443+3	4.64159+3	0.76753	0.063961	-1.	772.3	3240.	1.1
14	12	1000.0	2.15443+3	0.76753	0.063961	-1.	526.2	1504.	1.0
15	12	464.1589	1000.0	0.76753	0.063961	-1.	358.5	698.1	1.1
16	12	215.4434	464.1589	0.76753	0.063961	-1.	244.2	324.0	1.2
17	12	100.0	215.4434	0.76753	0.063961	-1.	166.4	150.4	1.3
18	12	46.41589	100.0	0.76753	0.063961	-1.	113.36	69.81	1.4
19	12	21.54434	46.41589	0.76753	0.063961	-1.	77.23	32.40	1.4
20	12	10.0	21.54434	0.76753	0.063961	-1.	52.62	15.04	1.3
21	12	4.641589	10.0	0.76753	0.063961	-1.	35.85	6.981	1.3
22	12	2.154434	4.641589	0.76753	0.063961	-1.	24.42	3.240	1.2
23	12	1.0	2.154434	0.76753	0.063961	-1.	16.64	1.504	1.2
24	12	0.4641589	1.0	0.76753	0.063961	-1.	11.336	0.6981	1.1
25	12	0.2154434	0.4641589	0.76753	0.063961	-1.	7.723	0.3240	1.1
26	25	0.0253	0.0253			10.	2.200	0.0253	1.1
	275	1.89574-1	2.15443-1		0.127922	-1.	6.217	0.2022	
	276	1.66810-1	1.89574-1		0.127922	-1.	5.832	0.1779	
	277	1.46780-1	1.66810-1		0.127922	-1.	5.470	0.1566	
	278	1.29155-1	1.46780-1		0.127922	-1.	5.131	0.1378	
	279	1.13646-1	1.29155-1		0.127922	-1.	4.813	0.1212	
	280	1.00000-1	1.13646-1		0.127922	-1.	4.515	0.1067	
	281	8.25404-2	1.00000-1		0.191883	300.	4.157	0.0905	
	282	6.81292-2	8.25404-2		0.191883	300.	3.781	0.0749	
	283	5.62341-2	6.81292-2		0.191883	300.	3.437	0.0619	
	284	4.64159-2	5.62341-2		0.191883	300.	3.125	0.0512	
	285	3.83119-2	4.64159-2		0.191883	300.	2.841	0.0423	
	286	3.16228-2	3.59381-2		0.191883	300.	2.582	0.0349	
	287	2.61016-2	2.78256-2		0.191883	300.	2.358	0.0288	
	288	2.15443-2	2.15443-2		0.191883	300.	2.132	0.0238	
	289	1.77828-2	1.46780-2		0.191883	300.	1.938	0.0197	
	290	1.46780-2	1.00000-2		0.191883	300.	1.761	0.0162	
	291	1.21153-2	1.46780-2		0.191883	300.	1.600	0.0134	
	292	1.00000-2	1.21153-2		0.191883	300.	1.454	0.0111	
	293	6.81292-3	1.00000-2		0.383766	300.	1.268	0.0085	
	294	4.64158-3	6.81294-3		0.383766	300.	1.047	0.0058	
	295	3.16227-3	4.64158-3		0.383766	300.	0.863	0.0039	
	296	2.15443-3	3.16227-3		0.383766	300.	0.714	0.0027	
	297	1.00000-3	2.15443-3		0.767532	300.	0.548	0.0016	
	298	1.00000-4	1.00000-3		2.302585	300.	0.334	0.0007	
	299	1.00000-5	1.00000-4		2.302582	300.	0.106	0.0001	

3.4. Other general characteristics of the BNAB-93 nuclear constants

As indicated above, in the BNAB-93 system of nuclear constants, two possible ways to take resonance selfshielding into account are envisaged: a) by using resonance selfshielding factors, and b) by using subgroups [7]. Resonance selfshielding factors are a function of two variables: the dilution cross section of the given nuclide by other nuclides in the mixture (σ_0), and the temperature of the mixture. The selfshielding factors are represented in the BNAB-93 system by a strictly defined grid of dilution cross sections applicable to all nuclides. However, the selfshielding factors are not determined for each individual case for all nodes of this grid, but only for the zeroth dilution cross section and for a few successive nodes of th grid:

$$\sigma_0 = 0,\ \sigma_0 = \sigma_{0,1}\times 10^N,\ \sigma_0 = \sigma_{0,2}\times 10^N \ldots\ \sigma_0 = \sigma_{0,k}\times 10^N.$$

The value of the indicator N is selected such that the selfshielding factor value for $\sigma_0=\sigma_{0,1}x10^N$ would be close to the selfshielding factor value for $\sigma_0=0$. The set of $\sigma_{0,1}$, $\sigma_{0,2}$, ...$\sigma_{0,k}$ is such that the value of the selfshielding factor for $\sigma_0=\sigma_{0,1}x10^N$ is close to the value of that factor for infinite dilution.

The standard set of $\sigma_{0,k}$ is entered into the table for which MF=0 and MT=2. Their sixteen values are:

$$\sigma_{0,1}=0;\ \sigma_{0,2}=0,1;\ \sigma_{0,3}=0,215;\ \sigma_{0,4}=0,464;\ \sigma_{0,5}=1;\ \sigma_{0,6}=2,154;\ \sigma_{0,7}=4,642;$$
$$\sigma_{0,8}=10;\ \sigma_{0,9}=21,544;\ \sigma_{0,10}=46,416;\ \sigma_{0,11}=100;\ \sigma_{0,12}=215,443;$$
$$\sigma_{0,13}=464,157;\ \sigma_{0,14}=1000;\ \sigma_{0,15}=2154,43;\ \sigma_{0,16}=4641,57.$$

Three temperatures are used in the determination of selfshielding factors in the BNAB-93 system: 300K, 900K and 1200K. The list of temperatures is given in the table for which MT=0 and MF=3. However, since the length of that table is short (LT=1, LC=3), none of the existing BNAB processing programs use it.

Another set of data, that is common to all nuclides, is the multiplier used in the Maxwellian spectrum averaging calculations of cross sections. The upper boundary of the thermal group of the BNAB-93 system is set by the user. If the thermal group cross section is determined by the 1/v dependence, and the neutron spectrum is a Maxwellian with a neutron gas temperature T_n, then the cross sections averaged over that spectrum will be proportional to the cross section at 0.0253 eV as given in the cross section table. If the upper boundary of the thermal range $T_{th}>>T_n$ then the proportionality coefficient is equal to $(\pi/2)x(293.7/T_n)^{1/2}$. If T_n is comparable to T_{th} however, then in order to obtain the group-averaged cross section, it is necessary to use the multiplier $C(T_{th}, T_n)$, the data for which is given in table [0,6] in the HEAD file. The format of that table corresponds exactly to the format of Westcott's g-factors which will be described below in chapter 4.7.

4. Nuclear Constants for the Calculation of Neutron Fields

4.1 Basic neutron constants

The following constitute the basic BNAB set of neutron constants:

σ_c - **capture cross section**, including all processes that lead to the disappearance of a neutron excluding the fission process

$$\sigma_c = \sigma_{n\gamma} + \sigma_{np} + \sigma_{n\alpha} + \sigma_{nd} + \sigma_{nt} + \ldots, \qquad (4.1)$$

σ_f - **fission cross section** including all precesses that lead to fission:

$$\sigma_f = \sigma_{nf} + \sigma_{n,n'f} + \sigma_{n,2nf} + \ldots, \qquad (4.2)$$

σ_e - **elastic cross section**

σ_{in} - **inelastic cross section** including all processes that are accompanied by the emission of a neutron, excluding fission and elastic scattering:

$$\sigma_{in} = \sigma_{n,n'} + \sigma_{n,2n} + \sigma_{n,3n} + \ldots + \sigma_{n,n'p} + \sigma_{n,n'\alpha} + \ldots, \qquad (4.3)$$

σ_t - **total cross section**, the sum of all partial processes:

$$\sigma_t = \sigma_c + \sigma_f + \sigma_e + \sigma_{in}, \qquad (4.4)$$

(The last equality in the BNAB tables is satisfied only approximately, namely with an accuracy that is assigned to the total cross section (usually to two significant figures); these total cross section values are redundant in the cross section tables and they are given principally only as a guide row for checking purposes; for calculational purposes, it is recommended to use the arithmetical sum of the partial cross sections as the total cross section).

r - neutron multiplicity, number of neutrons emitted in the inelastic process:

$$r = \frac{\sigma_{n,n'} + \sigma_{n,n'p} + \sigma_{n,n'\alpha} + \ldots + 2 \times \left(\sigma_{n,2n} + \sigma_{n,2np} + \ldots\right) + 3 \times \left(\sigma_{n,3n} + \ldots\right) + \ldots}{\sigma_{in}}, \qquad (4.5)$$

ν - **average number of neutrons**, emitted in the fission process (prompt as well as delayed);

μ - **cosine of the average elastic scattering angle**.

ξ - **average lethargy increment in elastic scattering**.

In addition to the above enumerated list of neutron data (see Table 4), the last column of the 28 group constants [1,0] table contains information on other neutron data (i.e., scattering matrices, selfshielding factors, etc...). That information is given in the form of a seven-digit word whose ten- thousandth position gives an indication whether a given data type is included in the BNAB library or not:

- the first four digits give an indication whether MF=2,3,4,5 tables are included and gives the number of such tables;
- the next position gives the indication whether MF=6 tables (which include subgroup resonance structure parameters) are included, and gives the number of individual temperatures for which these data are given;
- the next position gives an indication that the MF=7 table gives Westcott's g-factors for that group;

- the last position gives an indication whether subgroup information is included, this position has a few meanings: position= (3) means that basic subgroup constants are given for the given group in the MF=301 table, information as to which additional data must be used in subgroup calculations is also given; position=(1) means that in all subgroups of a given group, the value of the scattering cross section is constant, and has a group-averaged value; and that the capture cross section behaves accord to the 1/v law, and is normalized such that when it is group-averaged and weighted by the standard spectrum, the data entered in table [1,0] are group-averaged cross sections; position= (0)means that additional information is lacking.

For most materials, the basic neutron constants used in the BNAB-93 system are presented exclusively in the form of 28-group constants as given in table [1,0]. For the most important reactor and shielding materials, which are present in large concentrations and thus affect the neutron spectrum in the medium, or the presence of important processes such as fission, which would have the same effect, additional subgroup constants (such as in MF=301 and MT=0 tables) are introduced in addition to the 28-group data.

Table 4. Basic neutron group constants for iron

NAM=FE BIB=FOND MF= 1 MT= 0 AWR= 55.3650 DAT= .010393
LV = 10 LT = 28 LC= 10 LS= 10 LF = (I4,E7.0,2E9.0,E7.0,5E6.0,E9.0)
* 26-FE- 0
* g полное захват деление упр неупр множ ню мю кси list
*

-1	2.55	0.1668		1.22	1.155	1.394		.7789	.0080	1200003.
0	2.92	0.1506		1.58	1.186	1.048		.8359	.0060	1200003.
1	3.48	0.0828		2.11	1.292	1.001		.8200	.0065	1200003.
2	3.59	0.0294		2.28	1.281	1.000		.7024	.0107	1200003.
3	3.43	0.0113		2.35	1.063	1.000		.4977	.0181	1200003.
4	3.10	0.0035		2.27	0.825	1.000		.2954	.0255	1231103.
5	2.64	0.0032		2.25	0.385	1.000		.2839	.0257	1231103.
6	3.34	0.0055		3.31	0.023	1.000		.2006	.0283	1231103.
7	3.15	0.0062		3.13	0.019	1.000		.1135	.0319	1231103.
8	3.76	0.0077		3.72	0.032	1.000		.0461	.0346	1231103.
9	4.63	0.0119		4.60	0.021	1.000		.0120	.0357	1231103.
10	12.83	0.0166		12.74	0.068	1.000		.0120	.0357	1231103.
11	3.60	0.0060		3.59				.0120	.0357	0231103.
12	11.16	0.0156		11.15				.0120	.0357	0231103.
13	7.22	0.0055		7.22				.0120	.0357	0031103.
14	8.81	0.2225		8.58				.0120	.0357	0031103.
15	9.85	0.0124		9.84				.0120	.0357	0.
16	10.64	0.0239		10.62				.0120	.0357	1.
17	11.07	0.0326		11.04				.0120	.0357	1.
18	11.30	0.0495		11.25				.0120	.0357	1.
19	11.42	0.0739		11.35				.0120	.0357	1.
20	11.51	0.1093		11.40				.0120	.0357	1.
21	11.58	0.1608		11.42				.0120	.0357	1.
22	11.67	0.2368		11.43				.0120	.0357	1.
23	11.78	0.3479		11.43				.0120	.0357	1.
24	11.95	0.5099		11.44				.0120	.0357	1.
25	12.19	0.7496		11.44				.0120	.0357	1.
26	14.05	2.6165		11.44				.0120	.0357	1.

Subgroup constants are not necessarily used over the full energy range being investigated. They are used only for those wide energy groups of the 28-group set where the detailed description of the energy dependence of the cross sections is justified. In calculations using the multigroup approximation, nuclides for which subgroup data are not given, the same cross section values for all subgroups of a given group are used. If subgroup constants are given only for some groups, then those BNAB groups for which these constants are not given, either the group-averaged cross sections are assigned or the 1/v cross section dependence is assigned to that group.

All cross sections given in the MF=1 and MF=301 tables are given in barns. The nomenclature and format of the given basic neutron constants in the MF=1 and MF=301 tables are the same. Differences exist only in that the first four positions of the MF=1 table are dedicated to the number of the group, in the case of MF=301 table the first two positions are dedicated to the group number, and the two subsequent positions are dedicated to the number of the subgroup of that group.

4.2 Inelastic scattering transition matrix

The inelastic scattering matrices of intergroup transitions in the system of the 28-group neutron constants are given for two angular momenta: for the zeroth momentum (MF=2 and MT=0) and for the first angular momentum (MF=2 and MT=1 cross section, multiplied by the average cosine of the scattering angle which is accompanied by the given transition).
If there is even one non-zero inelastic scattering cross section value in any one group, it is mandatory that data library include either table [2,0] or [2,1]. If table [2,1] is excluded, the inelastic scattering for that nuclide will be considered to isotropic in the laboratory system of coordinates. The first angular momenta are determined from:

$$\sigma_{in}^{g\to g+k} = \sigma_{in,0}^{g\to g+k} \times \overline{\mu}_{in}^{g\to g+k}, \tag{4.6}$$

where $\overline{\mu}_{in}^{g\to g+k}$ the average cosine of the inelastic scattering angle for the transition.
The following normalization conditions must be satisfied:

$$\text{при MT=0} \quad \sum_{k=0}^{k\,\max} \sigma_{in,0}^{g\to g+k} = \sigma_{in}^{g} \times r^{g} \tag{4.7a}$$

$$\text{при MT=1} \quad \sum_{k=0}^{k\,\max} \sigma_{in,1}^{g\to g+k} = \sigma_{in}^{g} \times r^{g} \times \mu_{in}^{g}. \tag{4.7б}$$

Here, μ_{in}^{g} represents the average cosine of the inelastic scattering angle for the neutron group g. The groups for which inelastic transition cross sections are given, are assigned numbers from one to the number of the group which contains the inelastic scattering threshold at the lowest level of the target nuclide, but not exceeding g=10 (21.5 - 46.4 keV). The energy of the inelastically scattered neutrons is distributed in various groups starting with the one being considered and ending with group g=11 (10.0 - 21.5 keV), which is the recipient of all of the scattered neutrons having energies smaller than 21.5 keV. If there is a need to describe inelastic scattering for energies below 21.5 keV and the distribution of the inelastically scattered neutrons into groups lower than 10 keV, it is then necessary to use the inter-group transition table. An example for MF=2 and MT=0 is illustrated below:

NAM=U238 BIB=FOND MF= 2 MT= 0 DAT= .010393
LV = 10 LT = 12 LC= 14 LS= 14 LF = (I4,13E5.0)

* G/K	-1	0	1	2	3	4	5	6	7	8	9	10	11
-1	.130	.152	.204	.241	.332	.265	.184	.071	.022	.006	.001		
0	.038	.168	.186	.240	.281	.175	.103	.036	.010	.003	.001	.003	
1		.057	.181	.258	.325	.244	.153	.054	.015	.004	.001		
2			.082	.266	.358	.334	.171	.051	.015	.004	.001		
3				.117	.566	.114	.141	.076	.032	.012	.003	.002	
4					.134	.424	.245	.013	.006	.002	.001		
5						.013	.098	.154	.078	.024	.007	.011	
6							.012	.007	.002	.001	.001		
7								.014	.005	.001	.000		
8									.022	.009	.000		
9										.012	.009		
10											.025	.043	

For MT=1 the table has exactly the same form, except that it contains the first angular momenta of the transitions. In the BNAB-93 system, these tables are given only for A<20 nuclides. For heavier nuclides, anisotropy in inelastic scattering is unimportant. As concerns multigroup constants, probability data (not cross sections as in the case of 28 group sets) for the inter-group transitions are contained in MF=302 and MT=g tables, where g = 1,0,1,2...11, represents the number of the BNAB group which contains the subgroups from which scattering originates. The first two columns of these tables contain the group number and subgroup number which are the recipient of the transition. Beyond that, are as many columns as necessary, namely the number of subgroups in the given BNAB group. The data given in the table - basically the inelastic scattering transition probabilities for scattering from the subgroup specified by the column number of the group specified by the MT value, into the group and subgroup given in the first two columns of the corresponding rows.

The matrices of the average cosine of inelastic scattering accompanying the transition from subgroup to subgroup are entered in MF=302 and MT=g+100 tables. The format of these tables is the same as the tables of inter-subgroup transition probabilities. If there are no [302,g+100] tables in the BNAB system, the subgroup calculations are made with the use of the corresponding inter-group transition matrices. For those neutrons that remain in the same group after scattering are also assumed to remain in the same subgroup, but neutrons which slow down in any given group are distributed evenly among the subgroups of that group.

4.3 Elastic scattering transition matrices

Let us consider the differential elastic scattering cross section for the transition of neutrons from group g into group g+k, presented in terms of Legendre polynomials:

$$\sigma_e^{g\to g+k}\left(\vec{\Omega}\right) = \frac{\sigma_e^g \times p^{g\to g+k}}{4\pi} \times \sum_{l=0}^{l_{\max}} (2l+1) \times \omega_l^{g\to g+k} \times P_l(\mu). \qquad (4.8)$$

here $\omega_0^{g\to g+k} = 1$.

For the 28-group system, the MF=3 and MT=k ($k=0,1,2...k_{max}$) tables contain the quantities

$$\sigma_{e,l}^{g\to g+k} = \sigma_e^g \times p^{g\to g+k} \times \omega_l^{g\to g+k}, \tag{4.9}$$

(For $l=0,1...l_{max}$)

The first column, as usual, contains the value of the number of groups g, it is followed by $l_{max}+1$ of columns having the value $\omega_l^{g\to g+k}$ In the BNAB-93 system these columns contain the value $l_{max}=5$, for all nuclides except for hydrogen, for hydrogen that value is $l_{max}=15$. An example of table [3,0] is given below (scattering without slowing down out of the group).

Such a table is always entered for MT=1 ($k=1$) as well, since slowing down from a neighboring group is possible for elastic scattering and for all nuclides. Slowing down by skipping one group(MT=2) for nuclides heavier than lithium is not possible for any of the BNAB groups; therefore, no additional tables are needed to describe elastic slowing down for those nuclides. In the case of lithium, elastic transitions by skipping a group are possible, and tables MF=3 and MT=0,1, and 2 are given for the isotopes of lithium. In the case of hydrogen, transitions are possible, in principle, into any lower lying energy group and in the BNAB-93 system tables MT=0,1,...12 are given for hydrogen.

Elastic scattering angular momentum matrix for inter-group G→G transitions

NAM=FE BIB=FOND MF= 3 MT= 0 AWR= 55.3650 DAT= .010393
LV = 10 LT = 14 LC= 7 LS= 7 LF = (I4,6E11.0)

* G\L *	0	1	2	3	4	5
-1	0.4838	0.3890	0.3127	0.2733	0.2236	0.1670
0	0.9500	0.8241	0.7069	0.5739	0.4362	0.2945
1	0.9628	0.8119	0.6659	0.4964	0.3371	0.1861
2	0.9575	0.7044	0.5420	0.3799	0.2208	0.0883
3	0.9469	0.5118	0.3963	0.2436	0.1144	0.0272
4	0.9529	0.3157	0.2925	0.1197	0.0424	0.0038
5	0.9357	0.2944	0.2142	0.0517	0.0032	0.0001
6	0.9110	0.2253	0.0989	0.0160	0.0001	-.0007
7	0.9458	0.1270	0.0367	0.0060	0.0004	0.0000
8	0.9523	0.0623	0.0101	0.0013	0.0000	0.0002
9	0.9568	0.0257	0.0006	0.0000	-.0001	-.0000
10	0.9966	0.0130	0.0001	0.0000	-.0000	0.0000
11	0.9148	0.0394	0.0008	-.0002	0.0000	0.0000
12	0.9534	0.0272	0.0003	0.0000	-.0000	0.0000

As seen from the example given above, data are given only for groups $g=-1, 0,1,...12$. For groups $g=-1,0,...11$ the given data were derived by averaging the probability of transfer to a corresponding group over energy weighted by the standard spectrum and the elastic scattering cross section (for $l>0$ multiplied by the corresponding coefficient ω_l). For the 12th BNAB group, the data that are given were derived on the assumption that the elastic scattering cross section is constant within the confines of the group. For the 12th and for all lower lying energy groups, elastic scattering for all nuclides is practically isotropic in the centre of mass system; the group widths in that region of the lethargy scale are the same, and the resonance structure of the elastic scattering cross section for those nuclides which contribute significantly to the slowing down ability of the medium is insignificant.

Therefore, the data given for the 12th group can be applied as well to groups $g=13,14,...24,25$, providing that they are renormalized to the corresponding elastic scattering cross section. If $k_{max}>1$, then, for low energy groups g > 26-k_{max} the values $g+k$ will increase the group number of the very last 26th group (at least for k=k_{max}). The cross sections and the corresponding angular momenta of such "transitions"must be simply added to the matrix transition element of the 26th group.

The format of the presented data on the anisotropy of elastic scattering in the multigroup approximations is very close to that which is described. Differences exist only in the following: first of all, for $l=0$, the slowing down probabilities are given by $p^{(g,s)\to(g,s)+k}$ and for $l>0$, it is $\omega_l^{(g,s)\to(g,s)+k}$. Here (g,s) designates the subgroup s of group g, and (g,s)+k designates the subgroup which has a provisional number that is k times larger (the meaning of a provisional number will be explained below by an example). Furthermore, the first four positions of the table are occupied by two columns which contain the group number and that of its associated subgroups for which data are given. This is followed by $l_{max}+1$ columns containing data which describe transitions from one subgroup into a subgroup having a temporary number that is k times larger. As before, the value of k determines the value of MT (i.e.,MT=k). For instance for an MF=303 and MT=3 table, in rows, corresponding to the subgroup (g=4,s=5), scattering data are given in a row that accompanies the transition into subgroup (g=4,s=8) and which refers to the same BNAB group. In the next row, which corresponds to subgroup (g=4,s=6), scattering data that accompanies the transition into subgroup (g=5,s=1) are given since group g=4 contains only eight subgroup.

4.4 Hydrogen scattering parameters

In the case of elastic scattering in hydrogen, a neutron has a finite probability to be scattered into any given lower energy group , therefore, the number of non-zero matrix elements for inter-group elastic scattering transitions in hydrogen turns out to be considerable. Aside from that, the inter-group transition probability matrix for hydrogen can be represented by the product of two vectors. And what is more, the angular momentum matrix for the inter-group transitions for elastic scattering in hydrogen can also be represented by the product of two vectors.

In other words, the differential transition cross section for the elastic slowing down in hydrogen from group g to group g' can be represented by a set of equations given below. Let us note that these formulae are correct in their assumption to describe the isotropic scattering of neutrons in hydrogen in the centre of mass coordinates. At higher energies this proposal becomes not entirely correct. Thus, in the minus one group the cosine of the scattering angle in the centre of mass is equal to 0.017. Such a weak anisotropy usually have practically no influence on the characteristics of the neutron field. However, it can be taken into account if the scattering anisotropy in hydrogen is described not in terms of the α and β parameters, but by using the elastic transition matrix (i.e., MF=3 tables).

$$\sigma^{g\to g'}(\overline{\Omega}) = \frac{1}{4\pi}\sum_{l=0}^{\infty}(2\cdot l+1)\times\sigma_l^{g\to g'}\times P_l(\mu), \qquad (4.8.1)$$

$$\sigma_0^{g\to g'} = \alpha_0^{g'}\times\beta_0^{g} \quad \text{при } g'>g, \qquad (4.8.2a)$$

$$\sigma_0^{g\to g'} = \sigma_e^{g} - \beta_0^{g}\times\sum_{g'>g}\alpha_0^{g'}, \qquad (4.8.2б)$$

$$\sigma_1^{g\to g'} = \alpha_1^{g'}\times\beta_1^{g} \quad \text{при } g'>g, \qquad (4.8.3a)$$

$$\sigma_1^{g\to g'} = \frac{2}{3}\times\sigma_e^{g} - \beta_1^{g}\times\sum_{g'>g}\alpha_1^{g'}, \qquad (4.8.3б)$$

$$\sigma_2^{g\to g'} = \frac{3}{2}\times\alpha_2^{g'}\times\beta_2^{g} - \frac{1}{2}\times\alpha_0^{g'}\times\beta_0^{g} \quad \text{при } g'>g, \qquad (4.8.4a)$$

$$\sigma_2^{g\to g} = \frac{1}{4}\times\sigma_e^{g} - \sum_{g'>g}\sigma_2^{g\to g'}, \qquad (4.8.4б)$$

$$\sigma_3^{g\to g'} = \frac{5}{2}\times\alpha_3^{g'}\times\beta_3^{g} - \frac{3}{2}\times\alpha_1^{g'}\times\beta_1^{g} \quad \text{при } g'>g, \qquad (4.8.5a)$$

$$\sigma_3^{g\to g} = -\sum_{g'>g}\sigma_3^{g\to g'}, \qquad (4.8.5б)$$

$$\sigma_4^{g\to g'} = \frac{35}{8}\times\alpha_4^{g'}\times\beta_4^{g} - \frac{30}{8}\times\alpha_2^{g'}\times\beta_2^{g} + \frac{3}{8}\times\alpha_0^{g'}\times\beta_0^{g} \quad \text{при g'>g}, \qquad (4.8.6a)$$

$$\sigma_4^{g\to g} = -\frac{1}{48}\times\sigma_e^{g} - \sum_{g'>g}\sigma_4^{g\to g'}, \qquad (4.8.6б)$$

$$\sigma_5^{g\to g'} = \frac{63}{8}\times\alpha_5^{g'}\times\beta_5^{g} - \frac{70}{8}\times\alpha_3^{g'}\times\beta_3^{g} + \frac{15}{8}\times\alpha_1^{g'}\times\beta_1^{g} \quad \text{при g'>g}, \qquad (4.8.7a)$$

$$\sigma_5^{g\to g} = -\sum_{g'>g}\sigma_5^{g\to g'}. \qquad (4.8.7б)$$

The α and β parameters for the 28-group approximation are stored in the MF=70, MT=0 and MT=1 tables. Correspondingly, MF=370, MT=0 and MT=1 tables are used in a multigroup approximation. If slowing down in hydrogen is described in a 28-group approximation using the α and β parameters, then elastic scattering in hydrogen in the "thermal" group is assumed to be isotropic (to take the hydrogen atom bond in molecules or crystals into consideration). In a multigroup approximation, the α and β parameters are used to calculate the slowing down at energies lying above the boundary of the thermal region determined by the user. For calculations performed in the range lying below the thermal region boundary, it is necessary to use the thermalization matrix (however, it stands to reason that calculations to evaluate the slowing down into the thermal group must be performed with the use of the α and β parameters).

α parameter table used in a 28-group approximation

NAM=H BIB=BN93 MF= 70 MT= 0 AWR= .999167 DAT= .080493
LV = 10 LT = 28 LC= 7 LS= 7 LF = (I4,6E11.0)
* 1- H- 1

* MG	alfa0	alfa1	alfa2	alfa3	alfa4	alfa5
-1	6.0182E+06	2.4774E+10	1.0225E+14	4.2315E+17	1.7556E+21	7.3019E+24
0	3.4818E+06	1.2171E+10	4.2620E+13	1.4949E+17	5.2523E+20	1.8484E+24
1	4.0000E+06	1.1635E+10	3.4000E+13	9.9814E+16	2.9433E+20	8.7171E+23
2	2.5000E+06	5.7145E+09	1.3125E+13	3.0287E+16	7.0208E+19	1.6347E+23
3	1.5000E+06	2.6981E+09	4.8750E+12	8.8472E+15	1.6125E+19	2.9513E+22
4	1.1000E+06	1.5309E+09	2.1450E+12	3.0252E+15	4.2937E+18	6.1310E+21
5	6.0000E+05	6.2731E+08	6.6000E+11	6.9867E+14	7.4400E+17	7.9680E+20
6	4.0000E+05	3.0837E+08	2.4000E+11	1.8850E+14	1.4933E+17	1.1928E+20
7	2.0000E+05	1.0903E+08	6.0000E+10	3.3322E+13	1.8667E+16	1.0543E+19
8	1.0000E+05	3.8547E+07	1.5000E+10	5.8905E+12	2.3333E+15	9.3185E+17
9	5.3584E+04	1.4415E+07	3.9228E+09	1.0792E+12	3.0000E+14	8.4195E+16
10	2.4872E+04	4.5585E+06	8.4514E+08	1.5841E+11	3.0000E+13	5.7362E+15
11	1.1544E+04	1.4415E+06	1.8208E+08	2.3252E+10	3.0000E+12	3.9080E+14
12	5.3584E+03	4.5585E+05	3.9228E+07	3.4129E+09	3.0000E+11	2.6625E+13
13	2.4872E+03	1.4415E+05	8.4514E+06	5.0094E+08	3.0000E+10	1.8139E+12
14	1.1544E+03	4.5585E+04	1.8208E+06	7.3528E+07	3.0000E+09	1.2358E+11
15	5.3584E+02	1.4415E+04	3.9228E+05	1.0792E+07	3.0000E+08	8.4195E+09
16	2.4872E+02	4.5585E+03	8.4514E+04	1.5841E+06	3.0000E+07	5.7362E+08
17	1.1544E+02	1.4415E+03	1.8208E+04	2.3252E+05	3.0000E+06	3.9080E+07
18	5.3584E+01	4.5585E+02	3.9228E+03	3.4129E+04	3.0000E+05	2.6625E+06
19	2.4872E+01	1.4415E+02	8.4514E+02	5.0094E+03	3.0000E+04	1.8139E+05
20	1.1544E+01	4.5585E+01	1.8208E+02	7.3528E+02	3.0000E+03	1.2358E+04
21	5.3584E+00	1.4415E+01	3.9228E+01	1.0792E+02	3.0000E+02	8.4195E+02
22	2.4872E+00	4.5585E+00	8.4514E+00	1.5841E+01	3.0000E+01	5.7362E+01
23	1.1544E+00	1.4415E+00	1.8208E+00	2.3252E+00	3.0000E+00	3.9080E+00
24	5.3584E-01	4.5585E-01	3.9228E-01	3.4129E-01	3.0000E-01	2.6625E-01
25	2.4872E-01	1.4415E-01	8.4514E-02	5.0094E-02	3.0000E-02	1.8139E-02
26	2.1534E-01	6.6666E-02	2.3208E-02	8.6177E-03	3.3333E-03	1.3262E-03

4.5 Cross section resonance selfshielding factors

Cross section resonance selfshielding factors in the BNAB-93 system are given for a base temperature of 300K. For the 28-group approximation the data are given in the MF=4 tables, and for a multigroup approximation they are given in the MF=304 tables. Depending on the MT value, resonance selfshielding factors are given for the following reaction cross sections:

MT=1 - resonance selfshielding factors for the total cross section average weighted by the spectrum of the first angular harmonics of the neutron flux,

$$f_t(\sigma_0,T_0)=\frac{\left\langle \sigma_t(E,T_0) \Big/ \left[\sigma_t(E,T_0)+\sigma_0\right]^2 \right\rangle}{\left\langle \sigma_t(E,T_0)\right\rangle \times \left\langle 1 \Big/ \left[\sigma_t(E,T_0)+\sigma_0\right]^2 \right\rangle}; \qquad (4.10)$$

MT=2 - resonance selfshielding factors for the elastic scattering cross section, average weighted by the zeroth angular harmonics of the neutron flux:

$$f_e(\sigma_0,T_0)=\frac{\left\langle \sigma_e(E,T_0) \Big/ \left[\sigma_t(E,T_0)+\sigma_0\right]\right\rangle}{\left\langle \sigma_e(E,T_0)\right\rangle \times \left\langle 1 \Big/ \left[\sigma_t(E,T_0)+\sigma_0\right]\right\rangle}; \qquad (4.11)$$

MT=4 - resonance selfshielding factors for the inelastic scattering cross section, average weighted by the zeroth angular harmonics of the neutron flux:

$$f_{in}(\sigma_0,T_0)=\frac{\left\langle \sigma_{in}(E,T_0) \Big/ \left[\sigma_t(E,T_0)+\sigma_0\right]\right\rangle}{\left\langle \sigma_{in}(E,T_0)\right\rangle \times \left\langle 1 \Big/ \left[\sigma_t(E,T_0)+\sigma_0\right]\right\rangle}; \qquad (4.12)$$

MT=18 - resonance selfshielding factors for the fission cross section:

$$f_f(\sigma_0,T_0)=\frac{\left\langle \sigma_f(E,T_0) \Big/ \left[\sigma_t(E,T_0)+\sigma_0\right]\right\rangle}{\left\langle \sigma_f(E,T_0)\right\rangle \times \left\langle 1 \Big/ \left[\sigma_t(E,T_0)+\sigma_0\right]\right\rangle}; \qquad (4.13)$$

MT=102- resonance selfshielding factors for the capture cross section:

$$f_c(\sigma_0,T_0)=\frac{\left\langle \sigma_c(E,T_0) \Big/ \left[\sigma_t(E,T_0)+\sigma_0\right]\right\rangle}{\left\langle \sigma_c(E,T_0)\right\rangle \times \left\langle 1 \Big/ \left[\sigma_t(E,T_0)+\sigma_0\right]\right\rangle}. \qquad (4.14)$$

In the formulae given above, the angle brackets indicate group averaging weighted by the standard spectrum $\Phi(E)$ (see section 3.3).

$$\langle F\rangle = \frac{\int_{E=E_g}^{E_{g-1}} F(E)\ \Phi(E)\ dE}{\int_{E=E_g}^{E_{g-1}} \Phi(E)\ dE}. \qquad (4.15)$$

The evaluation of the neutron flux and current spectra is based on the assumption of a constant collision density in the resonance range and in the "approximation of the dilution cross section", when the cross sections of all nuclides that make up the medium, (except the one that is being investigated), is considered to be constant within the boundaries of the given group. In the last approximation, the summed macroscopic cross section of all the other nuclides, referring to the atomic density C_i of the investigated *ith* nuclide, is also constant:

$$\sigma_0=\frac{1}{c_i}\times\sum_{j\neq i} c_j\times\sigma_t^j\ , \qquad (4.16)$$

the magnitude of which determines the listed selfshielding factors.

The resonance selfshielding factors are given for 16 values of the following parameter: $\sigma_0 = 0$, $\sigma_0 = \sigma_{0.1} \times 10^N$, ..., $\sigma_0 = \sigma_{0.15} \times 10^N$. The numerical values of $\sigma_{0.1}$, .. $\sigma_{0.15}$ are given in the MF=0 and MT=2 tables. The value of the exponent N is chosen such that the value of the selfshielding factor evaluated for the value of $\sigma_0 = \sigma_{0.1}$ is close enough to the value of the selfshielding factor evaluated for the value of $\sigma_0 = 0$, and that the selfshielding factor evaluated for the value $\sigma_0 = \sigma_{0.15}$ be close to unity (namely to the value for infinite dilution).

The selfshielding factors are given only for those groups in which the resonance selfshielding cross section is significant. The group number for which selfshielding factors are given is indicated in the first column of the table. The value of the exponent N, which is used to describe the data required for the determination of the MT value in the given group, is given in the second column.

Due to their nature, the resonance selfshielding factors for the total cross section cannot exceed unity. Resonance selfshielding factors for partial cross sections also practically never exceed unity. Because of that, the data entered in the MF=4 and MF=304 tables are in the form of integers where the selfshielding factor values multiplied by 1000 are given as whole numbers (i.e., INT(1000 x $f(\sigma_0)$). Thus, for instance, for $f(\sigma_0) = 0.1232$ the value is 123, and for $f(\sigma_0) = 0.0778$ the value is 778, etc... Selfshielding factors whose values exceed 0.9995 are not included in the tables and their location is filled with blanks. In the implementation of these data tables, these factors must be taken to be equal to unity. Selfshielding factors given in MF=4 tables are not given for all cross sections; they are given if the data given in the MF=1 and/or MF=301 tables are not equal to zero. Cross sections for which selfshielding factors are not given, they are given the value of one. A table of selfshielding factors for the capture cross section of iron for a temperature of 300K is shown as an example below:

Resonance selfshielding factors for the iron capture cross section (T=300K)

```
NAM=FE        BIB=FOND  MF=  4  MT=102  T-0= 300.        DAT= .010393
LV = 90       LT =  11  LC= 18  LS= 18  LF = (I4,I2,1X,16I4)

 *  G N   0  .1  ... ...  1  ... ...  10 ... ... 100 215 465 1000...*10
 *
    4 0  968 970 971 974 979 985 990 995 997 999 999
    5 0  935 936 937 940 945 954 965 978 987 993 997 998 999
    6 0  653 665 676 698 732 779 836 891 936 966 983 992 996 998 999
    7 0  512 524 535 557 595 651 724 804 878 932 965 983 992 996 998 999
    8 0  449 461 473 494 530 585 661 749 835 904 949 974 988 994 997 999
    9 0  426 437 447 464 493 537 603 685 774 855 917 956 978 990 995 998
   10 0  386 407 427 462 512 574 643 714 785 853 908 948 973 987 994 997
   11 0  684 689 695 706 725 757 802 854 905 945 971 986 993 997 998 999
   12 0  768 770 772 777 786 804 833 872 914 949 973 986 993 997 999 999
   13 0  964 965 965 966 968 971 977 983 990 994 997 999 999
   14 1  273 289 305 339 398 493 618 749 855 924 962 982 992 996 998 999
```

Subgroup selfshielding factors are presented in the same format as the 28-group factors. The only difference being that selfshielding factor data are always given for every group. Thus, for each wide BNAB group in which resonance selfshielding is appreciable even in the case of a single group, the MF=304 table is apportioned as many rows as there are groups (the number

of the group is entered in the first column of each of these rows. The number of subgroups is not specified in the table - they are determined by the sequential number of the row which contains the number of the given group in the first column. The rows which correspond to those subgroups in which resonance selfshielding is not substantial, are filled completely with blanks (as already stated, in calculations they must be converted to ones).

The temperature dependence of the resonance selfshielding factors is given in the MF=5 tables, and in the MF=305 tables in the case of subgroup data. Depending on the value of MT, these tables are also used to store the Doppler effect on the resonance selfshielding factors for the total cross section (MT=1), for the elastic scattering cross section (MT=2), for the fission cross section (MT=18), or for the capture cross section (MT=102).

The Doppler effect is calculated from the following formulae:

$$\Delta_1(\sigma_0) = f(\sigma_0, T_1) - f(\sigma_0, T_0)\ ; \qquad (4.17a)$$

$$\Delta_2(\sigma_0) = f(\sigma_0, T_2) - f(\sigma_0, T_1)\ ; \qquad (4.17b)$$

The temperature values T_1, T_2, T_3 are 300K, 900K and 2100K. If the number of temperatures in this table exceeded three values, which are used in the BNAB-93 system, then the number of Doppler coefficients Δ would be larger. Doppler coefficients are given for the same dilution cross sections as for the resonance selfshielding factors. However, these coefficients do not have to be given for all MT values, which are assigned selfshielding factors, but for one, two, or three MT values only. The quantities Δ_1 and Δ_2 may not be given for all groups which are assigned selfshielding factors in the MF=5 tables and having the same MT value. If Doppler coefficients are not given, they are assigned a zero value. An example of a BNAB MF=5 table is given below.

Resonance selfshielding Doppler coefficients for capture (900K - 300K; 2100K - 900K)

```
NAM=FE        BIB=FOND  MF=  5  MT=102  T-1=  900.       T-2= 2100.
LV = 90       LT =  14  LC= 18  LS= 18  LF = (I4,I2,1X,16I4)
                                                                    N
*  G N   0  .1  ... ...  1  ... ...  10 ... ... 100 215 465 1000...*10
*
   6 0  46  47  47  46  43  38  31  23  15   8   4   2   1   0   0   0
        41  40  39  37  34  29  22  15   9   5   2   1   1   0   0   0
   7 0  32  33  34  35  37  38  38  33  24  15   8   4   2   1   0   0
        31  32  33  35  36  36  34  28  19  11   6   3   1   1   0   0
   8 0  36  37  38  39  41  42  41  36  27  18  10   5   3   1   1   0
        35  36  36  37  38  38  35  29  21  13   7   4   2   1   0   0
   9 0  40  42  43  45  48  51  52  49  43  32  20  12   6   3   1   1
        36  38  39  40  43  44  45  41  34  24  15   8   4   2   1   0
  10 0  42  45  47  49  50  48  41  32  23  15   8   4   2   1   0   0
        38  40  41  42  40  35  29  22  16  10   5   3   1   1   0   0
  11 0  31  31  30  30  29  28  26  22  17  11   6   3   2   1   0   0
        27  27  27  26  26  24  22  19  14   8   5   2   1   1   0   0
  14 1  50  54  58  64  73  82  80  65  43  24  12   6   3   1   1   0
        57  60  63  67  72  72  63  46  28  15   7   4   2   1   0   0
```

In the 28-group BNAB-93 system, it is assumed that the group-averaged cross sections are not temperature dependent, namely that the Doppler coefficients for infinite dilution are equal to zero. Strictly speaking, that is not entirely correct, because with an increase of temperature, resonances have a tendency to spread, and some of them "migrate" to the neighboring group. As a result, the value of the group-averaged cross section in the neighboring group increases, and the value of the cross section in the original group decreases correspondingly. As a rule, in the case of the wider of the 28 groups, these effects are not significant and temperature effects have a tendency to compensate each other. This fact served as a basis for the simplification of the mechanism concerning the temperature independence of group-averaged cross section. As a matter of fact, in the 28-group approximation, differences in the values of selfshielding factors, each one normalized to the group-averaged cross section at a given temperature, are used in the calculation of the Doppler effect. In a subgroup approximation it is not always possible to assume that subgroup-averaged cross sections are temperature independent. Therefore, in this case the Doppler effect has to be determined by

$$\Delta f = \frac{\sigma(\sigma_0, T_1)}{\sigma(\infty, T_0)} - \frac{\sigma(\sigma_0, T_0)}{\sigma(\infty, T_0)} \tag{4.18}$$

In the subgroups in which this effect is appreciable, the selfshielding Doppler coefficient is calculated in this manner. At the same time, it becomes evident that in some groups the Doppler effect is negative.

The format of the tabulated Doppler coefficients is analagous to the format used for the selfshielding factors themselves. The only difference is that for each group for which data are given, the MF=5 table has two rows instead of one: the first one contains the value of Δ_1, and the second contains the value of Δ_2. In the MF=305 tables, there are $2xNs_g$ rows for each group, where Ns_g is the number of subgroup in group g. The number of the group which are assigned selfshielding temperature effects are entered only in the first of the two rows. The subgroup number is not given in the MF=305 table, instead it is determined by the sequential number of each pair of rows, for each given group.

The following procedure is recommended for the calculation of the selfshielding factor for a given value of dilution cross section σ_0 and temperature T:

1) for $\sigma_0 \geq 10^{N+4}$ $f(\sigma_0, T) = 1$ for any given T value;

2) for smaller value of σ_0, the selfshielding factors are calculated for two dilution cross sections values which are closest to the one being investigated, for all three temperatures of the medium $\sigma_{0,i} \times 10^N \leq \sigma_0 \leq \sigma_{0,i+1} \times 10^N$.

for $\sigma_0 = \sigma_{0,i} \times 10^N$ or $\sigma_{0,i+1} \times 10^N$:

$f(\sigma_0, T_0)$ is taken from the MF=5 table for the corresponding MT reaction;

$$f(\sigma_0, T_1) = f(\sigma_0, T_0) + \Delta_1(\sigma_0); \tag{4.19a}$$

$$f(\sigma_0, T_2) = f(\sigma_0, T_0) + \Delta_1(\sigma_0) + \Delta_2(\sigma_0) = f(\sigma_0, T_1) + \Delta_2(\sigma_0). \tag{4.19б}$$

3) For each temperature value T, an interpolation of selfshielding factor values is performed for the required dilution cross section value:

- when $\sigma_0 < \sigma_0 \times 10^N = 0{,}1 \times 10^N$

$$f(\sigma, T) = f(0, T) + \left[f\left(0.1 \times 10^N, T\right) - f(0, T) \right] \times \frac{\sigma_0}{0.1 \times 10^N}; \qquad (4.20a)$$

- when $\sigma_{0,1} \times 10^N \le \sigma_{0,i} \le \sigma_0 \le \sigma_{0,i+1} \le \sigma_{0,15} \times 10^N$

$$f(\sigma_0, T) = f\left(\sigma_{0,i}, T\right) + \left(f\left(\sigma_{0,i+1}, T\right) - f\left(\sigma_{0,i}, T\right) \right) \times \frac{\ln\left(\sigma_0 - \sigma_{0,i}\right)}{\ln\left(\sigma_{0,i+1} - \sigma_{0,i}\right)} \qquad (4.20б)$$

- when $\sigma_0 > \sigma_{0,15} \times 10^N$ use the previous interpolation formula, and

$$i=15,\ \sigma_{0,16} = 10^{N+4},\ f\left(\sigma_{0,16}, T\right) = 1 \quad \text{for any value of T.}$$

4) Perform a parabolic interpolation of the temperature logarithm for the given temperature

$$\begin{aligned} f(\sigma_0, T) = {} & \frac{(\ln T - \ln T_1) \times (\ln T - \ln T_2)}{(\ln T_0 - \ln T_1) \times (\ln T_0 - \ln T_2)} \times f(\sigma_0, T_0) + \\ & + \frac{(\ln T - \ln T_0) \times (\ln T - \ln T_2)}{(\ln T_1 - \ln T_0) \times (\ln T_1 - \ln T_2)} \times f(\sigma_0, T_1) + \\ & + \frac{(\ln T - \ln T_0) \times (\ln T - \ln T_1)}{(\ln T_2 - \ln T_0) \times (\ln T_2 - \ln T_1)} \times f(\sigma_0, T_2). \end{aligned} \qquad (4.21)$$

This interpolation method of the temperature can be applied for 200K<T<2500K.

If the medium is composed of a number of nuclides which have resonances in their cross sections, two dilution cross sections must be used for each one of them in the iteration procedure described below; the first one denoted as before by σ_0 (it will be used in the calculation of the resonance selfshielding cross sections averaged over the spectrum of the zeroth harmonic of the neutron flux), and the second, denoted by σ_1 (it will be used for the calculation of the selfshielding of the total cross section whose averaging is weighted by the first harmonic of the neutron flux, i.e., weighted by the current).

In the case of the zeroth iteration of the ith nuclide,

$$\sigma_{1,i}^{(0)} = \frac{1}{c_i} \sum_{j \ne i} c_j \sigma_{t,j}, \qquad (4.22a)$$

where $\sigma_{t,j}$ is the group-averaged total cross section of nuclide j taken from the MF=1 table. After the dilution cross sections in the given approximation have been calculated for all of the nuclides in the medium, including the resonance structure in the group being investigated

(i.e., for which MF=4 tables have been given, or MF=304 tables in the case of subgroup data), let us consider the next iterations.

In the kth iteration, the following equation must be satisfied:

$$\sigma_{1,i}^{(k)} = \frac{1}{c_i} \sum_{j \neq i} c_j \sigma_{t,j} f_{t,j}\left(\sigma_{0,j}^{(k-1)}, T\right). \qquad (4.22б)$$

It is recommended to perform three iterations for $\sigma_{1,i}^{(k)}$, that is for $k_{max} = 3$. Next, let $\sigma_{1,i} = \sigma_{1,i}^{(k\,max)}$, a $\sigma_{0,i}^{(0)} = \sigma_{1,i}^{(k\,max)}$, and perform another three iterations, in order to derive $\sigma_{0,i}$

$$\sigma_{0,i}^{(k)} = \frac{1}{c_i} \sum_{j \neq i} c_j \left[\sigma_{e,j} f_{e,j}\left(\sigma_{0,}^{(k-1)}, T\right) + \sigma_{c,j} f_{c,j}\left(\sigma_{0,j}^{(k-1)}, T\right) + \right.$$
$$\left. + \sigma_{f,j} f_{f,j}\left(\sigma_{0,j}^{(k-1)}, T\right) + \sigma_{in,j} f_{in,j}\left(\sigma_{0,j}^{(k-1)}, T\right) \right]. \qquad (4.23)$$

4.6 Fission Neutron Spectra

4.6.1 Prompt neutron fission spectra

The prompt fission neutron spectra are not given in tabular form in the BNAB-93 system of nuclear constants. These spectra are recommended to be calculated by auxiliary programs with the assumption that they are described by the Watt spectrum formula:

$$\chi(E) = \frac{2\exp(-ab/4)}{a\sqrt{\pi ab}} \exp(-E/a) sh\sqrt{bE}. \qquad (4.24)$$

As shown in paper [12], this formula gives the possibility to incorporate existing results of recent prompt fission neutron spectra measurements to an accuracy commensurate to the uncertainties of those measurements. Furthermore, the a and b parameters for different fissile nuclide and for different neutron energies which can induce fission, lend themselves to simple systematics (energy is given in MeV):

$$a = 1{,}03 \qquad (4.25a)$$
$$b = 0{,}858\ \overline{\nu}\ + 0{,}465. \qquad (4.25b)$$

The average energy of fission neutrons is given by the following formula:

$$\overline{E} = 1{,}5a + 0{,}25a^2 b. \qquad (4.26)$$

In the case of thermal neutron (ν-bar= 2.432) fission of uranium-235, the average energy is calculated to be: E-bar = 1.976 MeV which agrees very well with the average value of measured quantities given by different authors (1.97± 0,02). Unfortunately, the calculated

value of the average fission neutron energy for this most important fuel nuclide, which is based on the evaluation of all of the measured differential experiments (see [12]), differs from the value of 2.03 MeV, which provides the best agreement between measured and calculated values of integral characteristics of cross sections averaged over the fission spectrum as well as over reactor spectra. In order to eliminate this discrepancy in the working version of the BNAB-93 system, the possibility exists to calculate the uranium-235 (and only for uranium-235) fission spectrum using the value of a=1.476, which guarantees a value of E-bar=2.03 MeV for the average neutron fission energy.

4.6.2 Characteristics of delayed fission neutrons

In order to represent the delayed fission neutrons in the BNAB-93 system, the delayed neutron precursors are subdivided into six groups. The intensity of the emitted delayed neutrons in energy group g , at a time t after the fission event in the isotope in question is represented by the following formula:

$$S_d(t) = F\ \nu_d \sum_{i=1}^{6} \alpha_i\ \gamma_i^g \exp\left(-\lambda_i\ t\right) \qquad (4.27)$$

where F is the number of fissions per event, ν_d is the number of delayed fission neutrons, α_i is the fraction of these neutrons belonging to the *I*-th group of delayed neutrons, γ^g_i is the probability that the delayed neutron will belong to the *g*-th energy group, λ_i is the decay constant for the *I*-th group of precursors.

The ν_d quantity in the BNAB-93 system is considered to be dependent on the energy of the incident neutron although that dependence is weak:

- for E_n <5 МэВ $\qquad \nu_d = \nu_d^{th}$. (4.28а)

- for E_n >7 МэВ $\qquad \nu_d = \nu_d^{fast}$. (4.28б)

- for 5 МэВ> E_n >7 МэВ $\qquad \nu_d(E_n) = \nu_d^{th} + (E_n - 5) \times \left(\nu_d^{fast} - \nu_d^{th}\right)/2$. (4.28в)

It follows from this dependence that:

- in groups *g=-1* и *g=0* $\qquad = \nu_d^{fast}$,

- in group *g=1* $\qquad \nu_d = 0{,}04 \times \nu_d^{th} + 0{,}96 \times \nu_d^{fast}$,

- in group *g=2* $\qquad \nu_d = 0{,}88 \times \nu_d^{th} + 0{,}12 \times \nu_d^{fast}$,

- in groups *g=3* по *g=26* $\qquad \nu_d = \nu_d^{th}$.

The example given in Table 5 shows delayed neutron data for uranium-235. The body of the table contains LT=8 columns. The first two rowss of the first column contain no information. The first row of the last six columns contains the delayed neutron fractions α_i, whereby the sum of the α_i is equal to 1. The average number of delayed neutrons emitted during fission of the considered nucleus by thermal neutrons ν_d^{th} is contained in the 8th column. The value of the decay constants λ_i (given in units of 1/s) is given in the second rows of the six columns. The average number of delayed neutrons emitted during fission of the considered nucleus by neutrons having an energy larger than 7 MeV - ν_d^{fast} - is given in the 8th column.

The third sequential row contains the following data:

- in the first column: the number of the BNAB energy group (in this variant, the numeration of the tables starts with the first group);

- in columns 2 - 7: the fraction of the spectrum corresponding to the delayed neutron group which lies within the considered BNAB energy group specified in the first column;

- in the 8th column: the fractions of the summed delayed neutron spectrum:

$$\chi_g = \sum_{i=1}^{6} \alpha_i \times \chi_g^i . \qquad (4.29)$$

Table 5. Delayed neutron fission data for uranium-235

```
NAM=U235      BIB=BN93  MF= 11  MT=  0                        DAT= .010393
LV = 10       LT =  13  LC=  8  LS=  8  LF = (I4,7E8.0)
* NG      1        2        3        4        5        6        vd
*
        .0350    .1807    .1725    .3868    .1586    .0664    .0166
        .0133    .0327    .1208    .3028    .8495   2.8530    .0093
*
    1   .0000    .0000    .0000    .0000    .0000    .0000    .0000
    2   .0000    .0000    .0000    .0000    .0000    .0000    .0000
    3   .0000    .0000    .0001    .0015    .0040    .0081    .0018
    4   .0060    .0083    .0142    .0516    .0500    .0601    .0360
    5   .1333    .1649    .1016    .1787    .1375    .1374    .1520
    6   .2646    .3402    .3573    .3263    .3056    .2960    .3267
    7   .2779    .2528    .2700    .2339    .2555    .2432    .2491
    8   .1608    .1136    .1463    .1212    .1413    .1307    .1293
    9   .0919    .0705    .0629    .0499    .0636    .0664    .0606
   10   .0384    .0268    .0277    .0217    .0226    .0254    .0246
   11   .0271    .0229    .0199    .0152    .0199    .0326    .0197
```

4.7 Westcott's G factors

Westcott's G factors are used to calculate cross sections in the thermal group if the thermalization effects are not calculated in detail, and the neutron spectrum in the thermal group is assumed to be Maxwellian:

$$\Phi(E) \approx M(E,T_n) = Const \times E \times \exp(-E/kT_n). \tag{4.30}$$

If the temperature of the neutron gas T_n in formula (4.30) is assumed to be given, it is calculated in the BNAB-93 system using the formula:

$$T_n = T_{th}\left[1+1{,}4\Sigma_a/(\xi\Sigma_e)\right], \tag{4.31}$$

where, Σ_a is calculated using the 26-group data (for E=0.0253) and the quantity $\xi\Sigma_e$ for the region lying immediately above the thermal group boundary E_{th}. This boundary may be chosen to be equal to one of the low-energy boundaries of the BNAB group: E=0.215 eV or E=0.464 eV.

In that case, the capture cross-section for the thermal group may be calculated as follows:

$$\sigma_c = \frac{\int_0^{E_{th}} \sigma_c(E)M(E,T_n)dE}{\int_0^{E_{th}} M(E,T_n)dE} = \frac{\sqrt{\pi}}{2}\frac{\sqrt{T_0}}{\sqrt{T_n}} \times \sigma_c^{26} \times C(E_{th},T_n) \times g(E_{th},T_n). \tag{4.32}$$

here, T_0 =293K ≈ 300K the normal temperature; and where g (E_{th}, T_n) is the Westcott g-factor defined by

$$g(E_{th},T_n) = \frac{1}{\sigma_c^{26}} \frac{\int_0^{E_{th}} \sigma_c(E)M(E,T_n)dE}{\int_0^{E_{th}} M(E,T_n)\sqrt{\frac{0{,}0253}{E(\text{eV})}}dE}; \tag{4.33}$$

and where $C(E_{th},T_n)$ is the normalization factor:

$$C(E_{th},T_n) = \frac{\int_0^{E_{th}} \left(\sqrt{0{,}0253}/\sqrt{E}\right)M(E,T_n)dE}{\int_0^{E_{th}} M(E,T_n)dE} \frac{2}{\sqrt{\pi}}\frac{\sqrt{T_n}}{\sqrt{T_0}}. \tag{4.34}$$

For $E_{th} \to \infty$: $C(E_{th}, T_n) \to 1$. The value of the function $C(E_{th},T_n)$ is entered in the MF=0 and MT=6 table. Westcott G-factors are entered in the MF=7 and MT=0 table for four value of E_{th} and for the same numbers of temperatures, so as to have enough space between them to perform a linear least squares interpolation on T_n. The last value of E_{th} being always equal to infinity. The absence of the MF=7 table means that the g-factors for the material under consideration may be given the value 1 to a high degree of probability.

4.8 Data on energy emission in neutron reactions

With regard to the characteristics of energy emission considered in the BNAB-93 system of nuclear constants, the energy from each interaction is considered independently: elastic scattering, capture, inelastic scattering and fission. The corresponding cross sections are given in the MF=1 table, and the resonance selfshielding factors for these cross sections are given in the MF=4 and MF=5 tables. Data on energy released locally due to the slowing down of charged particles as well as the emission of the total energy, including photon energy, are entered in the MF=8 table. In the case of elastic scattering, the local energy emission is associated with the recoil nuclei; in the case of capture and inelastic scattering, both nuclear recoil and charged particle release (if both capture and inelastic scattering emit charged particles) and in the emission of charged particles released in the decay of radioactive products of considered processes. In the latter case, only those radioactive products which have a half life smaller than three years are included.

Local energy emission in the fission process consists of the slowing down of fission products and charged particles emitted in the decay chains of radioactive products. In this case as well, only those decays which have a half life of less than three years are included. In addition to the local energy emission, both prompt gamma rays as well as gamma rays emitted in the decay of fission products contribute to the overall energy emission. The energy that is associated with the fission neutrons is not included in the overall energy emission.

When it is necessary to calculate residual energy emission generated by the radioactive decay of neutron reaction products (products that have accumulated in irradiated materials), use is made of data stored in MF=9 tables consisting of activation reaction cross sections, in MF=9 tables containing data on the radiation characteristics of radionuclides produced in neutron reactions and on energy emission in their decay, and in the MF-91 table containing data on the abundance and spectral distribution of photons emitted in the decay of nuclei.

In the BNAB-93 system it is possible to take time-dependent energy emission data into consideration. In order to take this time dependence into account, data on local and total delayed energy emission are entered in the MF=8 table in the form of a list of radionuclides that are the source of that energy.

The data needed to calculate the residual energy emission due to fission, are stored in the MF=74 table (inasmuch as the contribution to the delayed energy emission due to fission is only slightly dependent on the fissile nucleus, that contribution is not entered in the MF=8 table). If it were deemed to be necessary to include the energy of photons in the calculation of the total energy emission, the data due to local energy emission is available from the MF=8 table, and the data on photons emitted in neutron reactions is available from the MF=10 table, which contains the abundance and spectral photon data. The total energy due to photons is stored there as well.

The data on energy emission due to neutron reactions are given in the BNAB-93 system only in the form of 28-group sets. They are also meant to be used in sub-group calculations.

Data on energy emission for neutron reactions in sodium is shown in Table 6. All energies are given in MeV. The following nomenclature is used in the table:

- E-EL - local energy emission due to elastic scattering;
- E-C - local energy emission due to neutron capture;
- DE-C - local delayed energy emission due to neutron capture;
- T-C - total energy emission due to neutron capture;
- DT-C - total delayed energy emission due to neutron capture;
- E-IN - local energy emission due to inelastic scattering:
- DE-IN - local delayed energy emission due to inelastic scattering;
- T-IN - total energy emission for inelastic scattering;
- DT-IN - total delayed energy emission due to inelastic scattering
- R.N.LIST - list of identifiable numbers of radionuclides which contribute to the delayed energy emission and their decay half lives (in seconds).

Table 6. Energy emission data due to neutron reactions in sodium

NAM=NA BIB=FOND MF= 8 MT= 4 DAT= .010393
LV = 10 LT = 14 LC= 11 LS= 11 LF = (I4,E7.0,2(2E7.2,2E6.0),E8.0)

* G	E-EL	E-C	T-C	DE-C	DT-C	E-IN	T-IN	DE-IN	DT-IN	R.N.LIST
-1	3.93-1	12.99	14.28	2.343	2.536	0.677	12.997	.0116	.1430	90209.
0	3.24-1	10.01	11.42	2.259	2.836	0.508	10.559	.0006	.0072	11.0
1	2.26-1	6.02	6.70	2.102	3.391	0.438	4.566	.0	.0	100239.
2	1.77-1	3.65	3.80	1.971	3.785	0.307	2.398	.0	.0	37.2
3	1.26-1	0.168	14.61	0.553	4.674	0.205	1.387	.0	.0	110239.
4	1.05-1	0.080	13.53	0.553	4.674	0.134	0.598	.0	.0	53856.
5	6.03-2	0.045	12.69	0.553	4.674	0.069	0.509	.0	.0	110229.
6	4.30-2	0.025	12.22	0.553	4.674	0.036	0.476	.0	.0	8.206+7
7	2.16-2	0.001	11.92	0.553	4.674					
8	1.13-2	0.001	11.76	0.553	4.674					
9	5.09-3	0.001	11.69	0.553	4.674					
10	2.51-3	0.001	11.67	0.553	4.674					
11	1.16-3	0.001	11.65	0.553	4.674					
12	5.33-4	0.001	11.633	0.553	4.674					

This example includes radionuclides which contribute to the delayed energy emission, namely ^{20}F, ^{23}Ne, and ^{23}Na (which contribute to the energy emission through capture as a result of the (n,α), (n,p) and (n,γ) reactions), as well as ^{22}Na which contributes to the energy emission through inelastic scattering as a result of the (n,2n) reaction. Data may be entered in the MF=8 table either for all of the 28 groups or for the first 14 groups with *g=-1 ....g=12*, as illustrated in Table 6. In the last example, energy emission due to elastic scattering for groups 13 to 26 must be calculated starting from data of group 12, multiplying that quantity by the ratio of the group-averaged neutron energy E_n^g taken from table [0,2]:

$$E - EL_g = (E - EL)_{12} \times E_n^g / E_n^{12} . \qquad (4.35)$$

When calculating energy emission due to capture in low energy groups, the same method must be used as in the case of the group 12 calculation.

In the BNAB-93 system, the energy emission due to fission is taken to be independent of the energy of the neutron causing fission. The quantity E-F (local energy emission due to fission) is entered as the first parameter in the header rows of the MF=8 table; the quantity T-F (total energy emission due to fission) is entered as the second parameter. Since the nuclide under consideration in the example given in Table 6 is not fissile, these quantities are not given.

5. Nuclear Data for the Calculation of Photon Fields

5.1 Data on the generation of photons in neutron reactions.

In the BNAB-93 system, the generation of photons in neutron reactions is specified by the matrix $\lambda_r^{g,j}$ which determines the number of photons of group j, generated in reaction of type r ,due to neutrons of group g.

Three types of processes which lead to the generation of photons are considered:

- fission,
- capture, which, in addition to radiative capture includes reactions accompanied by the release of charged particles which are not accompanied by the release of secondary neutrons; and
- inelastic scattering, including reactions of type (n,2n) and (n,3n), as well as reactions accompanied by the release of charged particles and secondary neutrons.

The cross sections for each of these processes are given in MF=1, MT=0 tables.

In some of the first groups, starting with g=-1 the data for the last two types of processes may be combined, such that the $\lambda_r^{g,j}$ matrix in those groups considered as $\lambda_{non}^{g,j}$, i.e., they must be multiplied by the sum of the capture and inelastic scattering cross sections taken from the basic neutron constants.

In the case of the fission reaction, $\lambda_f^{g,j} = \lambda_f^j$, i.e., they are independent of the group number g, and is the same for all neutron groups.

The selfshielded capture and fission cross sections are calculated with the aid of the selfshielding factors and associated Doppler coefficients which are stored in the MF=4 and MF=5 tables and the subgroup parameters stored in the MF=6 tables. The total cross section for the generation of group j photons due to group g neutrons is equal to:

in groups where $\lambda_{non}^{g,j}$ is given:

$$\sigma_{tot}^{g,j} = \left[\sigma_c^{g,j} \times f_c^g(\sigma_0,T) + \sigma_{in}^g \times f_{in}^g(\sigma_0)\right] \times \lambda_{non}^{g,j} + \sigma_f^g \times f_f^g(\sigma_0,T) \times \lambda_f^j \qquad (5.1)$$

and in the other groups:

$$\sigma_{tot}^{g,j} = \sigma_c^g \times f_c^g(\sigma_0,T) \times \lambda_c^{g,j} + \sigma_{in}^g \times f_{in}^g(\sigma_0) \times \lambda_{in}^{g,j} + \sigma_f^g \times f_c^g(\sigma_0,T) \times \lambda_f^j \qquad (5.2)$$

The quantities λ_c , λ_{in}, and λ_f represent the contribution of photons generated by a nuclear reaction and by the decay of the radioactive products of that reaction whose half life is smaller than three years. In the calculation of these quantities, most of the generated photons having an energy which falls within an energy *j* must be corrected in order to take into account the difference between the energy of the photon and the group-averaged energy given in table [0,5]. Thus, the total energy carried by the photon in a group representation is conserved. This energy is stored in table [0,5] for each reaction *r=non, c, in, a*.

Table MF=10 is made up of 17 columns. The first column contains the number of the group. The other columns contain data associated with the group given in the first column. The following 15 columns contain the $\lambda_r^{g,j}$ data, and the last column contains the total energy carried by the photons. The sequential order of the groups and the meaning of the information stored in each row of the table are specified using the parameter BET - by the second parameter stored in the header row of the table: *nin*=INT(BET) the number of rows which contain the quantities $\lambda_{non}^{g,j}$ or $\lambda_{in}^{g,j}$ (from *g=-1 to g=nin-2*). Which of these quantities is stored in which rows will become clearer in the description that follows.

The quantities $\lambda_f^{g,j}$ are stored in the subsequent rows (*nin+1*). In the tables that contain non-fissile nuclides this row is filled with blanks. For tables containing fissile nuclides, the number of the group is not entered in this row (it is not needed, because the quantities λ_f^j do not depend on g).

The number of the highest energy group g_c , which contains the $\lambda_c^{g,j}$ data, is entered in first column of the (*nin*+2) row. This number g_c may be equal to *nin*-1; in that case, the quantities $\lambda_{non}^{g,j}$ are entered in all of the first *nin* rows. However, if g_c is smaller than *nin*-1, then the quantities entered in the first g_c +1 rows of the table have the meaning of $\lambda_{non}^{g,j}$ for groups ranging from g=-1 to g=g_c , and the meaning of $\lambda_{in}^{g,j}$ for those entered in the g_c +2 rows.

All $\lambda_c^{g,j}$ quantities must be specified for all groups having numbers g=g_c to g=26, i.e., for n=27-g_c groups. This may be done explicitly, then the total number of rows must be equal to LT=*nin*+28-g_c. But all of this information may also be given using one row, namely the last in the table, then LT=*nin*+2. In this case, the quantities $\lambda_c^{26,j}$ are entered in the last row (even though the number $g_c < 26$ is given in the first column. The quantities $\lambda_c^{g,j}$ for $g_c \le g \le 26$ are calculated using the algorithm, whose description follows.

First, let us consider the case in which the capture of a neutron is limited to radiative capture, and assume that the quantity A=1.

Let j_0^g be the minimal number of photon groups for which the following inequality is satisfied:

$$\sum_{j=1}^{j_0} \lambda_c^{26,j} \ge A . \qquad (5.3)$$

In an approximation, it can be assumed that photons entering into this group, essentially the initial photons, correspond to the transitions from the capture state. The total energy of these photons is:

$$Z = \sum_{j=1}^{j_0} \lambda_c^{26,j} E_\gamma^j \qquad (5.4)$$

In high energy groups, the total energy must be increased by an energy increment E'_n of the captured neutrons (in the given case, radiative capture is the only process under consideration). If thermal neutron capture provides a noticeable contribution to the reaction accompanied by the release of a charged particle, then the fraction of these reactions in the total capture process is defined by the parameter ALF, the first parameter to be entered in the header rows of the table. In this case, one must assume that A=1-ALF, and the total energy of the initial photons in group g must be increased by an increment $E_n^g \times A$.

On the assumption that this increase is not so big as to change the spectrum of the initial photons, which would require a correction of the total energy, a correction may be introduced by means of a correction in the generation of the initial photons:

$$\lambda_c^{g,j} = \lambda_c^{26,j} \times \left(Z + E_n^g \times A\right)/Z. \tag{5.5}$$

The table given above which is described by a rather complicated but economical structure is characterized by the designation MT=1. Aside from that, the data can be given in a more rigorous format characterized by the designation MF=0. The formats of the two tables are almost the same for both values of MT. MT=0 corresponds to the case when BET=28.0; inasmuch as this value is determined by the fact that it is not specified, the value of the second parameter, when MT=0, is not used in the processing of the table. The number of rows LT, in both MF=10 and MT=0 tabled is equal to 29. Thus, there is no room left over to enter the values and consequently, all values entered in the first 28 rows of the tables can always be represented by $\lambda_c^{g,j}$. Since $\lambda_{non}^{g,j}$ is not given, there is no need for the parameter ALF and it is not used in the case of MT=0. If necessary, the values $\lambda_f{}^j$ are entered in the last rows of the table.

Table 7. Group yield of photons in neutron reactions for aluminium

NAM=AL		BIB=FOND	MF= 10	MT= 1	ALF= 0.0		BET= 6.0	
LV = 10		LT = 8	LC= 16	LS= 9	LF = (I3,8E8.0)			
*G1	1	2	3	4	5	6	7	8
-1		0.1362	0.1620	0.1391	0.2121	0.5181	0.6691	0.4849
0		0.0744	0.1457	0.1307	0.1840	0.4787	0.6254	0.4459
1		0.0160	0.0630	0.0597	0.0904	0.3532	0.4425	0.2714
2		0.0000	0.0055	0.0057	0.0237	0.2395	0.3410	0.1761
3		0.0001	0.0000	0.0001	0.0016	0.0628	0.3304	0.0852
4		0.0002	0.0001	0.0002	0.0002	0.0002	0.0251	0.0000
5								
*								
4		0.3710	0.1200	0.2500	0.3160	0.2910	1.0200	0.0682
*								
*G1	9	10	11	12	13	14	15	E-SUM
-1	0.5579	0.1590	0.0000	0.0000	0.0000	0.0000	0.0000	7.9949
0	0.5495	0.1340	0.0000	0.0000	0.0000	0.0000	0.0000	6.9398
1	0.4865	0.0971	0.0000	0.0000	0.0000	0.0000	0.0000	4.1290
2	0.4665	0.0687	0.0000	0.0000	0.0000	0.0000	0.0000	2.3699
3	0.5734	0.0195	0.0000	0.0000	0.0000	0.0000	0.0000	1.6098
4	0.9344	0.0000	0.0000	0.0000	0.0000	0.0000	0.0000	0.9920
5	0.9310	0.0000	0.0000	0.0000	0.0000	0.0000	0.0000	0.9310
*								
4	0.0793	0.0784	0.0616	0.0192	0.0110	0.0055	0.0027	9.5157

The yield of photons in aluminium is given as an example in Table 7. In that example, g_c =4. Hence, the data entered in the table for groups g=-1,0,1,2,3 must be considered as $\lambda_{non}^{g,j}$ (except those given in the last column, which represent the corresponding summed energy) The values of $\lambda_{in}^{4,j}$ are entered in the fifth row, and $\lambda_{in}^{5,j}$ in the sixth row. (in this case *nin* is equal to six). The seventh row reserved for λ_f^j, is empty in the case of aluminium. In the following rows, the group number g_c =4 is specified, but at the same time, as it is the last row (LT=8), only one row for $\lambda_c^{26,j}$ is given, which is self evident since aluminium has only one isotope and the energy dependent experimental data λ_c^j for ^{27}Al is absent.

5.2. 15-Group photon constants

The energy boundaries and average group energies for photon groups are given in the BNAB MF=o and MT=4 tables. There are eight types of cross sections for each group:

SKN= - Compton scattering on atomic electrons cross section (assuming that these are free atoms, using the Klein-Nishina-Tamm formula) ;

SBD= σ_{comp} - Compton scattering cross section, derived on the assumption that these are atom bound electrons;

SN= σ^{pair} - pair production cross section;

SPH= σ^{photo} - photoelectric cross section;

STT= σ^{tot} = SBD + SN + SPH + σ^{coh} (where σ^{coh} is the coherent (Raleigh) scattering);

ST= σ^{t} = SBD + SN + SPH = STT - σ^{coh};

SA= σ^{abs} = ST - (SBD x f_{comp}) (where f_{comp} = the fraction of the energy scattered by Compton scattering;

SAE= = ST - (SN x f_{pair}) - (SPH x f_{photo}) - (SBD x f_{comp}) (where f_{pair} and f_{photo} are fractions of energy scattered during the pair production process and during the photoelectric process, as a result of Bremsstrahlung radiation, positron annihilation and luminescence radiation accompanying the photoelectric process).

For the majority of photon transport calculations, it is enough to know σ_t and σ_{comp}. The energy-angle indicator for the angular momenta from the zeroth to the 15th group in the 15-group representation of the data, calculated for a single free electron using the Klein-Nishina-Tamm formula are given in the MF=0 and MT=15 table. This indicator can be used to evaluate the angular distribution and photon spectra for scattering on bound electrons. Coherent scattering in this approximation can be neglected, and the photoelectric and pair production processes are considered as absorptions. For instance, if σ_{comp}^{K-N} and σ_{comp} differ slightly, then the use of the indicator calculated for scattering on free electrons is definitely justified. If the differences are signicant, then the extent to which they affect the problem under consideration must be determined. The BNAB photon groups are listed in Table 8.

Table 8. BNAB photon group constants

NAM=FE BIB= BN93 MF= 11 MT= 0 DAT= .010393
LV = 10 LT = 15 LC= 9 LS= 9 LF = (I4,F7.0,2F8.0,5F9.0)

GR	SKN	SBN	SN	SPN	STT	ST	SA	SAE
1	1.338	1.338	1.420	0.00	2.77	2.77	2.33	1.97
2	1.574	1.574	1.184	0.00	2.76	2.76	2.23	1.91
3	1.873	1.873	0.953	0.00	2.83	2.82	2.16	1.87
4	2.173	2.173	0.753	0.00	2.93	2.93	2.12	1.84
5	2.522	2.522	0.561	0.00	3.09	3.09	2.09	1.85
6	3.029	3.029	0.344	0.01	3.38	3.38	2.09	1.91
7	3.722	3.722	0.153	0.01	3.89	3.88	2.15	2.04
8	4.508	4.507	0.039	0.02	4.57	4.56	2.27	2.21
9	5.560	5.549	0.004	0.04	5.63	5.59	2.46	2.42
10	7.325	7.282	0.000	0.18	7.61	7.46	2.72	2.70
11	9.940	9.737	0.000	1.85	12.36	11.60	4.21	4.15
12	12.417	11.735	0.000	16.77	31.53	28.51	18.63	18.25
13	14.181	12.546	0.000	120.22	142.25	132.95	121.49	117.05
14	15.538	11.781	0.000	999.07	1039.66	1010.43	999.77	923.93
15	16.419	9.555	0.000	7006.02	7084.87	7012.98	7006.02	5962.42

Since the binding effect manifests itself only in the lowest energy groups, omitting the electron binding effect on the form of the energo-angular distribution of scattered photons is entirely acceptable (when considering the effect of this influence on the cross section). Knowing the difference between σ_{tot} and σ_t which is equal to σ_{coh}, makes it possible to solve the problem whether it is necessary to take Raleigh scattering into consideration. Generally speaking, this scattering process can be included without any problem in the Thompson approximation model, i.e., without considering form factors which were taken into consideration in the calculation of the cross section. The difference between SAE and SA gives an indication as to the importance of including secondary photons formed during the pair production and photoelectric processes. If absolutely necessary, some of the secondary photons, and in particular the annihilation photons, may be taken into consideration since the pair production cross section is known and the energo-angular distribution of the annihilation photons is known as well. Consideration of the finer influencing effects of electron-atom binding on the energo-angular distribution of scattered photons, consideration of the Bremsstrahlung radiation generated by the Compton and photoelectric electrons, and the positron generated luminescence radiation, all of these require additional data, which are not available in the current version of the BNAB library. On the basis of the data that are available, it is only possible to evaluate the degree to which these effects are important.

REFERENCES

[1] MANTUROV, G.N., NIKOLAEV,M.N., TSIBULYA, A.M., The BNAB-93 Group Constants System. Verification Report. TsNIIAI, Moscow (1995).

[2] Library of Recommended Evaluated Neutron Data - BROND-2. Problems in Nuclear Science and Technology, Series: Nuclear Constants, No. 2(3) (1991) [in Russian].

[3] NIKOLAEV, M.N., RYAZANOV, B.G., SAVOS'KIN, M.M., TSIBULYA, A.M., Multigroup Approximation of the Neutron Transport Theory. Ehnergoatomizdat, Moscow (1984) [in Russian].

[4] RSIC Shielding Routine Collection. PSR-171/NJOY91.13, Radiation Shielding Information Center, Oak Ridge National Laboratory.

[5] SINITSA V.V. , Program for the Calculation of Group Constants Using Libraries of Evaluated Neutron Data. Problems in Nuclear Science and Technology, Series: Nuclear Constants No. 5(59) (1984)34 [in Russian].

[6] ABAGYAN, L.P., BAZAZYANTS, N.O., BONDARENKO, I.I., NIKOLAEV, M.N., Group Constants for Nuclear Reactor Calculations, Atomizdat, Moscow (1964) [in Russian].

[7] NIKOLAEV, M.N., CHOKHLOV, V.F., A system of Subgroup Constants. Information Bulletin of the Nuclear Data Centre No. 4 (1967) 420 [in Russian].

[8] CHOCHLOV, V.F., SAVOS'KIN, M.M., NIKOLAEV, M.N., Complex of Computational Programs ARAMAKO for the Calculation of Group Macro- and Blocked Micro- Cross Sections on the Basis of the 26-Group System of Constants in Subgroup Representation. Problems in Nuclear Science and Technology, Series: Nuclear Constants No. 8(3) (1972) 3 [in Russian].

[9] ABAGYAN, L.P., BAZAZYANTS, N.O., NIKOLAEV, M.N., TSIBULYA A.M., Group Constants for the Calculation of Reactors and Shielding. Ehnergoizdat, Moscow (1981) [in Russian].

[10] NIKOLAEV, M.N., SAVOS'KIN, M.M., Current State of the ARAMAKO System. Problems in Nuclear Science and Technology, Series: Nuclear Constants No.5(59) (1984) 24 [in Russian].

[11] ABAGYAN, L.P., YUDKEVICH, M.S., Evaluated Neutron Data for the Calculation of Thermal Reactors. Problems in Nuclear Science and Technology, Series: Nuclear Constants No.4(43) (1981) 24 [in Russian].

[12] KHOMYAKOV, Yu.S., NIKOLAEV, M.N., DOLGOV, E.V., TSIBULYA, A.M., Evaluation of Prompt Fission Neutron Spectra for their Application in Engineering Calculations. Problems in Nuclear Science and Technology, Series: Nuclear Constants No. 1 (1992) 70 [in Russian].

A NUCLEAR REACTION CROSS-SECTION DATABASE FOR ION BEAM ANALYSIS

A.F. Gurbitch, V.A. Ershova

State Research Centre of the Russian Federation
Institute of Physics and Power Engineering, Obninsk

Abstract

A PC database containing most nuclear cross-sections used in ion beam analysis (IBA) has been developed. Excitation functions and yield curves, both in the form of graphs and tables, are presented in a easy to use format. Current information as well as previously compiled data published in handbooks and tables are included. Data available only in the form of published graphs were digitized using precise technological methods. Each of the references used in this compilation is discussed in a short comment in the text. The information used in the database may be used as a guide while planning an experiment or as a source of data used in spectra simulation computer programs.

The analysis of the composition and surface structure of materials using the Nuclear Reaction Analysis method [1] requires an extensive knowledge of charged particle induced nuclear reaction cross sections at low energies (e.g., E<10 MeV). These data are needed for two processes: as input to programs designed for the analysis of measured spectra obtained in the determination of the distribution and concentration of the composite elements, and for the determination of optimal conditions of planned experiments. With regard to the latter, it is also necessary to have a knowledge of the reaction data for all reactions that are possible in the given sample. Information pertinent to this analysis was generated primarily in the 1950-ies and 1960-ies in conjunction with intensive studies of the nuclear level structure, and is available in various publications. A large amount of data has also been generated recently specifically for the nuclear microanalysis method. Part of this information has been collected in handbooks [1-3]. However, the required availability of the data needed for nuclear microanalysis is far from being satisfied. The urgent need for the systematic compilation and evaluation of nuclear reaction cross section data is widely acknowledged [4]. The wide application of spectral analysis programs which have been written for PC's (personal computers) requires that the needed information be available in a format amenable for input in these programs.

Table 1. Composition of the NRABASE database.
(The numerals indicate the number of data files)

	p,p_0	p,α_0	p,γ	$p,\alpha\gamma$	$p,p'\gamma$	d,d_0	d,p_0	d,p'	d,α_0	d,α'	$^3He,p_0$	$^3He,p'$	$^3He,\alpha_0$	α,α_0	α,p_0
^2H							2				1				
^3He															
^6Li	5	3													
^7Li	8	10													
^9Be	1								1						
^{10}B	1	1							1	1					
^{11}B	1	1													
^{12}C	9		2			2	5				3	6	1	9	
^{13}C							1		1						
^{14}N	6					1		4	2	2		5	1	7	1
^{15}N		6		1					1						
^{16}O	3		1			2	4	6	6					10	
^{18}O	1	11													
^{19}F	7	4													
^{23}Na			2	2	2		1		1						
^{nat}Mg	1														
^{27}Al	2		2	1	2										
^{28}Si	3														
^{31}P			1	1											
^{32}S	2														
^{nat}Cl	1														
^{48}Ti	1														
^{52}Cr			1												
^{nat}Zn	1														
^{109}Ag	1														

This report describes the development of a database, called NRABASE, to be used on IBM PC's. This database contains most nuclear reaction cross sections required for surface analysis using ion beams. The data included in this database have been compiled from a large number of references published since 1953. The first version of this database contains nuclear data for charged particles reactions for both input and output channels (including non-Rutherford reverse scattering) and data for some (p,γ) reactions (see Table 1).

The nuclear reaction excitation functions and the output spectra are represented in the form of graphs and tables which are presented in a special "friendly" format. A significant amount of

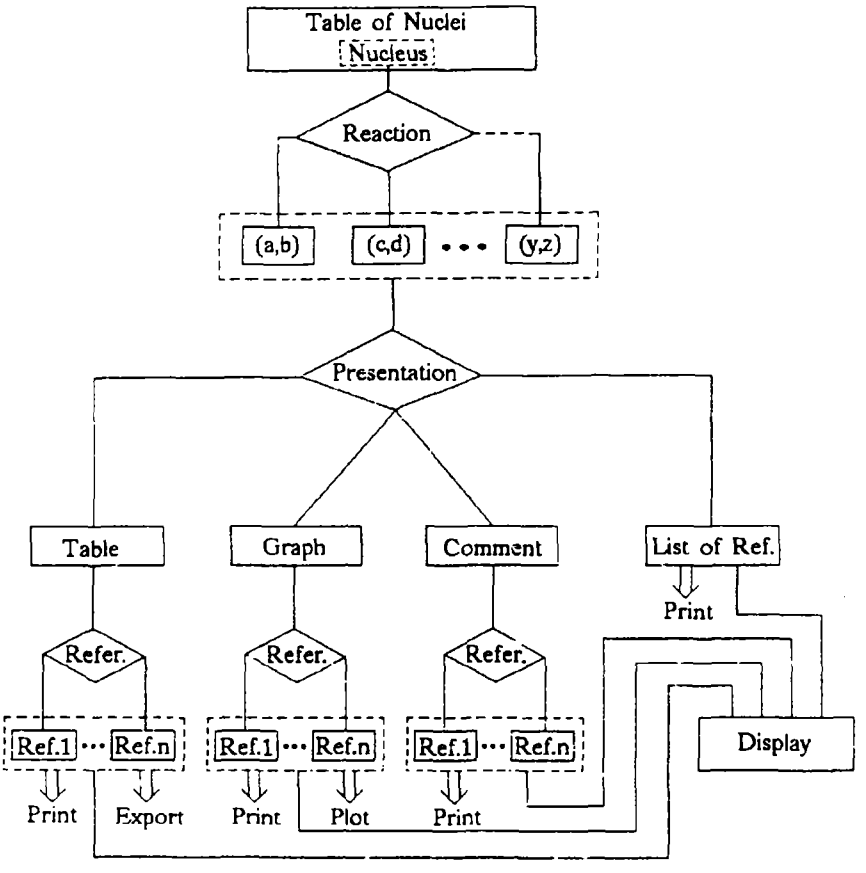

Figure 1. Structure of the NRABASE database

information which is published only in the form of graphs has been digitized using the following method. The graphs were scanned and displayed on the screen and the coordinates of selected points of the graphs were identified with the use of a marker which converted the data to the corresponding energy and cross section value pairs. In the course of this procedure, the image on the screen was adjusted for the inevitable skewing of the image in the scanning process. The results of the digitizing procedure were checked against the data that were published in both graphical as well as in tabular form. The uncertainties introduced by the digitizing process did not exceed 3%. It must be noted that these uncertainties included errors introduced in the course of the production of the final image and the distortion introduced in the final printing.

Two alternative possibilities to access data for the development of the database were implemented: to use the actual tabulated and plotted data from a given information source, and to use data from a selected number of different sources. The latter approach, considered by the

authors to be the most convenient, was actually used in this procedure. The structure of the database is shown in Figure 1.

The data stored in the NRABASE database were compiled from more than 100 published sources. Each reference is accompanied by a short comment which includes the experimental details of the measurement and the error analysis of the measured data. The graphical information is stored in a form that can be conveniently used by the plotting program designed to plot the data with the use of an HP printer. The total information stored in the database consists of approximately 3 Mb of data.

The NRABASE database can be obtained from the FTP SigBase archive through the Internet using the following addresses: ihn.gns.cri.nz or physics.isu.edu. The next version of NRABASE, which is currently being developed, will contain cross sections required for the analysis of hydrogen isotopes using the nuclear recoil method.

REFERENCES

[1] MAYER, J.W., RIMINI, E. , (Eds), Acad.Press, New York (1977).

[2] TESMER, J.R., NASTASI, M., (Eds), Handbook of Modern Ion Beam Material Analysis, MRS, Pittsburg (1995).

[3] SOROKA, V.I., Selected Data on the Low-Energy Elastic Scattering for the use in Nuclear Microanalysis, Preprint KIN-94-2, Kiev (1994).

[4] VICKRIDGE, I.C., Nucl.Instr.Meth. V.B66 (1992) 303.

SURVEY OF NEUTRON SPECTRA GENERATED BY THE FISSION OF HEAVY NUCLEI INDUCED BY FAST NEUTRONS

G.N.Lovchikova, A.M. Trufanov

State Research Centre of the Russian Federation
Institute of Physics and Power Engineering, Obninsk

Abstract

A review of neutron fission spectra measurements is presented. This review and the results of this analysis was performed with the participation of the authors. It is shown that there is a need for additional measurements of the energy and angular distributions of secondary neutrons in order to improve the understanding of the neutron emission mechanism in fission.

Introduction

Although fission neutron spectra of the actinides have been studied extensively for a long time, it is not apparent that this problem will be solved in the near future. The interest in the experimental and theoretical study of fission neutron spectra for the following two reasons.

1. The energy spectrum of secondary neutrons emitted at the time of neutron fission, which is one of the most important characteristic of the fission process, is used primarily in the design and calculations of nuclear reactors. Of the most important aspects of this process is the dependence of the neutron spectrum shape on the energy of the bombarding neutron, and the associated average energy of the secondary neutrons. Because of the considerable experimental difficulties inherent in the measurement of fission neutron spectra, the amount of published data is sparse and the results of the average neutron energy are noticeably disparate. This circumstance necessitates a thorough evaluation of the published data and the generation of recommended values.

2. The scientific aspect of this problem consists in the development of a model describing the mechanism of the emission of neutrons induced by the fission of heavy nuclei - a most complex transmutation of nuclear matter - with the objective of developing a theory of nuclear fission. The required information to create such a theory is derived from various energy and angular differential distributions of secondary neutrons. Due to the development of the measurement technology in the course of the last few years, it has been possible to improve the accuracy of the measured fission neutron spectra and to determine a number of new properties of this process, particularly its mechanism.

Experimental Technique

Without a doubt the most widely used method to study neutron energy spectra is neutron spectrometry in conjunction with the time-of-flight method. This method guarantees a high accuracy and high degree of reliability. Depending on the features of the problem, there are a variety of variants of this method. The study of prompt fission neutron spectra, especially in the case of neutron induced fission, imposes its own specific requirements on the construction of the detectors and the whole design of the experiment.

At the present time, time-of-flight spectrometers, mounted on the FEI accelerators KG-2.5 and EGP-10M, are used to measure integral prompt neutron spectra due to fast neutron induced fission in actinide nuclei. Each of the spectrometers, includes a multi sectional ionization fission chamber, a neutron detector, the shielding of the neutron detector, and the associated instrumentation for the control of the experiment and for the preprocessing and storage of the collected data. A schematic of a typical experimental geometry is shown in Figure 1.

The most important element of the neutron spectrometer is the fission fragment detector which to a large extent determines the reliability of the results. The fission fragment detector chosen for our experiments consisted of an ionization chamber with layers of fissile nuclides [1]. Due to the unique combination of these characteristics,: such as a fast response (with an attainable time resolution of 0.5 ns [2]), a highly effective registration of fission fragments, the simplicity of the construction, the high reliability and stability of its operation, this ionization chamber represents an optimal piece of instrumentation used in the study of nuclear fission. Using the concept of sectionalization, it was possible to solve a number of problems: namely, to reduce the dispersion in the flight path and to introduce corrections in the changes in each section of the flight path, to reduce the inherent electrical capacitance of the chamber, resulting in the improvement of the time resolution to 1.5 ns for an individual section. The most important achievement is that it was possible to record the time reference point independently of the fission fragment signal due to the choice and implementation of special preamplifiers. This method of obtaining a time reference has a number of advantages over the widely used method, in which the time correlation is triggered by the high frequency voltage of the collection electrode of the accelerator, and the fission chamber signals serve only to select those events which are related to fission (i.e., the measurements take place in the regime of "fast-slow" correlations). The ability to obtain an intermittent time reference independent of the signals from the fission fragment chamber, gives the possibility to use the accelerator in a continuous mode, and to realize a higher intensity of the neutron beam, and thus guarantee the necessary statistical accuracy of the measurement results. The continuous operation regime of the accelerator considerably improves the discrimination of the background and simplifies the procedure to introduce corrections to the background of random coincidences.

In the course of our work, we constructed and tested chambers with layers of ^{232}Th, ^{235}U, ^{237}Np and ^{239}Pu. The neutron detectors incorporated elements of monocrystaline stilbene having a diameter of 63 mm and a height of 39 mm connected to an FEU photomultiplier. The neutron detector which was situated within a specially designed shielding assembly, whose quality played a crucial role in the possibility to measure the desired effect. The optimum suppression of the neutron and gamma ray background was achieved by a carefully selected

shield geometry, the judicious arrangement of its individual components, and by a selected choice of shielding materials. In order to minimize the registration of gamma rays, the neutron and gamma rays were separated on the basis of their pulse shape. The total time resolution of the spectrometer was less than 2.5 ns for a flight path of 2 m. The absolute effectiveness of the neutron detector was determined by normalizing to the ^{252}Cf spontaneous fission neutron spectrum whose shape was taken from reference [3]. The basic component of the electronic assembly which was incorporated in the spectrometer was based on the KAMAK standard. The collection and preliminary processing of the information was performed with the aid of a personal computer.

Results of the fission neutron spectrum measurements

The experimental measurements of fission neutron spectra were performed for primary neutron energies ranging from 0.5 to 17.7 MeV for the ^{232}Th, ^{235}U, ^{237}Np, ^{238}U and ^{239}Pu nuclides. As mentioned above, all fission neutron spectra were measured with spectrometers using the time-of-flight method on the KG-2,2 and EGP-10M accelerators [4], as well as with the neutron spectrometer of the Central Institute of Nuclear Research at Rossendorf in Germany. The reactions D(d,n)^{3}He, T(d,n)^{4}He and T(p,n)^{3}He, using gaseous tritium, gaseous deuterium and solid tritium as targets, served as neutron sources. It must be noted that information on the measurement of fission neutron spectra for the indicated nuclides at the selected initial energies is absent in the open literature.

The results of measurements of fission neutron spectra at initial energies ranging from 0.5 to 6 MeV (i.e., up to the threshold of the (n,n'f)) were used to test the evaluations of the dependence of the average fission neutron energy as a function of initial neutron energies.

A typical example of the current status of the experimental information available on fission neutron spectra is the dependence of the average secondary neutron energy $\overline{E}$ on the energy of the primary neutron E_n for the widely used ^{235}U nuclide. Typical for this nuclide is the considerable scatter of the experimental data between the initial $\overline{E}$ value and E_n = 3 MeV, their complete absence between 7 MeV and 14 MeV and the significant disagreement among the existing evaluations of the actual dependence at even high energies of E_n [5]. An illustration of the state of the existing experimental information is given in Figure 2. In addition to the actual measurements [6-16], Figure 2 shows the evaluations of the $\overline{E}(E_n)$ dependence based on individual national libraries of microscopic nuclear data ENDF/B-VI (USA), JENDL-3 (Japan) and BROND-2 (Russia) as well as the latest version of the Russian BNAB-90 set of group constants used for reactor calculations. It can be seen that the scatter of the experimental points is not systematic and is due to the fact that the value of $\overline{E}$ in the energy range of $E_n < 3$ MeV is constant, as assumed in the ENDF/B-VI version, rather than to the increase of the $\overline{E}(E_n)$ function as is expected from theoretical considerations. Furthermore, the results published in reference [10] give a clear indication for an opposite tendency. Finally, the difference between the evaluations of $\overline{E}(E_n)$ based on the national libraries can be as high as 5% while the accuracy requirements range from 1-2 %. It must be noted, however, that all evaluations of the $\overline{E}(E_n)$ dependence given in Figure 2 are close to being linear, and have an approximately similar slope, which is characterized by the derivative $d\overline{E}/dN$ which is equal to 0.025 - 0.03 [16]. The same pattern of the $\overline{E}(E_n)$ dependence for the (n,f) reaction, can be observed for all investigated nuclides.

After analyzing all of the available experimental and evaluated data of the $\overline{E}(E_n)$ dependence it was decided to discard those data which did not satisfy that criteria characterized by the dispersion and discrepancy of the data. This resulted in a selection of consistent $\overline{E}(E_n)$ values for ^{235}U which were in better agreement with the evaluations incorporated in the BROND-2 and BNAB-90 group libraries [16].

The Table lists information on the average fission neutron characteristics of the investigated nuclides. The values of the average neutron energies resulting from the (n,f) reaction (i.e., in the case of a "clean" fission process), in which the emission of pre-fission neutrons is energetically impossible, were determined using two separate methods. In the first method, the temperature "T", which was used as the description parameter, was derived by using the least squares method of the observed Maxwellian distribution:

$$N_m(E) = 2(E/\pi \cdot T^3)^{1/2} \exp(-E/T) \quad (1)$$

This equation establishes the relationship between the average energy $\overline{E}$ and the temperature T, where

$$\overline{E}=3/2T \quad (2)$$

In the second method the value of E was determined in accordance with

$$\overline{E}=\int_0^\infty EN(E)dE \quad (3)$$

from the directly observed spectrum N(E), which for energies lower than the limiting condition $E<E_{min}$, equal to the energy threshold of the neutron detector, was extrapolated in accordance with the dependence given by equation (1). Both methods give values of $\overline{E}$ which agree within the limits of their uncertainties.

At primary neutrons energies, which are larger than the fission threshold energies, fissions of the remaining nuclides A-1 and A-2 occur in addition to the fissioning of the initial nuclide A. In this case, the experimental spectrum consists of the superposition of post-fission neutron spectra (prompt fission neutron spectra due to fission fragments from the A, A-1 and A-2 nuclides), and pre-fission neutrons (spectra of neutrons emitted before fission) registered in coincidence with fragments from the A-1 nuclides in addition to spectra of primary and secondary neutrons in coincidence with fragments from the A-2 nuclides. In this case, the $\overline{E}$ parameter was determined only by using the second method in accordance with equation (3).

The Table also lists the final values of the $\overline{E}(E)$ dependence; these data take into account corrections due to the effect of the angular "secondary neutron" - "primary neutron" correlation which occurs as a result of the angular anisotropy of the scattered fragments and the strong angular correlation between the forward motions of the post-fission neutrons and the fission fragments. The same method as that used in reference [6] was used for the correction to account for the angular correlation.

The errors listed in the Table combine the statistical errors, the errors in the corrections, and systematic errors due to the discrimination of part of the fragments in the fission detector.

Average fission neutron characteristics

Nuclide	Experiment			Theory [17]
	E_n, MeV	ΔE, MeV	$\overline{E}$, MeV	$\overline{E}$, MeV
^{232}Th	1.5	2.6 - 8.0	1.87 ± 0.04	1.82
	7.3	2.0 - 10.0	1.96 ± 0.08	1.88
	14.6	0.35 - 12.0	1.90 ± 0.04	2.09
	17.7	0.35 - 14.0	1.98 ± 0.04	-
^{235}U	0.5	0.3 - 12.0	1.98 ± 0.03	1.98
	1.5	2.0 - 10.0	1.95 ± 0.03	2.00
	5.0	0.3 - 13.0	2.12 ± 0.03	-
^{237}Np	4.9	0.3 -12.0	2.19 ± 0.04	2.17
	7.8	1.5 - 12.9	2.03 ± 0.08	2.17
^{238}U	16.0	0.3 - 11.0	1.92 ± 0.04	-
	17.7	0.3 - 13.0	1.98 ± 0.04	-
^{239}Pu	1.5	2.0 - 10.0	2.06 ± 0.04	2.11
	7.5	0.6 - 6.3	2.24 ± 0.10	2.23
	10.0	0.6 - 6.3	2.11 ± 0.10	2.29

Annotation: theoretical $\overline{E}$ values agree with those given in Ref.[17], correspond only to post fission neutron spectra.

These inaccuracies are inevitable and unfortunately present difficulties in their exact evaluation. In addition to the errors inherent in the determination of $\overline{E}$, one can add such factors as the narrowness of the energy range of the secondary neutrons and the high neutron registration threshold.

As an example, Figures 3 and 4 portray experimentally determined spectra together with those determined theoretically. Even though the use of prompt fission neutrons spectra approximated by Maxwellian or Watt distribution is practically convenient, it does not reflect the process of neutron emission from fission fragments. Therefore, it is more sensible to use the calculational method to determine prompt fission neutron spectra using the statistical theory. All measured neutron spectra resulting from the (n,f) reaction are comparable with those calculated using the statistical approach as developed by Madland and Nicks, and later improved by the work of Maerten and Seeliger [18-20]. The statistical description of fission neutron spectra is based on the theoretical analysis of spectra of neutrons emitted by fission fragments in the framework of the Hauser-Feshbach theory, and the analysis of the fission fragment distributions according to their mass, spin and energy in various approximations.

Based on results obtained from statistical theory, and on the totality of models used, it can be said that theory can be used to determine fission neutron spectra, however, there are still differences between theory and experimentally determined results.

Spectra of neutrons emitted in the second and third plateau of the fission cross section

Experiments to measure secondary fission neutrons of heavy nuclides in the little-studied neutron energy range of $E_n < 14$ MeV, were initially designed primarily to satisfy practical requirements; it is only later that these studies acquired a significant physical interest. This was due partly to the results of experimental works conducted at the V.G. Khlopin Radium Institute together with scientists of the FEI [6]. They discovered a certain characteristic of emissive fission, characterized by the presence of an excess of neutrons in the soft part of the spectrum (below 2 MeV) in comparison to the results obtained from calculations using statistical models and traditional representations of the emission mechanism of post-fission neutrons based on the totality of accelerated fission fragments.

The nature of the increase in the fraction of neutrons in the hard part of the spectrum when the energy of the bombarding neutrons was increased, was explained as a manifestation of the mechanism of emission of pre-fission neutrons. In order to investigate the interpretation of the observed manifestation in the soft part of the spectrum, it was necessary to analyze the energy and angular dependencies of the anomalously emitted secondary neutrons - whose characteristics would provide an answer to this problem. As a result of this conclusion, the ensuing research was devoted to an increase in the experimental information on the low energy anomaly in the neutron spectra resulting from the emissive fission of actinides. In order to substantiate the measurement results obtained earlier at the Radium Institute, measurements of the secondary neutron spectra were repeated at the FEI at an energy of $E_n = 14.6$ MeV for the ^{232}Th under new experimental conditions using a fission fragment detector. These results were described in reference [6]. The resulting spectra obtained at an energy of $E_n = 14.6$ MeV compared well with the earlier measurements at an energy of $E_n = 14.7$ MeV [4].

Currently, measurements are being conducted of the energy distribution of neutrons emitted in the ^{232}Th(n,xn'f) reaction for an initial neutron energy of 17.7 MeV as well as in the ^{238}U(n,xn'f) reaction for initial neutron energies of 13.2 MeV, 16.0 MeV and 17.7 MeV using an ionization fission chamber which was constructed at the Radium Institute [6]. The measurements conducted in this experiment, used the relative method which consisted in the simultaneous measurement of the spectrum of the fissioning isotope and that of the well known ^{252}Cf spontaneous fission spectrum standard. This method does not only eliminate a number of experimental errors, but also allows the direct determination of the ratio of the fission neutron spectrum of the investigated nuclide to the spontaneous fission spectrum of ^{252}Cf, thereby giving the possibility to reveal fine effects related to the registration of pre-fission neutrons against the background of the spectrum of neutrons emitted by the exited fission products. As an example of these measurements, Figure 5 shows the fission neutron energy spectra for the investigated ^{238}U nucleus for two primary neutron energies of 16.0 MeV and 17.7 MeV measured at an exiting neutron angle of 90^0 relative to the beam of the primary neutrons [21]. These spectra represent the sum of a few components: pre-fission neutrons

emitted prior to the fissioning of the (n,n'f) and (n,2n'f) reactions, and neutrons emitted by the exited fragments. Due to the addition of the nonequilibrium mechanism of the pre-fission emission of hard neutrons, step-like features could be observed in the spectra in the energy range of $E = E_n - B_f^{A-1}$, where B_f^{A-1} is the height of the fission barrier of the A-1 nuclide.

However, the representation of neutron spectra of emissive fission is not informative enough for the qualitative analysis of such an effect because the fraction of pre-fission neutrons in the total spectrum is not large enough. In order to have a reliable understanding of the effect played by pre-fission neutrons from the (n,n'f) reaction, it was necessary to obtain the ratio of the prompt neutron spectra for induced fission of the investigated isotopes to the spectrum of the spontaneous fission of ^{252}Cf. Figure 6 shows the energy dependence of the ratio of the two types of spectra represented by the following equation

$$R(E,E_n) = N(E,E_n) \,/\, N_{Cf}(E) \tag{4}$$

for the ^{238}U nuclide. In the analysis of the experimental data, all measured spectra were normalized to unity, and included the contribution of neutrons having energies below the neutron registration threshold, i.e.,

$$\int_0^\infty N(E,E_n)dE = \int_0^\infty N_{Cf}(E)dE = 1 \tag{5}$$

The energy distributions of the $R(E,E_n)$ ratios which were determined for the investigated isotopes of ^{232}Th and ^{238}U in the region of emissive fission are similar. It can be seen from the Figure, that a maximum can be observed in the high energy part of the $R(E,E_n)$ spectrum. In the low energy part of the $R(E,E_n)$ spectrum, a rise can be observed for secondary energies lower than 2 MeV. The question regarding the nature of the observed maximum in the high energy part of the spectrum is considered in the work described in reference [6] - that is the manifestation of the mechanism of the nonequilibrium emission of pre-fission neutrons

As the energy of the bombarding neutrons is increased from E_n = 13.2 MeV to E_n =17.7 MeV, a shift of the high energy maximum in $R(E,E_n)$ along the energy scale in accordance with the relationship $E_{max} = E_n - B_f^{A-1}$ can be observed for both isotopes being investigated. This proves that the observed characteristic in the $R(E,E_n)$ ratio in the high energy part of the spectrum is not due to bad statistics or effects in the instrumentation, but supports the correctness of the chosen physical interpretation of the observed effect.

In order to explain the observed rise in the low energy part of the $R(E,E_n)$ ratio it is necessary to performed a thorough statistical analysis of the energy relationships of $R(E,E_n)$ obtained experimentally for various initial energies so as to clarify the physical nature of these neutrons. However, the main and most important step to be taken in these investigations is the performance of more informative experiments in order to study the energy distribution of neutrons at angles ranging from 0^0 to 90^0 with respect to the direction of the fragment movement. Using a large difference in the angular distributions of two components (namely pre-fission and post-fission) it would be possible to isolate the spectrum of the pre-fission neutrons and at the same time to confirm the proposition regarding the mechanism that causes

the excess of soft neutrons. Information on the average characteristics of emissive fission neutrons for the ^{232}Th and ^{238}U nuclides are also listed in the Table. It must be noted that experimental measurements of fission neutron spectra for fast neutron fission are very sparse, and are completely absent at energies above 14 MeV, a comparison of the results can therefore be done only with the aid of systematics [17]. The use of this method produces results based on theoretical calculations of fission neutron spectra and their average energies with the inclusion of a highly probable emissive fission. All emissive fission data are significantly lower than the theoretical values of $\overline{E}$. The most probable reason for such a discrepancy is related to the contribution of an anomalously soft component which is not reproducible in the framework of those neutron emission mechanisms which are at the basis of the curve calculated from systematics.

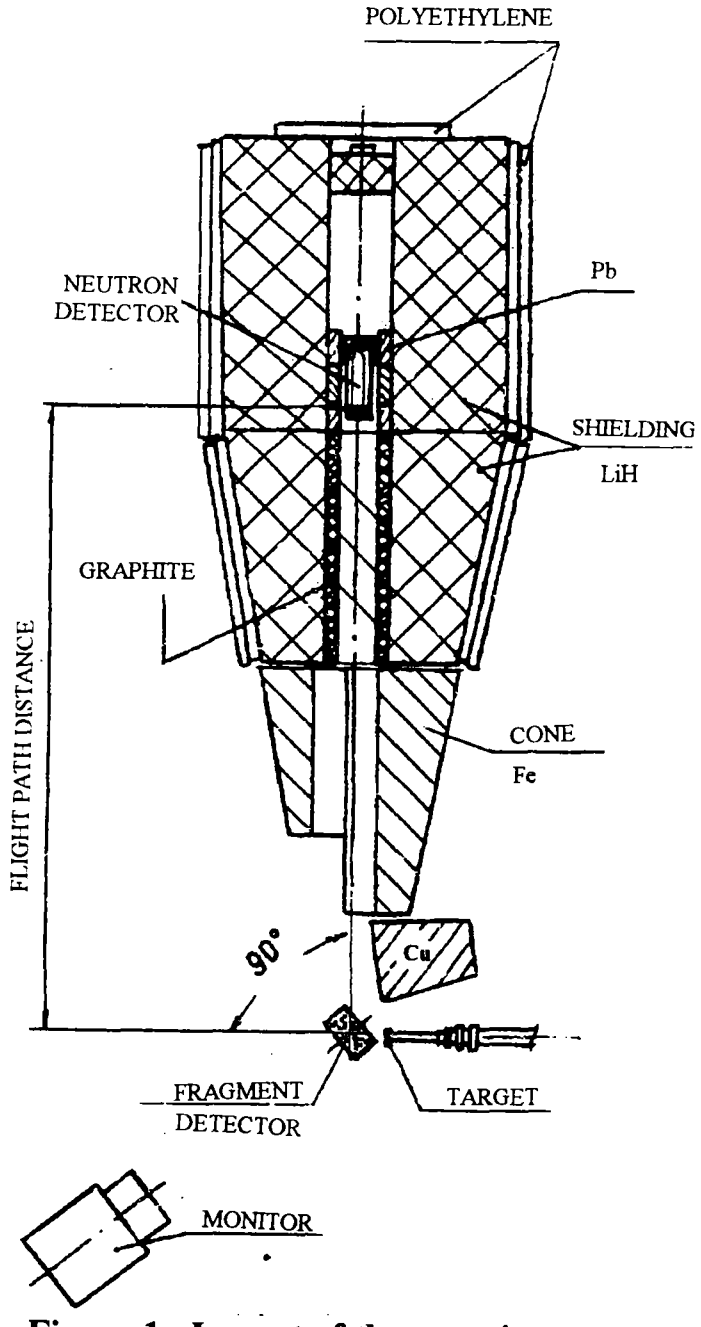

Figure 1. Layout of the experiment

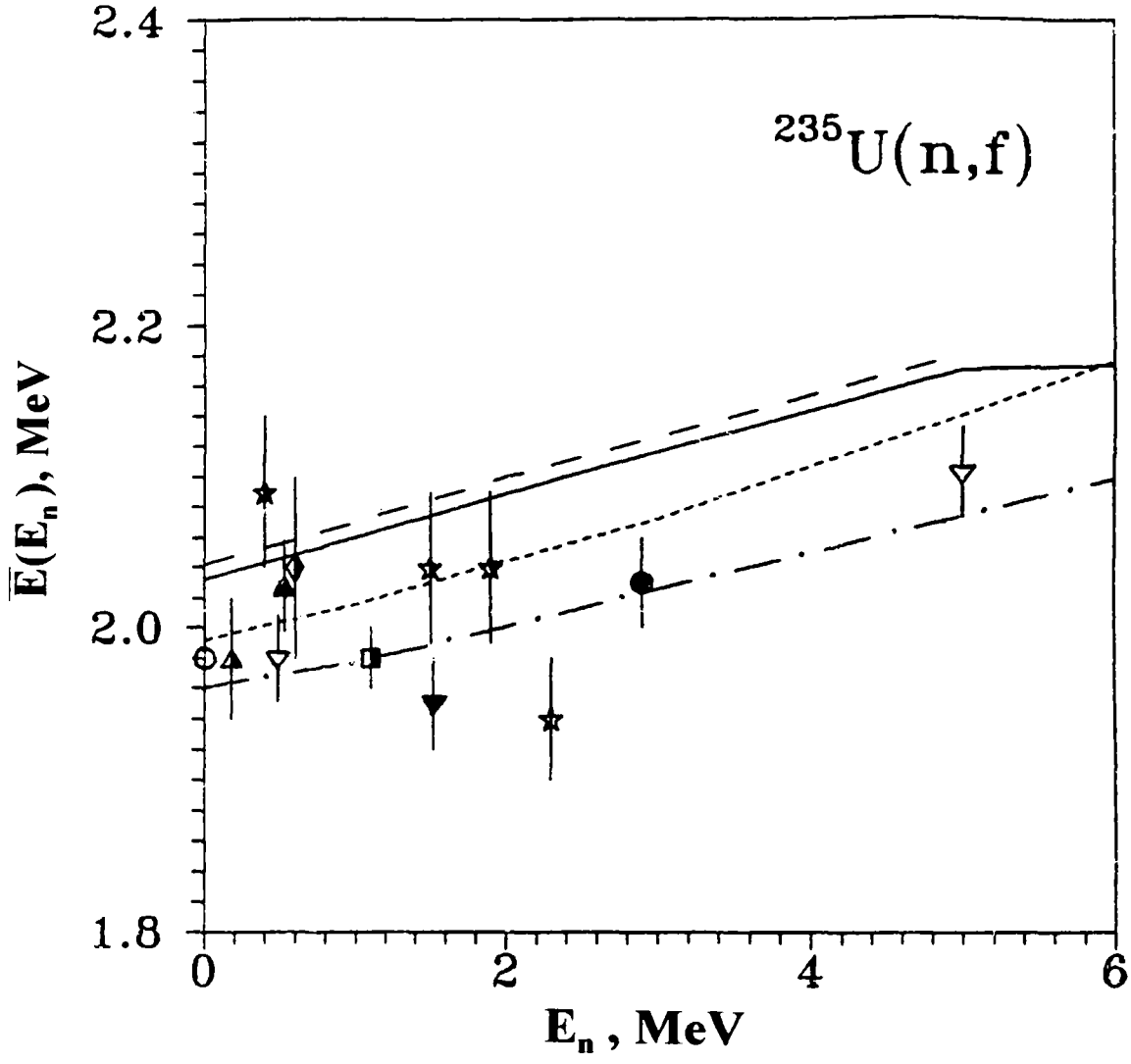

Figure 2. Dependence of the average fission energy $\overline{E}$ for the $^{235}U(n,f)$ reaction as a function of the bombarding neutron energy E_n.

Experimental data: o thermal values (E_n= 0) [7-9]

☆ - [10], ☆ - [10], ◭ - [11], ▲ - [12], ◆ - [13], ◨ - [14], ▼ - [15], ● - [6], ▽ - [16].

Curves representing evaluations: continuous - ENDF/B-VI; dashed - JENDL-3; dotted-dashed -.- BROND-2; dotted ... BNAB-90.

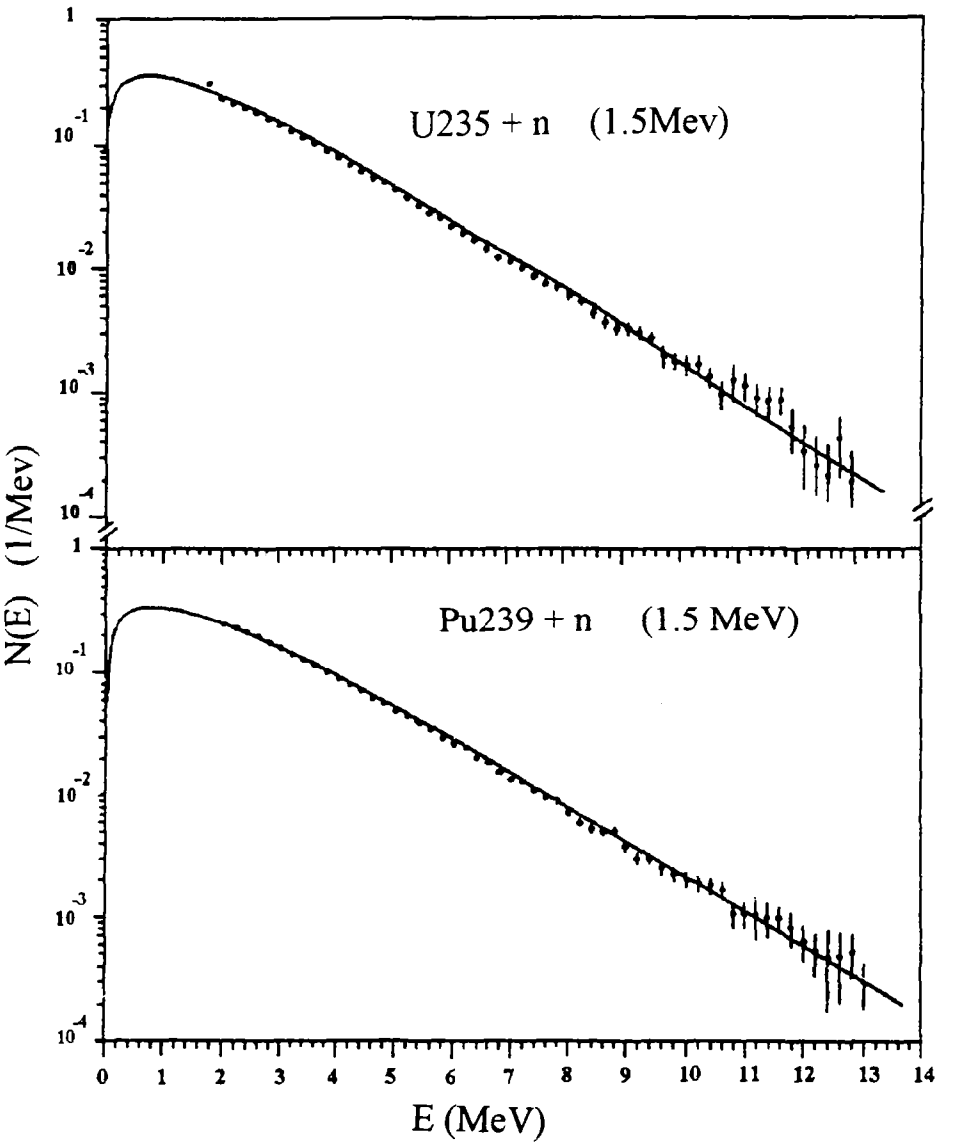

Figure 3. Measured fission neutron spectra of the ^{235}U and ^{239}Pu nuclides compared with those calculated using the FINESSE model [18].

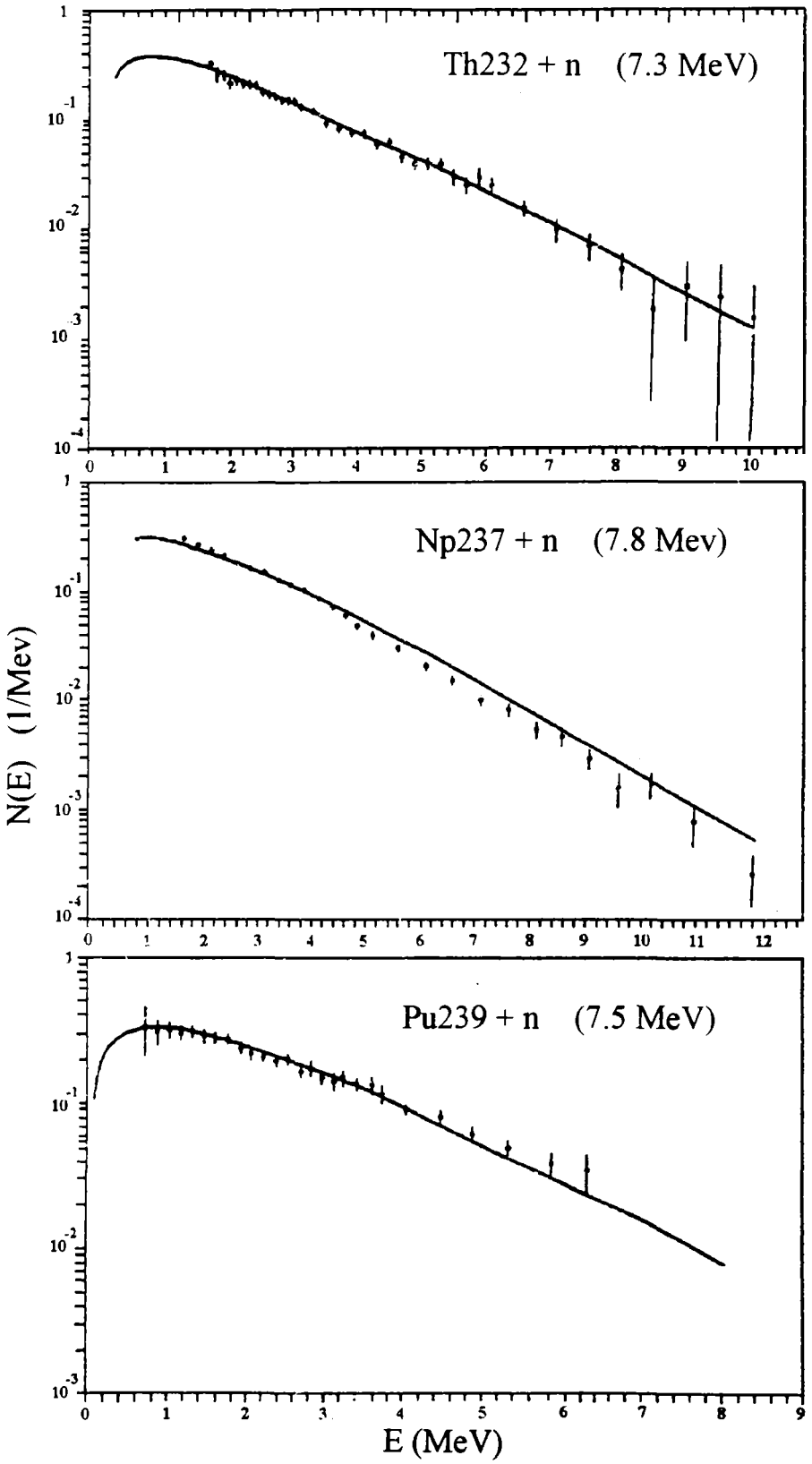

Figure 4. Measured fission neutron spectra of the ^{232}Th, ^{237}Np, and ^{239}Pu nuclides compared with those calculated using the FINESSE model [18]

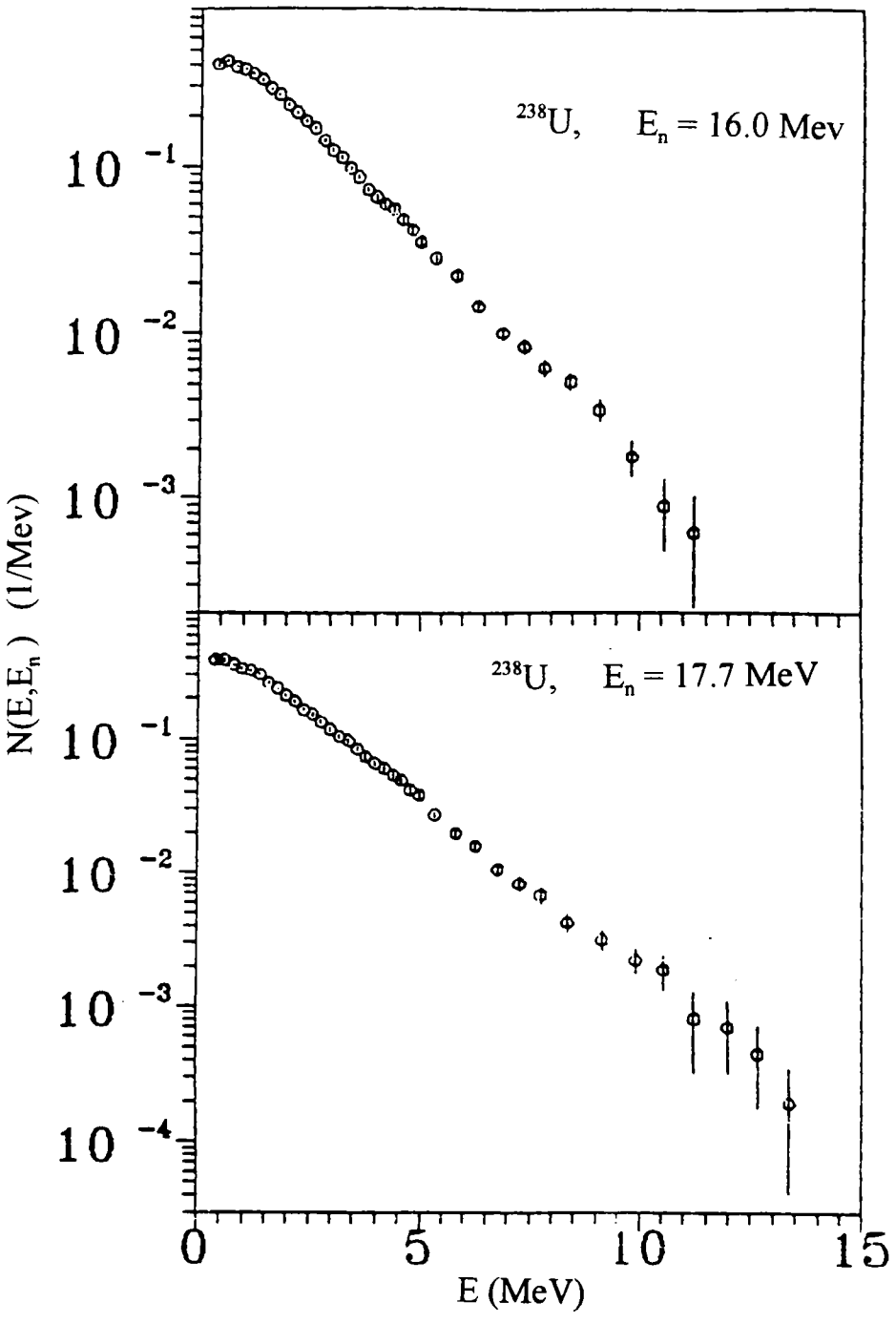

Figure 5. Fission neutron energy spectra for ^{238}U for a neutron scattering angle of 90^0

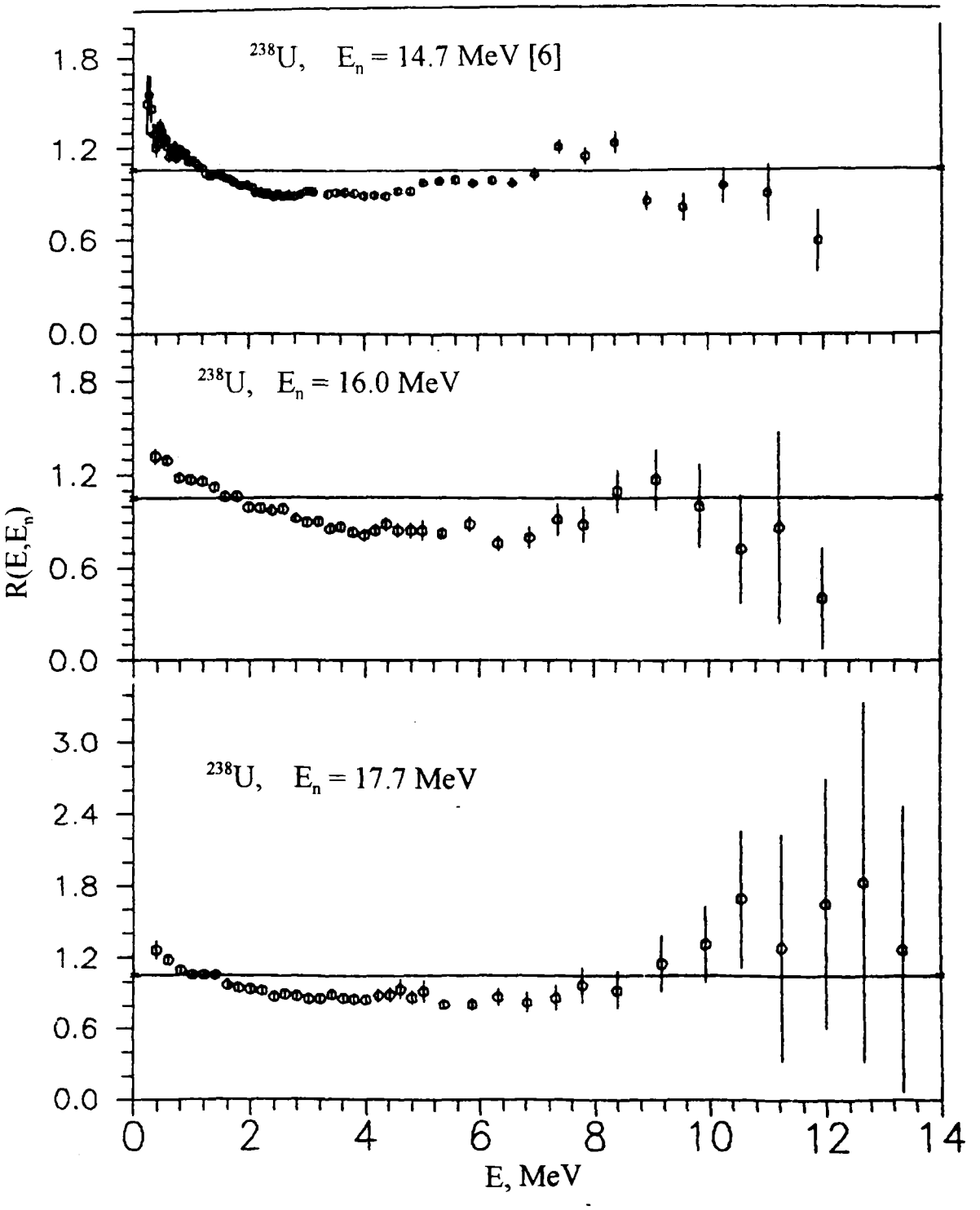

Figure 6. The R(E,E_n) ratio of the fission neutron spectra for the ^{238}U + n reaction to the ^{252}Cf spontaneous fission spectrum for initial neutron energies of 14.7, 16.0 and 17.7 MeV.

References

[1] SUCHICH, S. Eh., et al., Preprint FEI-1927, Obninsk (1988) [in Russian].

[2] AVDEEV, S.P. et.al., Preprint OIYaI P 3-61-667, Dubna (1981) [in Russian].

[3] MANNHART, W., Properties of Neutron Sources, Report IAEA-TECDOC-410, IAEA, Vienna (1987) 158.

[4] SMIRENKIN G.N., et al., Preprint FEI 2439, Obninsk (1995) [in Russian].

[5] CHOMYAKOV, Yu.S. et al., Problems in Nuclear Science and Technology, Series: Nuclear Constants 4 (1992) 70 [in Russian].

[6] BOYKOV, G.S., et al., Yadernaya Fizika 53 3 (1991) 628 [in Russian].

[7] STAROSTOV, B.N., et al., Problems in Nuclear Science and Technology, Series: Nuclear Constants 2 37 (1980) 37 [in Russian].

[8] STAROSTOV, B.N., et al., Problems in Nuclear Science and Technology, Series: Nuclear Constants 3 (1985) 16 [in Russian].

[9] YUFENG, W., et al., Chin.J. Nucl. Phys. 11 (1989) 47.

[10] KNITTER, H.H., et al., in Proc. Prompt Fission Neutron Spectra, IAEA, Vienna (1972) 41.

[11] JOHANSSON, P.I., et al., (Proc. International Conference on Nuclear Cross Sections and Technology, Washington, DC, 1975), NBS Special Publication 425, 2 (1975) 572.

[12] JOHANSSON, P.I., HOLMQVIST, B., Nucl. Sci. Engin. 62 (1977) 695.

[13] BERTIN, F., et al., (All-Union Conf. on Neutron Physics, Kiev, TsNIIatominform, Moscow, 1976) Vol.5 (1975) 349 [in French].

[14] HOWERTON , R.J., DOYAS, R., Nucl .Sci. Engin. 6 (1971) 414.

[15] POLYAKOV, A.V., et al., in Proc. International Conf. Nuclear, Leningrad, Fission - 50 Years, 2 (1989) 50 [in Russian].

[16] TRUFANOV, A.M., et al., Yadernaya Fizika 57 4 (1994) 606 [in Russian].

[17] DURING I, et al., (Proc. Cons. Meeting, Vienna, IAEA, 1990) Rep. INDC(NDS)-251, IAEA, Vienna (1991) 159.

[18] MAERTEN, H., SEELIGER, D., Nucl. Sci. Engin. 93 (1986) 370.

[19] MAERTEN, H., et al., (Proc. 15th Intern. Symposium on Nuclear Physics), Rep. ZFK-592, Dresden (1986) 1.

[20] DURING, I., et al., (Prog. on Nuclear Data Research in the Federal Republic of Germany), Rep. NEANDC(E)-322 and INDC(Ger)-36 and KFK-4953 (1991) 52.

[21] SMIRENKIN, G.N., er al., Yadernaya Fizika (1996) in print.

LOW ENERGY ^{231}Pa PHOTOFISSION CROSS SECTION

A.S. Soldatov, V.E. Rudnikov
G.N. Smirenkin (deceased)

State Research Centre of the Russian Federation
Institute of Physics and Power Engineering, Obninsk

Abstract

Results of the measurement of the ^{231}Pa photofission cross section and yield, measured at the bremsstrahlung end point energy of 5-9 MeV, performed on the FEI microtron, are presented. Measurements in the 7-9 MeV energy range were performed earlier. The dependence of the ^{231}Pa cross-section on gamma ray energy was derived from experimental yield data using the minimal directional divergence method. Relative measurements were performed using track detectors, and the ^{238}U photofission cross section as the standard. The samples consisted of layers of ^{231}Pa and ^{238}U having a thickness of 0.33 and 0.74 mg/cm^2 respectively. The fissionability of the ^{231}Pa(γ,f) reaction was compared with that of the ^{230}Th(^{3}He,df) reaction.

Introduction

Among all of the stable isotopes, the odd-Z nuclides constitute a minority, and among the actinides they are suitable in the preparation of targets used in the experimental study of the fission process. As a rule they are odd-even nuclides; the exception of these are rare isotopes of the ^{242m}Am type which exist in a long-lived isomeric state. Thus, among the odd-Z nuclides, those that are amenable for the study of the (γ,f) reaction are basically odd-even fissile nuclides, and those that are amenable for the study of the (n,f) reaction are odd-odd nuclides, and only direct reactions, because of their diversity do they represent a universal method for the study of low energy fission.

This work is devoted to the study of the photofission cross section of the ^{231}Pa nuclide; there are a number of reasons for the interest in this reaction. First, the ^{231}Pa(γ,f) reaction was investigated in only one study [1] in which microtron bremsstrahlung radiation was used as the source of gamma rays; in this experiment, measurements were made in the 5 to 7 MeV energy range where emphasis was given to the sub-barrier region and the related resonance structure region of the cross section. Second, the studied nuclide falls into a group of light actinides which are characterized by the so-called thorium anomaly of the fission probability and of the fission barriers [2]. Third, the results of experiments reported in references [3 and 4] devoted to the study of the fission of ^{231}Pa in the ^{230}Th(^{3}He,df) reaction are significantly different.

In this experiment, we report the results of our experiment performed in the 7 to 9 MeV range which extends and concludes the earlier measurements which were reported in reference [1]. All experimental data, combining the results of this experiment with those reported in reference [1], were analyzed.

Experimental part. Measurement results and their analysis.

As in the case of the earlier measurements reported in reference [1], the experiment used the electron beam from the FEI microtron. The bremsstrahlung radiation was generated using a target in the form of 1 mm thick tungsten disc and an aluminium absorber of those electrons that penetrated the disc. Using this type of gamma ray source, which has a continuous spectrum $N(E,E_{max})$, the experiment does not consists in the measurement of the cross section but of the photofission yield

$$(E_{max}) = C \int_0^{E_{max}} \sigma_f(E) N(E, E_{max}) dE, \qquad (1)$$

where E_{max} is the energy end point of the bremsstrahlung radiation, C is a multiplier determined by the number of nuclei in the fissioning target, and the distance between the target and the gamma ray source in the bremsstrahlung target [5]. It turns out that from the left part of the experiment equation (1) is not the correct way of stating the problem, its solution is obtained by using the minimal directional divergence method [6].

In that experiment as well as in our earlier measurements of the photofission cross sections (i.e., references [5,7]), the method used consisted of relative measurements which did not determine the photofission yield $Y(E_{max})$ of the investigated nuclide, but its ratio to the photofission yield $Y_0(E_{max})$ of the standard nuclide

$$R(E_{max}) = \frac{Y(E_{max})}{Y_0(E_{max})} = \frac{\int_0^{E_{max}} \sigma_f(E) N(E, E_{max}) dE}{\int_0^{E_{max}} \sigma_f^0(E) N(E, E_{max}) dE}, \qquad (2)$$

where $\sigma^0(E)$ is the standard cross section. The photofission cross section of ^{238}U was used as the standard as it is known to a better degree of accuracy than any other nuclide. The evaluated value of $\sigma_f^0(E)$ which was used was taken from reference [5]. Knowing the standard cross section and the gamma ray spectrum $N(E,E_{max})$ [8], it is easy to reduce equation (2) to equation (1), whose solution was discussed above (see also [5,7]). In accordance with the requirements regarding relative measurements of fissioning target, layers of oxides of ^{231}Pa and ^{238}U having thicknesses of 0.33 and 0.74 mg/cm^2 respectively, were deposited on thin aluminium substrates positioned next to each other. For the detection of fission fragments, mica track detectors were positioned parallel to the targets. For the standardization of the fissioning targets, they were irradiated by monoenergetic neutrons, whose fission cross sections for both isotopes are known better than those of the (γ,f) reaction.

The yield ratios $R(E,E_{max})$ which were obtained in this experiment and in the earlier measurements [1], are given in Table 1 and in the upper part of Figure 1. Photofission cross sections $\sigma_f(E)$ which were obtained as a result of the solution of equation (1) using the method described in reference [6] for a single dependence of $R(E_{max})$ in the energy range 5 to 9 MeV, are given in Table 2 and in the lower part of Figure 1. The values of $\sigma_f(E)$ shown in Figure 1 are somewhat different from those reported in reference [1]. The reason for this is the widening of the measurement energy range, the improvement in the value of the standard cross section and the perfection of the data processing [5].

Discussion of the result

Figure 2 shows the comparison between the fission probabilities (fissionability) of ^{231}Pa(γ,f) and ^{230}Th(^{3}He,df). For this purpose, the photofission cross sections results obtained in these measurements were converted to fission probabilities (fissionability)

$$P_f(E)=\sigma_f(E)/\sigma_c(E) \qquad (3)$$

using the photoabsorption cross section σ_c(E) based on the results reported in reference [9]. The experimental data of σ_c(E) measured for a large number of nuclides for energies ranging from 9 to 18 MeV unfortunately did not include data for ^{231}Pa; these were approximated by summing two lorenzian functions whose parameter values made it possible to obtained the required dependence for energies E smaller than 9 MeV. Values of σ_c(E) for the ^{232}Th nuclide [9], which lie close to the group of nuclides that includes the ^{231}Pa nuclide, were used to determine the photofissionability P_f(E) of ^{231}Pa.

As can be seen from Figure 2, the photofissionability of ^{231}Pa in the low energy part of the range, down to the neutron binding energy B_n=6.82 MeV, is in good agreement with earlier measurement values on the fissionability of the ^{230}Th(^{3}He,df) reaction [3]. The last series of measurements was devoted especially to that energy range. At the end of the investigated energy range (i.e., E> 6.9 MeV) our results differ from those reported in reference [3], and are more in agreement with those given in reference [4]; these measurements were performed up to 10.5 MeV and were devoted particularly to the high energy range. In the overlapping range of these two sets of measurements [3] and [4], the data differ by not less than a factor of two; such a discrepancy cannot be explained by errors in the individual measurements which are reported in reference [4] to be approximately 10%. For energies E>7.5 MeV, the value of the photofissionability of ^{231}Pa is approximately $P_f = 0.5\pm0.1$. From reference [4], it can be seen that the fissionability decreases rapidly for values of $E > B_n$. The value of $P_f = 0.5$ is in agreement with the systematics of the ratio of average neutron widths and fission widths taken from references [9-11]

$$\Gamma_n/\Gamma_f=P_f^{-1}-1, \qquad (4)$$

using the assumption that P_f = constant and that Γ_n / Γ_f = constant, which is traditional for the so-called fissionability plateau of $8 \le E \le 12$ MeV.

Conclusions

Together with the earlier measurements [1], the measurements performed in this experiment have given the possibility to determine the photofission cross section of the ^{231}Pa nuclide in a broad range in the vicinity of the fission threshold, namely E = 5-9 MeV. A comparison of the photofissionability of ^{231}Pa evaluated by us with the fissionability of the same nuclide in the direct reaction ^{230}Th(^{3}He,df) [3,4], has shown that it is in better agreement with the results given in reference [3] in the immediate vicinity of the threshold E < 7 MeV, and with the results published in reference [4] in the middle of the P_f(E) plateau.

Table 1. Ratios of the ^{231}Pa yields R to the ^{238}U yield standard as a function of the bremsstrahlung spectrum end point energy E_{max}

E_{max}, MeV	R	ΔR
4,725	0,1129	0,0152
4,775	0,1475	0,0142
4,825	0,1554	0,0126
4,875	0,1924	0,0092
4,925	0,2373	0,0147
4,975	0,2005	0,0094
5,025	0,2079	0,0100
5,125	0,2793	0,0207
5,225	0,3297	0,0162
5,325	0,3507	0,0123
5,425	0,3990	0,0120
5,525	0,4935	0,0138
5,625	0,5701	0,0160
5,725	0,7700	0,0223
5,825	1,043	0,029
5,925	1,230	0,033
6,025	1,326	0,036
6,125	1,362	0,037
6,225	1,318	0,036
6,325	1,280	0,036
6,425	1,391	0,039
6,525	1,398	0,039
6,625	1,479	0,040

E_{max}, MeV	R	ΔR
6,725	1,464	0,040
-	-	-
6,925	1,451	0,039
7,025	1,638	0,072
7,125	1,551	0,067
7,225	1,621	0,068
7,325	1,793	0,079
-	-	-
7,525	1,842	0,074
7,625	1,914	0,088
7,725	1,914	0,092
7,825	1,970	0,095
7,925	1,957	0,092
8,085	1,885	0,057
8,185	2,021	0,101
8,285	1,954	0,098
8,385	1,873	0.094
-	-	-
-	-	-
8,685	1,978	0,079
8,785	2,080	0,083
-	-	-
8,925	2,105	0,080

Table 2. ^{231}Pa photofission cross section σ_f (E) as a function of energy E

E, MeV	σ_f, mb	$\Delta\sigma_f$, mb
4,750	$6,66 \cdot 10^{-4}$	$2,06 \cdot 10^{-4}$
4,800	$7,21 \cdot 10^{-4}$	$2,59 \cdot 10^{-4}$
4,850	$1,64 \cdot 10^{-3}$	$6,23 \cdot 10^{-4}$
4,900	$2,50 \cdot 10^{-3}$	$2,00 \cdot 10^{-4}$
4,950	$7,90 \cdot 10^{-4}$	$1,34 \cdot 10^{-4}$
5,000	$5,25 \cdot 10^{-3}$	$7,87 \cdot 10^{-4}$
5,075	$1,55 \cdot 10^{-2}$	$1,70 \cdot 10^{-3}$
5,175	$2,56 \cdot 10^{-2}$	$2,30 \cdot 10^{-3}$
5,275	$7,16 \cdot 10^{-2}$	$5,01 \cdot 10^{-3}$
5,375	$1,59 \cdot 10^{-1}$	$1,58 \cdot 10^{-2}$
5,475	$4,88 \cdot 10^{-1}$	$4,88 \cdot 10^{-2}$
5,575	1,49	0,11
5,675	4,39	0,44
5,775	7,21	0,61
5,875	7,36	0,81
5,975	8,17	0,53
6,075	8,75	0,70
6,175	8,97	0,76
6,275	10,48	1,10
6,375	13,50	1,35

E, MeV	σ_f, mb	$\Delta\sigma_f$, mb
6,475	13,47	1,48
6,575	14,47	1,52
6,675	15,71	1,73
6,825	19,96	2,59
6,975	26,84	3,76
7,075	30,04	4,21
7,175	34,47	4,47
7,275	35,68	5,35
7,425	34,40	5,16
7,575	33,41	4,68
7,675	32,50	4,55
7,775	32,24	4,84
7,875	32,89	5,26
8,005	35,35	5,83
8,135	39,42	7,88
8,235	42,29	8,88
8,335	47,36	10,42
8,535	53,55	12,85
8,735	58,22	14,55
8,855	59,29	16,60

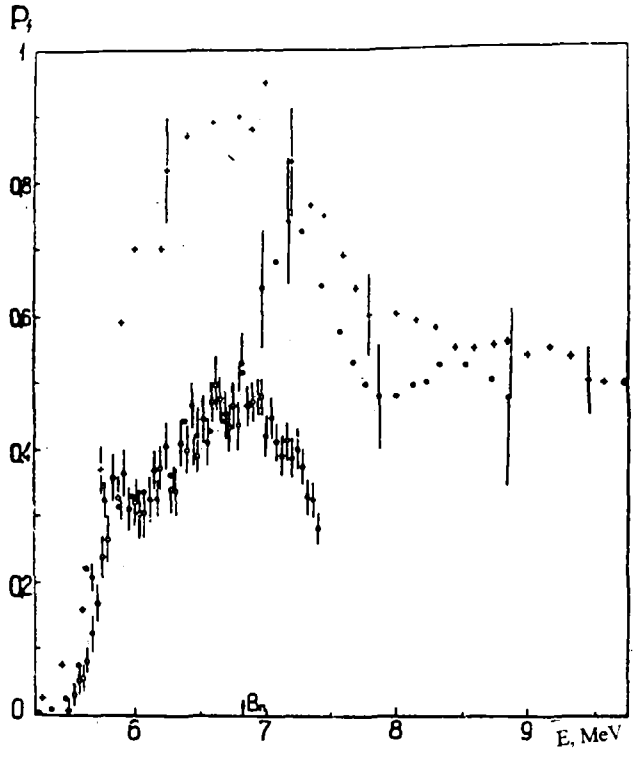

Figure 1. Ratios of the ^{231}Pa and ^{238}U photofission yields $R(E_{max})$ and the $\sigma_f(E)$ photofission cross sections of the ^{231}Pa(γ,f) reaction

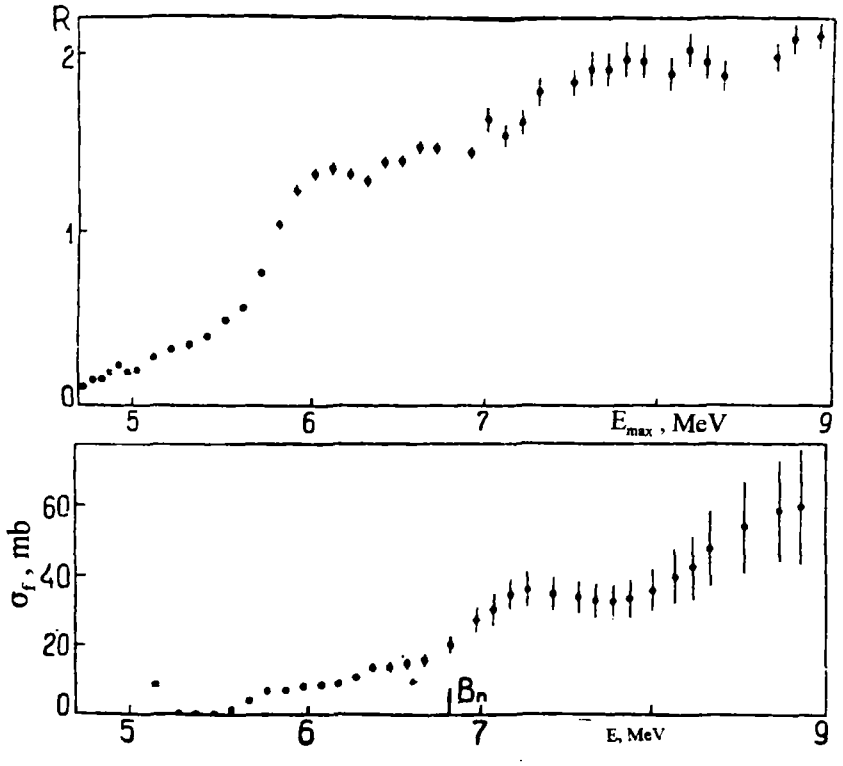

Figure 2. Fissionabilities of the ^{230}Th(^{3}He,df) and of the ^{231}Pa(γ,f) reactions: O Ref [3] , + Ref. [4], • this experiment

References

[1] SOLDATOV, A,S., et al., Yadernaya Fizika 46 (1987) 695 [in Russian].

[2] BJORNHOLM, S., LYNN, J.E., Rev. Mod. Phys. 52 (1980) 725.

[3] BACK, B.B., et al., Phys. Rev. C 10 (1974) 1948.

[4] GAVRON, A., et al., Phys. Rev. C 13 (1976) 2374.

[5] SOLDATOV, A.S., SMIRENKIN, G.N., Yadernaya Fizika 55 (1992) 3153 [in Russian].

[6] TARASKO, M.Z., Preprint FEI-1446, Obninsk (1983) [in Russian].

[7] SOLDATOV, A.S., et al., Atomnaya Energiya 68 (1990) 257 [in Russian].

[8] TARASKO. M.Z., et al., Atomnaya Energiya 65 (1988) 290 [in Russian]

[9] CALDWELL, J., et al., Phys. Rev. C 21 (1980) 1215.

[10] BERMAN B., et al., Phys. Rev. C 34 (1986) 2201.

[11] ISTEKOV, K.K., et al., Yadernaya Fizika 29 (1979) 1156 [in Russian].

MEASUREMENT OF THE $^{58}Ni(n,\alpha)^{55}Fe$ REACTION

V.V. Ketlerov, A.A. Goverdovskij, V.F Mitrofanov
Yu.B. Ostapenko, V.A. Khryachkov

State Research Centre of the Russian Federation
Institute of Physics and Power Engineering, Obninsk

Abstract

Results of the measurement of the $^{58}Ni(n,\alpha)^{55}Fe$ reaction in the 3.5 - 6.8 MeV energy range is presented. The measurements were performed using a gridded ionization chamber with a gas mixture of 95% Xe and 3% CO_2. The corrections made to the experimental data, which took a large number of factors into account, are presented. The nature of the measured cross-section uncertainties are discussed, and the results are compared with the data of other authors.

Introduction

The cross section of neutron induced reaction accompanied by the emission of alpha particles play an extremely important role in the solution of the problem of helium accumulation in structural materials of nuclear power plants. As a rule, experimental investigations to measure these cross sections are impeded by the relatively low probability of the (n,α) process. As a result, spectrometric investigations, which presuppose the use of very thin samples made of isotopically pure materials, are performed rarely and at barely acceptable energy resolutions. This situation leads to the unattainability of vital information, and limits theoretical analysis, which is at the present time the basis of the prediction and evaluation of the (n,α) reaction induced by fast neutrons in intermediate weight nuclides. The data on angular distributions of alpha particles is sparse as well.

The principle experimental method used at the present time consists of a multi-detector system (based primarily on semi-conductor spectrometry) and activation analysis installations. In the course of the last five years, the Tohoki University [1] and the FEI institute in Russia, have developed (practically simultaneously) a highly precise method for the measurement of double differential (n,α) reaction cross sections using ionization chambers.

This article describes the results of the $58Ni(n,\alpha)^{55}Fe$ reaction cross section measurement. Principle attention is given to the procedure used to obtain exact absolute values of the $\sigma_{n,\alpha}$ cross section.

1. Experimental Method

The ionization chamber consists of a set of electrodes (cathode-grid-anode) separated by a gap filled with a gas. Pulses, generated on each of the three chamber electrodes, contains information on such charged particle parameters as kinetic energy and the angle of the emitted particle with respect to the axis perpendicular to the cathode element. The process of the induction of the charges in a simple flat parallel chamber is described in reference [2]. As a result of slowing down, the fragment leaves a track in the gas medium consisting of positively charged ions and free electrons. As a result, an electric field of intensity E is created across the gap between the electrodes. The created field initiates a movement of positive ions towards the cathode with a velocity v_i and of the electrons toward the anode with a velocity v_e. Assuming that the effect of recombination can be neglected, and omitting the effects related to the generation of magnetic fields, the charge which is induced on the anode by a single electron located at a distance x from the point of emission from the cathode, can be expressed by the following equation:

$$Q_{An}^{-} = -\frac{ev^{-}}{D}\frac{D - x\cos(\Theta)}{v^{-}} = -e\left(1 - \frac{x\cos(\Theta)}{D}\right).$$

It follows then, that the total charge on the anode due to all of the electrons which produce a track is:

$$Q_{An}^{-} = \int_0^R -\rho(x)\left(1 - \frac{x\cos(\Theta)}{D}\right)dx,$$

where $\rho(x)$ is the ionization density of the gas along the track.

Taking into account the total number of generated electrons n_0, we obtain

$$Q_{An}^{-} = -n_0 e + \frac{\cos(\Theta)}{D}\int_0^R x\rho(x)dx = -n_0 e\left(1 - \frac{\overline{x}}{D}\cos(\Theta)\right),$$

$$\text{where} \quad \overline{x} = \frac{1}{n_0}\int_0^R x\rho(x)dx,$$

here, $\overline{x}$ is the location of the centre of mass of the ionization along the track.

Let us examine the Frisch grid ionization chamber and assume that the grid element is perfect: i.e., that the electrons moving in the space between the cathode and the grid do not generate any pulses on the anode and that the electrons, after having passed through the grid, are not deposited on the wire coils. Under such conditions, all of the electrons will cover the same distance between the Frisch grid and the anode; consequently the anode pulse will be equal to:

$$Q_{An}^{-} = -n_0 e$$

It is evident that the Frisch grid does not have any effect on the cathode. The expression for the charge induced on the cathode is analogous to that of a chamber without a grid, namely:

$$Q_{Cat}^{-} = n_0 e\left(1 - \frac{\overline{x}}{D}\cos(\Theta)\right),$$

where D is the distance between the grid and the cathode.

All of the consideration presented above apply to the case of a perfect grid. The problems that arise from using real Frisch grids are described in detail in the definitive work published in reference [2. It is emphasized in that reference that the choice of the grid geometry, as well as the voltage applied to the electrodes must be done carefully so as to avoid the loss of electrons on the grid and to shield the anode from the effect of space charges moving between the cathode and the grid to a maximum degree. In the case of a perfect grid the anode pulse is proportional to the number of electrons generated by the slowing down of the particles in the gas. For the case of an "imperfect" grid, the pulse can be expressed by the following expression:

$$P_{An} \propto n_0(1-\lambda)\left(1+\sigma\left(1-\frac{\overline{x}}{D}\cos(\Theta)\right)\right),$$

where λ is the fraction of electrons that was captured by the grid. As shown in reference [2], the charge excess induced on the anode due to the incomplete shielding of the grid is equal to

$$\Delta P_{An} = \sigma n_0 e\left(1-\frac{\overline{x}}{D}\cos(\Theta)\right),$$

where σ is the so-called ineffectiveness of the grid, which is constant for fixed geometry grids. The distortion generated by the incomplete shielding of the anode by the grid, can be corrected at the data processing stage. The losses incurred by the capture of electrons on the grid are not amenable to be corrected because λ is a function of the emission angle of the particle and the location of the origin of the track in the working volume of the chamber. The reliable operation of the chamber is possible only if λ=0. This condition can only be achieved if no electric field lines within the chamber terminated on the grid. In such a case, an electrical lens, which focusses electrons away from the coil windings, is formed in the space between the coils. In this case, electrons will not be captured by the coils. However, strictly speaking, another condition must be satisfied, namely, that the drift velocity of the electrons must be substantially larger than the diffusion velocity of the electrons. These last conditions are met practically for all used working gases if the ratio of the voltage of the electric field to the gas pressure (E/P) is larger than 0.5 Torr.volts/cm.

It is shown in reference [2] that the lines of force do not terminate on the grid if the following condition is met:

$$\frac{V_{An}-V_{Grd}}{V_{Grd}-V_{Cat}} > \frac{Y(1+\rho)+2l\rho}{a(1-\rho)-2l\rho},$$

where V_{an}, V_{grd} and V_{cat} are the voltages applied to the anode, the grid and the cathode respectively; Y is the distance from the anode to the grid, so that

$$\rho = 2\pi\frac{r}{d},$$

where r is the radius of the grid coils, d is the distance between the coil windings;

$$l = \frac{d}{2\pi}\left(\frac{1}{4}\rho^2 - \ln(\rho)\right);$$

where a is the distance between the cathode and the grid.

For the detector used in this experiment $\frac{V_{Cat} - V_{Grd}}{V_{Grd} - V_{An}} > 0.60$

For σ, obtained by the method of conformal mapping, the following expression holds true:

$$\sigma = \frac{1}{l + Y},$$

where *l* and Y are defined above. The evaluation of σ can be determined using the simplified equation

$$\sigma = \frac{d}{2\pi Y} \ln\left(\frac{d}{2\pi r}\right).$$

For the chamber under consideration, σ = 0.026.

To a first approximation, excluding the dependence on σ, P_{cat} can be defined by

$$P_{Cat} = n_0 e\left(1 - \frac{\overline{x}}{D}\cos(\Theta)\right)$$

It is not difficult to obtain a formula for the correction of the anode pulse in the case of incomplete shielding of the anode

$$P_{An}^{T} = P_{An} - \sigma P_{Cat}$$

and for the cosine of the angle

$$\cos(\Theta) = \frac{P_{Cat}(0, E) - P_{Cat}(\cos(\Theta), E)}{\overline{X} / D(P_{An})}$$

A two-dimensional spectrum for 128x128 channels was constructe in order to obtain the dependence of $\overline{X}/D$ on P_{an}. After having obtained the $\overline{X}/D$ on P_{an} dependence, it is possible to calculate the cosine of the emission angle for each of the emitted alpha particles.

As the alpha particle is emitted from the target, a certain amount of energy is lost due to its attenuation in the target layer. As the value of the cosine decreases, the average distance x which the alpha particle traverses in the target layer increases in accordance with the following relationship:

$$x = \frac{D}{2\cos(\Theta)},$$

During data processing, it is absolutely necessary to introduce a correction to account for the energy loss of the alpha particle in the target layer. This is accomplished by constructed a dependence of the location of the centres of well separated alpha trajectories as a function of $1/\cos\theta$. The slope of this curve corresponds to the losses sustained by the alpha particles as they are emitted in a perpendicular direction.

2. Measurement procedures

The measurements were performed relative to the ^{238}U fission cross section, a widely used standard in the monitoring of the neutron flux. In this experiment, both uranium and nickel targets were mounted on a separate cathode element of the ionization chamber. The thickness of the uranium oxide layer was 260 mg/cm^2. The absolute number of nuclei was determined by measuring the alpha activity of the sample. The detector assembly on the side of the uranium layer was set up so as to establish a counting regime of the detector (i.e., only the beginning section of the fragment track was used to suppress the alpha particle emission and the effect of the target layer.

The measurements were made in the neutron energy range from 3.5 MeV to 6.8 MeV. The D(d,n)^{3}He reaction in a solid deuterium target having a thickness of 1.4 mg/cm^2 was used as the neutron source. Two ^{58}Ni targets (with an isotopic enrichment of 95.9%) having a thickness of 250 mg/cm^2 and 155 mg/cm^2 respectively, were used in this experiment. This made it possible to determine the role played by the target parameters in the (n,α) cross sections. The first target was irradiated using the KG-2.5 accelerator; the second was irradiated using the EG-1 accelerator, both at the FEI institute.

Two spectra were constructed for each incident neutron energy: the ^{238}U fission fragment spectrum in the monitor channel, and the two-dimensional (angle-energy) set of alpha particle data emitted by the excited nickel in the main channel. The ionization chamber was filled with a mixture of Xe + 3% of CO_2 to a pressure of 2.5 at, permitting the registration of alpha particles with energies up to 9 MeV. A crucial role in this experiment was played by the determination of the optimal distance between the neutron generating target and the detector. This was due to the considerable influence of the inevitable gamma ray background on the energy resolution of the detector δE_α. If the value of δE_α was 72 keV for the spontaneous decay of ^{252}Cf, then the value for the beam flux would be 170 keV.

3. Corrections and uncertainties

To eliminate distorting factors in the measured data, a number of corrections have been introduced in the reaction cross section ratio $^{58}Ni(n,\alpha)/^{238}U(n,f)$ data. These can be subdivided into three groups.

A. Determination of the number of ^{238}U nuclei in the target.

- The loss of particles in the uranium target leading to the loss in counting efficiency by (1.1±0.3)%.
- Taking into account of the alpha spectrum tail which has an effect on the target thickness introduced a correction of (0.5±0.2)%.
- Taking into account of the dead time in the alpha particle counting: 0.2% (this includes the time for data registration and for recording the data on disk).

B. Determination of the incident neutron beam density.

- Loss of fission fragments due to their absorption in the uranium target with the assumption that the transit equivalent in uranium dioxide is 5 mg/cm^2; the correction

for this effect is (2.6±1.3)%.

- Counting efficiency of the fission fragments which leave the target layer is estimated at (99.4±0.3)%, (including the pulse discrimination level).
- Background due to room return and electronic noise: <0.1%.
- The fissioning of incidental isotopes by fast neutrons were disregarded, (the ^{238}U enrichment in the target was 99.99%).
- Uranium fission events due to neutrons scattered by structural materials in the detector assembly were calculated by the Monte Carlo method; this correction amounted to (2.5±0.5)%.
- The fissioning in traces of ^{235}U by thermal neutrons had an effect of less than 0.1%.
- The difference between the neutron flux densities incident on the nickel and uranium targets was taken into account by means of a correction coefficient: (2.1±0.5)%.
- The background of neutrons originating from the $D(d,n)^3He$ reaction in the deuterium target substrate for neutron energies > 5.5 MeV, contributed a correction of approximately (1.0±0.5)%.
- Photo fission in ^{238}U was neglected.
- Kinematics effects in the $D(d,n)^3He$ reaction contributed to the distortion of the measured ratio by (0.8±0.4)%on the average.

C. Counting of alpha particles originating in the $^{58}Ni(n,\alpha)$ reaction.

- The loss of alpha particles in the target: (1.2±0.7)%. (This correction was introduced for each neutron energy taking the angular distribution of the alpha particles into account).
- Background in the two-dimensional matrix: (1.0±0.5)% (omitting the nitrogen peak).
- Consideration of the isotopic composition of the nickel target gave a correction of (4.3±0.1)%.
- Alpha counting efficiency (94±3)%.
- Geometry counting efficiency (99±1)%.
- Kinematics effects in the (n,α) reaction: (3±1)%.

The total uncertainty of the measured quantities is made up of statistical and systematics components. The statistical error component, determined for both counting channels, namely for fragments and alpha particles, was less than 5%, (for most of the points the uncertainty was 1.5 to 2.5 %). The systematic error consists of all correction errors Δ_1 , the error in the determination of the number of nuclei in the nickel target Δ_2 (2%) and uncertainties in the ^{238}U fission cross section Δ_3.

The energy dependence of Δ_1 is as follows:

- for $E_n < 5.5$ MeV it is 1.7%;
- for $E_n < 6$ MeV it is 2.3 %;
- for $E_n > 6$ MeV it is 3.4 %.

The energy dependence of Δ_3 is as follows:

- for $E_n < 5$ MeV it is 2.4 %;
- for $E_n < 6$ MeV it is 3.3 %;
- for $E_n > 6$ MeV it is 3.9 %.

Thus, the total error of the measured $^{58}Ni(n,\alpha)^{55}Fe$ reaction cross section is less than 8.5%.

4. Measurement results

The measurement results are listed in the Table. In addition, the Table also lists the corresponding reference values for ^{238}U.

For reasons given in reference [3], the authors used results given in reference [4] in the region of the first fission probability, instead of using the recommended σ_f values given in the ENDF file. Figure 1 shows the total $^{58}Ni(n,\alpha)^{55}Fe$ reaction cross section measurement results in the 4.8 MeV to 5.2 MeV neutron energy range, which is the range in which the measurements using the KG-2.5 and EG-1 accelerators overlap. The measurements were made using nickel targets of two different thicknesses. As can be seen in the figure, the data fall within the error bars of the two measurements.

Figure 2 shows the total set of data measured in this experiment together with data measured by other authors [5-9]. Leaving the physical analysis of the results aside, it is worthy to note the presence of a fine structure in the $\sigma(n,\alpha)$ cross section at the neutron energy region of approximately 5 MeV. It must noted that our data lie somewhat lower than those of the other authors. The structure of the $\sigma_{n\alpha}(E_n)$ function can be observed in detail only at higher energy resolution.

At incident neutron energies larger than 6 MeV, the absolute values of the cross sections are by and large in relatively good agreement with those of other authors. However, in the region of the "plateau", the scatter of the data is considerably higher and exhibit a significant increase in their error bars. It can be stated that the energy dependencies of $\sigma_{n\alpha}$ of all of the given experiments are not in good agreement. Not only can the evaluations of the data given in the BROND, JEF-2 and ENDF files resolve the differences in the experimental data, but neither can they give an adequate description of the real situation and explain the differences in their data.

Measurement results of the $^{58}Ni(n,\alpha)^{55}Fe$ reaction cross section

N	$E_n + \Delta E_n$ MeV	σ_Γ мб	$\sigma_{n,\alpha}$ мб	$\pm\Delta\ \sigma_{n,\alpha}$ мб
1	3,55±0,11	533	5,51	0,40
2	3,75±0,09	544	7,68	0,61
3	3,95±0,08	545	10,2	0,7
4	4,14±0,08	547	13,4	1,0
5	4,26±0,08	548	17,0	1,4
6	4,36±0,07	548	19,6	1,5
7	4,47±0,07	549	21,9	1,7
8	4,59±0,07	549	24,9	2,1
9	4,69±0,06	541	25,3	2,1
10	4,81±0,06	534	27,8	1,8
11	4,92±0,06	533	25,5	1,6
12	4,95±0,06	534	26,4	1,9
13	5,04±0,05	533	26,9	1,7
14	5,05±0,05	533	27,0	1,7
15	5,13±0,05	536	29,6	2,1
16	5,18±0,05	536	32,7	2,2
17	5,32±0,05	538	38,3	2,6
18	5,44±0,05	545	44,5	3,0
19	5,56±0,05	548	47,6	3,3
20	5,69±0,05	572	52,9	3,6
21	5,82±0,05	588	54,8	3,6
22	5,94±0,04	610	55,3	3,7
23	6,08±0,04	642	59,7	4,5
24	6,21±0,04	686	55,3	4,1
25	6,35±0,04	752	63,3	5,2
26	6,47±0,04	799	70,7	5,3
27	6,60±0,04	840	72,4	5,5
28	6,72±0,04	872	78,0	5,9
29	6,83±0,04	897	68,0	5,3

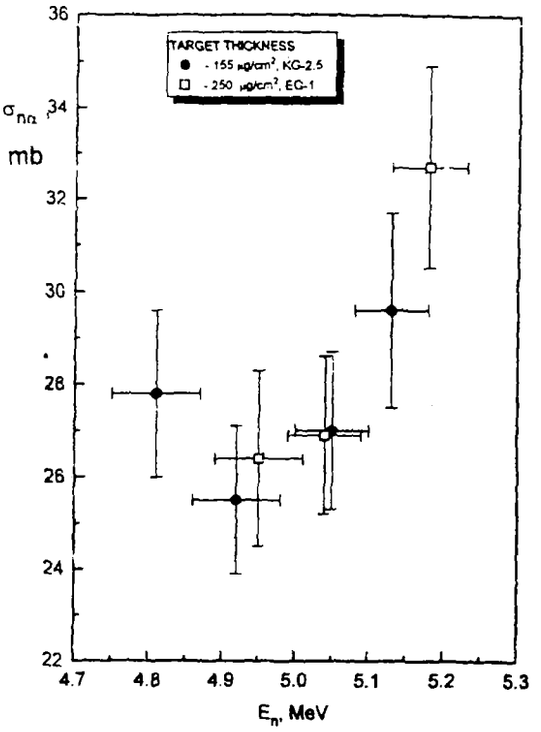

Figure 1. The $^{58}Ni(n,\alpha)^{55}Fe$ reaction cross sections measurement results in the 4.8 MeV to 5.2 MeV neutron energy range showing the data measured in the range in which the measurements using the KG-2.5 and EG-1 accelerators overlap.

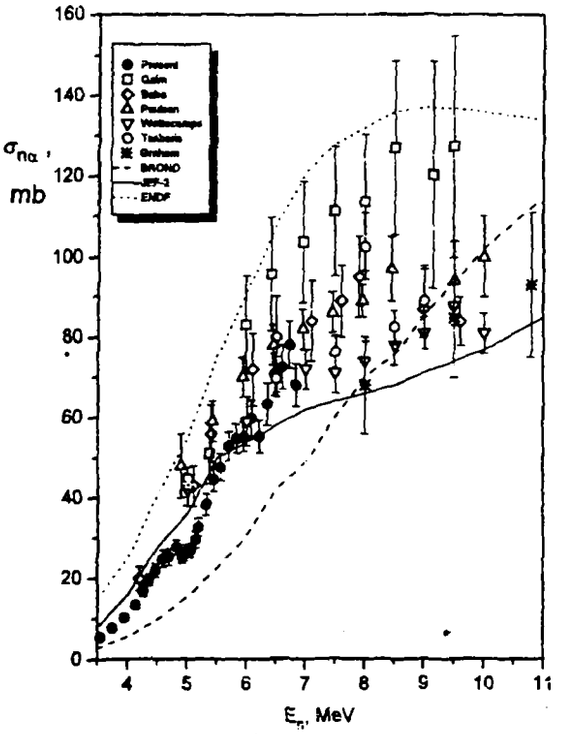

Figure 2. Comparison of the ^{58}Ni (n,α) cross section measurement results with those obtained by other authors [5-9].

REFERENCES

[1] ITO, N., BABA, M., MATSUAMA, S., et al., NIM A337 (1994) 474.

[2] BUNEMANN, O., CRANSHOW, T.E., HARVEY, J.A., Can. J. Research A27 (1949) 191.

[3] GOVERDOVSKY, A.A., (Proc. Advisory Group Meeting, Geel, 1984), IAEA TECDOC-335 (1984) 89.

[4] MEADOWS, J.W., Rep. ANL/NDM-83, ANL, USA (1983).

[5] QAIM, S.M., WOLFDE, R., RAHMAN, M.M., OILIG, H., Nucl. Sci. Engin. 88 (1984)143.

[6] PAULSEN, A., LISKIEN, H., ARNOTTE, F., WIDERA, R., Nucl. Sci. Engin. 78 (1981)377.

[7] WATTEKAMPS, E., in Proc. Intern. Nuclear Data Conf., Juelich, Germany (1991)310.

[8] TSABARIS, C., WATTEKAMPS, E., ROLLIG, G., in Proc. Intern. Nuclear Data Conf., Gatlinburg, USA, 1 (1994) 282.

[9] GRAHAM, S.L., AHMAD, M., GRIMES, S.M., Nucl. Sci. Engin. 95 (1987) 60.

THE FORMULATION OF THRESHOLD REACTION SYSTEMATICS

A.I. Dityuk, A.Yu. Konobeev, V.P. Lunev, Yu.N. Shubin*

State Research Centre of the Russian Federation
Institute of Physics and Power Engineering, Obninsk
** Obninsk Institute of Atomic Energy*

Abstract

Using an analysis of existing experimental (n,np), (n,d), (n,t) and (n,α) threshold reaction data for incident neutron energies between 14 to 15 MeV and the theoretical representation of the interaction mechanism of neutrons with atomic nuclei, a set of semi-empirical equations, designed for the evaluation of these threshold reactions, are proposed. The derivation of these equations is based on the relationship of the pre-equilibrium hybrid exciton and evaporation models. In comparison with empirical systematics made earlier by other authors, the proposed formulas provide a better agreement between experimental data and theory.

1. Introduction

At the present time, in order to determine reaction cross sections in the 14 to 15 MeV range, formulas derived from the analysis of the systematic dependence of cross sections on the number of neutrons and protons in nuclides are being used. In a number of cases, the determination of cross-sections using formulas is both practicable and reliable. Alternative approaches are difficult for two reasons: experimental measurements present difficulties in the set up of the experiments, and results obtained from calculations based on theory have a high degree of uncertainty.

The (n,α), (n,t), (n,d) and (n,np) reaction cross sections [1-11] which were derived earlier from systematics were strictly empirical, and were based on analytical representations of cross sections in the form of exponentials whose exponents depended on the characteristics of the target nuclei. The shape of such cross sections was determined from the statistical evaporation model whose use in the derivation of such systematics served only to emphasize their empirical character. The reason for this is related to the fact that the evaporation model does not adequately take into account the non-equilibrium nature of the emitted particles which contributes significantly to the cross sections of the investigated reactions in intermediate and heavy nuclides [12].

The shortcomings of empirical dependencies is manifested by the unreliability of the prediction of the cross sections for nuclides which are removed from the Z and A nuclides in the region where the parameters were adjusted.

In this work we propose a new semi-empirical systematics for the (n,α), (n,t), (n,d) and (n,np) reaction cross sections at an energy of approximately 14.5 MeV. These are based on formulas derived from the pre-equilibrium exciton model and the evaporation model. A comparison with the results of other works shows that the proposed systematics are more successful in describing the experimental data at 14.5 MeV than various empirical dependencies.

2. Basic principles in the development of systematics

The models used in the development of cross section systematics in this work, consists of the closed form of the pre-equilibrium exciton model and Weisskopf's evaporation model.

In accordance with the exciton model, the expression used for the calculation of the pre-equilibrium particle emission spectrum, is written as follows

$$\frac{d\sigma^{pre}}{d\varepsilon_x} = \sigma_{non}(E_n)\sum_{n=n_0}^{\bar{n}} \frac{(2S_x+1)m_x\varepsilon_x\sigma_x^{inv}(\varepsilon_x)}{\pi^2\hbar^3}\frac{\omega(p-1,h,U)}{\omega(p,h,E)}R_x(n) \qquad (1)$$

$$\frac{D(n)}{\lambda_+(n,E)+\lambda_-(n,E)+\lambda_0(n,E)+\gamma(n,E)}$$

where ϵ_x is the energy of the emitted particle, σ_{non} is the nonelastic cross section for the interaction of the incident neutron having an energy E_n with the nucleus, S_x and m_x are the spin and the reduced mass of the particle of type x, σ_{inv} the inverse reaction cross section, ω(p,h,E) the density of the exciton states consisting of p particles and h holes (p+h=n) for an excitation energy E, and where $R_x(n)$ is a factor which determines the fraction of type x particles in a n-exciton state, λ_+ and λ_- are the velocities of transition into a state with n+2 and n-2 excitons, γ is the sum of the emission velocities which enter in the composition of an n-exciton configuration, D(n) is the exciton "depletion" factor, U and E are the excitation energies of the residual and compound nucleus, and n_0 the initial number of excitons.

The approximation formula for the calculation of pre-equilibrium particle emission spectra under the effect of neutrons of approximately 14.5 MeV may be obtained using equation (1), taking the following conditions into consideration.

In the range of considered excitation energies, the velocity of intra-nuclear transitions, corresponding to an increase in the complexity of the n-exciton configuration, shows a noted increase in the velocities of the other processes, namely $\lambda_+ >> \lambda$ and $\lambda_+ >> \gamma$. The basic contribution to a pre-equilibrium emission spectrum creates a state which has an initial number of excitons equal to three. In the description of the emission of complex particles (e.g., d, t, α), the $R_x(n)$ factor which enters into equation (1) determines the probability of the formation of such particles in the process of a pick-up reaction [13]. The investigated process takes place with a much larger probability for a combination of one particle which is at an energy that is higher than the Fermi energy and a corresponding number of particles at an energy lower than the Fermi energy [13]. Using the Strutinsky-Erickson formula [14] for the calculation of the exciton state density ω(p;h,E), and the Williams [15] formula for the calculation of λ_+, one obtains the following approximate expression which describes the pre-equilibrium particle emission spectrum:

$$\frac{d\sigma}{d\varepsilon_a} = \sigma_{non}(E_n)\frac{(2s_a+1)m_a\varepsilon_a\sigma_a^{inv}(\varepsilon_a)}{2\pi^3\hbar^2 g^4 E_0^3|M|^2}F_{1,3}(\varepsilon_a)\sum_{n_0}(U_a/E_0)^{n-2}p(n^2-1), \quad (2)$$

where $|M|^2$ is the average square of the matrix element of the residual interaction, Q_{nx} is the (n,x) reaction energy, whereas for the emission of compound particle which has a_x nucleons equal to

$$R_x = F_{1,a_x-1}, \quad (3)$$

where the values of the factors F_{1,a_x-1} are calculated in reference [13].

Using expressions (2) and (3), it is possible to obtain an equation for the calculation of the pre-equilibrium component of the reaction cross section σ_{pre} accompanied by the formation of compound particles. Using a "drastically abridged" form of this (?) equation to represent the inverse reaction cross section, and by approximating the values of the F_{1,a_x-1} factor using a linear dependence, one obtains the following approximation of the σ^{pre}

$$\sigma_{(n,t)} = \sigma_{non}(E_n)\frac{4}{3}\frac{(2s_t+1)m_t\sigma_{geom}}{\pi^3\hbar^2 g^4 E_0|M|^2}\left(\frac{E_n+Q_{(nt)}-V_t}{E_0}\right)^3 \times \\ \times\left\{0.5\alpha(E_n+Q_{(n,t)}-V_t)+\alpha(V_t+Q_t)+\beta\right\} \quad (4)$$

where $|M|^2 = KA^{-3}E^{-1}$, $g = A/13$ is the single particle density, V_x is the Coulomb potential for particle x, $\sigma_{geom}=\pi R^2$ where R is the radius of the nucleus, and where the coefficients C_1 and C_2 approximate the quantity F_{1,a_x-1} taken from reference [13]: $F_{1,a_x-1} = C_1(\varepsilon_x + Q_x) + C_2$, where ϵ_x and Q_x are the kinetic energy and the binding energy of the charged particle emitted from the nucleus, respectively.

Weisskopf's equation was used to calculate the equilibrium component of the cross section, accordingly the particle emission velocity is equal to:

$$W_x = \frac{(2s_x+1)m_x\varepsilon_x}{\pi^2\hbar^3}\sigma_x^{inv}(\varepsilon_x)\frac{\rho(U)}{\rho(E)}, \quad (5)$$

where $\rho(U)$ and $\rho(E)$ are th level densities of the residual compound nucleus having excitation energies of Y and E.

Using known thermodynamic relationships which link level densities with the entropy of the nucleus and the nuclear temperature, it is possible to obtain the following approximate expression to calculate the equilibrium emission spectrum of the particle:

$$\frac{d\sigma^{eq}}{d\varepsilon_x} = \sigma_{non}(E_n)(1-P^{pre})\frac{1}{\sum_{x'}\Gamma_{x'}}\frac{(2s_x+1)m_x}{\pi^2\hbar^2}\varepsilon_x\sigma_x^{inv}(\varepsilon_x)exp(-\frac{\varepsilon_x+Q_x}{T_x}), \qquad (6)$$

where P^{pre} is the probability for all non-equilibrium processes, which take place during the interaction of the incident neutron with the nucleus, where T_x is the nuclear temperature corresponding to the x channel, $\Gamma_{x'}$ is the width of the equilibrium emission of the type x' particle, is equal to:

$$\Gamma_{x'} = \frac{(2s_{x'}+1)m_{x'}}{\pi^2\hbar^2}\int_0^{E_n+Q_{(n,x')}}\varepsilon_{x'}\sigma_{x'}^{inv}(\varepsilon_{x'})exp(-\frac{\varepsilon_{x'}+Q_{x'}}{T_{x'}})d\varepsilon_{x'}, \qquad (7)$$

Assuming that the neutron width is significantly larger than the widths of the other channels, and disregarding the differences in the values of nuclear temperatures for various channels, it is possible to obtain the following approximate formula which describes the equilibrium component of the reaction cross section with the formation of a charged particle:

$$\sigma_{(n,x)}^{eq} = \sigma_{non}(E_n)(1-P^{pre})\frac{(2s_x+1)m_x}{(2s_n+1)m_n}exp(-\frac{V_x-Q_{(n,x)}}{T}) \qquad (8)$$

The equations derived above were used to calculate the systematics of the (n,α), (n,t), (n,d) and (n,np) reaction cross sections.

3. The (n,α) reaction

3.1. Formulas for the construction of the systematics.

In this work, the (n,α) reaction cross section was represented by the sum of three components consisting of the direct mechanism for the formation of alpha particles, the pre-equilibrium component and the evaporation emission component:

$$\sigma_{(n,\alpha)} = \sigma_{(n,\alpha)}^{dir} + \sigma_{(n,\alpha)}^{pre} + \sigma_{(n,\alpha)}^{eq} \qquad (9)$$

The direct component of the (n,α) reaction cross section was calculated using the formula given in references [16,17]:

$$\sigma^{dir}_{(n,\alpha)} = \left(d\sigma/d\epsilon\right)_{obs}\left(E_n + Q_{(n,\alpha)} - E_{eff}\right), \qquad (10)$$

where $(d\sigma/d\epsilon)_{obs}$ is the experimental value of the alpha particle emission spectrum in the hard part of the spectrum, E_n is the energy of the incident neutrons, $Q_{n\alpha}$ is the (n,α) reaction energy, and where E_{eff} is the cut-off energy.

The σ^{pre} and σ^{eq} components were calculated using equations (4) and (8).

It follows from the semi-empirical mass equation, that the effective (n,α) reaction threshold (V_α - $Q_{n\alpha}$) exhibits the following dependence on the number of neutrons and protons in the nucleus:

$$V_\alpha - Q_{(n,\alpha)} = \beta_1\left(\frac{N-Z+1}{A}\right)^2 + \beta_2\left(\frac{N-Z+0.5}{A}\right) + \beta_3 Z/A^{1/3} + \beta_4 , \qquad (11)$$

where β_i are constants.

Using equations (4), (8), (10) and (11) for the construction of the (n,α) reaction cross section systematics, the following 12-parameter equation can be suggested:

$$\sigma_{(n,\alpha)} = \pi r_0^2\left(A^{1/3}+1\right)^2\left\{\begin{array}{l} A^{\alpha_1}\left(\alpha_2 S^2 + \alpha_3 P + \alpha_4 Z/A^{1/3} + \alpha_5\right)^{\alpha_6}\left(\alpha_7 P + \alpha_8\right) \\ + exp\left(\alpha_9 S^2 + \alpha_{10} P + \alpha_{11} Z/A^{1/3} + \alpha_{12}\right) \end{array}\right\}, \qquad (12)$$

where $S = (N - Z + 1)/A$, $P = (N - Z + 0{,}5)/A$, $r_0 = 1{,}3$ фм, , α_i are parameters, N, Z and A represent the number of neutrons, protons and nucleons in the target nucleus.

The first member of the expression within the braces in equation (12) describes the non-equilibrium alpha particle emission, the second member represents the formation of particles at the evaporation stage of the reaction. Instead of two components, corresponding to the direct and pre-equilibrium channels, an additional componentr having an effective order α_6 was introduced in equation (12) so as to reduce the number of free parameters. As the probability of all pre-equilibrium processes P^{pre} (which is part of equation (8)) undergoes a smooth transition as it applies from one nucleus to the next, it is not included in equation (12). The fitting of equation (12) to various sets of experimental data, as given in reference [4] for example, or as presented below, leads to the following conclusions: i) because expression $\alpha_2 S^2+\alpha_3 P+\alpha_4 Z/A^{1/3}+\alpha_5$ in equation (12) is smaller than zero, the minimum value of χ^2 is achieved for all $Z \leq 50$ nuclides when the non-equilibrium component is equal to zero; ii) for a number of elements in the range of $50<Z<65$, because of the increase in the value of the pre-equilibrium component, the monotone dependence of the cross section on the neutron excess parameter (N-Z)/A breaks down, which is not corroborated by other calculations and experimental data.

The following 7-parameter formula is proposed to be used for the construction of the systematics of the (n,α) reaction cross section:

$$\sigma_{(n,\alpha)} = \pi r_0^2 (A^{1/3} + 1)^2 exp\left(\alpha_1 S^2 + \alpha_2 P + \alpha_3 Z / A^{1/3} + \alpha_4\right), \quad \text{for } Z \leq 50 \qquad (13a)$$

$$\sigma_{(n,\alpha)} = \pi r_0^2 (A^{1/3} + 1)^2 (\alpha_5 P + \alpha_6)^3, \quad \text{for } Z > 50 \qquad (13b)$$

where $S = (N-Z+1)/A$, $P = (N-Z+0,5)/A$, $r_0 = 1{,}3$ фм, , and α_i are parameters.

3.2. Comparison of various systematics using the cross section library from reference [4]

A comparison of various systematics, using a file of experimental data which was compiled in the framework of the same effort. This comparison included the systematics presented in reference [3] as well as various other empirical dependencies proposed in reference [4]. The systematics which was recognized to be the best consisted of an 8-parameter formula [4]:

$$\sigma_{(n,\alpha)} = \alpha_1 (A^{1/3} + 1)^2 exp\left(\alpha_2 R + \alpha_3 R^2 + \alpha_4 A\right), \quad \text{for } Z \leq 50 \qquad (14a)$$

$$\sigma_{(n,\alpha)} = \alpha_5 (A^{1/3} + 1)^2 exp\left(\alpha_6 R + \alpha_7 A\right), \quad \text{for } Z > 50 \qquad (14b)$$

where R = (N-Z)/A, and α_i are parameters whose values are derived in reference [4].

Not too long ago, another empirical formula was proposed in reference [5]:

$$\sigma_{(n,\alpha)} = \alpha_1 (A^{1/3} + 1)^2 exp\left(\alpha_2 S + \alpha_3 / A + \alpha_4 / A^{1/2}\right), \qquad (15)$$

where S = (N-Z+1)/A, α_i are parameters; whereby $\alpha_4 = 0$ for odd A nuclides, $\alpha_4 > 0$ for odd-odd nuclides, and $\alpha_4 < 0$ for even-even nuclides.

In this work, the results from formulas (12), (13) and (15) were added to the experimental data given in reference [4]. In this context, the parameter values in these formulas were chosen such that the following equation (16) had a minimum value:

$$\Sigma = \sum_{i=1}^{N} \left\{ \frac{(\sigma_i^{calc} - \sigma_i^{exp})}{\Delta\sigma_i^{exp}} \right\}^2, \qquad (16)$$

where σ^{calc} is the value of the cross section as calculated using formulas (12), (13) and (15), where σ^{exp} and $\Delta\sigma^{exp}$ are the experimental cross section values and their uncertainties, respectively, at 14.5 MeV, and where N is the number of nuclides in the experimental data library.

The value of χ^2 was calculated using equation $\chi^2 = \Sigma/(N-m)$, where Σ was determined from reference (16), and m is the number of free parameters. The program described in reference [18] was used to minimize equation (16).

The results of the comparisons of various systematics are shown in Table 1. As can be seen, the smallest value of χ^2 is obtained with formula (13) by using the experimental data from reference [14]. The relative sum of the squares Σ is smallest for formula (12). However, taking into account the breakdown of the monotone dependence of the cross section on the (N-Z)/A parameter in formula (12), which has been observed for some elements but is not corroborated by independent calculations or by experimental data, the systematics that gives the best description of the experimental (n,α) reaction cross section data is formula (13).

It is interesting to compare the (n,α) reaction cross section calculation results obtained with formula (13) with those obtained with formula (14) for different groups of nuclides. The results of these comparisons, made for 62 nuclides of atomic number $Z \leq 50$ and 52 nuclides with $Z > 50$ are listed in Tables 2 and 3.

Table 2 shows that using the semi-empirical formula (13a) leads to better results than the calculations using the empirical formula (14a). The comparison results given in Table 3 show that the 2-parameter formula (13b), which was obtained by using the pre-equilibrium exciton model, gives a better description of the experimental data than the empirical formula (14b) with a larger number of parameters.

The analysis of the results of the data obtained by means of various formulas shows that the systematics based on formula (13) gives the best agreement with experimental data.

Table 1. Calculation results obtained using various formulas to fit 114 experimental (n,α) reaction cross sections given in reference [4]

Formulas	Σ	χ^2	Number of parameters	Reference
(13)[1]	512.76	4.79	7	this work
(12)[2]	497.91	4.88	12	this work
Forrest, (14)[3]	527,70	4.98	8	[4]
Kumabe, Fukuda	653.03	6.16	8	[3]
Ait-Tahar (15)[4]	802.10	7.36	5	[5]
Levkovskiy	995.46	8.89	2	[1]

1. Parameter values: α_1= 153.11, α_2= 1.4848, α_3= 0.20170, α_4= 0.58348, α_5= 1.4284, α_6 =0.35901
2. Parameter values: α_1= 1.9207, α_2= 107.08, α_3= 39.797, α_4= 0.03105, α_5= 3.8513, α_6= 0.23368, α_7= 583.77, α_8= 129.23, α_9= 152.36, α_{10}= 1.6650, α_{11}= 0.19992, α_{12}= 0.58756
3. Parameters taken from reference[4], the values of Σ and χ^2 in reference [4] are 528.8 and 4.99 as a result of a mistake in the value of ^{209}Bi in the data library (see [4], p.65).
4. Parameter values: α_1= 6.5921, α_2= 31.243, α_3= 85.256, α_4= 0 for odd A nuclides, α_4= 2.1597 for odd-odd nuclei, α_4= 1.0997 for even-even nuclei.

Table 2. Results of fitting various formulas to 62 values of cross sections obtained from reference [4] resulting from the analysis of experimental data for Z ≤ 50 nuclides

Formula	Σ	χ^2	No. of parameters
(13a)	350.11	6.04	4
Forrest, (14a)	354.09	6.11	4

Table 3. Results of fitting various formulas to 52 values of cross sections obtained from reference [4] resulting from the analysis of experimental data for Z > 50

Formulas	Σ	χ^2	No. of parameters
(13b)	162.65	3.25	2
Forrest, (14b)	173.61	3.54	3

3.3. New data library resulting from the analysis of 14.5 MeV experimental data.

The new (n,α) reaction cross section library is based on the compilations published in references [4] and [19] and data from the EXFOR library as of the end of 1994.

Evaluated data for 55 nuclides were taken from references [4] and [19], and the values for 65 nuclides were re-analyzed or supplemented to the library. Results of earlier experiments included in the EXFOR data library, together with data that had been measured in the course of the last few years, were used in the evaluation of the data. Because of their questionable reliability some experimental data which were included in reference [4] were not included in this evaluation. Most data obtained before 1970 were also not included in the compilation published in reference [19]. The complete bibliography of the experimental data that were used in the generation of this new library of 14.5 MeV (n,α) reaction cross sections is given in reference [20]. In the process of obtaining the reaction cross section, it was necessary to extrapolate and interpolate the experimental data on the basis of energy dependencies which were determined with the aid of the pre-equilibrium exciton model and the evaporation model, and to include data from well known libraries.

The new 14.5 MeV (n,α) reaction cross section data library which contains data for 120 nuclides, is included in reference [20].

3.4. Systematics of the (n,α) reaction cross section at 14.5 MeV

In order to obtain the systematics on the basis of formula (13), the required parameters were chosen so as to minimize the value of χ^2 in the description of the data in the new library [20].

The following formula was obtained for the Z≤ 50 nuclides:

$$\sigma_{(n,\alpha)} = \pi r_0^2 (A^{1/3} + 1)^2 exp\left(-209.11S^2 + 8.4723P - 0.19253Z / A^{1/3} - 0.96249\right), \quad (17a)$$

and for the Z > 50 nuclides:

$$\sigma_{(n,\alpha)} = \pi r_0^2 (A^{1/3} + 1)^2 (-16462P + 0.39951)^3, \quad (17b)$$

where S=(N-Z+1)/A, P=(N-Z+0.5)/ A, r_0=1.3 Fm, and N, Z, and A are the number of neutrons, protons and nucleons in the target nucleus, respectively.

The values of Σ and χ^2 corresponding to the description of the experimental data in the new library [20], and determined using the systematics (17), were found to be equal to Σ=44.26, and χ^2=3.6 [1]. In comparison, the fitting of the parameters of the empirical formula (14) to the same data taken from reference [20], calculated in this work, yields values of Σ=478.3 and χ^2=4.7 [2] Figure 1 shows the ratio of the data based on the analysis of the experimental data [20] to the values calculated using formula (17).

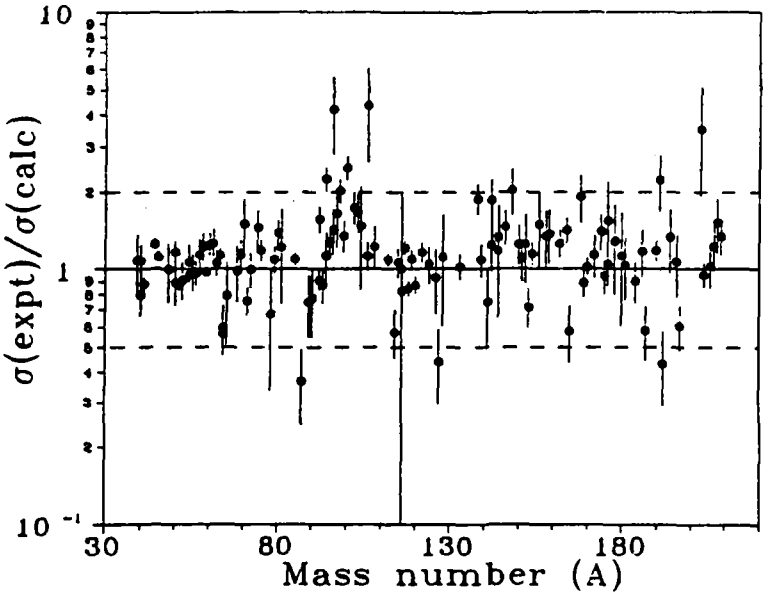

Figure 1. Ratio of the (n,α) reaction cross sections obtained from the analysis of the experimental data taken from reference [20] to data calculated with the aid of systematics

1. For Z≤50: Σ=309.29, χ^2 = 4.69; and for Z>50: Σ=137.98 and χ^2=2.87.
2. For Z≤ 50 : Σ=320.85, χ^2=4.86 and for Z>50: Σ = 157.58 and χ^2 = 3.35

4. The (n,t) reaction

4.1. formulas for the construction of the systematics

It was demonstrated in reference [21] that in the construction of the systematics of the (n,t) reaction cross section, it was only necessary to take the pre-equilibrium component of the cross section (formula (4)) into account. This conclusion is in agreement with the results described in references [13,22], according to which the basic contribution to the (n,t) reaction cross section for intermediate and heavy nuclides results in a non-equilibrium emission of tritons.

Measurements of (n,t) reaction cross sections at 14.5 MeV yield sharply different values in their dependence on the parity of the target nucleus. In order obtain systematics which describe the experimental data, it is necessary to alter formula (4) to take the evaporation effect into account when calculating the densities of exciton states. Consideration of such effects, consistent with reference [23], results in a displacement of the excitation energy of the residual nucleus in the Strutinsky-Erickson formula [14] by a quantity δ which is dependent on parity. This in turn calls for the displacement of the reaction energy $Q_{(n,t)}$ in formula (1) by a quantity δ. Considering that the square of the matrix element of the residual interaction $|M|^2$ depends on the excitation energy (E) and on the mass number (A) in the following manner: $|M|^2 = KA^{-3}E^{-1}$, and that the single-particle density is equal to g=A/n, where K and n are constants, the approximation formula for the evaluation of the (n,t) reaction cross section may be written in the following form:

$$\sigma_{(n,t)} = \pi r_0^2 (A^{1/3} + 1)^2 \frac{3.1 \times 10^{-2} n^4}{K A^{1/3} E_0^3} (E_n + Q_{(n,t)} - V_t + \delta)^3 \times \times \{0.5\alpha (E_n + Q_{(n,t)} - V_t + \delta) + \alpha (V_t + Q_t) + \beta\} \quad (18)$$

where σ_{non} in formula (4) is substituted by the expression $\pi r_0^2 (A^{1/3} + 1)^2$, δ=0 for even-even target nuclei, $\delta = -11/A^{1/2}$ for odd A nuclei, and $\delta = -22/A^{1/2}$ for odd nuclei.

In order to obtain systematics for the (n,t) reaction cross section it is necessary to take the difference in the values of the (n,t) reaction threshold for nuclei of different parity. The indicated differences are illustrated by the data shown in Figure 2. Figure 2 shows the values of $-Q^{(nt)} + V^t$ for 625 stable nuclides and unstable nuclides having a half-life larger than one hour and A>40. These values were calculated using mass data from the tables of isotopes and on the basis of the approximation approach put forward by Meiers, Sviatetskiy and Lisekil. The quantities V_t were calculated on the basis information given in reference [21]. By comparing the data given in Figure 2, it can be seen that the quantity $-Q^{(nt)} + V^t$ are noticeably different for even-even nuclides, odd A nuclides and odd-odd nuclides.

According to the semi-empirical mass formula, the reaction energy $Q_{(n,t)}$ depends on the neutron excess parameter (N-Z)/A; even-odd differences in the $Q_{(n,t)}$ value are described by that member of the mass formula that is proportional to $A^{-3/4}$. Substituting the quantity $-Q^{(nt)} + V^t$ in formula (18) by the expression $\beta_i (N-Z)/A + \beta_2 Z/A^{1/3} + \beta_3 A^{-3/4} + \beta_4$ and taking into account that the $(E_n + Q_{(n,t)} - V_t)^3$ multiplier is most sensitive to the magnitude of the reaction energy, one obtains the following formula to describe the systematics of the (n,t) reaction cross section:

$$\sigma_{(n,t)} = \pi r_0^2 (A^{1/3} + 1)^2 A^{-1/3} \times \\ \times \left(\alpha_1 + \alpha_2 (N - Z)/A + \alpha_3 Z / A^{1/3} + \alpha_4 / A^{3/4} + \alpha_5 / A^{1/2}\right)^3 \quad (19)$$

where r_0 = 1.3 Fm, Z, N, A are the characteristics of the target nucleus, α_i are parameters which are determined by the conditions which would best describe the experimental data, whereby α_1, α_2 and α_3 have the same value for nuclides having different parity; according to the mass formula, $\alpha_4 < 0$ for even-even nuclides, $\alpha_4 = 0$ for odd A nuclides and $\alpha_4 > 0$ for odd-odd nuclides, the relationship of the α_5 parameters for different parities correspond to the quantity δ in formula (18).

4.1.1 Even-even nuclei.

The formal implementation of expression (19) leads to a four-parameter formula for the calculation of the (n,t) reaction cross section applied to even-even nuclides, including members proportional to (N-Z)/A, $Z/A^{1/3}$ and $A^{-3/4}$. It is sensible, however, to use formulas having fewer numbers of parameters in the description of a relatively small number experimental data (namely 18 nuclides [4,8]).

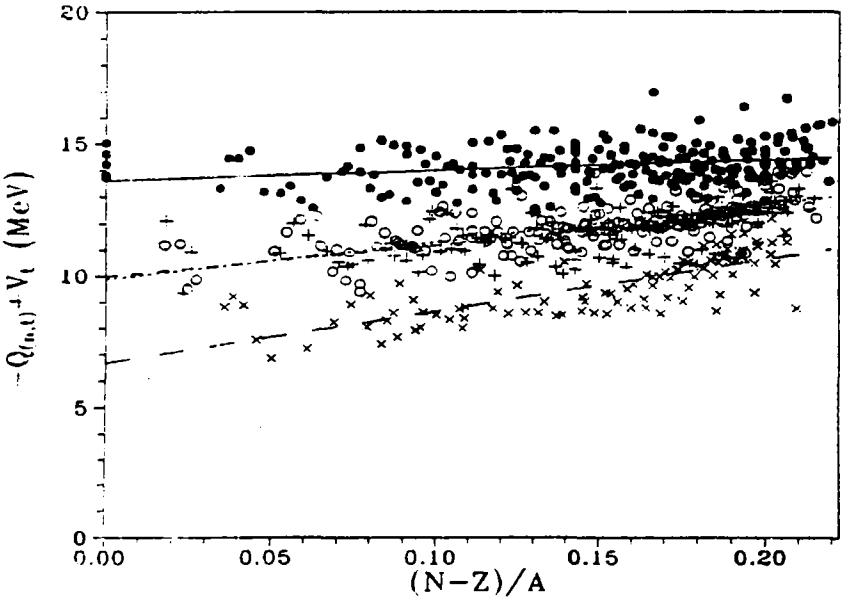

Figure 2. Effective (n,t) $-Q^{(m)} + V^t$ reaction threshold for 625 stable nuclides and unstable nuclides with a halflife larger than one hour, and A>40, calculated with the aid of the table of isotopic masses using the Meyers, Sviatinsky and Lisekil approximation. Even-even nuclides are shown as black circles, even-odd nuclides as open circles, odd-even nuclides as a + sign, and odd-odd nuclides as a cross x. The curves for nuclides of different parity were calculated using the least squares method: solid curve for even-even nuclides, short dashes for even-odd nuclides, intermediate dashes for odd even nuclides, and long dashes for odd-odd nuclides.

The following expression is proposed to be used in the construction of the systematics:

$$\sigma_{(n,t)} = \pi r_0^2 (A^{1/3} + 1)^2 A^{-1/3} \left(\alpha_1 + \alpha_2 (N - Z)/A + \alpha_3 Z / A^{1/3}\right)^3, \qquad (20)$$

where α_1 , α_2 and α_3 are determined from the conditions which give the best description of the experimental data for even-even nuclides.

4.1.2 Odd-even and even-odd nuclides.

It can be deduced from the table of isotope masses and from the determination of δ (see (18)) that the difference of the quantity $(\alpha_1+\alpha_2(N-Z)/A+\alpha_3 Z/A^{1/3}+ \alpha_4/A^{3/4}+$ (which enters into formula (19)), between odd A and even-even nuclides is $\alpha_4/A^{3/4} + \alpha_5/A^{1/2}$, whereby $\alpha_4 > 0$ and $\alpha_5 < 0$. It follows therefore that for odd A nuclides, the systematics for the (n,t) reaction cross section it is proposed to use the following formula:

$$\sigma_{(n,t)} = \pi r_0^2 (A^{1/3} + 1)^2 A^{-1/3} \times \\ \times \left(\alpha_1 + \alpha_2 (N - Z)/A + \alpha_3 Z / A^{1/3} + \alpha_4 / A^{3/4} + \alpha_5 / A^{1/2}\right)^3, \qquad (21)$$

where α_1 , α_2 and α_3 are parameters whose values are arrived at in the process of fitting of formula (20) to the experimental data of even-even nuclides. The values of α_4 and α_5 are determined from the conditions which best describe the measured odd A nuclide cross sections. (Because of the lack of experimental data for even-odd A>40 nuclides ,only odd-even nuclide are taken into consideration in this analysis).

4.1.3. Odd-odd nuclides

The difference of the quantity $(\alpha_1+\alpha_2(N-Z)/A+\alpha_3 Z/A^{1/3}+ \alpha_4/A^{3/4}+\alpha_5/A^{1/2})$ between odd-odd and even-even nuclides is equal to $2(\alpha_4/A^{3/4}+\alpha_5/A^{1/2})$, where the α_i parameters are determined in the other cases considered above. The (n,t) reaction cross section for odd-odd nuclides can be evaluated with the aid of the following formula:

$$\sigma_{(n,t)} = \pi r_0^2 (A^{1/3} + 1)^2 A^{-1/3} \times \\ \times \left(\alpha_1 + \alpha_2 (N - Z)/A + \alpha_3 Z / A^{1/3} + 2\alpha_4 / A^{3/4} + 2\alpha_5 / A^{1/2}\right)^3, \qquad (22)$$

where α_1, α_2 and α_3 are parameters obtained from the process of fitting formula (20) to the experimental data for even-even nuclides, and the values of parameters α_4 and α_5 are determined from the process of fitting formula (21) to the experimental data of odd A nuclides.

4.2. Experimental data.

The measurements of the (n,t) reaction cross section data of a number of nuclides were performed prior to the year 1986. There are two relatively complete data libraries [4,8] of 14.5 MeV (n,t) reaction cross sections which were derived from the analysis of the existing experimental data. The reaction cross sections given in reference [4], consist of data measured with the use of the activation method, which were normalized to the results of subsequent measurements using standard reaction cross sections. Therefore, the cross section data used in this work for the construction of systematics were taken from reference [4].

It must be noted that the data for most nuclides given in reference [4] had been measured at an energy of 14.6 MeV.

4.3. Comparison of different systematics.

A comparison of various systematics formulas using the experimental cross section data taken from the work of Forrest published in reference [4] has been performed. Parameters of the proposed formulas given in references [4] and [5], and the systematics proposed in references [4,6 and 9] were evaluated so as to obtain a minimum value for the sum of the squares of the relative deviation Σ (see formula (16)).

4.3.1. Even-even nuclides

The comparison included expression (20) and the following two- and three-parameter empirical formulas:

Qaim and Stocklin [6]:

$$\sigma_{(n,t)} = \alpha_1 (A^{1/3} + 1)^2 \exp(\alpha_2 (N - Z)/A), \quad (23)$$

Forrest [4]:

$$\sigma_{(n,t)} = \alpha_1 (A^{1/3} + 1)^2 \exp(\alpha_2 (N - Z)/A + \alpha_3 A^{1/2}), \quad (24)$$

Lishan [9]:

$$\sigma_{(n,t)} = \alpha_1 (A^{1/3} + 1)^2 \exp(\alpha_2 (N - Z + 1)/A), \quad (25)$$

Ait-Tahar [5]:

$$\sigma_{(n,t)} = \alpha_1 (A^{1/3} + 1)^2 \exp(\alpha_2 (N - Z + 1)/A + \alpha_3 / A). \quad (26)$$

The quantities Σ and χ^2 corresponding to the description of the experimental data [4] together with the aid of the proposed semi-empirical formula (20) and the empirical formulas (23) to (26) are listed in Table 4.

Table 4. Results of fitting various formulas to 18 experimental cross sections values taken from reference [4] for even Z nuclides

Formulas	Σ	χ^2	Parameters, mkbr
(20)	21.35	1.42	α_1=0.047995, α_2=0.35627, α_3=0.0045118
Qaim (23)	30.20	1.89	α_1=6.9880, α_2=14.450
Forrest (24)	21.86	1.46	α_1=1.516, α_2=24.35, α_3=0.2670
Lishan (25)	28.92	1.81	α_1=9.8116, α_2=15.804
Ait-Tahar	27.6	1.84	α_1=20.864, α_2=18.701, α_3=33.834

It can be seen from the data given in Table 4, that the minimum value of the sum of the squares of the relative deviations Σ and χ^2 occurs for formula (20) which is based on the pre-equilibrium exciton model.

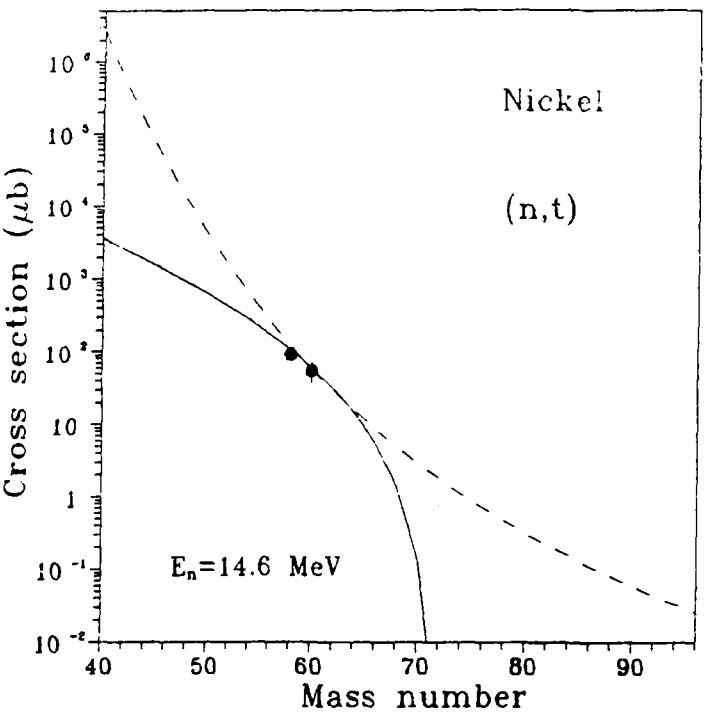

Figure 3. The (n,t) reaction cross section at 14.6 MeV for isotopes of nickel having an even number of neutrons, calculated with the aid of the semi-empirical formula (20) derived in this work (solid curve) and with the aid of formula (24) given in the work of Forrest [4] (dashed curve). Experimental data taken from reference [4] are represented by black circles.

Even though the values of χ^2 for the semi-empirical formula (20) and for the empirical formulas, such as (24), are close, there is a significant difference between them. Figure 3 shows (n,t) reaction cross sections for the even N nickel isotopes (Z=28) calculated with the aid of formulas (20) and (24) using parameter values given in Table 4. It can be seen in Figure 3 that for the region where there are experimental data, the cross section values obtained using various systematics are practically the same. Significant differences can be observed for unstable isotopes with relatively small and large mass numbers. The cross section values of such isotopes which were predicted by the empirical formula (24) prove to be incorrect. As can be seen from the data in Figure 3, the (n,t) reaction cross sections for light isotopes, which were calculated with the aid of formula (24), shows an increase in the value of the total reaction cross section. In the case of heavy isotopes, the cross section values predicted by formula (24), does not reflect the fact that the (n,t) reaction energy $Q_{(n,t)}$ decreases as the mass number (A) increases, and that it is smaller than -14.6 MeV for some values of A (see Figure 4), at the same time the (n,t) reaction cross section becomes equal to zero.

4.3.2. Odd A nuclides.

The suggested formula (21), which has two free parameters, and the empirical formulas identified below were used in the comparison of these nuclides:

Qaim, Stocklin [6]:

$$\sigma_{(n,t)} = \alpha_1 (A^{1/3} + 1)^2 \exp(\alpha_2 (N - Z)/A), \quad (27)$$

Forrest [4]:

$$\sigma_{(n,t)} = \alpha_1 \exp(\alpha_2 (N - Z)/A). \quad (28)$$

The result of the fitting formulas (21), (27) and (28) to the experimental data [4] are given in Table 5. The comparison of these data shows that the semi-empirical formula (21) best describes the experimental data.

Figure 5 shows the (n,t) reaction cross sections calculated for the isotopes of cobalt (Z=27), having even numbers of neutrons with the aid of formulas (21) and (28) using the parameters given in Table 5. It can be seen that, as in the case of even-even nuclides, the prediction of the empirical systematics using formula (28) for unstable nuclides proves to be incorrect as well. For light isotopes, the (n,t) reaction cross sections calculated with aid of formula (28), has the effect of increasing the value of total reaction cross section. For heavy isotopes, the cross section values predicted by formula (28) proved to be different from zero in spite of the fact that the (n,t) reaction energy $Q_{(n,t)}$ is smaller than the energy of the incident neutron energy of 14.6 MeV (see Figure 3).

Table 5. Results of fitting various formulas to seven experimental cross section data points for odd Z nuclides taken from reference [4].

Formulas	Σ	χ^2	Parameters, mkbr
(21)	39.81	7.96	α_4=4.7774, α_5=1.0881 [1)]
Qaim (27)	41.32	8.26	α_1=334.77, α_2=28.153
Forrest (28)	40.78	8.16	α_1=5082.5, α_2=22.638

[1)] Values for the α_1, α_2, α_3 are given in Table 4

4.4 Systematics of the (n,t) reaction cross section.

Using the pre-equilibrium exciton model, the results of the work given in reference [21] and the experimental data from reference [4], results in a new semi-empirical formula for the evaluation of the (n,t)reaction cross section at 14.6 MeV which has the following form:

$$\sigma_{(n,t)} = \pi r_0^2 (A^{1/3} + 1)^2 A^{-1/3} \times \times \left(-0.35627(N - Z)/A + 0.0045118Z/A^{1/3} + 0.047995 + \Delta\right)^3, \quad (29)$$

where $\Delta = 0$ for even-even nuclides,
$\Delta = 4.774/A^{3/4} - 1.0881/A^{1/2}$, for odd A nuclides,
$\Delta = 9.5548/A^{3/4} - 2.1762/A^{1/2}$. for odd-odd nuclides,

where r_0 = 1.3 Fm, Z, N, A are the number of protons, neutrons and nucleons in the target nuclide.

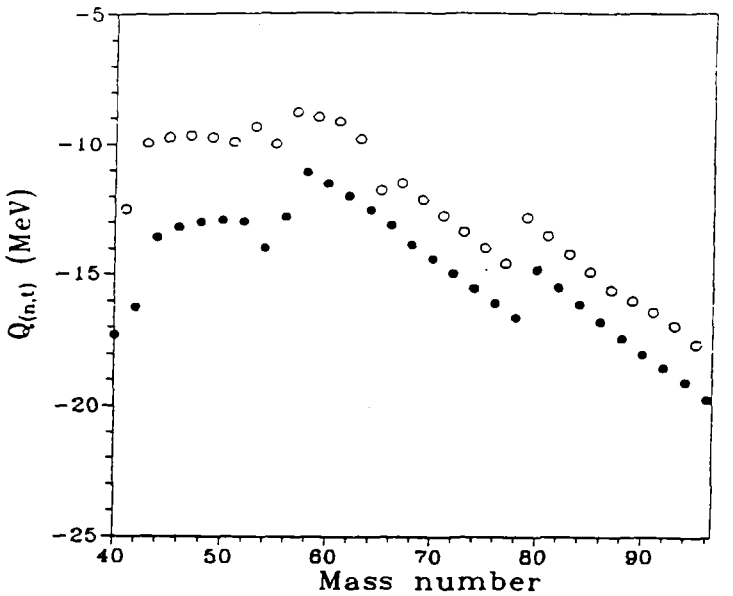

Figures 4. (n,t) reaction energy calculated with the aid of isotope mass tables on the basis of the approximation proposed by Meyers, Sviatetskiy and Lisekil, for nickel isotopes (represented by black circle) and for cobalt isotopes (represented by open circles), having even numbers of neutrons.

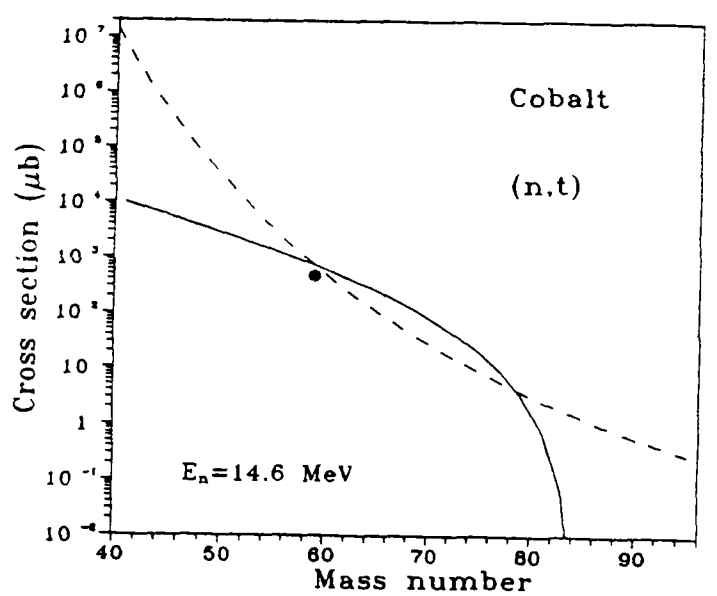

Figure 5. (n,t) reaction cross sections at 14.6 MeV for cobalt isotopes having an even number of neutrons calculated with the aid of the semi-empirical formula (21) (represented by the solid curve, and the empirical formula (28) taken from reference [4] (represented by the dashed curve). The experimental cross section value (represented by the black circle) was taken from reference [4].

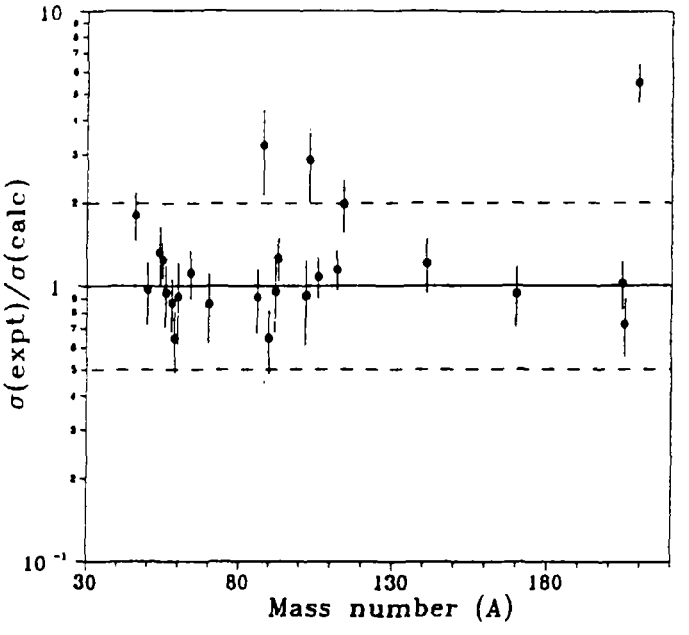

Figure 6. Ratio of the (n,t) reaction cross sections obtained from the analysis of experimental data from reference [4] to the cross sections calculated with the aid of formula (29) proposed in this work.

The values of Σ and χ^2 are calculated with the aid of formula (29) corresponding to the description of the experimental cross sections [4] have the following values:Σ=61.17 and χ^2=3.06. For even-even nuclides Σ=21.35 and χ^2=1.42, and for odd A nuclides Σ = 39.81, and χ^2 = 7.96.

The ratio of the experimental cross section values [4] to the cross sections calculated with the aid of the systematics formula (29) is shown on Figure 6. The comparison of the results obtained with formula (29) to the empirical systematics proposed by other authors shows that the semi-empirical formula (29) gives a more exact description of the experimental data. In addition, it appears that for nuclides that fall away from the valley of stability, formula (29) can be used to generate more realistic cross section values than those predicted by empirical systematics.

5. The (n,d) reaction

5.1 Analysis of the experimental data.

The experimental (n,d) reaction cross sections at 14.8 to 15.0 MeV for A>40 nuclides were obtained using the charged particle detection method described in references [25-28].

The following general observation may be made regarding the (n,d) experimental data. In most cases, experimental (n,d) reaction cross sections measured with the activation measurement method are in agreement with those calculated with the aid of systematics of the

sum of the (n,d) and (n,np) reaction cross sections. However, it was noted that the measured (n,d) reaction cross sections of ^{95}Mo and ^{96}Mo are not in agreement with the value predicted by the systematics of the (n,d)+(n,np) cross sections. Similar discrepancies have been observed in the experimental (n,d) reaction cross sections of ^{51}V, ^{65}Cu, ^{89}Y, ^{93}Nb and ^{96}Mo nuclides and in various values of the summed (n,d) and (n,np) reaction cross sections calculated using the semi-empirical systematics described in reference [29] which was obtained with the use of a new compilation of measured (n,d)+(n,np) cross sections.

Experimental cross section values are limited to nuclides of $A \leq 96$. An attempt to construct a systematics for the (n,d) reaction cross section on the basis of available measured data has led to the following results. Fitting of the various formulas to the body of experimental cross section values has shown that the predictions obtained from systematics in the region of intermediate and heavy nuclides are not correct. For these nuclides, the systematically determined (n,d) reaction cross section values turned out to be much higher than the summed (n,d)+(n,np) values measured by the activation method. Figure 7 shows the measured (n,d) cross section values, the curve determined from systematics, as well as the summed values of the (n,d)+(n,np) cross sections at 14.5 MeV obtained from the analysis of experimental data given in reference [29] for 49 nuclides. It can be seen from the figure that the (n,d) reaction cross section values predicted by the empirical $\alpha \exp(\beta(N-Z)/A)$ systematics in the nuclide range where experimental data are absent, are sharply higher in comparison to the sum of the measured values of the (n,d) and (n,np) reaction cross sections.

5.2. Calculation of the (n,d) reaction cross sections on the basis of theoretical models.

The construction of a systematic on the basis of experimental data leads to contradictions. Experimental data used for the prediction of (n,d) reaction cross sections in the range of intermediate and heavy nuclides, may be supplemented by theoretical calculations.

It is shown in reference [12] that the neutron emission spectra in nuclear reactions may be calculated for a broad range of incident particle energies and target nuclei mass numbers on the basis of a proposed poly-phenomenological approach.

The differential deuteron emission cross section is represented by the sum of three components, describing the direct process of the formation of the deuteron, a pre-equilibrium component and an evaporation emission component:

$$\frac{d\sigma}{d\varepsilon_d} = \frac{d\sigma^{dir}}{d\varepsilon_d} + \frac{d\sigma^{pre}}{d\varepsilon_d} + \frac{d\sigma^{eq}}{d\varepsilon_d} \qquad (30)$$

The direct component ($d\sigma^{dir}/d\epsilon_d$) and the pre-equilibrium component ($d\sigma^{pre}/d\epsilon_d$) are calculated in reference [12] using a hybrid exciton model [23]. Whereby the input to the direct processes is described phenomenologically.

The direct process is described as the formation of the deuteron as a result of the interaction of a primary nucleon with another nucleon which is lower than the Fermi level. The input stage can be represented by the configuration 1p0h, where p and h represent the number of particles and holes in the given exciton configuration. It is considered that the emission of the deuteron at the pre-equilibrium stage occurs after the formation of the 2p1h state. The coalescence model including the pick up of the particle is used to describe this process [13].

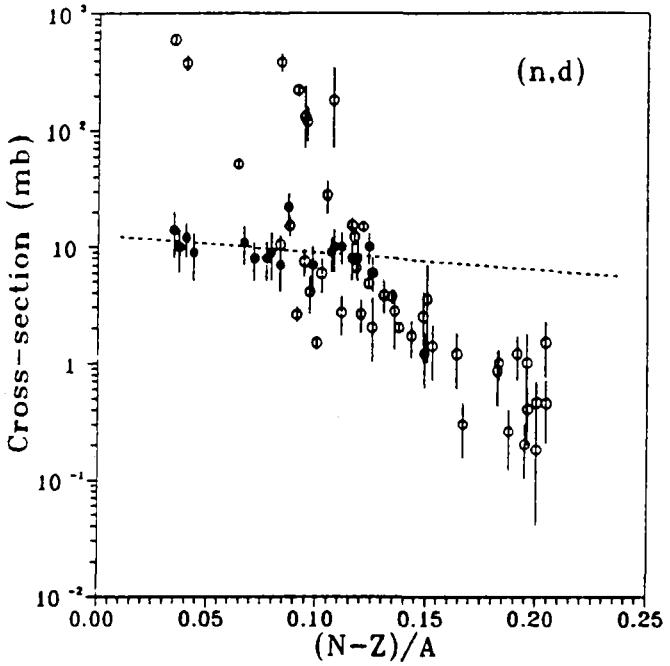

Figure 7. Experimental values of the (n,d) reaction cross section [25-28] (represented by black circles), the systematics curve $\alpha\exp(\beta(N-Z/A)$ constructed with the aid of experimental (n,d) reaction cross sections (represented by the dotted curve), the sum of the (n,d) and (n,np) reaction cross sections at 14.5 MeV obtained from the analysis of experimental data [29] (represented by open circles).

The differential cross section describing the formation of the deuteron at the direct stage of the reaction is calculated in the following manner:

$$\frac{d\sigma^{dir}}{d\varepsilon_d} = \sigma_{non}\frac{\omega^*(U)}{\omega(1p,0h,E)}\frac{\lambda_c^d(\varepsilon_d)/g_d}{\lambda_+^d(\varepsilon_d)+\lambda_c^d(\varepsilon_d)/g_d}g_d, \qquad (31)$$

where σ_{non} is the nonelastic interaction cross section of the primary nucleon with the nucleus, $\omega(p,h,E)$ is the density of exciton states which have p particles and h holes (p+h=n) for an excitation energy E, where $\omega^*(U)$ is the density of excited states of the nucleus which is formed after the emission of the deuteron, λ^d_+ is the velocity of the internal transition corresponding to the absorption of the excited deuteron by the nucleus, λ^d_c is the velocity of the emitted deuteron, and g_d is the density of one-particle states of the deuteron (g_d = A/28).

The density of final states ω^* of the nucleus after the emission of the deuteron can be represented by the following expression:

$$\omega^*(U) = \omega(0p,1h,U)\,\gamma/g_d\,, \qquad (32)$$

where γ is the parameter which characterizes the deuteron formation process.

The calculation of the pre-equilibrium deuteron spectrum is performed with the aid of the following expression:

$$\frac{d\sigma^{pre}}{d\varepsilon_d} = \sigma_{non}\sum_{n=3l+m=2}^{\bar{n}}\sum F_{l,m}(\varepsilon_d)\frac{\omega(p-l,h,U)}{\omega(p,h,E)}\times\frac{\lambda_c^d(\varepsilon_d)/g_d}{\lambda_+^d(\varepsilon_d)+\lambda_n^d(\varepsilon_d)/g_d}g_d D_n, \qquad (33)$$

where $F_{l,m}(\epsilon_d)$ is the formation probability of the deuteron having an energy ϵ_d out of l excited and m unexcited quasi-particles in the nucleus [13], D_n is the "depletion " factor and n is the exciton state.

The deuteron emission velocity which is a member of formulas (31) and (33), is determined by the following equation:

$$\lambda_{\tilde{n}}^{d} = \pi^{-2}\hbar^{-3}(2S_d + 1)\mu_d \varepsilon_d \sigma_{inv}^{d}(\varepsilon_d), \qquad (34)$$

where S_d and μ_d are the spin and the reduced mass of the deuteron, σ^{d}_{inv} is the inverse deuteron reaction.

The transition velocity corresponding to the absorption of the excited deuteron by the nucleus, is equal to:

$$\lambda_{+}^{d} = 2W_{opt}^{d} / \hbar \ , \qquad (35)$$

where W^{d}_{opt} is the imaginary part of the optical potential for deuterons interacting with nuclei.

The deuteron spectra presented in reference [12] are calculated with th aid of formulas (33) - (35) were compared to experimental data for nuclides of different atomic masses which were irradiated by neutrons and protons having energies from 14 to 90 MeV. It was shown that good agreement could be obtained with measured spectra by using the same value of γ, equal to ($2x10^{-3}$), for all nuclides, and by using the value of $\Sigma F_{l,m}=0.3$ for the sum of probabilities for the formation of deuterons for the pre-equilibrium stage of the reaction.

In this work, the approach given in reference [12] was used for the description of deuteron spectra which were used to obtain the (n,d) reaction cross section at 15 MeV.

When comparing the calculational results with the experimentally determined deuteron spectra in such reactions, it turned out that the use of the quantity $\gamma = (2x10^{-3})$, which was obtained in reference [12] as a result of the analysis of experimental data at incident particle energies up to 90 MeV, made it possible to achieve good agreement with measured spectra for odd-even target nuclides. For even-even nuclides, better agreement was observed using $\gamma = (4x10^{-3})$. Figures 8 and 9 shows calculated and experimental deuteron spectra resulting from the irradiation of nuclides of various parity with neutron of approximately 15 MeV. The non-equilibrium component of the spectra were calculated on the basis of the approach described above. The equilibrium spectra were calculated on the basis of the Hauser-Feshbach model using the program STAPRE [30]. The nuclear level densities were calculated using the superfluid model with effective parameters taken from reference [31]. It can be seen from Figures 8 and 9, that there is good agreement between the calculated and experimental spectra.

The calculational method described above, was used for the calculation of the (n,d) reaction cross section at 15 MeV for stable nuclides ranging between Ar and Bi. The equilibrium deuteron spectra were calculated with the aid of the Weisskopf model, which in comparison to the Hauser-Feshbach model, gives similar values for the integral of the evaporation spectrum as a function of energy.

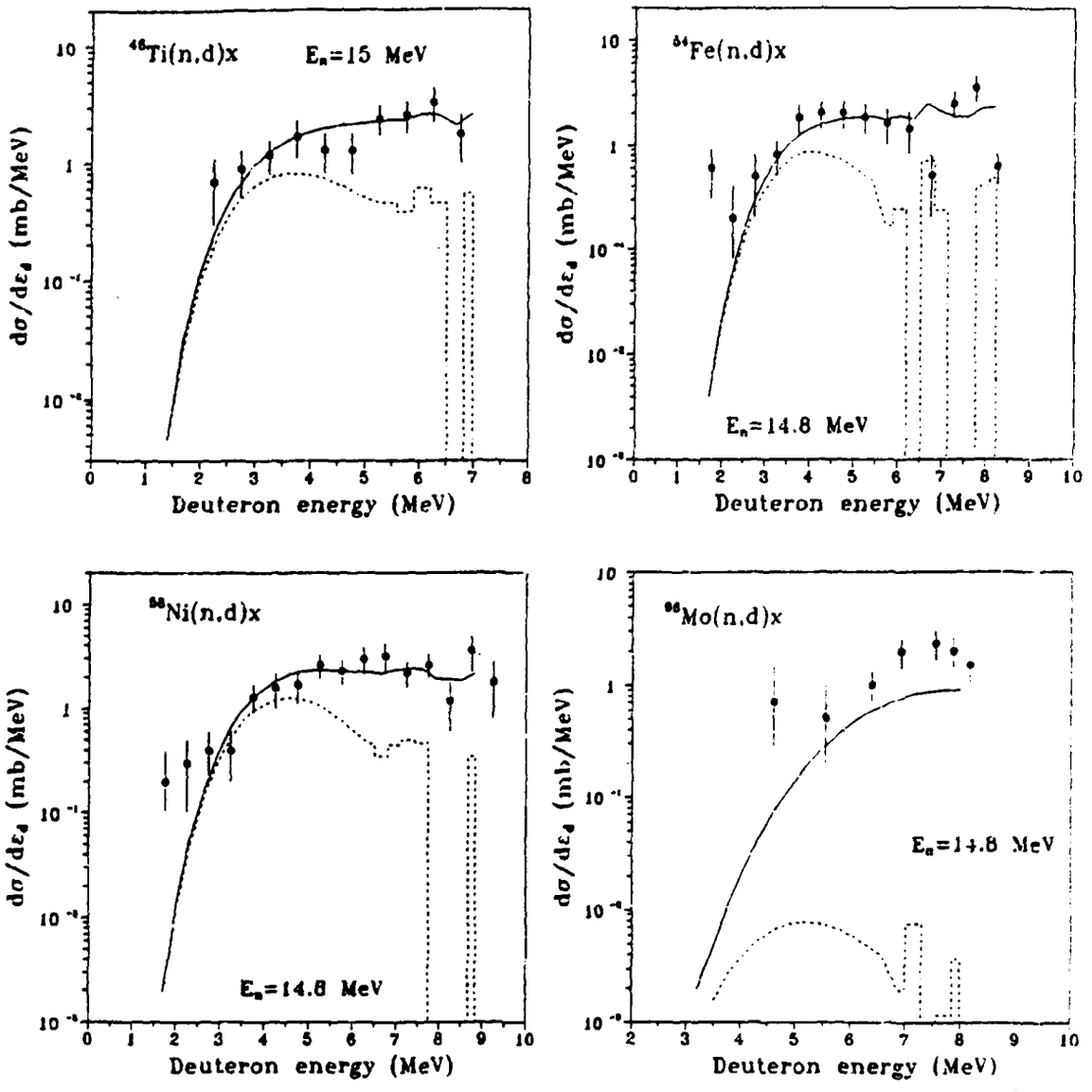

Figure 8. Deuteron spectra, calculated in this work and measured in references [25-28] for reactions taking place as a result of irradiation of even-even nuclides by 15 MeV neutrons. The total spectrum is shown by the solid curve, the equilibrium spectrum is shown by the dotted curve.

The (n,d) reaction cross section was calculated for 245 stable nuclides for atomic numbers ranging from 18-83. The results of these calculations, together with the experimental data, for the (n,d) and (n,d)+(n,np) reactions are given in Figure 10.

5.3. Systematics of the (n,d) reaction cross section

The calculated (n,d) reaction cross sections at 15 MeV for stable nuclides ranging from $40 \leq A \leq 209$, described above, may be used for various practical applications. However, it is necessary to make the following important observation.

In order to perform calculations, such as the ones made above, it is necessary to know the values of all individual parameters of each calculational model (e.g., γ, or the level density parameter), for all considered nuclides. If these parameters are not known, their values may be chosen by using neighboring nuclide data or approximate values of parameters for a large number of nuclides. However, such a procedure to choose unknown parameters leads to statistical uncertainties of the calculated cross section values. The systematics derived on the basis of the calculated cross section values must be designed so as to eliminate, albeit partly, such uncertainties. It must therefore be expected that the sum of the squares of the deviation of the experimental data from the calculated cross section values shall cause an increase in the analogous sum of the experimental data and the systematics, which was obtained exclusively on the basis of calculated cross section values.

The above statement could be illustrated by using the (n,p) and (n,α) reaction cross section as an example inasmuch as these reactions have been measured many times at 14.5 MeV.

The reaction cross sections considered here were calculated for 245 stable nuclides having atomic numbers ranging from Z=18-83. Pre-equilibrium proton spectra were calculated with the use of a hybrid exciton model, depending on the geometry [23]. The coalescence model including the particle pickup process [13] together with the hybrid model was used to describe the alpha particle emission, as illustrated in reference [32]. Weisskopf's model was used to calculate the evaporation spectra. The level densities were calculated with the aid of the Fermi gas model using the level density parameter a = A/9.

Having obtained the cross sections, the sum of the squares of the deviations (Σ) (see Formula (16) were calculated for the following quantities:

- cross sections derived from the analysis of experimental data for 156 nuclides ((n,p) reaction)), and for 120 nuclides ((n,α) reaction) given in references [33,20], and calculated cross section values,

- cross sections derived from the analysis of experimental data given in references [33,20], and cross section values calculated with the aid of various systematics.

In the latter case, the systematics parameters were obtained from fitting the formulas to 245 calculated cross section values. In the case of the (n,p) reaction, the simple empirical Levkovskiy formula [34], the empirical formula given in reference [4] and the semi-empirical systematics derived in reference [12]. Levkovskiy's formula [1] and the semi-empirical formula given in reference [20] were used to describe the (n,α) reaction.

The obtained values of the sum of squares of the deviation Σ are given in Tables 6 and 7.

By comparing the Σ values listed in Tables 6 and 7, it can be seen that the systematics obtained on the basis of calculated cross section values are better conveyed by experimental cross section values than by the calculated data used for the construction of the systematics.

On the basis of what has been said above, it follows that in order to predict the (n,d) reaction cross sections of intermediate and heavy nuclides, it makes sense to use the systematics obtained on the basis of calculated data.

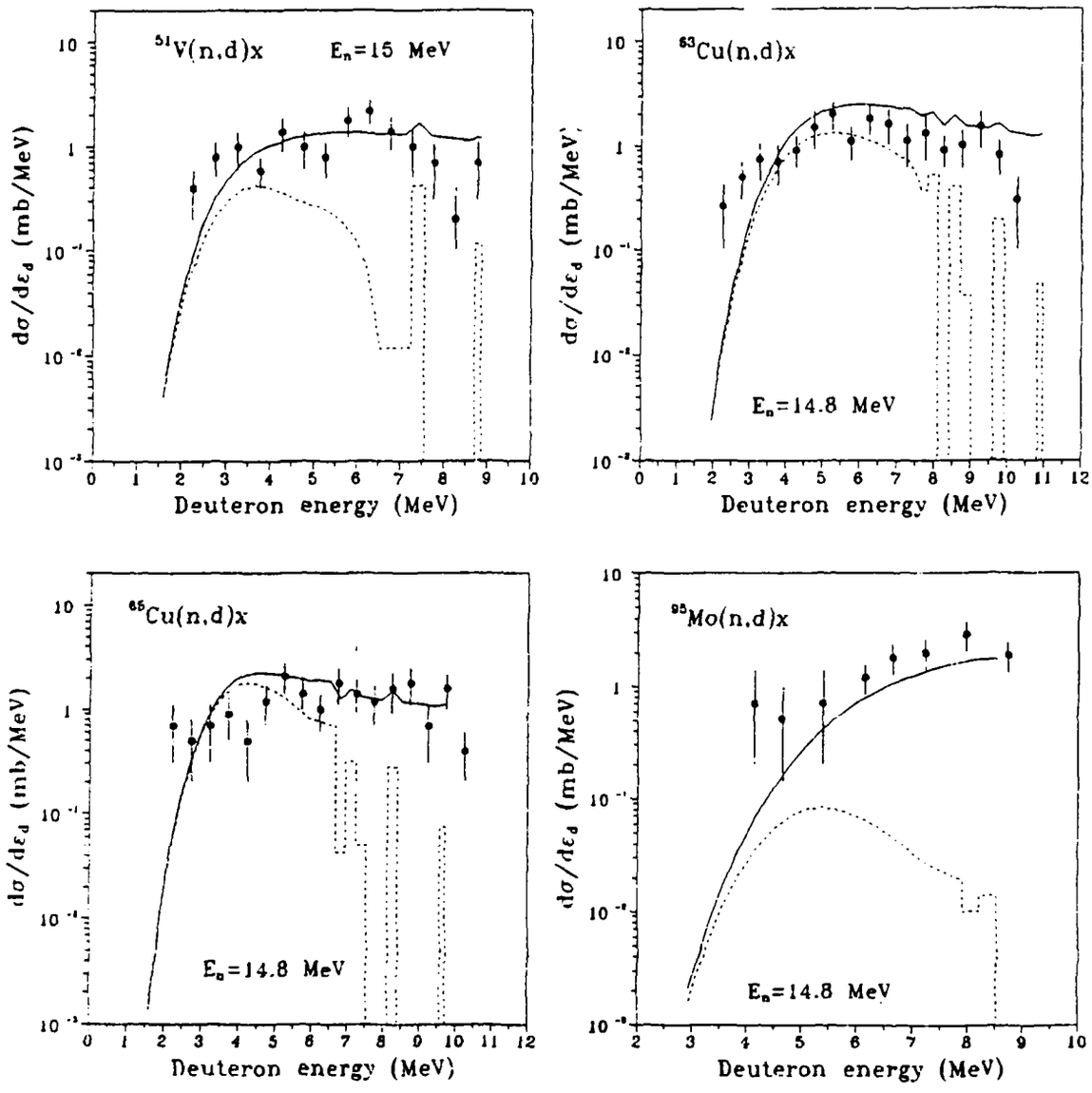

Figure 9. Deuteron spectra calculated in this work and measured spectra reported in [26-28] for reactions induced by the irradiation of odd-even nuclides with 15 MeV neutrons. The total spectrum is represented by the solid curve, and the equilibrium spectrum by the dotted curve.

For most stable nuclides with A ≥ 40, the non-equilibrium component of the (n,d) reaction cross section is significantly larger than the equilibrium component. Therefore, in the construction of the systematics of the (n,d) reaction cross section, it is possible to use the formula which describes the contribution of the non-equilibrium processes in the course of that reaction, as it was done in reference [35] for the (n,t) reaction.

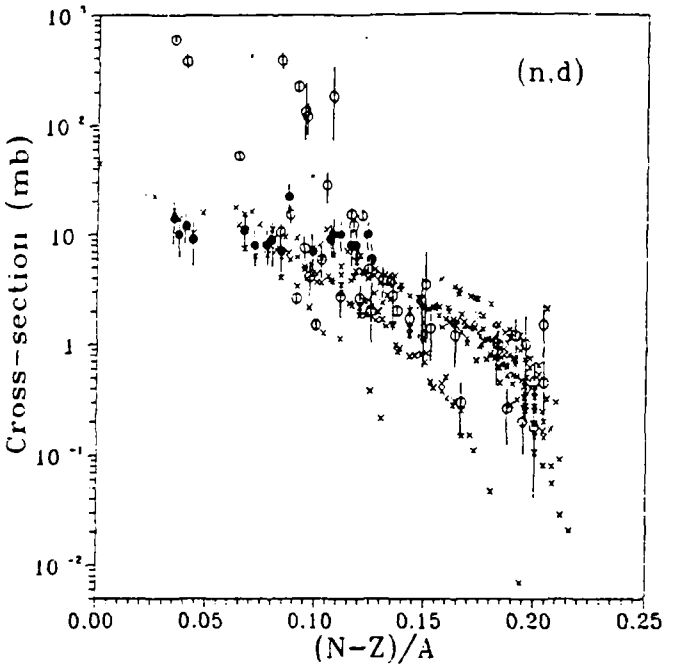

Figure 10. The (n,d) reaction cross sections calculated in this work for 245 stable nuclides (shown as crosses x), experimental values of the (n,d) reaction cross sections [25-28] (shown as black circles), the sum of the (n,d) and (n,np) reaction cross sections obtained in reference [29] based on the analysis of experimental data (shown by open circles).

Using the formula which is analogous to the one used for the construction of the (n,t) systematics in reference [35]:

$$\sigma_{(n,d)} = \pi\, r_0^2\left(A^{1/3}+1\right)^2 A^{-1/3}\left[\alpha_1(N-Z)/A + \alpha_2 Z/A^{1/3} + \alpha_3\right]^3, \qquad (36)$$

where r_o = 1.3 Fm, α_i are parameters chosen from conditions which best describe the experimental data.

In this work, the formula (36) parameters resulted from fitting them to 245 calculated (n,d) reaction cross sections shown in Figure 10. The sum of the squares of the deviation was minimized with the aid of the program taken from reference [18]. As a result, the following systematics was derived:

$$\sigma_{(n,d)} = \pi\, r_0^2\left(A^{1/3}+1\right)^2 A^{-1/3}\left[-24647(N-Z)/A + 0.019731Z/A^{1/3} + 0.30672\right]^3, \qquad (37)$$

where r_o = 1.3 Fm, N,Z, A are the number of neutrons, protons and nucleons in the target nucleus.

The resultant formula (37) may be used for the evaluation of (n,d) reaction cross sections for the interaction of 14.8 MeV neutrons with A≥ 40 nuclides. Used in this manner, namely applying the systematics of formula (37), rather than using calculated values of the cross section, which are included in their foundation, is much more expedient for the reasons that have been mentioned above.

Table 6. Values of (Σ), calculated with the use of formula (16) and the corresponding methods to calculate σ^{calc} for the (n,p) reaction for 14.5 MeV incident neutrons. The systematics parameters were determined by fitting the formula to 245 calculated cross section values. The σ^{exp} quantities were obtained from the analysis of experimental data given in reference [33]. The number of experimental points was N=156.

Cross section calculation method	Number of systematics parameters	Σ
Hybrid exciton and evaporation model	-	2730
Empirical systematics [34]	2	1965
Empirical systematics [4]	4	1939
Semi-empirical systematics [12]	7	1912

Table 7. Values of (Σ), calculated with the use of formula (16) and the corresponding methods to calculate σ^{calc} for the (n,α) reaction for 14.5 MeV incident neutrons. The systematics parameters were determined by fitting the formula to 245 calculated cross section values. The σ^{exp} quantities were obtained from the analysis of experimental data given in reference [20]. The number of experimental points was N=120.

Cross section calculation method	Number of systematics parameters	Σ
Hybrid exciton and evaporation model	-	3809
Empirical systematics [1]	2	3088
Semi-empirical systematics [20]	7	963

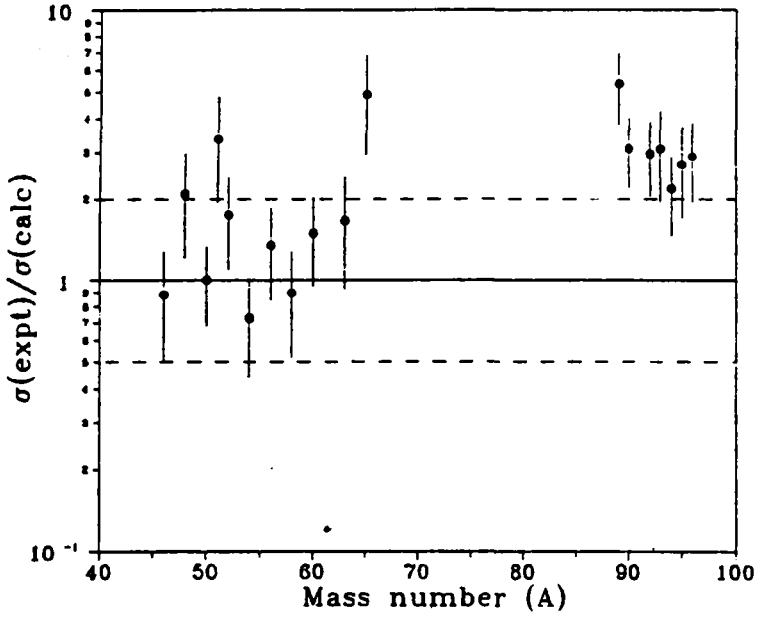

Figure 11. Ratio of experimental (n,d) reaction cross sections to calculations using systematics (37).

Figure 11 shows the ratio of 18 experimental cross sections taken from references [25-28] to cross sections calculated using formula (37). It must be noted that the most significant differences were observed for those nuclides for which the experimental (n,d) reaction cross sections exceed the (n,d)+(n,np) cross section sum calculated with the aid of systematics (see section 5.1).

6. The (n,np) reaction

6.1. Formulas for the construction of the (n,np) reaction cross section systematics.

The (n,np) reaction cross section consists of the sum of three component cross sections:

$$\sigma(n,np) = \sigma(n,n+p) + \sigma(n,p+n) + \sigma(n,d), \qquad (38)$$

where $\sigma(n,n+p)$ is the cross section for the reaction accompanied by the subsequent emission of a neutron and a proton, $\sigma(n,p+n)$ is the cross section for the reaction with the emission of a proton and a neutron and $\sigma(n,d)$ is the (n,d) reaction cross section.

The analysis of the experimental cross section values [25-28] for the reaction accompanied by the emission of a deuteron has shown that the contribution of the (n,d) channel to the total cross section of the (n,n+p)+(n,p+n)+(n,d) reactions is small and is therefore not considered any further in this work.

The (n,n+p) and (n,p+n) reaction cross sections can be represented by

$$\begin{aligned} \sigma(n,n+p) &= \sigma^{pre}(n,n+p) + (1 - P^{pre})\sigma(n,n+p) , \\ \sigma(n,p+n) &= \sigma^{pre}(n,p+n) + (1 - P^{pre})\sigma(n,p+n) \end{aligned} \qquad (39)$$

where $\sigma^{pre}(n,n+p)$ and $\sigma^{pre}(n,p+n)$, $\sigma^{eq}(n,n+p)$ and $\sigma^{eq}(n,p+n)$ are the contributions of the pre-equilibrium and the equilibrium components to the total (n,n+p) and (n,p+n) cross sections, and where P^{pre} is the probability for all of the pre-equilibrium processes.

Simple analytical expressions for the calculation of the σ^{pre}(n,np) and σ^{eq}(n,np) cross sections can be obtained from theoretical models described in section 6.2, taking the following conditions into consideration.As illustrated by the analysis of 246 stable nuclides having mass numbers ranging from 40 - 209, which was performed in the work referenced in [29]:

- 208 nuclides (85%) satisfy conditions $Q_n<Q_p+V_p'; Q_n'<Q_p'+V_p'; Q_n''<Q_p''+V_p''$;
- 36 nuclides (14%) satisfy conditions $Q_n<Q_p+V_p'; Q_n'>Q_p'+V_p'; Q_n''<Q_p''+V_p''$
- and 2 nuclides (1%) satisfy all of the remaining relationships between the considered quantities,

(where Q_n and Q_p are the energies of neutron and proton separation from the compound nucleus (A+1,Z), where Q'_n and Q'_p are the energies of separation of the particle from the target nucleus (A,Z), Q''_n and Q''_p are the energies of separation of the particle from the nucleus formed after the emission of the proton from the compound nucleus (A,Z-1), where V_p, $V_{p'}$ and $V_{p''}$ are the Coulomb potential for the proton corresponding to the (A+1,Z), (A,Z) and (A,Z-1) nuclei). (The Coulomb potential is calculated using the following formula: $V_p(A,Z)=).5(Z-1)/r_o((A-1)^{1/3} + 1)$ MeV, where Z is the charge of the target nucleus)

For 625 unstable nuclides in the range of $40 \leq A \leq 209$ and having half lives larger than 1 hour,

- 451 nuclides (72%) satisfy conditions $Q_n<Q_p+V_p;\ Q_{n'}<Q_{n'}+V_{p'};\ Q_{n''}<Q_{p''}+V_{p''}$,
- 90 nuclides (15%) satisfy conditions $Q_n<Q_p+V_p;\ Q_{n'}>Q_{p'}+V_{p'}\ Q_{n''}<Q_{p''}+V_{p''}$[1],
- and 84 nuclides (13%) satisfy all of the remaining relationships between the separation energies of the neutron and the proton.

It can be shown that the equilibrium component of the (n,np) reaction cross section corresponding to two rather common widespread cases relating to the relationship between Q_n and Q_p will have the following form under the condition that

$$Q_n<Q_p+V_p;\ Q_{n'}<Q_{p'}+V_{p'};\ Q_{n''}<Q_{p''}+V_{p''}:$$

$$\sigma^{eq}(n,np) = \sigma^{eq}(n,n+p) + \sigma^{eq}(n,p+n) =$$

$$C^{eq} e^{\frac{Q'_{(n,p)}-V_p}{T}} \left\{ 1 - \left(1 + \frac{(E_n - E_{th})}{T} + \frac{1}{2}\frac{(E_n - E_{th})^2}{T^2} + \frac{1}{6}\frac{(E_n - E_{th})^3}{T^3} \right) e^{-\frac{(E_n - E_{th})}{T}} \right\} +$$

$$+ C^{eq} e^{\frac{Q_{(n,p)}-V_p}{T}} \left\{ 1 - \left(1 + \frac{(E_n - E_{th})}{T} \right) e^{-\frac{(E_n - E_{th})}{T}} \right\}, \qquad (40a)$$

$$Q_{(n,np)} = - Q_{p'}(A,Z),$$

$$Q_{(n,p)} = Q_n(A+1,Z) - Q_p(A+1,Z), \qquad Q'_{(n,p)} = Q_{n'}(A,Z) - Q_{p'}(A,Z),$$

$$C^{eq} = \sigma_n^{non}(E_n)(1 - P^{pre}), \qquad E_{th} = -Q_{(n,np)} + V_p.$$

For $Q_n<Q_p+V_p;\ Q_{n'}>Q_{p'}+V_{p'};\ Q_{n''}<Q_{p''}+V_{p''}$:

$$\sigma^{eq}(n,np) = C^{eq} \left\{ 1 + e^{\frac{(Q_{(n,p)}-V_p)}{T}} \right\} \left\{ 1 - (1 + \frac{E_n - E_{th}}{T}) e^{-\frac{(E_n - E_{th})}{T}} \right\}. \qquad (40b)$$

The formulas for the evaluation of the pre-equilibrium component of the (n,np) reaction cross section, corresponding to the two most common and widespread cases relating to the relationship between the quantities of the neutron and proton separation energy, have the following form.

For the condition: $Q_n<Q_p+V_p;\ Q_{n'}<Q_{p'}+V_{p'};\ Q_{n''}<Q_{p''}+V_{p''}$:

$$\sigma^{pre}(n,np) = \sigma^{pre}(n,n+p) + \sigma^{pre}(n,p+n) =$$

$$= C_n^{pre} \frac{e^{\frac{(Q'_{(n,p)}-V_p)}{T}}}{T^2} \left\{ \left(3E_{th}T^4 + 8T^5\right) - (E_n - E_{th})\left(3T^4 + 2T^3E_{th}\right) + \right.$$

$$+ (E_n - E_{th})^2 \left(\frac{E_{th}T^2}{2} \right) + (E_n - E_{th})^3 \frac{T^2}{6} - \qquad (41a)$$

$$\left. - e^{-\frac{(E_n - E_{th})}{T}} \left(3E_{th}T^4 + 8T^5 + (E_n - E_{th})\left(5T^4 + E_{th}T^3\right) + T^3(E_n - E_{th})^2\right) \right\} +$$

$$+ C_p^{pre} \left\{ \frac{1}{6}(E_n - E_{th})^3 + \frac{Q_{n'}}{2}(E_n - E_{th})^2 \right\};$$

and for the condition: ; $Q_n<Q_p+V_p$; $Q_n'>Q_p'+V_p'$; $Q_n''<Q_p''+V_p''$:

$$\sigma^{pre}(n,np)=C_n^{pre}\left\{\frac{E_n(E_n-E_{th})^2}{2}-\frac{(E_n-E_{th})^3}{3}\right\}+C_p^{pre}\left\{\frac{1}{6}(E_n-E_{th})^3+\frac{Q_{n''}}{2}(E_n-E_{th})^2\right\}, \quad (41b)$$

where $C_{n(p)}^{pre}=\sigma_n^{non}(E_n)\dfrac{8(2s_{n(p)}+1)m_{n(p)}r_0^2A^{2/3}R_{n(p)}(3)}{\pi^2\hbar^2E_0|M|^2g^4}$,

$g=A/12$ MeV^{-1}, $|M|^2=150$ A^{-3} E$_o^{-1}$ MeV, $r_0=1.3$ Fm and $R_n(3)=0.5$.

The (n,np) reaction cross section for nuclides that belong to other groups can be readily identified by their magnitude. As shown in Figure 12,
- nuclides for which $Q_n<Q_p+V_p$; $Q_n'<Q_p'+V_p'$; $Q_n''<Q_p''+V_p''$,
  have a significantly smaller magnitude of the (n,np) reaction cross section at 14.5 MeV,
- than those for which $Q_n<Q_p+V_p$; $Q_n'>Q_p'+V_p'$; $Q_n''<Q_p''+V_p''$.

This is due to the fact that nuclides having an energy of 14.5 MeV,
- and for which $Q_n<Q_p+V_p$; $Q_n<Q_p'+V_p'$; $Q_n''<Q_p''+V_p''$
  is relatively near to the effective reaction threshold E_{th}= -Q(n,np) + V_p.

As a result of calculations performed for the (n,np) reaction cross section [29] based on the pre-equilibrium - evaporation models for stable nuclides and taking the set of conditions $Q_n<Q_p+V_p$; $Q_n'<Q_p'+V_p'$; $Q_n''<Q_p''+V_p''$ into account, the pre-equilibrium component of the (n,np) reaction cross section at 14.5 MeV significantly exceeds the equilibrium component. Nuclides for which $Q_n<Q_p+V_p$; $Q_n'>Q_p'+V_p'$; $Q_n''<Q_p''+V_p''$, the contribution of the equilibrium emission dominates the (n,np) reaction cross section.

The noted conditions makes it possible to significantly simplify the expressions for the calculations of (n,np) reaction cross sections of nuclides belonging to various groups.

Nuclides for which $Q_n<Q_p+V_p$; $Q_n'<Q_p'+V_p'$; $Q_n''<Q_p''+V_p''$ at 14.5 MeV:

$$\sigma(n,np)\equiv\sigma^{pre}(n,np)\approx C^{pre}\frac{Q_{(n,p)}-Q_{(n,np)}}{2}(14.5-E_{th})^2, \quad (42a)$$

Nuclides for which $Q_n<Q_p+V_p$; $Q_n'>Q_p'+V_p'$; $Q_n''<Q_p''+V_p''$:

$$\sigma^{eq}(n,np)=C^{eq}\left\{1+e^{\frac{(Q_{(n,p)}-V_p)}{T}}\right\}\left\{1-(1+\frac{14.5-E_{th}}{T})e^{-\frac{(14.5-E_{th})}{T}}\right\}. \quad (42b)$$

In deriving formulas (42a) from (41a) it was assumed that

$$(14,5 - E_{th})/E_{th} << 1. \quad (43)$$

It can be seen from formulas that the (n,np) reaction cross section depends on the (n,np) and (n,p) reaction energies. Using the semi-empirical mass formula, it can be shown that the (n,np) reaction energy displays the following dependence on the number of neutrons and protons in nuclei

$$Q_{(n,np)}(A,Z)\equiv\beta_1\left(\frac{N-Z+\beta_2}{A}\right)^2+\beta_3\left(\frac{N-Z+\beta_4}{A}\right)+\frac{\beta_5}{A^{1/3}}+\beta_6, \quad (44)$$

where β_1 - β_6 are constants. A similar dependence can also be seen for the (n,p) reaction energy.

Based on the expressions (42) and (44), the following formula is proposed for the construction of the (n,np) reaction cross section systematics:

$$\sigma(n,np) = \pi r_0^2\left(A^{1/3}+1\right)^2\left\{A^{-1/3}(\alpha_1 S+\alpha_2)^2 + exp\left(\alpha_3 S^2+\alpha_4 S+\alpha_5\right)\right\}, \qquad (45)$$

where $S=\left(\frac{N-Z+\alpha_6}{A}\right)$, r_o = 1.3 Fm and α_1 - α_6 are parameters.

The first member of the sum in expression (45) describes the pre-equilibrium component and the second, describes the equilibrium component of the (n,np) reaction cross section. As the probability for all pre-equilibrium processes P_{pre} is a smoothly changing function as it passes from nuclide to nuclide, P_{pre} is therefore not included in expression (45) in its explicit form.

6.2. Comparison of various (n,np) reaction cross section systematics

The following empirical systematics for the (n,np) reaction cross section have been presented in references [4,10,11].

The work by Qaim [11,4]:

$$\sigma(n,np) = \begin{cases} \alpha_1 exp(\alpha_2 s), \xi > 0 \\ \alpha_3 \sigma(\xi > 0), \xi < 0 \end{cases} \qquad \begin{aligned} s &= \left(\frac{N-Z}{A}\right), \\ \xi &= Q_p(A,Z) - Q_n(A,Z), \end{aligned} \qquad (46)$$

where α_1 - α_3 are parameters; N, Z, A are the number of neutrons, protons and the mass number of the target nucleus; Q_p (A,Z), Q_n (A,Z) is the binding energy of the proton and neutron in the target nucleus.

The work by Forrest [4]:

$$\sigma(n,np) = \alpha_1\left(A^{1/3}+1\right)^2\left(1+\alpha_2 tanh(\xi+1)\right)exp\left(\alpha_3 s+\alpha_4 A^{-1}\right), \qquad (47)$$

where α_1 - α_4 are parameters, and $\xi = Q_p(A,Z) - Q_n(A,Z)$.

The work of Ikeda et al [10]

$$\sigma(n,np) = \alpha_1(A^{1/3}+1)^2 exp\left(\alpha_2 s+\alpha_3 s^2+\alpha_4 s^3\right) \qquad (48)$$

where α_1 - α_4 are parameters.

A new (n,np) reaction cross section library obtained from the analysis of experimental data given in reference [29] was used for the comparison of the systematics. The α_i parameters in expressions (45) - (48) were chosen so as to minimize the value of expression (16).

The results of the comparison of the systematics are presented in Table 8. As can be seen from these data, the fitting of the evaluated data taken from reference [29] produced minimum values of Σ and χ^2 by using formula (45).

Formula (45) produces minimum values of Σ and χ^2 by using experimental data contained in other compilations as well. For instance, the evaluated (n,np) reaction cross section data given at 14.7 MeV in reference [4] contains data for 35 nuclides ranging from ^{44}Ca to ^{199}Hg. The results of the fitting of expressions (45) - (48) are presented in Table 9.

It is interesting to compare the data obtained by using the systematics (45) with the calculational results obtained on the basis of contemporary theoretical models which have been performed in reference [36]. The(n,np) reaction cross sections were calculated using the pre-equilibrium exciton model and the evaporation model in the framework of the Hauser-Feshbach approximation. Level densities were calculated using the superfluid model of the nucleus. The sum of the squares of the relative deviations, corresponding to the results of calculation [36] and the evaluated cross sections from reference [29], is given in Table 8. It is evident that the data predicted by the systematics using formula (45) are more exact than the calculational results obtained on the basis of theoretical models. This conclusion is related to the currently unavoidable uncertainty in the parameters of calculational models which lead to the deviation of calculational results from the data [37].

All of the above-mentioned commentary suggests that formula (7) provides the best description of the experimental data in comparison to systematics or calculations made on the basis of theoretical models.

6.3. Systematics of the (n,np) reaction cross section

As a result of this work, a new 6-parameter formula for the evaluation of the sum of the (n,np), (n,pn) and (n,d) reaction cross sections at 14.5 MeV has been derived:

$$\sigma(n,np) = \pi r_0^2 \left(A^{1/3} + 1 \right)^2 \left\{ A^{-1/3} \left(-1.2496S + 0.29702 \right)^2 + exp\left(-1424.1S^2 + 277.85S - 14.302 \right) \right\}, \quad (49)$$

where r_0 = 1.3 Fm, and S = (N-Z+3.5)/A , and where N, Z and A are the numbers of neutrons, protons and mass number of the target nucleus.

A comparison of the pre-equilibrium component of the (n,np) reaction cross section, calculated with the aid of formula (49), and on the basis of the hybrid exciton model [29], is presented in Figures 13 and 15. An analogous comparison is presented in Figures 14 and 16 for the sum of the pre-equilibrium and equilibrium components of the cross section calculated using formula (49) and the model described in reference [29]. As an illustration, these comparisons were made for the isotopes of nickel and zirconium.

It can be seen from these figures, that not only does the new systematics describes the experimental data well, but it also reproduces the pre-equilibrium and equilibrium contributions to the (n,np) reaction cross section.

Figure 17 shows the ratio of the experimental cross section values to the values calculated with aid of formula (49).

Table 8. Results of fitting various formulas to 49 experimental (n,np) cross section values at an energy of 14.5 MeV [29].

Formula	Σ	χ^2	Source
(45) [1)]	157.96	3.67	This work
Forrest [2)]	218.99	4.8664	[4]
Ikeda et al [3)]	491.92	10.931	[10]
Qaim [4)]	739.96	16.086	[11]
pre-equilibrium and equilibrium model	642.64	-	[36]

Parameter values:
1) $\alpha_1 = -1.2496$, $\alpha^2 = 0.29702$, $\alpha_3 = -1424.1$, $\alpha_4 = 277.85$, $\alpha_5 = -14.302$, $\alpha_6 = 3.5$;
2) $\alpha_1 = 1842.7$, $\alpha_2 = -0.47433$, $\alpha_3 = -57.122$, $\alpha_4 = -150.10$;
3) $\alpha_1 = 6008.5$, $\alpha_2 = -222.91$, $\alpha_3 = 1566.5$, $\alpha_4 = -4027.4$;
4) $\alpha_1 = 34.953$, $\alpha_2 = -25.245$; $\alpha_3 = 3.8324$.

Table 9. Results of fitting various formulas to 35 experimental (n,np) cross section values at an energy of 14.5 MeV [4].

Formula	Σ	χ_2	Source
(45) [1)]	171.85	5.93	This work
Forrest [2)]	273.26	8.81	[4]
Ikeda et al [3)]	513.12	15.55	[10]
Qaim [4)]	1028.80	32.15	[11]
pre-equilibrium and equilibrium model	2131.11	-	[36]

Parameter values:
1) $\alpha_1 = -1.3454$, $\alpha^2 = 0.32162$, $\alpha_3 = -1556.8$, $\alpha_4 = 309.73$, $\alpha_5 = -16.148$, $\alpha_6 = 3.5$;
2) $\alpha_1 = 2425.8$, $\alpha_2 = -0.37779$, $\alpha_3 = -58.354$, $\alpha_4 = -166.12$;
3) $\alpha_1 = 31168$, $\alpha_2 = 268.01$, $\alpha_3 = 1992.0$, $\alpha_4 = 5198.9$;
4) $\alpha_1 = 44.706$, $\alpha_2 = -22.805$; $\alpha_3 = 1.0652$.

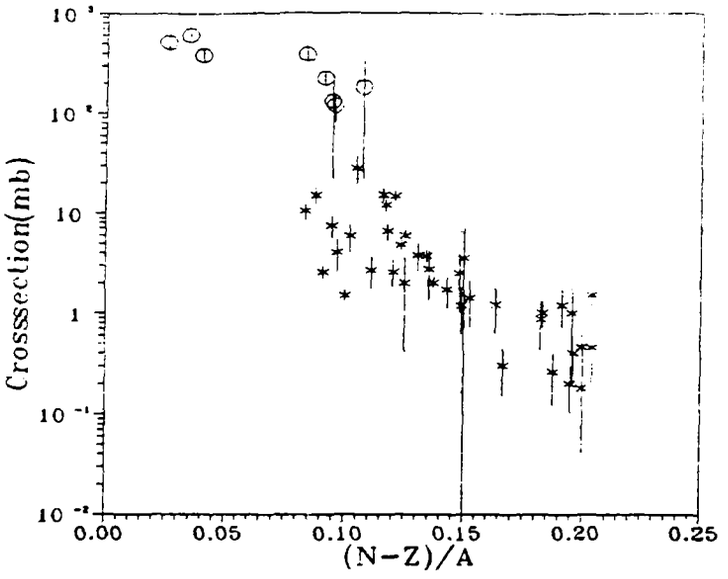

Figure 12. Evaluated (n,np) reaction cross section data at 14.5 MeV calculated in this work plotted as a function of (N-Z)/A)

(*) Target nuclei which satisfy condition $Q_n<Q_p+V_p$; $Q_{n'}<Q_{p'}+V_{p'}$; $Q_{n''}<Q_{p''}+V_{p''}$;

(o) Target nuclei which satisfy condition $Q_n<Q_p+V_p$; $Q_{n'}>Q_{p'}+V_{p'}$; $Q_{n''}<Q_{p''}+V_{p''}$.

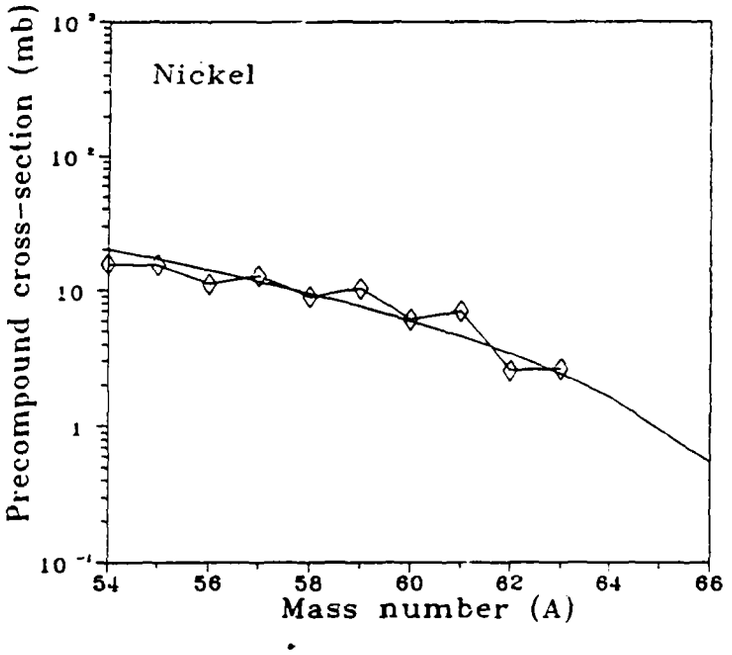

Figure 13. Pre-equilibrium component of the (n,np) reaction cross sections at 14.5 MeV for nickel isotopes. (◇) calculated values on the basis of the hybrid exciton and the evaporation models reported in reference [29]; solid curve, values calculated with systematics formula (49) recommended in this work.

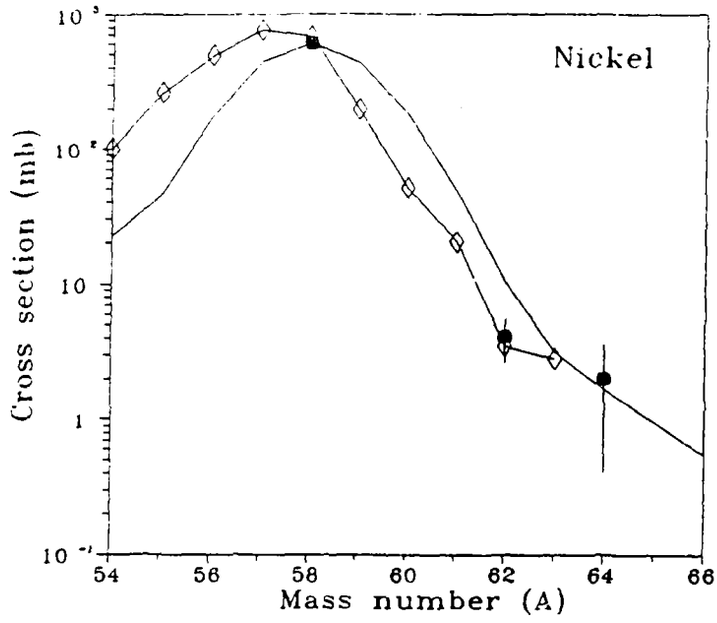

Figure 14. The (n,np) reaction cross sections for nickel isotopes at 14.5 MeV.
(●) values obtained from analysis of experimental data; (◊) values calculated on the basis of the hybrid exciton and evaporation models reported in reference [29]; solid curve calculated with the use of the systematics formula (49) recommended in this work.

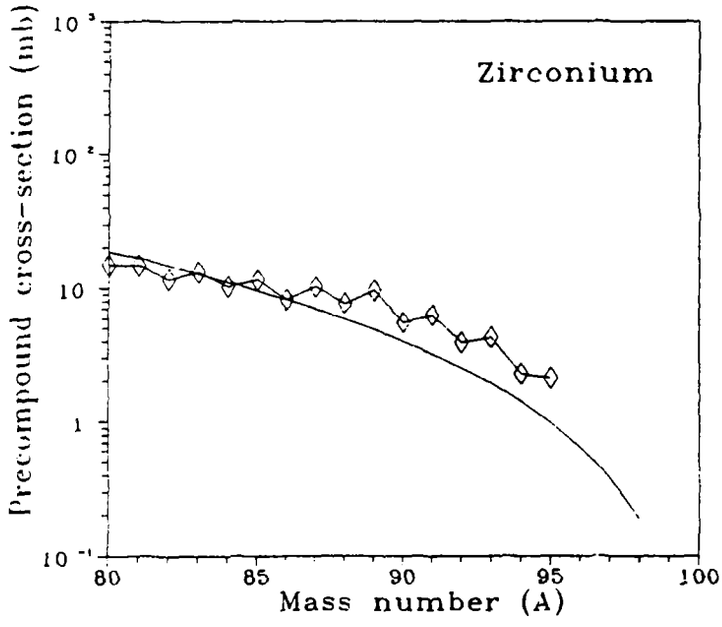

Figure 15. Pre-equilibrium component of the (n,np) reaction cross section at 14.5 MeV for zirconium isotopes. (◊) values calculated on the basis of the hybrid exciton and evaporation models reported in reference [29]; solid curve calculated with the use of the systematics formula (49) recommended in this work.

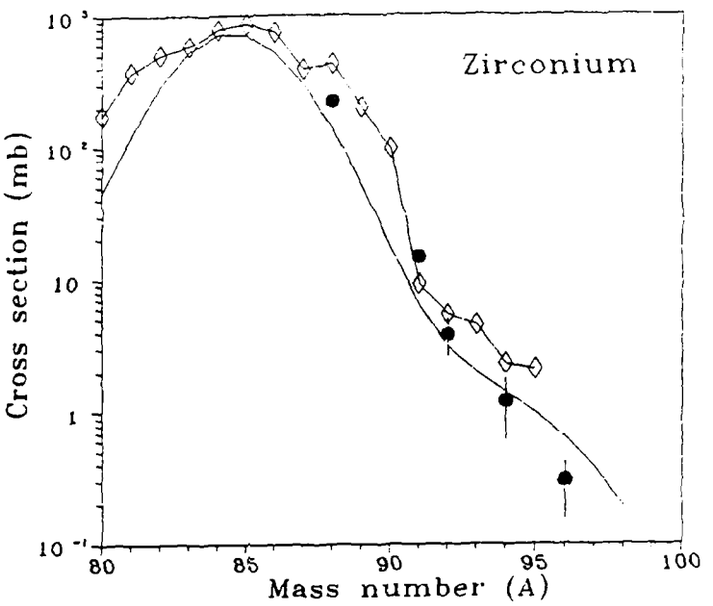

Figure 16. The (n,np) reaction cross sections for zirconium isotopes at 14.5 MeV.
(●) values obtained from analysis of experimental data; (◊) values calculated on the basis of the hybrid exciton and evaporation models reported in reference [29]; solid curve calculated with the use of the systematics formula (49) recommended in this work.

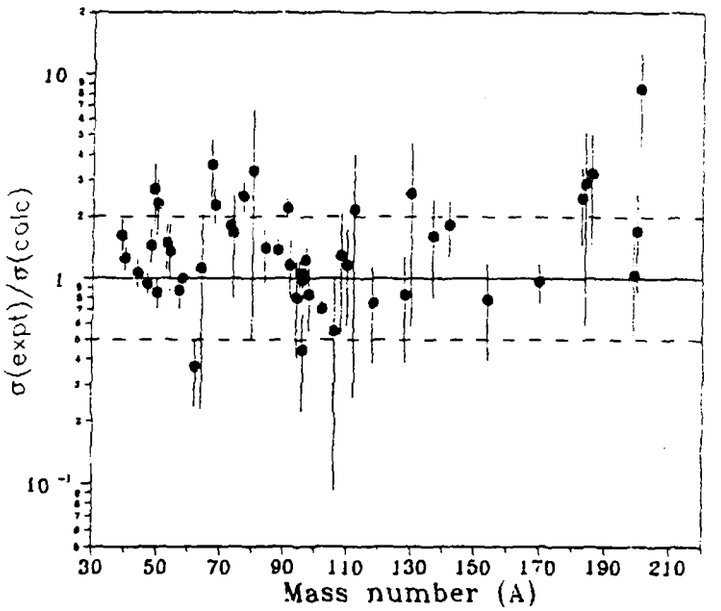

Figure 17. Ratio of cross section values obtained from the analysis of experimental data reported in reference [29], to the cross section values calculated with the aid of the systematics formula (49) as a function of mass number.

References

[1] LEVKOVSKIY, V.N., J. Exp. Theo. Fiz. 6 (1958) 1174 [in Russian].

[2] GARDNER, D.G., YU,Y., Nucl. Phys. 60 (1964) 49.

[3] KUMABE, I., FUKUDA, K., Rep. NEANDC(J), 65/U (1978) 45.

[4] FORREST, Rep. AERE-R 12419 (1986).

[5] AIT-TAHAR, S., Z. Phys. A348 (1994) 289.

[6] QAIM, S.M., STOCKLIN, G., Nucl. Phys. A257 (1976) 233.

[7] WOO, T.W., SALAITA, G.N.,(Proc.Int. Conf. Nuclear Cross Sections for Technology, Knoxville, 1979) Rep. NBS Spec. Publ. 594 GC 12 (1979) 853.

[8] BODY, Z.T., MIHALY, K., Compilation of (n,t) Cross Sections Around 14 MeV, Rep. INDC(HUN)-22, IAEA, Vienna (1985).

[9] LISHAN, Y., Comm. Nucl. Data Progr. 7 (1992 85.

[10] IKEDA, Y., et al., (Proc. Int. Conf. Nucl. Data for Science and Technology, Mito, 1988.

[11] QAIM, S.M., Nucl. Phys. A382 (1982) 255.

[12] SHUBIN, Yu., et al., IAEA Rep. INDC(CCP)-385, Vienna (1995).

[13] IWAMOTO, A., HARADA, K., Phys. Rev. C26 (1982) 1527.

[14] STRUTINSKY, V.M., (Proc. Cong. Int. Phys. App., Paris, 1958), Adv. Phys. 9 (1960) 425.

[15] WILLIAMS, F.C., Phys. Lett. 31B (1970) 184.

[16] BLOKHIN, A.I., et al., Izv. Akad. Nauk, Ser. Physics, 49 (1985) 962. [in Russian].

[17] ZELENETSKIY, A.V., PASCHCHENKO, A.B., Problems in Science and Technology, Series: Nuclear Constants 3 (1990) 53 [in Russian].

[18] SILIN, I.N., Preprint OIYaI 11-3362, Dubna (1967) [in Russian].

[19] BYCHKOV, V.M., et al., Neutron cross sections of threshold reactions, Ehnergoizdat, Moscow (1982) [in Russian].

[20] KONOBEEV, A.Yu., LUNEV, B.P., SHUBIN, Yu.N., Semi-empirical systematics of the (n,α) reaction cross section at an approximate energy of 14.5 MeV, Preprint FEI-2409 (1995) [in Russian].

[21] KONOBEEV, A.Yu., et al., Nucl. Instr. Meth. B93 (1994) 409.

[22] JINGSHANG, Zh., SHIWEI, Y., CUILAN, W., Z. Physik C28 (1983) 1475.

[23] BLANN, M., VONACH, H.K., Phys. Rev. C28 (1983) 1475.

[24] BLANN, M., BIPSLINGHOF, J., Rep. UCID-19614, Lawrence Livermore Laboratory (1982).

[25] GRIMES, S.M., HAIGHT, R.C., ANDERSON, J.D., Nucl. Sci. Eng. 62 (1977) 187.

[26] GRIMES, S.M., HAIGHT, R.C., ANDERSON, J.D., Phys. Rev. C17 (1978) 508.

[27] GRIMES, S.M., et al., Phys. Rev. C19 (1979) 2127.

[28] HAIGHT, R.C., et al., Phys. Rev. C23 (1981) 700.

[29] DITYUK, A.I., et al., (n,np) reaction cross section systematics at 14.5 MeV, Preprint FEI-2492 (1996) [in Russian].

[30] UHL, M., STROHMAYER, B., Rep. IRK-76/01, Vienna (1976).

[31] GRUDZEVICH, O.T., et al., (Proc. First Int. Conf. on Neutron Physics, Kiev 1987), TsNIIATOMINFORM, Moscow, 2. (1988) 96.[in Russian]

[32] KONOBEEV, A.Yu., KOROVIN, Yu. A., Kerntchnik 59 (1994) 72.

[33] PASHCHENKO, A.B., Cross sections for reactions induced by 14.5 MeV neutrons, spontaneous Cf-252 neutrons and U-235 fission spectra, Report N-0236, TsNIIATOMINFORM, Moscow (1990) [In Russian].

[34] LEVKOVSKIY, V.N., JETF 18 (1964) 213 [in Russian].

[35] KONOBEEV, A.Yu., LUNEV, V. P., SHUBIN, Yu.N., Semi-empirical systematics for the (n,t) reaction cross sections at an approximate energy of 14.5 MeV, Preprint FEI-2491(1996) [in Russian].

[36] GRUDZEVICH, O.T., et al., Problems of Atomic Science and Technology, Series: Nuclear Constants 3-4 (1993) [in Russian].

[37] GRUDZEVICH, O.T., et al., Problems of Atomic Science and Technology, Series: Nuclear Constants 1 (1992) 57 [in Russian].

ANALYSIS OF THE Nb(n,xn) AND Bi(n,xn) REACTION IN THE 5-27 MeV INCIDENT NEUTRON ENERGY RANGE

V.P. Lunev, V.G. Pronyaev, S.P. Simakov

State Research Centre of the Russian Federation
Institute of Physics and Power Engineering, Obninsk

Abstract

Results of a detailed study of the generation of neutron emission spectra, taking into account the contribution of the pre-equilibrium decay and direct reaction mechanisms to the formation of the compound nucleus are presented. Main consideration is given to the determination of the nuclear level density in the neutron inelastic scattering channel which is the primary contributor to the shape of the soft part of neutron emission spectra. A good description of the experimentally observed spectra over the whole energy range was obtained. The level density parameters which were determined are in good agreement with those taken from well known systematics in the case of Nb, but not in the case of Bi.

Introduction

In spite of the relative long time that has been devoted to the efforts to understand the fundamental mechanisms to describe the nucleon-nucleus reaction in the MeV energy range, exhausting all possible approaches, it still has not been possible to understand the interaction mechanisms and the properties of the exited states of the nucleus. Accordingly, the models and methods which would have the ability to give qualitative predictions of the reaction cross section , and the energy and angular distribution of secondary particles to an accuracy to which they are now determined experimentally, have not yet been developed.

The (compound) equilibrium mechanism of a reaction has been formalized rigorously in the Hauser-Feshbach model [1]. Nevertheless, even in this case, there are uncertainties which arise in the modeling of the nuclear level densities. Even in the case of the simplest phenomenological models, such as the Fermi-gas model [2], as well as in the case of the latest models, which take shell effects, evaporation and collective effects into consideration [3], the theoretical calculations do not always agree with the observed energy dependence of the excitation function, nor do they have the required accuracy.

Primary unresolved difficulties are still encountered in the theoretical interpretation of the non-equilibrium mechanisms of the direct inelastic scattering and in the case of pre-equilibrium emission of nucleons from intermediate (incoming) states. Initially, all increases above the compound state were attempted to be described by the pre-equilibrium nucleon emission in the framework of the exciton model [4]. However, as the number of reaction analyses grew, more unresolved problems became apparent. On the other hand, a definite success was achieved in the understanding of the direct excitation mechanism of the lowest collective states of nuclei. The first attempt to create a single quantum-mechanical theory which would explain the

process of a nuclear reaction in terms of an evolution of complex open and closed configurations was undertaken by Feshbach, Kerman ad Kunin [5]. However, since that time there has been no significant progress in the theory of nuclear reactions.

The work presented here, which could be considered as another step in this direction, attempts to describe quantitatively the relationship between various mechanisms on the basis of a quantitative description of the doubly differential neutron cross sections for the Nb(n,xn) and Bi(n,xn) reactions for incident neutron energies from 5 to 27 MeV. In this context, this analysis is based on rather fundamental models and their parameters.

2. Experimental information on the Nb(n,xn) and Bi(n,xn) reaction cross sections

Double differential neutron emission (DDC) have been measured in various laboratories in the course of the last ten years. A list of these measurements, and their characteristics are given in Table 1. As can be seen, there are seven independent experiments for Nb, and six for Bi. All of these measurements were performed using the time-of-flight method which is considered to be the most accurate for the spectrometry of fast neutrons. Taken together, these measurements cover the incident neutron energy range from 5 to 26 MeV. There are three independent experiments at 14 MeV.

The range of secondary neutrons having an energy (E), is given in the next column of Table 1. The minimum energy of the secondary neutron spectrum is determined by the detector threshold or by the dynamic range of the spectrometer. The upper limit of the spectrum depends on whether the elastically scattered neutron spectrum could be differentiated from the total spectrum. In those measurements where the spectrum of elastically scattered neutrons could be separated from (using a special method devised by the authors) the secondary neutron spectrum, a minus sign is entered in the fourth column of Table 1. Such experimental data play an important role in the analysis process because the spectrum of neutrons resulting from the (n,xn) reaction is not affected by the elastically scattered neutrons.

The range of angles at which the spectrum of secondary neutrons were measured is important in the analysis of angular distributions. Experimental conditions are usually such that it is possible to make measurements at angles ranging from 30 to 150 degrees. On the average, the number of angles at which measurements were made was six to eight. This was deemed sufficient to identify the characteristic tendencies of the angular distributions of secondary neutrons.

It must be also noted that typical energy resolution is on the order of hundreds of keV. At such resolutions, the measured spectra appear as uninterrupted distributions having irregularities in the hard part of the spectrum which correspond to the unresolved low-lying levels of the target nucleus.

As can be seen from Table 1, there are three independent measurements performed at an incident neutron energy of 14 MeV at different laboratories. The results of these measurements are compared with each other in Figures 1 and 2 (for the energy spectra of secondary neutrons) and in Figures 3 and 4 (for the angular distributions).

As can be seen, the data from three measurements fall within reasonable agreement with each other, which enhances their reliability. The divergence of the data at energies above 10 to 12 MeV may be explained by the contribution of elastically scattered neutrons, which had not been subtracted in the experiments reported in [8,9], in contrast to the experiments described in [7,13].

Experimentally determined data, which resulted from the experiments reported in [6-10. 12, 13], were used as a basis for our theoretical analysis given below. The data reported in reference [11] are evidently erroneous, as their value are approximately 30% lower than the results reported in reference [10], and their measurements were made at one angle only.

Table 1. Measurements of differential neutron emission cross sections for the Nb(n,xn) and the Bi(n,xn) reactions.

Nucleus	E_o MeV	$\bar{E}$ MeV	Elastic peak	Angles degrees	No. of angles	Reference
Nb	5,2	0,6-4,3	-	30-150	6	6
	6,2	0,6-5,3	-	30-150	6	6
	6,2	0,6-6,4	-	30-150	6	6
	8,0	0,6-7,2	-	30-150	6	6
	14,1	1,0-13	-	45-135	5	7
	14,1	0,9-14	+	30-150	8	8
	14,1	0,8-14	+	15-160	16	9
	18,0	1,8-18	+	30-150	7	8
	20,1	3,6-19	+	30-135	6	10
	20,6	0,5-17	+	90	1	11
	25,6	12,5-25	+	25-125	7	12
Bi	5,0	0,6-4,2	-	30-150	6	6
	6,0	0,6-5,0	-	30-150	6	6
	7,0	0,6-6,0	-	30-150	6	6
	8,1	0,6-7,0	-	30-150	6	6
	14,1	0,4-12	-	30-150	5	13
	14,1	0,7-14	+	15-150	15	9
	14,1	0,9-14	+	30-150	8	8
	18,0	1,8-18	+	30-145	7	8
	20,6	0,5-20	+	90	1	11
	25,6	12,5-25	+	25-125	7	12

3. Reactions with the formation of a compound nucleus

The Hauser-Feshbach model [1] which takes the conservation of spin and parity, as well as the characteristics of low-lying levels of the residual nucleus into account was used for the description of reaction cross sections with the formation of a compound nucleus at neutron incident energies below 14 MeV. Taking realistic nuclear level schemes into consideration is important for low incident neutrons energies when the maximum excitation energy is relatively low, and the transition to discrete states which leads to irregularities in the spectra of secondary neutrons have noticeable contributions.

At energies of 18 MeV and above, the ALICE [14] program was used to perform calculations. This program incorporates Weisskopf's expression to calculate neutron spectra from all intermediate nuclei formed after neutron or proton emission.

The model parameters, which were derived from the neutron optical potential, were used for the calculation of transmission coefficients in the Hauser-Feshbach model, and the neutron absorption cross section in Weisskopf' approximation. In this experiment, following the analysis of all of the available information, the neutron potential parameters were taken from reference [15] for Nb and [16] for Bi. The potentials suggested in reference [17] were used in the calculations of charged particles emitted in competing channels.

However, to a large extent, the energy dependence of the secondary neutron spectra and of the partial reaction cross sections are derived from the level densities of excited nuclei. There are a few approaches or models for its description. The simplest and most widely used is the Fermi-gas model with reverse shift; using this model, the energy dependence can be expressed as follows:

$$\rho(u) = \frac{\sqrt{\pi}}{24} \frac{\exp\left\{2\sqrt{a(U-\Delta)}\right\}}{a^{1/4}(U-\Delta)^{5/4}} \frac{2I+1}{2\sqrt{2\pi}\sigma^3} \exp\left\{-\frac{(I+1/2)^2}{2\sigma^2}\right\}, \qquad (1)$$

where a is the level density energy dependence parameter, Δ is the reverse shift which takes even-odd effects into consideration, σ is the spin dependence of the.of nuclear level densities:

$$\sigma^2(U) = 0,00957\,\eta\sqrt{\frac{(U-\Delta)}{a}} r_0^2 A^{5/3}. \qquad (2)$$

The a and Δ are parameters usually based on conditions derived from the simultaneous description of low-lying levels and neutron resonances for those nuclides for which there is such information. In addition there is the dependence of these parameters on the mass number, as it is done in Dilg's systematics [18].

However, there exists a certain interest in the independent procedure used to determine the nuclear level density parameters from the results of fitting the Hauser-Feshbach model formula to the energy and angular neutron distributions. Since the contribution of neutrons from the (n,2n) reaction had not yet been taken into account, only experimental data for incident

neutron energies in the 5 to 8 MeV range were chosen in this procedure. The analysis focussed on the low energy part of the neutron spectrum (<2MeV) in which the contribution of neutrons which originated from the non-equilibrium processes is negligibly small.

The density parameters determined in this manner, together with those derived from Dilg's systematics are listed in Table 2. In the latter, the relative moment of inertia η turns out to be an independent parameter which could assume a value of 1 or 0.5 (in the method developed in this work, however, we were spared this shortcoming because the moment of inertia originates from the angular distribution of inelastically scattered neutrons). A comparison shows that in the case of niobium, the density parameters obtained in this work are close to the parameters derived from Dilg's systematics for a value of η equal to 0.5. For bismuth, however, the data show a noticeable divergence in the values of all three parameters.

In the course of the last decade, the theory concerning density values of excited states of nuclei has experienced further development. Methods have been developed to take the influence of pair correlations (superfluid) and collective degrees of freedom [3] into account. From a general point of view, in the framework of this model, the expression for level densities can be written as follows:

$$\rho(U,J) = \rho_{bcs}(U,J)\, K_{vibr}(U)\, K_{rot}(U) \qquad (3)$$

where $\rho_{bcs}(U,J)$ is the level density in the independent quasi-particle model, K_{vibr} and K_{rot} are the vibrational and rotational amplification coefficients of the nuclear level densities.

Table 2. Nuclear level density parameters

Nucleus	U_c, MeV	a, MeV^{-1}	Δ, MeV	η	Reference
^{93}Nb	1.7	11.2	-0.2	0.51±0.17	This work
	1.16	11.42	-0.69	0.5	[18]
	1.16	11.98	-0.76	1.0	[18]
		8.7		1.0	[3]
^{209}Bi	3.3	12.7	1.6	0.29±0.04	This work
	1.0	10.12	-1.36	0.5	[18]
	1.0	11.43	-1.23	1.0	[18]
		13.1		1.0	[3]

An important aspect of this model is the recognition that there exists a phase transition point, in other words, that there is an excitation energy U_{kr} at which there is a break-up of the pair correlation and a transition into an independent Fermi-particle state. For the nuclides under consideration, that energy is U_{kp} = 5.2 MeV for Nb and 0 MeV for Bi. This means that the pair correlation is absent altogether or that its effect becomes apparent at small excitation energies.

4. Pre-equilibrium nucleon emission

The calculation of pre-equilibrium nucleon spectra was carried out on the basis of the dependence of the hybrid exciton model geometry (GDH) [19]. Th calculations were performed using the following equation:

$$\frac{d\sigma^{pre}}{d\varepsilon_x} = \pi\lambda^2 \sum_{l=0}^{\infty}(2l+1)T_l \sum_{n=n_0}^{\bar{n}} R_x(n) \frac{\omega(p-1,h,E-Q_x-\varepsilon_x)}{\omega(p,h,E)} \frac{\lambda_c^x}{\lambda_c^x+\lambda_+^x} g D_n, \quad (4)$$

where χ is the wavelength of the incident particle, T_r is the partial transmission coefficients calculated using the optical model, ϵ_x is the energy of the nucleon emitted by the nucleus, Q_x is the binding energy of the compound nucleus, ω(p,h,E) is the density of the exciton states having p particles and h holes (p+h=n) for an energy E, λ_c is the velocity of the internal transition corresponding to the absorption of the nucleon in the nucleus, g=A/14.0 is the density of single particle states, R_x (n) is the number of particles of type x in the n-exciton state, D_n is the depletion factor of the exciton state n, taking into account changes in the populated states due to emissions at previous stages, and where n_0 is the initial number of excitons (n_0 = 3).

The density of excited states was calculated with the aid of the Strutinsky-Erickson formula:

$$\omega(p,h,E) = \frac{g(gE-A)^{n-1}}{p!\,h!\,(n-1)!}, \quad (5)$$

where A is the correction for Pauli's principle:

$$A = (p^2+h^2+p-3h)/4. \quad (6)$$

The nucleon emission velocity was calculated using expression:

$$\lambda_c^x = \frac{(2s_x+1)\mu_x\varepsilon_x\sigma_{inv}^x(\varepsilon_x)}{\pi^2\hbar^3 g_x}, \quad (7)$$

where s_x and μ_x are the spin and the reduced mass of particle type x, σ_{inv} is the inverse reaction cross section for the particle being investigated, g_x is the density of single particle states which is equal to N/14 for neutrons and Z/14 for protons.

The nucleon absorption velocity was calculated using the formula:

$$\lambda_+^x = V\sigma_0(\varepsilon_x)\rho_l \quad (8)$$

where V is the velocity of the nucleon inside of the nucleus, σ_0 is the nucleon-nucleon interaction cross section which takes Pauli's principle into account, and where p_l is the nuclear matter density. In the initial state (2p1h), average values of the nuclear density corresponding to the distance from the centre of the nucleus $l\chi<r_l<(l+1)\chi$ were taken into account for each partial wave and each value of the radius r. Density values for the other exciton states were averaged over the volume of the nucleus.

The factor R_x (n) which is a constituent of formula (2) was calculated for neutron reactions in the following manner:

$$R_n(3) = (Z + 2A)/(2Z + A), \tag{9a}$$

$$R_p(n) = 2 - R_x(3), \tag{9b}$$

$$R_x(n) = R_x(3) + (n-3)/4. \tag{9c}$$

In performing the calculations, multiple pre-equilibrium nucleon emission was taken into account in an approximate form only. In accordance with [17] it was assumed that the number of particles emitted from one and the same exciton state is equal to:

$P_{np} = P_n P_p$ (for the emission of neutrons and protons) (10a)

$P_{nn} = P_n P_n / 2$ (for the emission of two neutrons) (10b)

whereby P_n and P_p are the total number of neutrons and protons emitted by the n-exciton configuration being investigated. The pre-equilibrium components of the (n,n'), (n,2n) and (p,np) reactions were calculated by using the following equations:

$$\sigma^{Z,A}(E_n - \varepsilon) = \frac{C_n}{\sigma_n} \frac{d\sigma_n(\varepsilon)}{d\varepsilon}, \tag{11a}$$

$$\sigma^{Z,A-1}(E_n + Q_{(n,2n)} - \varepsilon - \bar{\varepsilon}_n) = \frac{C_{nn}/2}{\sigma_{2n}} \frac{d\sigma_n(\varepsilon)}{d\varepsilon}, \tag{11b}$$

$$\sigma^{Z-1,A-1}(E_n + Q_{(n,np)} - \varepsilon - \bar{\varepsilon}_{p(n)}) = \frac{C_{np}}{2\sigma_{np}} \left(\left(1 - V_p/\varepsilon\right) \frac{d\sigma_n(\varepsilon)}{d\varepsilon} + \frac{d\sigma_p(\varepsilon)}{d\varepsilon} \right), \tag{11c}$$

where Ż and A are the characteristics of the target nucleus, E_n is the energy of the primary neutrons, $Q_{(n,2n)}$ and $Q_{(n,np)}$ are the reaction energies of the (n,2n) and (n,np) reactions, V_p is the Coulomb potential for the protons, C_n , C_{nn} and C_{np} are the emission of a single pre-equilibrium neutron, the simultaneous emission of two pre-equilibrium neutrons from the same exciton state, and the emission of a neutron and a proton from such states, respectively, where σ_n and σ_{2n} represent the values of the integrals of the total pre-equilibrium neutron spectra ($d\sigma_n/d\epsilon$) in the energy range corresponding to the (n,n'), (n2n) reactions, and where σ_{np} represents the integrated pre-equilibrium neutron spectrum ($d\sigma_n/d\epsilon$) for energies ranging from 0 to $E-B_n-B_p$ respectively, and where $\bar{\epsilon}_n$ and $\bar{\epsilon}_p$ are the average kinetic energies of the second neutron and proton corresponding to the kinetic energy ϵ of the first emitted particle.

5. Contributions of the direct processes in inelastic scattering

In the framework of the generalized model of the nucleus, the direct excitation cross section was calculated either by using the strong coupling channels [21]formalism, or by using the first order distorted wave Born approximation (DWBA) [22].

In the distorted wave method, the cross section for the direct excited state of the target nucleus is represented by the following equation:

$$\sigma_{if}^{\lambda} = \sum_{\mu} \left| \sum_{jijf} C_{jijf}^{\lambda\mu}(\theta) \int_{0}^{\infty} \Psi_{ji}(r) F_{\lambda}(r) \Psi_{jf}(r) dr \right|^2 , \qquad (12)$$

where $C_{jijf}^{\lambda\mu}(\theta)$ are the kinematic coefficients determined by the law of angular momenta summation, $\Psi^*_{ji}(r)$ and $\Psi_{jf}(r)$ are the radial wave functions of the optical model for incident and scattered neutrons, $F_\lambda(r)$ is the form factor of the excited level of the target nucleus. For the case of direct inelastic scattering, there is a high probability for the excitation of collective states of the target nucleus. In the framework of the generalized model of the nucleus [23], using a phenomenological approach, the form factor is usually expressed by:

$$F_{\lambda}(r) = \frac{\beta_{\lambda} R_0}{(2\lambda+1)^{1/2}} \frac{dV(r)}{dr} , \qquad (13)$$

where β_λ is the dynamic deformation parameter for the multipole excited state λ , $R_o = r_o A^{1/3}$ is the radius of the nucleus, and V(r) is the optical model potential.

Thus, in order to evaluate the contribution of the direct processes in inelastic scattering one has to have spectroscopic information on the spin, parity and deformation parameters of the excited states of the target nucleus, as well as information on the optical potential parameters for the scattered particle in the energy range that is being investigated.

For the even-even spherical nuclei, the lowest lying excited levels are analyzed in the framework of the generalized model and are considered as excitation of surface oscillations of different multipolarities. The excitation of neighboring states of odd nuclei can be analyzed in terms of a model of weak coupling of odd nucleons with excited states of even-even nuclear core.

Using that approach, let us analyze the lowest lying levels of the ^{93}Nb nucleus. In the excited energy range of 0.8 to 1.1 MeV, one can observe in the niobium nucleus a quintet of states with spins ranging from $1/2^+$ to $13/2^+$, whereby the centre of gravity of these states (0.934 MeV) coincide with the location of the 2^+ level of the neighboring even-even ^{92}Zr nucleus, and the sum of the electromagnetic transitions probabilities to a state belonging to that quintet, is close to the electromagnetic transition probability of the 2^+ nucleus of ^{92}Zr [24]. Such a coincidence indicates that the averaged characteristics of excited states of the ^{93}Nb nucleus can be analyzed in terms of a weak odd proton coupling model in the $g^{9/2+}$ shell with excited states of an even-even ^{92}Zr core. The necessary information regarding the location E_λ, the spin λ, the parity and the dynamic deformation parameter β_λ for the ^{92}Zr nuclide was taken from reference [23]. The data in that reference were obtained from the analysis of experimental data on inelastic scattering of protons having an initial energies of 19.4 to 12.7 MeV. Large deformation parameters values for the 2^+ and 3^- levels, indicate a strong correlation of these levels with the ground state 0^+ and that circumstance demands that strong channel coupling method be used in the calculations of the direct excitation cross section in inelastic scattering. Not only were the cross sections for the direct excitation of single phonon states calculated in the framework of the strong channel coupling method, the calculations extended to the excitation of two-phonon states obtained as a result of a twofold excitation of strong single-phonon states 2^+ and 3^-, namely: $\{2^+ \otimes 2^+\}$, $\{3^- \otimes 3^-\}$ and $\{2^+ \otimes 3^-\}$.

The status of the two-phonon state was determined in terms of a harmonics approximation as the sum of the energies of single-phonon states, forming two-phonon states.

The experimental data on the locations and spins of the ^{92}Zr levels are well known up to the excitation energy of 4.43 MeV and the multipolarities are known only up to -5; it is therefore necessary to supplement the information with data derived from theoretical calculations based on poly-microscopic models [26-28] of excited states. In such calculations, which are differentiated from one another by the chosen effective strengths, it is nevertheless possible to not only reproduce experimental data on low-lying collective states of even-even nuclides, but to obtain information on other excitations of the nucleus, such as on the multipolar resonances. Data resulting from theoretical calculations for ^{92}Zr were taken from reference [28].

The optical potential parameters for the calculation of the direct inelastic scattering of neutrons for ^{93}Nb were taken from reference [15]. The magnitude of the imaginary part of the optical potential was reduced by 30% in the calculations using the strong channel coupling method.

A similar approach was used for the ^{209}Bi nucleus. Having the experimental information on the locations, spins and parity of the excited states from reference [29] made it possible to analyze the ^{209}Bi in the framework of the weak coupling model in the $2f_{7/2}$ state of the odd proton together with the vibrational states of the even-even ^{208}Pb core of the nucleus. The optical potential parameters for the calculation of the inelastic scattering of neutrons were taken from reference [16].

6. Discussion of the calculational results.

The comparison of the calculational results with the experimental differential cross sections integrated over angle given in the form of integral spectra of secondary neutrons is shown in Figures 5 to 10. All data are represented in the centre of mass system. For the purpose of demonstrating the tendencies of the data, they are shown at two extreme energies (5 MeV and 25 MeV) and at an average energy (14 MeV) taken from the analyzed range of incident neutron energies.

As can be seen from the figures, the compound reaction mechanism is the dominating contribution to the low energy part of the secondary neutron spectra. This contribution falls off exponentially as a function of increasing neutron energy E, or correspondingly as a function of decreasing excitation energy U, which is a consequence of the energy dependence of the nuclear level density function. In the case of ^{209}Bi(n,xn) reaction, because of the relatively low density and high energy of transition from resolved levels to the continuum, there is a distinct increase in irregularities in the spectrum which correspond to the discrete levels of the residual nucleus (see Figure 6). In all appearances, for incident neutron energies of E_0 = 5 MeV it is possible to achieve a better description of the neutron inelastic scattering spectrum for that reaction in the energy range E=0.5 to 2.0 MeV if the spectroscopic information on higher lying excited levels (U > 3.3 MeV) of the ^{209}Bi nucleus had been known.

As indicated, the energy dependence (slope) of secondary neutron spectra is determined from the nuclear level densities. Figures 7 and 8 show the calculational results based on the statistical model using different density functions derived from the Fermi gas model with inverse shift (expressions 1 and 2) and on the superfluid model taking collective effects into consideration (3). In case of the first approach, the a and Δ parameters were chosen on the basis on the conditions which gave the best description of the spectrum for incident neutron energies below 8 MeV; in the case of the second approach, the values of these parameters were taken from the systematics described in reference [13]. As can be seen, in the case of Nb, both approaches give approximately the same description which are in good agreement with the experimental data. In the case of Bi on the other hand, the results from the systematics given in [13] predict too steep a slope of the secondary neutron spectrum.

On this basis, the following conclusion could be reached: that known level density parameter systematics cannot predict the density of excited states for specific nuclei with the required accuracy. In order to be able to describe experimental data to a satisfactory level it is necessary to resort to a fitting procedure, which is without a doubt, easier to achieve using simple expressions for the density function such as the Fermi-gas model.

In contrast to the compound mechanism, the direct inelastic scattering process provides the dominant contribution at the highest energy (hard) part of the secondary neutron spectrum. As can be seen, the theoretical approach used in this work, predicts the structure and magnitude of the observed differential cross sections. This means that, for the energies considered here, the direct mechanism is determined by the collective (vibrational) states of the target nucleus to a significant extent. As a rule, these consists of the first quadrupole or octupole vibrational modes of even-even or magic nuclei. As the configuration of the excited state becomes more complex (e.g., multiphonon levels), or in the case of transition to a single particle level, the probability of direct excitation diminishes.

As can be seen in figures 5 and 6, for the lowest incident neutron energies (5 MeV), the compound and direct mechanism contributions are enough to satisfactorily describe the experimental data. However, further improvements could be achieved in the framework of these mechanisms if more information on the structure of the nucleus were available. For incident neutron energies of 14 MeV and above, there is a gap in the theoretical calculations in the intermediate secondary neutron energy interval, in which the contributions of the equilibrium and direct mechanisms become sparse. In this work it was attempted to include calculations on pre-equilibrium models, as described in Chapter 4, above. If one used proven model parameters (e.g., optical potential, internal transition velocities, etc...), one would obtains an excessive contribution to the pre-equilibrium mechanism. In order to obtain a satisfactory description of the experimental data in the form of a sum of three processes, it would be necessary to lower the pre-equilibrium emission contribution by a factor of two.

Finally, Figures 11 and 12 show the incident neutron energy dependence of the integral contributions of the equilibrium, direct and pre-equilibrium mechanisms for the Nb and Bi target nuclei, respectively. Both nuclei show similar tendencies in that the contribution of the compound mechanism falls off from 90% to 50% at energies ranging from 5 to 25 MeV. The contribution of the direct mechanism, which is hardly energy dependent, amounts to approximately 10% - 15%. The remaining part of the (n,xn) reaction cross section, is attributed to the pre-equilibrium neutron emission whose contribution increases from 0 to 30% - 35%.

7. Conclusion

The following conclusions have been reached as a result of the work performed in the calculations and analysis of the experimental data on the ^{93}Nb(n,xn) and ^{209}Bi(n,xn) differential reaction cross sections for incident neutron energies ranging from 5 to 27 MeV.

At low incident neutron energies (up to 10 MeV) the reaction mechanism consists of equilibrium and direct processes. In order to obtain quantitative descriptions of the reaction cross sections and energy-angular distributions of secondary neutrons, it is necessary to use the Hauser-Feshbach model and the model of strong coupling channels or the deformed wave Born approximation formalism. These models produce correct quantitative evaluations if the model parameters used in these calculations (optical potential, spectroscopic characteristics of excited levels, etc...) have been obtained from the analysis of other reactions or from calculations using microscopic approaches. The determination of parameters used in the excited states density functions requires an independent approach because known systematics do not always predict these parameters to the required accuracy.

At higher energies (E>14 MeV), the compound mechanism contribution becomes noticeably smaller, and the direct contribution does not change significantly (partly, this is due to the difficulty in the calculation of the direct excitation of high-lying states due to the absence of the information of their nature). In order to obtain a satisfactory description of the data, it is necessary to introduce pre-equilibrium neutron emission; however, the calculations of the respective models must be normalized to experimentally determined data. This attests to the fact that the contribution of the pre-equilibrium emission of nucleons at intermediate energies is not sufficiently substantiated.

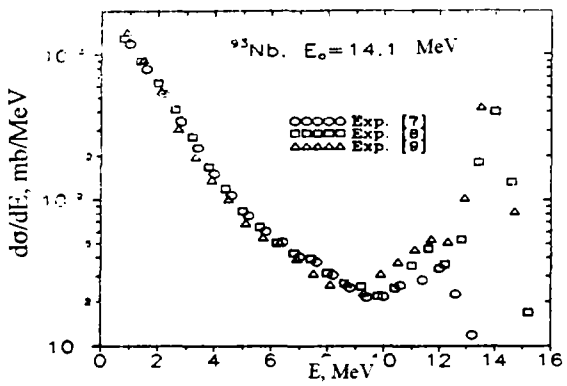

Figure 1. Integral spectra of secondary neutrons for the Nb(n,xn) reaction at 14 MeV

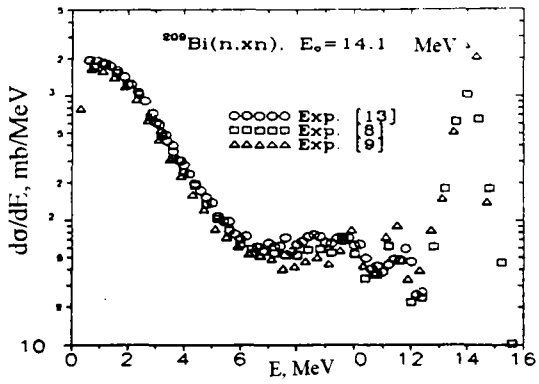

Figure 2. Integral spectra of secondary neutrons for the Bi(n,xn) reaction at 14 MeV

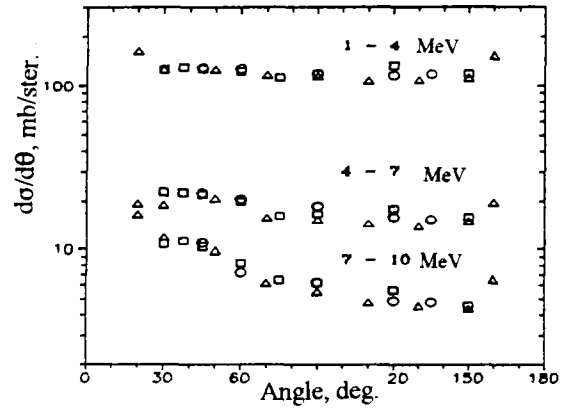

Figure 3. Angular distribution of secondary neutrons in the centre of mass system for the Nb(n,xn) reaction at 14 Mev

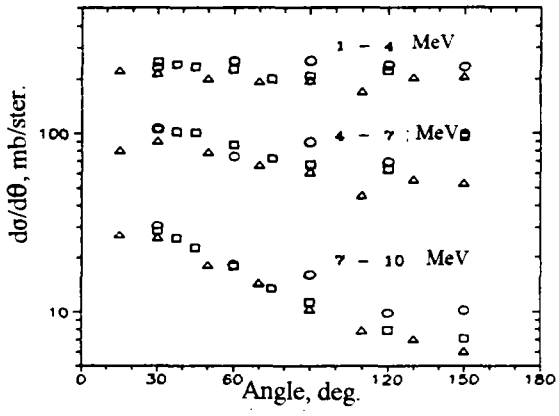

Figure 4. Angular distribution of secondary neutrons in the centre of mass system for the Bi(n,xn) reaction at 14 Mev

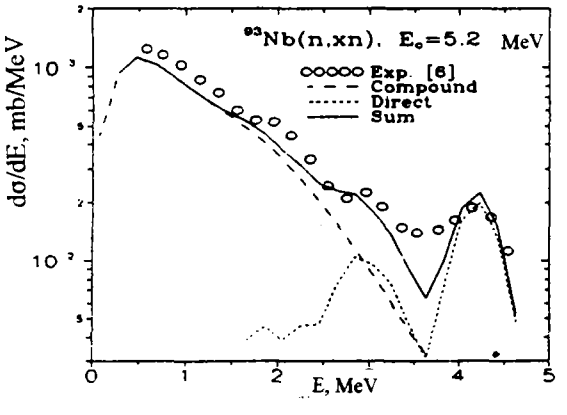

Figure 5. Experimental and calculated neutron spectra for the Nb(n,n') reaction at 5.2 MeV

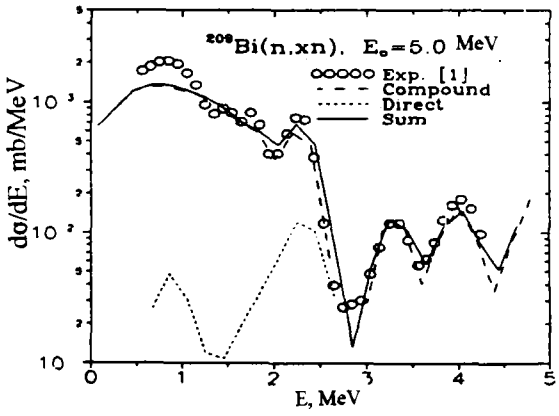

Figure 6. Experimental and calculated neutron spectra for the Bi(n,n') reaction at 5.2 MeV

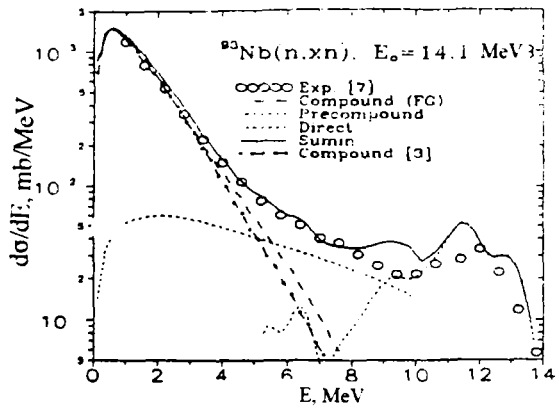

Figure 7. Experimental and calculated neutron spectra for the Nb(n,xn) reaction at 14.1 MeV

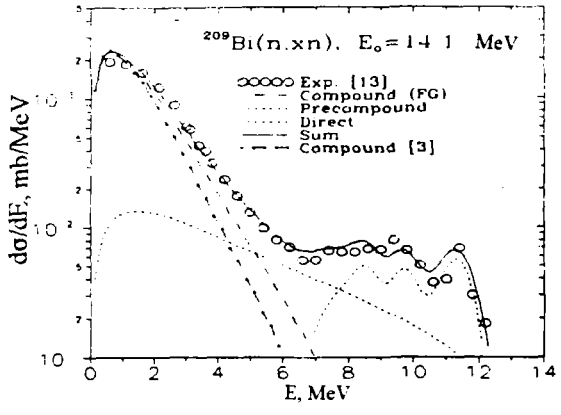

Figure 8. Experimental and calculated neutron spectra for the Bi(n,xn) reaction at 14.2 MeV

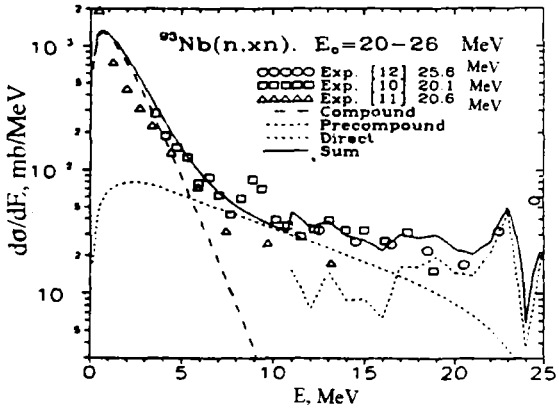

Figure 9. Experimental and calculated neutron spectra for the Nb(n,xn) reaction at 20-26 MeV

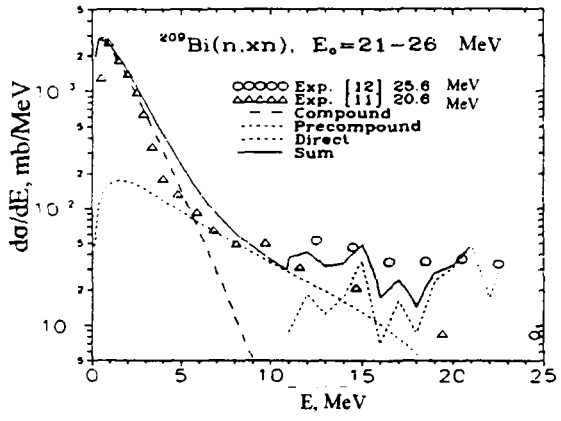

Figure 10. Experimental and calculated neutron spectra for the Bi(n,xn) reaction at 20-26 MeV

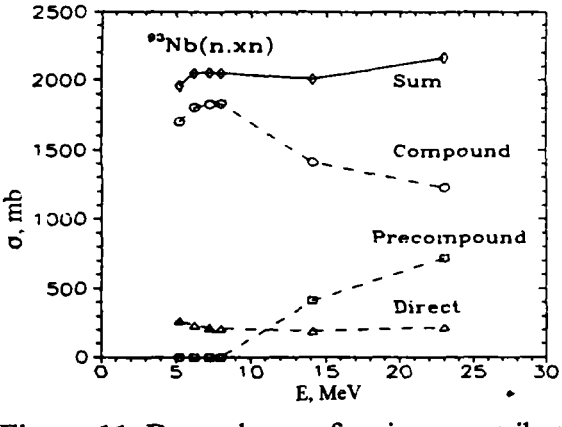

Figure 11. Dependence of various contributing mechanisms of the Nb(n,xn) reaction on incident neutron energy

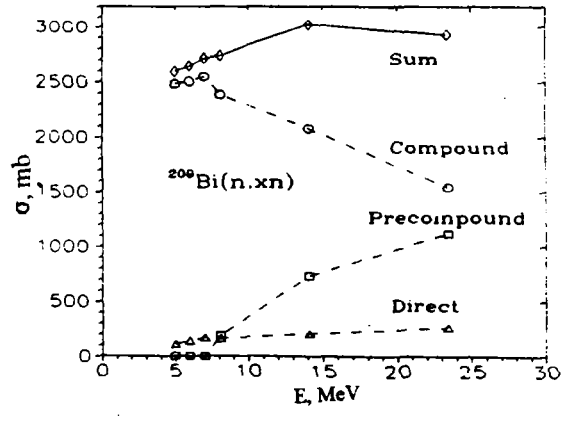

Figure 12. Dependence of various contributing mechanisms of the Bi(n,xn) reaction on incident neutron energy

References

[1] HAUSER, W., FESCHBACH, H., Phys. Rev. 87 (1952) 366.

[2] BETHE, H.A., Phys. Rev. 50 (1936) 332.

[3] IGNATYUK, A.V., Statistical Properties of Excited Atomic Nuclei, Ehnergoatomizdat, Moscow (1983) [in Russian].

[4] GRIFFIN, J.J., Phys. Lett. B24 (1967) 5.

[5] FESCHBACH, H., Ann. of Physics 125 (1980) 429.

[6] SIMAKOV, S.P., et al., Rep. INDC(NDS)-272, IAEA, Vienna (1992).

[7] LYCHAGIN, A.A., et al., Sov.J. At. En., 57 (1984) 266.

[8] BABA, M., J. Nucl. Sci. Techn. 31 (1994) 757.

[9] TAKAHASHI, A., OKTAVIAN, Rep. A-92-01, 2 Osaka (1992).

[10] LOVCHIKOVA, G.N., et al., Rep. FEI-1603, Obninsk (1984).

[11] PROKOPETS, G.A., Proc. Fifth All-Union Conf. on Neutron Physics, TsNINatominform, Moscow, Vol. 2 (1980) 54 [in Russian].

[12] MARCINKOWSKI, A., et al., Nucl. Sci. Eng. 83 (1983) 13.

[13] SIMAKOV, S.P., et al. Rep. INDC(CCP)-315, IAEA, Vienna (1990).

[14] BLANN, M., BISPLINGHOFF, J. , Rep. UCID-20169, Lawrence Livermore Laboratory, Livermore (1985).

[15] LAGRANCHE, Ch., LEJEUNE, A., Phys. Rev. C25 (1985) 2278.

[16] FINLAY, R.W., et al., Phys. Rev. C30 (1984) 796.

[17] BLANN, M., VONACH, H.K., Phys. Rev. C28 (1983) 1475.

[18] DILG, W., et al., Nucl. Phys. A217 (1973) 269.

[19] BLANN, M., Phys. Rev. Lett. 28 (1972) 757.

[20] KIKUCHI, K., KAWAI, M., Nuclear Matter and Nuclear Interactions, North Holland, Amsterdam (1968).

[21] TAMURA, T., Rev. Mod. Phys. 37 (1965) 679.

[22] AUSTERN, N., Direct Nuclear Reaction Theories, Wiley Interscience, New York (1969).

[23] BOR, O., MOTTELSON, B., "Structure of the atomic nucleus", 2 Mir, Moscow (1977) [in Russian].

[24] VAN HEERDEN, I.J., et al., Z. Physik 260 (1973) 9.

[25] STAUTBERG, M.M., et al., Phys. Rev. 151 (1966) 969.
DICKENS, J.K., et al., Phys. Rev. 168 (1968) 1355.

[26] SOLOVIEV, V.G., in Selective Topics on the Atomic Nucleus Structure. OIYaI (1976) 146 [in Russian].

[27] BERTSCH, G., TSAI, S.F., Phys. Rev. C18 (1975) 125.

[28] BLOKHIN, A.I., IGNATYUK, A.V., in Topics on Nuclear and Cosmic Rays, Higher Educational Institution, Vol. 7, Kharkov (1977) 100 [in Russian].
VDOVIN, A.I., SOLOVIEV, V.G., EhTchAYa 14 (1983)237 [in Russian].

[29] WAGNER, W.T., CROWLEY, G.M., Phys. Rev. C11 (1975) 486.
WAGNER, W.T., CROWLEY, G.M., Phus. Rev. C12 (1975) 757.

Nuclear Data Section
International Atomic Energy Agency
P.O. Box 100
A-1400 Vienna
Austria

e-mail, INTERNET: SERVICES@IAEAND.IAEA.OR.AT
fax: (43-1)20607
cable: INATOM VIENNA a
telex: 1-12645 atom a
telephone: (43-1)2060-21710

online: TELNET or FTP: IAEAND.IAEA.OR.AT
username: IAEANDS for interactive Nuclear Data Information System
username: ANONYMOUS for FTP file transfer
username: FENDL for FTP file transfer of FENDL files
For users with web-browsers: http://www-nds.iaea.or.at